Regulation of histidine catabolism in *Pseudomonas fluorescens* SBW25

A thesis submitted in partial fulfillment of the requirements for
the degree of
Doctor of Philosophy
in
Microbiology & Genetics

at Massey University, Auckland, New Zealand

Naren

2019

Abstract

The pathway of histidine utilization (*hut*) has been a model for studying bacterial gene expression, particularly the coordination between cellular carbon and nitrogen metabolisms. Early studies in enteric bacteria led to the concept of catabolite repression, which explains the inhibitory effects of glucose on the utilization of alternative carbon sources such as histidine and lactose. Briefly, transcription of *hut* genes is activated by the catabolite-activating protein (CAP) charged with cAMP and the NtrBC/NAC cascade when histidine is used as a source of carbon and nitrogen, respectively. However, this well-defined paradigm does not hold for many non-enteric bacteria, including the closely related *Pseudomonas*.

This work aims to define the molecular basis of *hut* gene expression in *Pseudomonas*, using the plant growth-promoting bacterium *P. fluorescens* SBW25 as a model. Previous work identified all *hut* genes involved in histidine uptake and subsequent enzymatic breakdown, which are organized in three transcriptional units in the *hut* locus: *hutF*, *hutCD* and *hutU-G*. Like in enteric bacteria, histidine-induced expression of *hut* operons is mediated by the HutC repressor with urocanate, the first intermediate of the histidine degradation pathway, as the effector molecule. However, the precise interactions between HutC and its *hut* operator sites remain elusive; more importantly, recent progress suggests a new role of HutC in global gene regulation beyond histidine catabolism. Moreover, two two-component systems CbrAB and NtrBC are involved in *hut* activation, but it remains unknown whether they act in a direct or indirect manner.

In this study, I first examined the molecular interactions between His_6-tagged HutC protein and probe DNAs of the P_{hutU} and P_{hutF} promoters. Results of electrophoretic mobility shift assay (EMSA) and DNase I footprinting indicate that HutC binds to a consensus sequence of TGTA-N_2-TACA (named Phut site), and involves complex oligomerization in response to varying concentrations of urocanate. A novel weak HutC binding sequence (termed Pntr site) was identified in the P_{hutF} promoter, which may help strengthen the repression of *hutF*. Significantly, this Pntr site shows no sequence similarity to the previously recognized Phut site, instead it is homologous to the NtrC-binding consensus sequence (GCACCA-N_3-TGGTGC).

Next, the Phut consensus sequence was used to predict HutC target genes in the genome of *P. fluorescens* SBW25. This led to the identification of 88 candidate promoters, eight of which were subject to experimental verification by EMSA and DNase I footprinting. Phenotypic analysis of the *hutC* deletion mutant showed that *hutC* is involved in cell motilities. The data is consistent with the predicted global regulatory role of HutC.

Histidine utilization poses a significant challenge as it produces excess nitrogen over carbon. The rate of histidine utilization (*hut*) thus must be carefully regulated. Here we show, for the first time, that expression of *hut* genes is positively regulated by two global regulators CbrAB and NtrBC in a *direct* manner, while subjecting to histidine concentration-dependent negative control of the HutC repressor. *hut* expression is further regulated at the post-transcriptional level by the CbrAB-CrcYZ-Crc/Hfq cascade in response to the presence of succinate (the most preferred carbon source for *Pseudomonas*). When growing in nutrient-complex conditions such as a minimal salts medium supplemented with succinate and histidine wherein histidine is the sole nitrogen but less-preferred carbon source, CbrAB is involved in directly activating *hut* transcription but indirectly repressing *hut* translation. Under this condition, NtrBC plays the dominant role in transcriptional activation of *hut* genes, but it requires assistance from the HutC repressor. A combination of genetic and biochemical analyses show that HutC acts as a governor to monitor and control the histidine catabolic rate, preventing production of excess ammonium and consequent inactivation of the NtrBC system. HutC additionally recognizes the NtrC binding site responsible for *ntrBC* expression, which provides a negative feedback for NtrBC autoregulation.

Together, data presented in this thesis extend our understanding of carbon catabolite repression to the cellular nitrogen catabolism of *Pseudomonas*: carbon/nitrogen metabolic balance is maintained by the interplay of CbrAB and NtrBC at the *hut* operator site, and it requires the local regulator HutC to prevent *hut* expression from exceeding a critical upper limit. The finding that the HutC regulator is capable of recognizing two distinct DNA binding motifs (Phut and Pntr) has broader implications in gene regulation. Further biochemical analysis is required to unravel the molecular basis of the observed dual site recognition.

Acknowledgements

After this challenging and exciting PhD, I have gained not only the ability to conduct research, but also a logical way of thinking and positive attitude when facing difficulties. Here, I have many people to thank. First and foremost, I would like to thank my supervisor Dr. Xue-Xian Zhang for providing me with this fascinating project to work on, for his advice and continuous support. I am really grateful for all his valuable insights into my project and helpful discussions throughout my study.

I appreciate the continuous support and encouragement from my co-supervisor at Massey University, Distinguished Professor Paul B. Rainey. Thanks also to all the members of the Rainey Lab and Hendrickson Lab for helping me here and there, particularly, Dr. Elena Colombi, Dr. Christina Straub and Dr. Gayle Ferguson for sharing their experience in research work, and Dr. Daniel Rexin and Danielle Kok for managing our lab building so well.

I would like to thank Kiran Jayan for sharing with me his research progress on HutC in *Pseudomonas aeruginosa*. I also want to express my gratitude to Dr. Yunhao Liu for his help and tips on my experiments, this made the beginning of my PhD study easier. Thanks to all the past and present members of Xue-Xian's Lab. These guys contributed to a pleasant working environment and made my journey here full of joy and happiness.

Thanks to my family for their unconditional love, patience and support, which accompanied me throughout my study towards my Doctorate. A special thanks to Simon Chang for respecting all my life decisions and always being by my side. I will never forget all the delicious dinners he made, which filled me with energy to conquer all the long nights of thesis writing.

Table of Contents

List of Figures

List of Tables

List of Abbreviations

APS	Ammonium persulphate
ATP	Adenosine triphosphate
BLAST	Basic local alignment search tool
BSA	Bovine serum albumin
bp	Base pairs
ºC	Degrees Celsius
Da	Dalton
DMSO	Dimethyl sulfoxide
DNA	Deoxyribonucleic acid
DNase I	Deoxyribonuclease I
dNTP	Deoxynucleotide triphosphate
EDTA	Ethylenediamine tetraacetic acid
g	Gravitational force
h	Hour
HEPES	n-2-hydroxylethylpiperazine-n′-2-ethanesulphonic acid
IPTG	Isopropyl-β-D-thiogalactoside
kb	Kilobase pairs
kDa	KiloDaltons
LB	Lysogeny broth
M	Molar
mM	Millimolar
µM	Micromolar
mg	Milligram
ml	Milliliter
µl	Microliter
min	Minute
MW	Molecular weight
MWCO	Molecular weight cut-off
ncRNA	non-coding ribonucleic acid
nm	Nanometre
nM	Nanomolar
OD	Optical density

ORF	Open reading frames
PAGE	Polyacrylamide gel electrophoresis
PCR	Polymerase chain reaction
PMSF	Phenylmethylsulfonyl fluoride
RNA	ribonucleic acid
rpm	Revolution per minute
SDS	Sodium dodecyl sulphate
TBE	Tris-borate-EDTA
TCA	tricarboxylic acid
TEMED	N,N,N',N'-Tetramethylethylenediamine
UV	Ultraviolet

Chapter 1

Introduction

Amino acids, such as histidine, are a good nutrient source for many bacteria. Historically, the pathway for histidine utilization (*hut*) has been used as a genetic model for studying the coordination of cellular carbon and nitrogen metabolism (reviewed by Bender, 2012). Early studies in enteric bacteria have led to the establishment of at least three important paradigms in bacterial gene expression: first, the concept of catabolite repression that explains glucose-mediated inhibition on expression of the enzymes involved in the utilization of alternative carbon sources such as histidine and lactose (i.e. the so-called 'glucose effects'); second, NtrBC as the first two-component signal transduction system and a master regulator of cellular nitrogen metabolism; third, autoregulation of bacterial regulators. Briefly, the *hut* operon is subject to positive control by the catabolite activator protein (CAP) whose activity is modulated by cAMP in response to glucose availability when histidine is used as a carbon source. When histidine is used as a nitrogen source, the *hut* operon is activated by the nitrogen assimilation control protein (NAC) under the control of the NtrBC system. The negative control of *hut* is mediated by the HutC repressor, which regulates expression of *hut* genes, including *hutC* itself, in a histidine concentration-dependent manner.

However, it has long been known that this well-defined model of *hut* expression does not hold for many non-enteric bacteria, including the closely related genus *Pseudomonas*. This literature review will describe the histidine catabolism in different bacterial species with a focus on the emerging new role of HutC in global gene regulation and its contribution to the ecological performance of bacteria when colonizing eukaryotic hosts. This section will also discuss the latest progress on carbon catabolite repression (CCR) in *Pseudomonas*, which occurs at the post-transcriptional level. My discussion will specifically focus on previous work on *P. fluorescens* SBW25, a plant growth-promoting bacterium used as the model organism for studying the molecular mechanisms of *hut* gene expression in *Pseudomonas*.

1.1 Histidine catabolism in bacteria

The ability to degrade histidine is widely distributed among bacteria (Itoh *et al.*, 2007). The histidine degradation is achieved by either a four-step or five-step enzymatic pathway. The first three steps are common among all bacteria (Bender, 2012; Itoh *et al.*, 2007). As shown in Figure 1.1, histidine is first deaminized by histidase (HutH) to yield urocanate, and then urocanase (HutU) hydrates urocanate to give imidazolone propionate (IP), which is further catabolized into formiminoglutamate (FIGLU) by imidazolone propionate hydrolase (HutI). Further breakdown of FIGLU differs in different organisms. In most enteric bacteria (e.g. *Klebsiella aerogenes* and *Salmonella typhimurium*) and Gram-positive bacterium *Bacillus subtilis*, FIGLU is directly hydrolyzed by formiminoglutamase (HutG[4]) to produce glutamate with formamide secreted as a waste product (Chasin & Magasanik, 1968; Goldberg & Magasanik, 1975; Kaminskas & Magasanik, 1970; Smith & Magasanik, 1971). In most *Pseudomonas* and *Streptomyces* species, FIGLU is catabolized by formiminoglutamate iminohydrolase (HutF) and formylglutamate amidohydrolase (HutG) through a two-step reaction with formate and glutamate as the end products (Hu & Phillips, 1988; Kendrick & Wheelis, 1982). Glutamate can be hydrolyzed to yield ammonia and α-ketoglutarate, which provides carbon and energy for bacterial growth through the TCA cycle (Itoh *et al.*, 2007). Of note, the distribution of these two histidine degradation pathways does not always correlate with the phylogenetic position of bacteria. Some enteric bacteria, such as *Erwinia amylovora* and *Serratia proteamaculans*, utilize histidine via the 5-step pathway (Bender, 2012). Additionally, several *Pseudomonas* species, such as *P. alcaliphila*, *P. fulva* and *P. mendocina*, do not possess *hutF* in their genome, suggesting that the 4-step pathway is employed to degrade histidine.

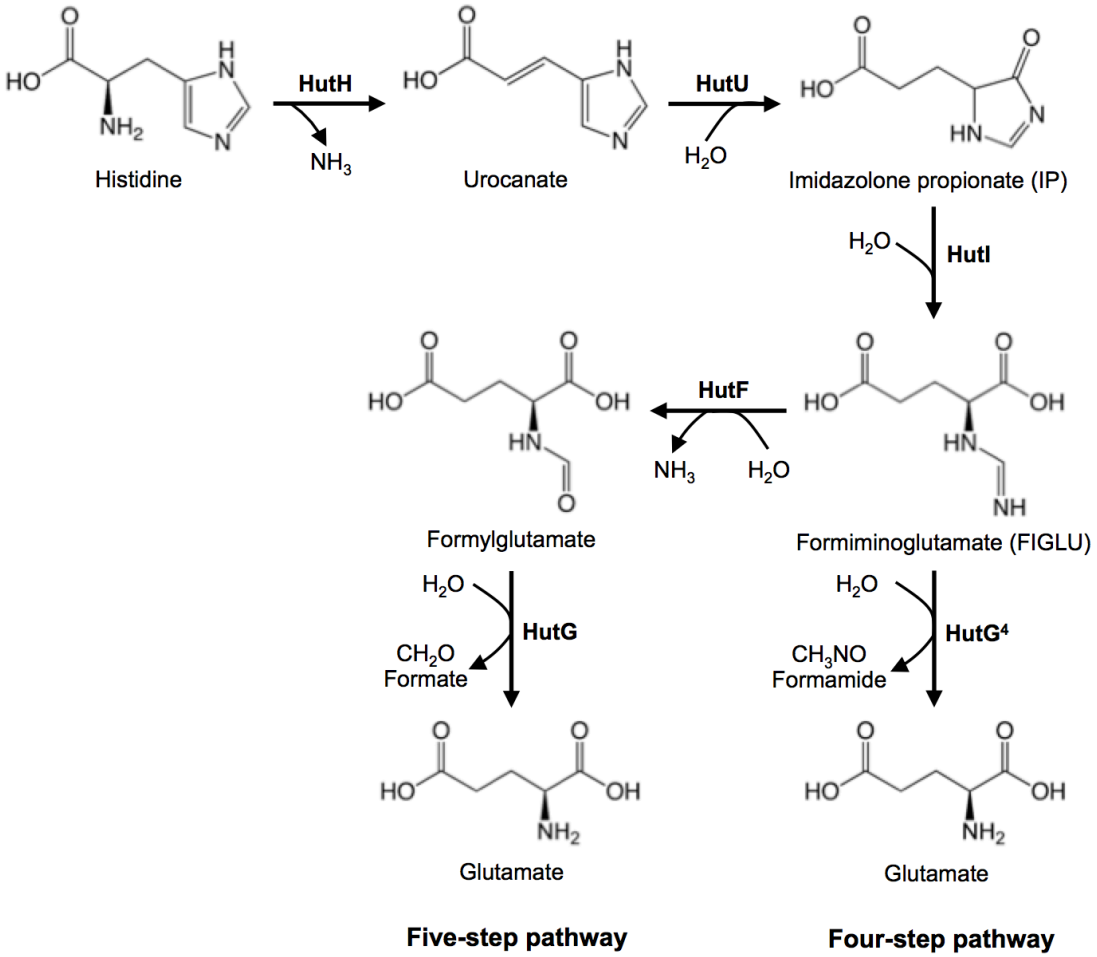

Figure 1.1. Histidine catabolic pathways in bacteria. The five-step pathway of histidine degradation is sequentially catalyzed by the following five enzymes: HutH, histidase; HutU, urocanase; HutI, imidazolone propionate hydrolase; HutF, formiminoglutamate iminohydrolase; HutG, formylglutamate amidohydrolase. The final step of the four-step pathway is catalyzed by formiminoglutamase (HutG^4).

1.2 Genes for histidine utilization and their expression

1.2.1 *Klebsiella pneumoniae*

Enteric bacterium *K. pneumoniae* has been a model organism for studying the Hut system, and the regulation of *hut* genes is best characterized for this organism. It possesses a *hut* locus with the order of genes *hutIG*^{4}*CUHT* (Figure 1.2). *hutIG*^{4}*UH* encode the enzymes for histidine degradation via the 4-step pathway. *hutT* encodes a putative urocanate transporter, and HutC is a transcriptional repressor of the *hut* genes (Boylan & Bender, 1984; Goldberg & Magasanik, 1975). The *hutUH* genes form an operon, which is transcribed from a promoter located between *hutC* and *hutU*

(Nieuwkoop & Bender, 1988; Nieuwkoop *et al.*, 1984). *hutT* is suggested to be one part of *hutUHT* operon based on its relative position to *hutUH* (Bender, 2012). *hutC* is transcribed independently, and HutG activity is also independent of the P_{hutI} promoter (Schwacha *et al.*, 1990). However, *hutIGC* can be co-transcribed as an operon (Schwacha & Bender, 1990). In the absence of histidine and urocanate, HutC represses the transcription of *hut* operons by binding to the operator site in the *hut* promoters, and the repression is relieved via molecular interaction between HutC and the effector, urocanate (Goldberg & Magasanik, 1975; Magasanik *et al.*, 1965). Urocanate is the direct inducer; the histidine-induced expression is achieved by intracellular conversion of histidine to urocanate (Schwacha & Bender, 1990). A 20-bp DNA sequence (ATGCTTGTATAGACAAGTAT) in the *hutU* promoter region was identified critical for HutC recognition according to a DNA deletion analysis (Osuna, Schwacha*, et al.*, 1994). The HutC-mediated negative control of *hut* genes is highly conserved among Gram-negative bacteria.

In *K. pneumoniae*, the positive regulation of *hut* genes is mediated by catabolite-activating protein (CAP) and nitrogen assimilation control protein (NAC). When histidine is used as a carbon source, transcription of the *hutU* operon is activated by CAP charged with cAMP (Prival & Magasanik, 1971). Accordingly, the *hutU* expression is subject to carbon catabolite repression (CCR) provoked by glucose (see details in Section 1.6.1). When histidine is utilized as a nitrogen source, the *hutU* transcription is activated by NAC, which is regulated by NtrBC in response to nitrogen limitation (Pomposiello *et al.*, 1998).

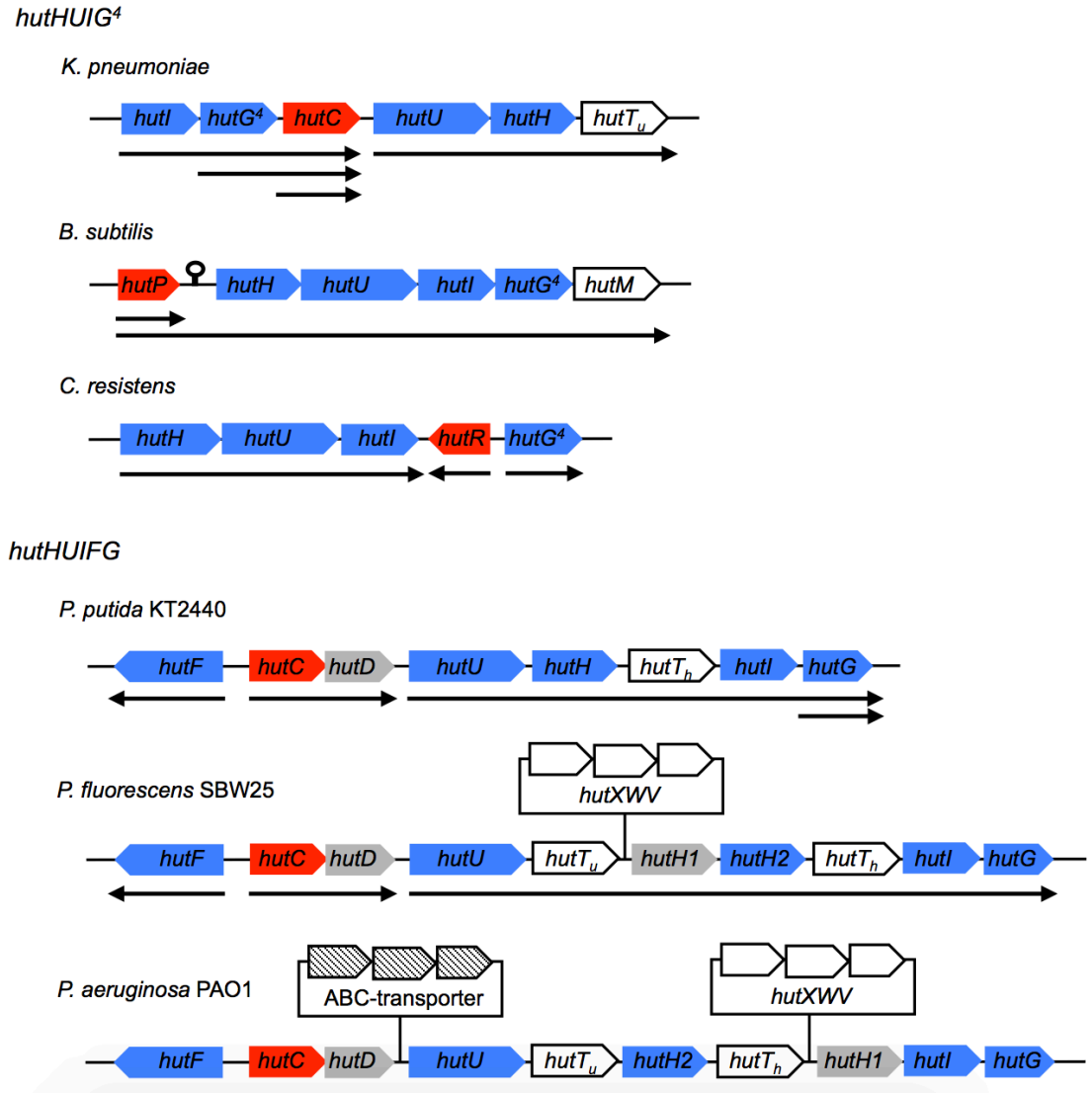

Figure 1.2. Genetic structure of the histidine utilization (*hut*) genes. Genes encoding regulatory proteins are shown in red. Enzymatic *hut* genes are marked in blue. Genes with no colour encode putative transporters for histidine or urocanate. The function of genes in grey is undetermined. The striped arrows denote genes presumed irrelevant to histidine utilization. A stem-loop structure between *hutP* and *hutH* of *Bacillus subtilis* is as indicated. Genes with the same name are homologous. Arrows under the genes indicate transcription units and directions.

1.2.2 *Bacillus subtilis*

The organization and induction of *hut* genes in the gram-positive bacterium *B. subtilis* are considerably different from those in gram-negative bacteria. The *hutPHUIC*^{4}*M* genes form a single operon in *B. subtilis* (Kimhi & Magasanik, 1970) (Figure 1.2). *hutM* encodes the histidine transporter (Yoshida *et al.*, 1995). *hutP* encodes a positive

regulator for the downstream *hut* genes, which mediates induction of the *hut* genes via an antitermination mechanism (Wray & Fisher, 1994). Transcription of the *hutPHUIC*[4] operon initiates upstream of *hutP* (Oda *et al.*, 1988), however, a stem-loop structure between *hutP* and *hutH* terminates the transcription (Figure 1.2). HutP acts at the stem-loop structure, allowing readthrough of the termination signal and consequent transcription of the downstream *hut* genes (Wray & Fisher, 1994). The effector molecule of HutP and also the inducer of *hut* genes is histidine instead of urocanate (Chasin & Magasanik, 1968). X-ray crystallography has revealed that a HutP hexamer binds histidine followed by a conformational change, and binds a Mg^{2+} leading to another conformational change. Then the HutP-histidine-Mg^{2+} complex interacts with the GC-rich stem-loop structure, destabilizing the structure and abolishing termination (Kumarevel *et al.*, 2005). Other divalent ions have also been found to support the histidine-induced antitermination of the *hut* operon such as Zn^{2+} (Dhakshnamoorthy *et al.*, 2013). Furthermore, in the presence of histidine, HutP also activates the *hut* promoter for about 5 folds, however, the underlying mechanism remains unknown (Oda *et al.*, 1992; Wray & Fisher, 1994).

Transcription of the *hut* genes in *B. subtilis* is negatively regulated by CcpA, a regulatory protein that blocks gene transcription by binding to a *cre* site (Shivers *et al.*, 2006). A putative *cre* site was identified in the coding region of *hutP*, which is likely responsible for the CcpA-mediated repression (Oda *et al.*, 1992). The CcpA protein is one of the key players in the glucose-induced carbon catabolite repression (CCR) (Wray *et al.*, 1994). The mechanism of CCR of histidine utilization in *B. subtilis* will be described in Section 1.6.2.

1.2.3 Pseudomonads

In *Pseudomonas* species, the organization of *hut* genes is conserved (Itoh *et al.*, 2007). The *hut* locus of *P. fluorescens* and *P. putida* have been well characterized (Figure 1.2). In *P. fluorescens* SBW25, the *hut* genes are organized in three transcriptional units, *hutF*, *hutCD* and *hutU-G* (Zhang & Rainey, 2007). The enzymes for histidine degradation are encoded by *hutH2*, *hutU*, *hutI*, *hutF* and *hutG* as presented above. Another copy of *hutH*-like gene *hutH1*, whose product exhibits 36% sequence identity with HutH from *P. putida*, is nonfunctional for histidine degradation (Zhang & Rainey,

2007). *hutT*$_h$ and *hutT*$_u$ encode specific transporters for histidine and urocanate, respectively. *hutXWV* encodes an ABC-type transporter playing a minor role in histidine uptake. HutC negatively regulates the three *hut* operons, including itself, and urocanate is the effector molecule to relieve the HutC-mediated repression (Hu *et al.*, 1989; Zhang & Rainey, 2007). In *P. putida*, HutC binds to an additional site preceding the *hutG* gene, which possesses an independent promoter. The *hutF*, *hutCD* and *hutUHIG* operons are induced by urocanate only, whereas either urocanate or formylglutamate is able to relieve the HutC-mediated repression of *hutG*. Moreover, formylglutamate does not interfere the induction of *hutF* and *hutUHIG* by urocanate, suggesting that HutC contains a binding site for formylglutamate, which is separate from that for binding urocanate (Hu *et al.*, 1989; Hu & Phillips, 1988).

A study on *P. putida* analyzed the HutC-binding site in the *hutU* promoter region, suggesting that a 16-bp dyad symmetry located near the transcription start site is recognized by HutC (Hu *et al.*, 1989). However, the assays for protein-DNA interaction were performed with crude cell lysates instead of purified HutC protein. Thus, the precise DNA sequence recognized by HutC has not been determined, and the mode of action of HutC interacting with DNA is unknown.

Most *Pseudomonas* species degrade histidine via a 5-step pathway. However, it has been recently found that some species, such as *P. alcaliphila*, *P. fulva* and *P. mendocina*, possess the formiminoglutamase (HutG^4) enzyme specific for the 4-step *hut* pathway. Interestingly, the two pathways co-exist in *P. aeruginosa*. The *hutRE* operon allows *P. aeruginosa* to degrade the intermediate formiminoglutamate (FIG) via the 4-step pathway. *hutE* encodes the formiminoglutamase for converting FIG to glutamate and formamide. HutR is a transcriptional activator for the *hutRE* expression with FIG as the inducer. The 4-step pathway is dispensable when the 5-step route is present and *vice versa*. However, the two pathways are not ecologically redundant as the 4-step route is advantageous when histidine is the sole carbon source (Gerth *et al.*, 2012).

The expression of *hut* genes is positively regulated by two two-component signal transduction systems CbrAB and NtrBC in response to the intracellular carbon and nitrogen status. In *P. fluorescens* SBW25, when histidine is the sole carbon source, CbrAB is required for transcription of the *hutU-G* operon, which is initiated by a σ^{54}-dependent promoter. When histidine is the sole nitrogen source, either CbrAB or the

nitrogen regulator NtrBC is required for the expression of *hutU-G* (Zhang & Rainey, 2008). Moreover, in *P. aeruginosa*, histidase activity was abolished in the *cbrAB* mutants growing on histidine (Nishijyo *et al.*, 2001). However, it is still a question whether the regulation of *hut* genes by CbrB and NtrC is direct or indirect.

1.2.4 *Corynebacterium resistens*

A novel mode of *hut* regulation has been observed in a human pathogen *Corynebacterium resistens* DSM 45100, a gram-positive bacterium, instead of the HutP-mediated antitermination in *B. subtilis* (Schroder *et al.*, 2012). A transcriptional regulator of the IclR superfamily, named $HutR^C$, was identified in the *hut* locus of *C. resistens* DSM 45100, which comprises three transcription units: *hutHUI*, $hutR^C$, and $hutC^4$ (Figure 1.2). $HutR^C$ binds to the promoter region of *hutH* and the intergenic region between $hutR^C$ and $hutC^4$ *in vitro* by recognizing a 14-bp motif TCTGwwATwCCAGA. The $HutR^C$ regulator might function as an activator given that the deduced $HutR^C$-binding site is located upstream of the -35 promoter region. The molecular interactions between $HutR^C$ and the *hut* promoter DNAs are not abolished by histidine or urocanate *in vitro*.

1.3 The transcriptional regulator HutC

1.3.1 The HutC domain structure

HutC protein belongs to the GntR/HutC protein family of transcriptional regulators. Members of this family are present widely in bacteria and participate in various biological processes (Suvorova *et al.*, 2015). The GntR family is one of the largest prokaryotic transcription factor families and is named after the gluconate operon repressor from *B. subtilis* (Rigali et al., 2002). Transcriptional regulators from the GntR family are typically comprised of a N-terminal DNA-binding domain and a C-terminal effector-binding and oligomerization (E-O) domain (Suvorova *et al.*, 2015). The DNA-binding domain is formed by the winged helix-turn-helix (wHTH) motif, which is a common feature of the GntR family (Resch *et al.*, 2010). wHTH motif is a subfamily of the helix-turn-helix (HTH) motif and contains a third α-helix and a contiguous

antiparallel β-sheet that forms the 'wing' (Aravind *et al.*, 2005). The C-terminal E-O domain of GntR family is highly diverse, which is used to categorize the subfamilies: FadR, HutC, MocR, YtrA, PlmA and AraR (Suvorova *et al.*, 2015).

HutC is the second largest subfamily, which comprises about 30% of the GntR transcription factors (Rigali *et al.*, 2002). It was named after the member HutC from *P. putida* (Allison & Phillips, 1990). The E-O domain of HutC subfamily is a UTRA (UbiC transcription regulator-associated) domain as it shares the same fold with the catalytic domain of chorismate lyase (*ubiC* gene product of *Escherichia coli*) (Aravind & Anantharaman, 2003).

HutC works as a typical one-component signal transduction system comprising a sensor input domain and a functional output domain. Signal transduction in prokaryotes is dominated by such systems (Ulrich *et al.*, 2005). It is proposed that the C-terminal E-O domain allows HutC to specifically recognize the effector molecule, urocanate, and the effector-binding E-O domain modulates affinity of the DNA-binding domain to DNA via an allosteric mechanism, thereby resulting in dissociation of HutC from the operator sites (Resch *et al.*, 2010). Though HutC has long been known as the representative of this subfamily, the crystal structure of full-length HutC is not available and little is known about the mode of HutC action.

1.3.2 The role of HutC in global gene regulation

There has been growing evidence in literature show that HutC plays a significant role in global gene regulation beyond histidine catabolism. These include cell motility, biofilm formation and the production of many virulence factors. The HutC-mediated global regulation is better studied in a zoonotic pathogen *Brucella abortus*. In that organism, HutC acts as a coactivator for transcription of the *virB* operon, which encodes a type IV secretion system (T4SS). The T4SS of *B. abortus* is a multicomponent protein machinery involved in the translocation of virulence effector molecules in host cells (Sieira *et al.*, 2010). HutC activates expression of the *virB* operon by directly binding to its promoter. The binding affinity of HutC to the *virB* promoter is 30 times lower than that to the *hut* promoter, and much lower concentration of urocanate is required to abolish HutC binding to the *virB* promoter. The difference in binding

affinity is crucial for HutC to coordinate between cellular metabolism and virulence during the process of host colonization. Moreover, a newly identified regulator MdrA (MarR-like sodium deoxycholate-responsive activator) also activates the *virB* promoter. MdrA is a MarR-family transcriptional regulator and shares 44% similarity with the MarR protein of *E. coli*. The target DNA sequences of MdrA and HutC overlap (Figure 1.3), and these two regulators activate the *virB* expression to similar extents, they are thus functionally redundant (Sieira *et al.*, 2012). Additionally, HutC is also involved in the regulation of bacterial attachment to host cell surface. This is achieved by direct activation of *btaE* gene, encoding a trimeric autotransporter adhesin required for attachment to the host extracellular matrix (Sieira *et al.*, 2017). Unlike the *virB* promoter, HutC and MdrA act in concert for the control of *btaE* promoter activity and the attachment of *B. abortus* to HeLa cells (Figure 1.3).

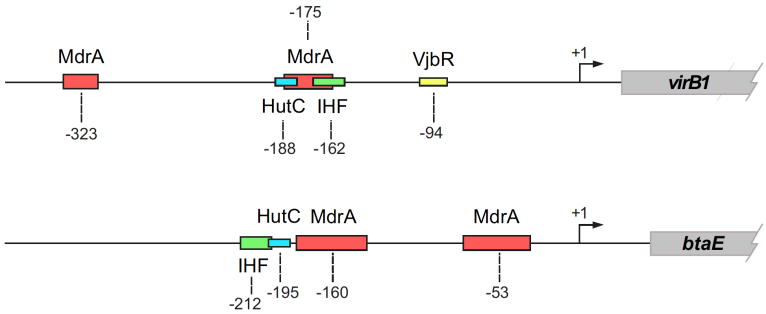

Figure 1.3. The promoter region of *virB* and *btaE* in *Brucella abortus* showing operator sites for HutC and MdrA regulators. Footprints of the regulators on DNA are indicated as boxes, with their relative positions to the transcription start site (+1). (Figure from Sieira *et al.*, 2017)

Yersinia pseudotuberculosis is an enteric food-borne pathogen of human and animals (Achtman *et al.*, 1999). A recent study by Joshua *et al.* (2015) showed that the *hutC* deletion mutant of *Y. pseudotuberculosis* was abolished in biofilm formation during colonization on *Caenorhabditis elegans*, while its swimming motility was enhanced. HutC is involved in the expression of *flhDC* encoding a master regulator controlling expression of the flagella genes at the top of the regulatory hierarchy (S. Atkinson *et al.*, 2008). Mutations in *flhDC* attenuate the biofilm formation of *Y. pseudotuberculosis*. Moreover, FlhDC is also involved in the regulation of a wide variety of metabolic, regulatory, transport and virulence genes on the basis of a transcriptomic analysis. The expression of *flhDC* was 5-fold higher in the *hutC* mutant compared with the wild-type strain after growth for 12 hours (Joshua *et al.*, 2015).

P. aeruginosa is a human opportunistic pathogen that is a common cause of hospital-acquired infections. An early study by Rietsch *et al.* (2004) suggested a link between *hut* catabolism and expression of the type III secretion genes. A transposon insertion mutant of *P. aeruginosa* PAO1 was defective in the ability to intoxicate eukaryotic cells in a type III effector-dependent manner. The insertion was located in the *hut* locus, resulting in overexpression of the *hut* genes. The defect in cytotoxicity depends on the presence of histidine and is likely caused by excessive uptake and catabolism of histidine. A separate study on *P. aeruginosa* PA14, conducting transposon mutagenesis for genes involved in swarming motility, identified HutC as a potential regulator. The Δ*hutC* mutant displayed a marked defect in swarming motility (0.09±0.07 fold change compared to wild type) and reduced swimming motility (0.50±0.04 fold change compared to wild type), but exhibits an increased ability to form biofilm (Yeung *et al.*, 2009). Additionally, a transcriptomic analysis of *P. aeruginosa* PAO1 showed that the expression of *hutC*, *hutH*, *hutU* and *hutTu* was significantly downregulated during biofilm formation compared with the planktonic stationary-phase cell sample, suggesting a regulatory link between histidine catabolism and biofilm formation (Patell *et al.*, 2010).

A recent study on plant pathogen *Xanthomonas oryzae pv. oryzae* found that the *hut* genes, including *hutC*, play an important role in the regulation of resistance to bismerthiazol, a bactericide used for controlling bacterial rice leaf blight (Liang *et al.*, 2018). Expression of both *hutC* and the enzymatic *hut* genes were significantly reduced by bismerthiazol treatment based on RNA-sequencing analysis. The Δ*hutG* and Δ*hutU* mutants were hypermotile, produced less biofilm and displayed reduced virulence compared with the wild type, indicating that the *hut* pathway contributes to bacterial virulence. Overexpression of *hutGU* reduced the effect of bismerthiazol treatment. Thus, bismerthiazol reduces the bacterial virulence by inhibiting the expression of *hut* genes.

In a previous work in this lab with *P. fluorescens* SBW25, it has been shown that HutC plays an important role in bacterial colonization on plants (Zhang & Rainey, 2007). Specifically, deletion of *hutC* caused a significant reduction in competitive ability to colonize the surfaces of sugar beet plants. The Δ*hutC* mutant displayed a fitness of −2.28 ± 0.30 and −1.9 ± 0.39 [selection rate constant (Lenski, 1991)] relative to the wild type in the shoot and rhizosphere, respectively (of note, fitness zero indicates that

the mutant and wild type are equally fit, while a negative or positive value indicates reduction or increase in fitness relative to wild type). In contrast, the effects of *hutC* deletion on bacterial fitness was very minor in laboratory medium with or without histidine. In addition, histidine was estimated to be at a very low concentration of 3.87 μM on the surface of sugar beet plants (Zhang & Rainey, 2006). Thus, the severe fitness reduction of Δ*hutC in planta* cannot be explained by its effect on *hut* expression alone.

On the basis of evidence described above, Zhang *et al*. (2013) proposed a new hypothesis that urocanate accumulated on certain tissues, such as skin, acts as a host-specific signaling molecule that elicits infection via interactions with the bacterial regulatory protein HutC. Urocanate is not commonly present in non-host environments such as soil and water (Gibbs *et al.*, 2008). As a host-derived nutrient, urocanate potentially acts as a cue activating expression of virulence factors of pathogenic bacteria. For example, production of virulence factor (alkaline protease) by *Vibrio alginolyticus* is stimulated by urocanate (Bowden *et al.*, 1982). In *Brucella abortus*, urocanate induces expression of VjbR at the post-transcriptional level. VjbR is a quorum-sensing regulator controlling expression of many genes, including virulence determinants (Arocena *et al.*, 2012). HutC, as the urocanate receptor, plays a significant role in regulating the production of virulence factors and promotes bacterial infection.

Together, evidence available to date strongly indicate the significance of HutC in global gene regulation and the ecological success of bacteria in natural environment. However, the mechanisms underlying the HutC-mediated regulation in some cellular processes have not been fully unveiled, and no systematic analysis of HutC-regulated candidate genes is available.

1.4 Maintenance of carbon/nitrogen metabolic balance in bacteria

Bacteria utilize multiple external nutrients to produce biomass and proliferate. Nutrients in the natural environment are usually present in changing availability and abundance. A coordinated way to uptake and catabolize various nutrients is thus necessitated for bacterial survival and growth. Carbon and nitrogen are two of the most important building blocks of all living organisms. Metabolism of carbon and nitrogen must be tightly coupled. For that, bacteria have evolved signalling mechanisms to sense

C/N status and control C/N metabolic balance (Zhang *et al.*, 2018). Carbon metabolism is under the control of carbon-derived signals and also subject to the availability of nitrogen nutrient. Similarly, nitrogen metabolism in bacteria is also regulated by the condition of carbon sources in addition to its cognate metabolic signals (Commichau *et al.*, 2006).

1.4.1 PII signalling system for nitrogen regulation

Regulation of cellular nitrogen metabolism is best understood in enteric bacteria (Merrick & Edwards, 1995). As shown in Figure 1.4, the current model indicates the central role of the NtrBC two-component signal transduction system, whose activity is control by the PII protein in response to changes of intracellular C/N ratio (specifically, the relative abundance of α-ketoglutarate and glutamine) (Arcondeguy *et al.*, 2001).

PII proteins are signal transduction proteins controlling expression of many genes involved in nitrogen metabolism. *E. coli* possesses two PII paralogues, GlnB and GlnK, whose activity is modulated via uridylylation by the bifunctional uridylyltransferase/uridylylremovase enzyme (UR/UTase), the *glnD* product (Forchhammer, 2004). Under nitrogen-poor conditions, intracellular glutamine level declines relative to α-ketoglutarate (Chubukov *et al.*, 2014). GlnD catalyzes uridylylation of the PII protein, then the uridylylated PII protein activates the two-component system NtrBC (Forchhammer, 2004). NtrBC is a master regulator for the expression of numerous nitrogen-regulated genes. NtrB possesses both kinase and phosphatase activities (Pioszak & Ninfa, 2004). In the conditions of nitrogen limitation, the uridylylated PII protein inhibits the phosphatase activity of NtrB, and the response regulator NtrC is thus phosphorylated by the NtrB kinase activity (Forchhammer, 2004). The phosphorylated NtrC then activates the expression of genes in a σ^{54}-dependent manner, including *nac* (encoding the nitrogen assimilation control protein, NAC), *glnA* (encoding glutamine synthetase, GS) and *amtB* (encoding high affinity ammonium transporter AmtB) (Hervas *et al.*, 2008).

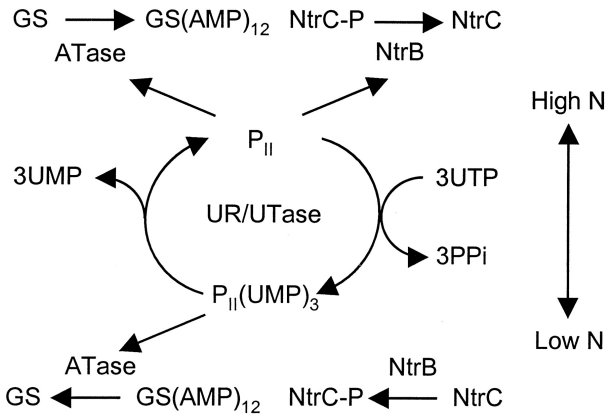

Figure 1.4. Nitrogen regulation (Ntr) system of enteric bacteria. The activities of NtrC and GlnE (ATase) are controlled by the PII protein in response to the intracellular carbon/nitrogen status. GlnE catalyzes the adenylylation and deadenylylation of GS. (Figure from Arcondeguy *et al.*, 2001)

In addition to NtrBC, GlnE is also a receptor of PII regulation, which is a bifunctional enzyme that modulates the activity of GS by adenylylation/deadenylylation. The non-modified PII activates the adenylyltransferase activity of GlnE, while the uridylylated PII stimulates its adenylylremovase activity. Accordingly, in the nitrogen-limited conditions, GS is activated via deadenylylation by GlnE, which is mediated by the uridylylated PII protein (Maheswaran & Forchhammer, 2003) (Figure 1.4). The number of identified PII targets has been increasing and the study on that is not yet complete (Huergo *et al.*, 2013).

In addition to uridylylation/deuridylylation, PII protein is also modulated by molecular interaction with the effector molecule α-ketoglutarate (Jiang *et al.*, 1998). Three binding sites for α-ketoglutarate were identified in the trimeric PII protein. When α-ketoglutarate is present at high concentrations, the binding sites on PII are fully occupied, which impairs the phosphatase activity of NtrB due to lack of the non-modified PII, thereby activating NtrC.

PII homologues are widely present in bacteria, archaea and also plants (Ninfa & Jiang, 2005). In *Pseudomonas*, the mechanism of PII regulation is also valid, which is evidenced by the presence of all the major components of PII signalling system (Itoh et al., 2007). But in some bacteria, the modification of PII is not achieved by uridylylation. In the Gram-positive actinomycetes, the PII protein is modified via adenylylation at Tyr51 (Hesketh *et al.*, 2002). Moreover, in cyanobacteria, PII is

regulated by phosphorylation at a seryl residue responding to the intracellular α-ketoglutarate level (Fadi Aldehni *et al.*, 2003).

1.4.2 The role of PTS in maintaining C/N balance in enteric bacteria

In many bacteria, some sugars are phosphorylated and transported through the phosphoenolpyruvate:carbohydrate phosphotransferase system (PTS). The basic components of PTS are similar in all the bacteria studied (Huergo & Dixon, 2015), including two general proteins enzyme I (EI) and histidine protein (HPr), and a set of sugars-specific multidomain permeases (EII) for sugar uptake (Postma & Lengeler, 1985). EII typically consists of an integral membrane domain and a cytoplasmic domain, which can be formed by either fused or separated proteins. For instance, the glucose-specific EII of *E. coli* is composed of the cytosolic component $EIIA^{Glc}$ and the integral membrane component $EIIBC^{Glc}$ (Huergo & Dixon, 2015). Phosphoenolpyruvate (PEP) is the phosphoryl donor for PTS. The transfer of phosphate group starts from PEP through EI and HPr to EII allowing uptake and phosphorylation of sugars (Postma *et al.*, 1993) (Figure 1.5).

The sugar PTS was found to be involved in a regulatory linkage of carbon and nitrogen metabolism. In *E. coli*, α-ketoglutarate, which accumulates in conditions of nitrogen limitation, inhibits the EI activity of the glucose-specific PTS, and thus directly blocks glucose uptake *in vivo*. This inhibition enables rapid modulation of glycolytic flux without perturbing glycolytic intermediates. A quantitative modeling confirms that the regulation of EI by α-ketoglutarate is, in principle, sufficient to match glucose consumption to cellular nitrogen conditions to balance the carbon and nitrogen metabolism (Doucette *et al.*, 2011).

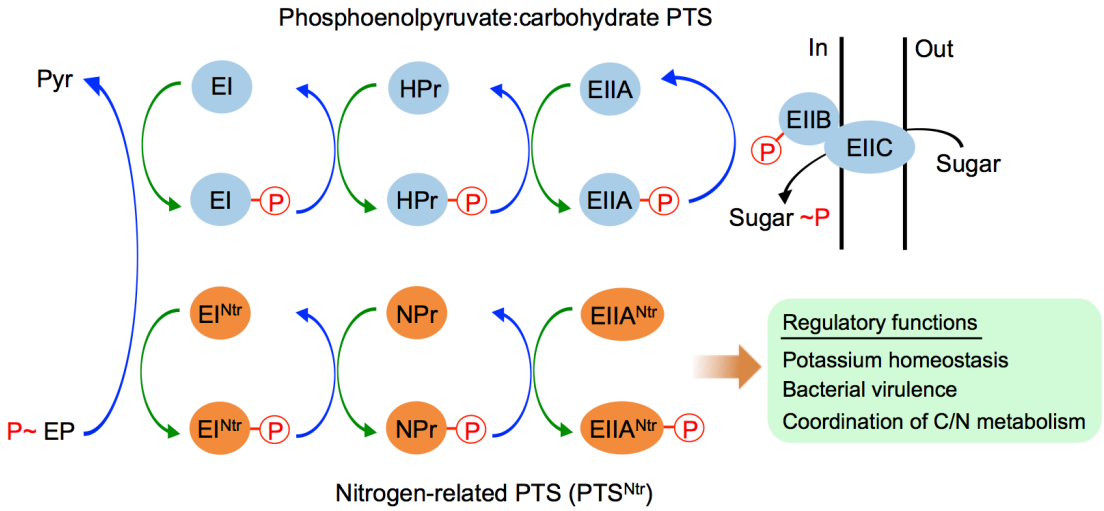

Figure 1.5. Phosphotransferase systems in bacteria.
The sugar PTS (phosphoenolpyruvate:carbohydrate PTS) is present in a wide range of bacteria and dedicated to carbohydrate uptake. It is basically composed of two general proteins EI and HPr and a set of sugars-specific permeases EII. EII proteins are commonly composed of a cytoplasmic domain (EIIA) and an integral membrane domain (EIIBC), which can be formed by either fused or separated proteins. Phosphoenolpyruvate (PEP) is the phosphoryl donor for PTS. The phosphate group of PEP is transferred through EI and HPr to EII, which couples phosphorylation and uptake of a specific sugar. PTS^{Ntr} is present in most proteobacteria, it is unrelated to sugar transport, but exerts regulatory functions. PTS^{Ntr} comprises EI^{Ntr}, NPr and $EIIA^{Ntr}$, which are paralogs of the sugar PTS. The required domains for transport are lacking in the EII^{Ntr} component. EI^{Ntr} acquires phosphate group from PEP and then catalyzes phosphorylation of NPr and subsequently $EIIA^{Ntr}$. No specific substrate phosphorylated by $EIIA^{Ntr}$ has been demonstrated. The sugar PTS and PTS^{Ntr} are functionally independent, but cross talk to each other under certain conditions through phosphate group transfer.

1.4.3 PTS^{Ntr} plays a central regulatory role in coordination of C/N metabolism in enteric bacteria

Apart from the canonical sugar PTS, most proteobacteria possess a so-called nitrogen-related PTS (PTS^{Ntr}), which is unrelated to carbohydrate transport, but exerts regulatory functions in a post-translational fashion (Chavarria *et al.*, 2012). PTS^{Ntr} comprises EI^{Ntr} (encoded by *ptsP*), NPr (encoded by *ptsO*) and $EIIA^{Ntr}$ (encoded by *ptsN*), which are paralogs of the sugar PTS (Reitzer, 2003) (Figure 1.5). *ptsO* and *ptsN* are located adjacent to the *rpoN* gene, which encodes the alternative sigma factor σ^{54} required for transcription of some genes related to nitrogen assimilation. This organization of *pts* genes is conserved in proteobacteria (Deutscher *et al.*, 2006). Accordingly, PTS^{Ntr} was originally thought to be involved in regulation of nitrogen metabolism. The EI^{Ntr} acquires phosphate group from PEP and passes it through NPr to $EIIA^{Ntr}$ (Pfluger-Grau &

Gorke, 2010). The domains required for transport are lacking in the EII component, and no specific substrate phosphorylated by PTS^{Ntr} has been demonstrated (Lee *et al.*, 2013).

Increasing evidence indicate that PTS^{Ntr} is a major player in the coordination of carbon and nitrogen metabolism. A study on *E. coli* showed that a *ptsN* insertion mutant failed to grow on several sugars and TCA cycle intermediates as the carbon source when providing an amino acid or nucleoside base as the nitrogen source. However, this growth defect was relieved by supplying ammonium salts (Powell *et al.*, 1995).

EI^{Ntr} carries a GAF signalling domain at its N-terminus, which is also a feature in the NifA family of bacterial transcription regulators (Reizer *et al.*, 1996). The GAF signalling domain is involved in sensing cellular nitrogen status and has been known to bind α-ketoglutarate (Martinez-Argudo *et al.*, 2004). A study on *E. coli* demonstrated that two signal molecules, glutamine and a-ketoglutarate, reciprocally regulate phosphorylation of the PTS^{Ntr} by directly modulating the EI^{Ntr} autophosphorylation, and the GAF domain of EI^{Ntr} is required for such regulation (Lee *et al.*, 2013). This finding reinforces the notion that PTS^{Ntr} plays a regulatory role in linking carbon and nitrogen metabolism.

In non-enteric bacteria *Azotobacter vinelandii* and *P. putida*, PTS^{Ntr} regulates polyhydroxyalkanoates (PHAs) accumulation (Noguez *et al.*, 2008; Velazquez *et al.*, 2007). PHAs accumulation significantly reduced with the loss of EI^{Ntr} and NPr, but increased in a mutant devoid of $EIIA^{Ntr}$. As carbon storage compounds, PHAs are usually accumulated under conditions of carbon overflow and nitrogen limitation (Pfluger-Grau & Gorke, 2010).

Notably, sugar PTS and PTS^{Ntr} cross talk to each other through phosphate group transfer. *P. putida* possesses a sugar PTS devoted exclusively to fructose uptake, PTS^{Fru}, and a PTS^{Ntr}. Glucose transport in *P. putida* is not through PTS (Chavarria *et al.*, 2012). The polyprotein EI-HPr-EIIA of PTS^{Fru} (the product of *fruB* gene) can phosphorylate $EIIA^{Ntr}$ both *in vitro* and *in vivo* when cells are grown on fructose (Pfluger & de Lorenzo, 2008). Additionally, FruB and EI^{Ntr} transfer phosphate group to $EIIA^{Ntr}$ equally well (Chavarria *et al.*, 2013). Similar results have also been observed in *E. coli*, both the energy coupling phosphotransferases EI^{Ntr}-NPr and EI-HPr contribute to the phosphorylation of $EIIA^{Ntr}$ (Zimmer *et al.*, 2008).

Additionally, PTS^{Ntr} is involved in regulation of diverse cellular processes. It plays a significant role in potassium homeostasis in *E. coli* by regulating potassium uptake in a concentration-dependent manner. At high K^+ concentrations, $EIIA^{Ntr}$ inhibits K^+ uptake by binding to the low affinity K^+ transporter TrkA to avoid overaccumulation of intracellular K^+ (Lee *et al.*, 2007). At low K^+ concentrations, $EIIA^{Ntr}$ promotes K^+ uptake by stimulating the potassium sensor KdpD kinase activity, which is required for synthesis of the high affinity K^+ transporter KdpFABC (Luttmann *et al.*, 2009). Furthermore, PTS^{Ntr} is involved in controlling production of virulence factors in some pathogen bacteria. In *P. aeruginosa*, EI^{Ntr} negatively regulates pyocyanin production by enhancing the transcription of QscR (quorum sensing control repressor), which represses the quorum-sensing LasR-LasI and RhlR-RhlI systems involved in pyocyanin production (Xu *et al.*, 2005). A recent study by Cabeen *et al.* (2016) found that biofilm formation of *P. aeruginosa* is hindered in the absence of PTS^{Ntr}-mediated phosphotransfer but in the presence of $EIIA^{Ntr}$, indicating that unphosphorylated $EIIA^{Ntr}$ negatively regulates biofilm formation.

1.4.4 Coordination between carbon and nitrogen metabolisms in *Pseudomonas*

Signal transduction in bacteria is predominantly mediated by two-component systems (TCS) consisting of a sensor histidine kinase (HK) and a cognate response regulator (RR). HK possesses a signal input domain sensing external signals and a histidine kinase domain responding to the signal by autophosphorylating at a conserved histidine residue. The phosphorylated HK transfers the phosphoryl to RR harboring a receiver domain and a regulatory output domain. RRs are usually DNA-binding transcriptional regulators. The phosphorylated RR then activates expression of the target genes (Groisman, 2016; Zschiedrich *et al.*, 2016).

Recent progress in *Pseudomonas* suggests that cellular C/N metabolic balance is maintained by the interplays between two two-component systems (Figure 1.6). Like in enteric bacterial, the cellular nitrogen metabolism of *Pseudomonas* is regulated by the NtrBC system with assistance of the PII protein. However, the CbrAB system is placed at the top of the regulatory hierarchy for cellular carbon metabolism. *Pseudomonas* species use succinate (and other intermediates of TCA cycle) as the most preferred carbon source (Rojo, 2010). Thus, the glucose-dependent regulatory circuits such as

the PTS systems found in enteric bacteria play little or no role in the central carbon metabolism in *Pseudomonas*. As shown in Figure 1.6, in the CbrAB regulatory system, CbrA is the sensor kinase with a transmembrane domain at its N-terminal and a cytoplasmic domain of histidine kinase activity at the C-terminal. Under conditions of carbon limitation (absence of a preferred carbon source), CbrA autophosphorylates with ATP and transfers the phosphate group to CbrB, the response regulator. Then the phosphorylated CbrB activates genes transcribed from a σ^{54}-dependent promoter (Amador *et al.*, 2010; Itoh *et al.*, 2007). However, the signal that controls the CbrA sensor is still unknown. A preferred carbon source (carbon-replete condition) might inhibit any step(s) of CbrB phosphorylation or promote CbrB dephosphorylation, thus reducing the CbrB activity (Itoh *et al.*, 2007). Under conditions of nitrogen limitation (intracellular glutamine level declines relative to α-ketoglutarate), like in enteric bacteria, GlnD (UR/UTase) catalyzes uridylylation of the PII protein, followed by activation of the NtrBC system by the uridylylated PII. The phosphorylated NtrC then transcriptionally activates genes for nitrogen metabolism in a σ^{54}-dependent manner (Arcondeguy *et al.*, 2001; Huergo *et al.*, 2013).

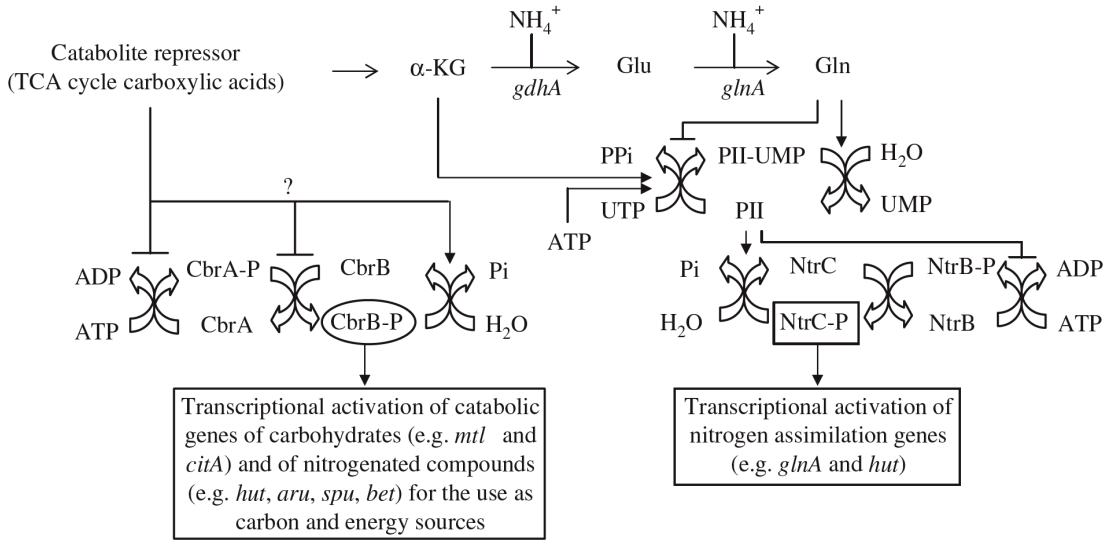

Figure 1.6. Regulatory circuits of the CbrAB and NtrBC two-component regulatory systems. Under conditions of carbon limitation, CbrA autophosphorylates with ATP and transfers the phosphate group to CbrB, which activates transcription of genes for catabolism of carbohydrates and nitrogenated compounds. Under nitrogen-limited (or carbon excess) conditions, uridylylation of the PII protein is catalyzed by GlnD (UR/UTase). The uridylylated PII inhibits the phosphatase activity of NtrB, resulting in phosphorylation of NtrC by the NtrB kinase activity. The phosphorylated NtrC then transcriptionally activates genes for nitrogen metabolism. The ammonia assimilation pathway is catalyzed by glutamine synthetase (*glnA* product) and glutamate dehydrogenase (*gdhA* product). α-KG, α-ketoglutarate; Glu, glutamate; Gln, glutamine. (Figure from Itoh *et al.*, 2007)

The CbrAB system was first identified in *P. aeruginosa* PAO1 and is exclusive of Pseudomonadaceae. It is required for utilization of many amino acids, sugars, polyamines and organic acids as carbon (and nitrogen) source (Barroso *et al.*, 2018; Itoh *et al.*, 2007). In *P. aeruginosa*, deletion of *cbrAB* abolished the utilization of a variety of organic compounds as the sole carbon source (Li & Lu, 2007). A *cbrB* mutant of *P. putida* was unable to grow on ornithine or tyrosine as the carbon source or carbon + nitrogen source. This *cbrB* mutant also showed reduced growth on histidine, proline, arginine and glutamate as the carbon source or carbon + nitrogen source (Amador *et al.*, 2010). Moreover, a Biolog phenotypic microarray analysis of *P. fluorescens* SBW25 growing on 190 carbon and 95 nitrogen substrates showed that deletion of *cbrB* abolished the growth on 20 carbon sources, and the *ntrC* mutant was unable to grow on 28 nitrogen substrates. Additionally, the mutant devoid of both *cbrB* and *ntrC* failed to utilize further 14 nitrogen sources, including histidine, proline, leucine, isoleucine and valine (Zhang & Rainey, 2008).

The CbrAB system works coordinately with NtrBC to maintain the C/N metabolic balance. A study on *P. aeruginosa* selected suppressors of the *cbrAB* mutant from minimal medium with arginine as the sole source of carbon and nitrogen (Li & Lu, 2007). The *cbrAB* mutant was unable to grow on this medium, while the suppressor mutants that restored the growth contain mutations mapped to *ntrB*. The mutations reduced the phosphatase activity of NtrB, which makes the Ntr system constitutively active. Thus, these two regulatory systems interrelate functionally. The dual involvement of CbrAB and NtrBC was also observed in the expression of histidine catabolic genes in *P. fluorescens* (Zhang & Rainey, 2008). When histidine is the sole carbon source, CbrB is required for transcription of the *hut* genes. When histidine is used as the sole nitrogen source, either CbrB or NtrC is required. Furthermore, the utilization of proline in *P. aeruginosa* is subject to dual control by CbrAB and NtrBC. Deletion of *cbrB* or *ntrC* had moderate or no effect on the growth on proline as the carbon or nitrogen source, whereas double deletion of *cbrB* and *ntrC* clearly impaired the growth (Amador *et al.*, 2010).

1.5 Carbon catabolite repression (CCR) in bacteria

Most heterotrophic bacteria preferentially utilize certain carbon sources over others in a nutrient-complex environment. Presence of preferred carbon sources represses the expression of catabolic genes of alternative carbon sources. This process is known as carbon catabolite repression (CCR) (Romero-Rodriguez *et al.*, 2018). CCR is important for bacterial competition in natural environments as it allows bacteria to acclimate rapidly to preferred carbon and energy sources, thereby maximizing growth rate (Liu *et al.*, 2017; Rojo, 2010). The classic example of CCR comes from *E. coli*, which preferentially utilizes glucose over lactose when both are present in the medium (Liu *et al.*, 2017). CCR is a fundamental regulatory phenomenon, with as many as 5-10% of bacterial genes are subject to CCR control (Gorke & Stulke, 2008). The molecular mechanisms driving CCR are very different among bacterial species. The molecular basis and main factors involved in CCR have been extensively studied in enteric bacterium *E. coli*, Gram-positive bacterium *Bacillus subtilis* and *Pseudomonas*.

1.5.1 Mechanisms of CCR in enteric bacteria

Glucose is the preferred carbon source for *E. coli*. It is transported into cells and phosphorylated through a phosphotransferase system (PTS) (Postma *et al.*, 1993). As mentioned above, the PTS system consists of two general proteins, enzyme I (EI) and histidine protein (HPr), and sugar-specific permease (EII) (Postma & Lengeler, 1985). In *E. coli*, the glucose-specific EII is composed of the cytosolic component $EIIA^{Glc}$ and the membrane-bound component $EIIBC^{Glc}$. The phosphoryl group is transferred from phosphoenolpyruvate (PEP) to glucose via EI, HPr, $EIIA^{Glc}$ and finally $EIIBC^{Glc}$ (Postma *et al.*, 1993). CCR is achieved by modulating the phosphorylation state of $EIIA^{Glc}$ through two different regulatory mechanisms (Bruckner & Titgemeyer, 2002; Gorke & Stulke, 2008; Rojo, 2010) (Figure 1.7). First, when glucose is transported and phosphorylated to glucose-6-phosphate, $EIIA^{Glc}$ is predominantly dephosphorylated due to the transfer of phosphate group to glucose. The nonphosphorylated $EIIA^{Glc}$ interacts with the transporters for non-PTS sugars, thereby inhibiting these sugars from entering into the cell. Consequently, the corresponding catabolic genes are poorly expressed due to the lack of inducer. This regulatory mechanism was termed 'inducer exclusion'. On the other hand, the nonphosphorylated $EIIA^{Glc}$ impedes transcription of the catabolic genes

for non-PTS sugars by reducing the cAMP-CAP complex formation. The activity of adenylate cyclase (AC) required for production of cAMP depends on the phosphorylation of EIIA^{Glc}. In the conditions with glucose being assimilated, the cAMP level is low because of the nonphosphorylated EIIA^{Glc}. Thus, CAP is present in a monomeric state instead of the cAMP-CAP complex. It is unable to activate the target genes for assimilation of the non-PTS sugars, such as lactose, glycerol and maltose.

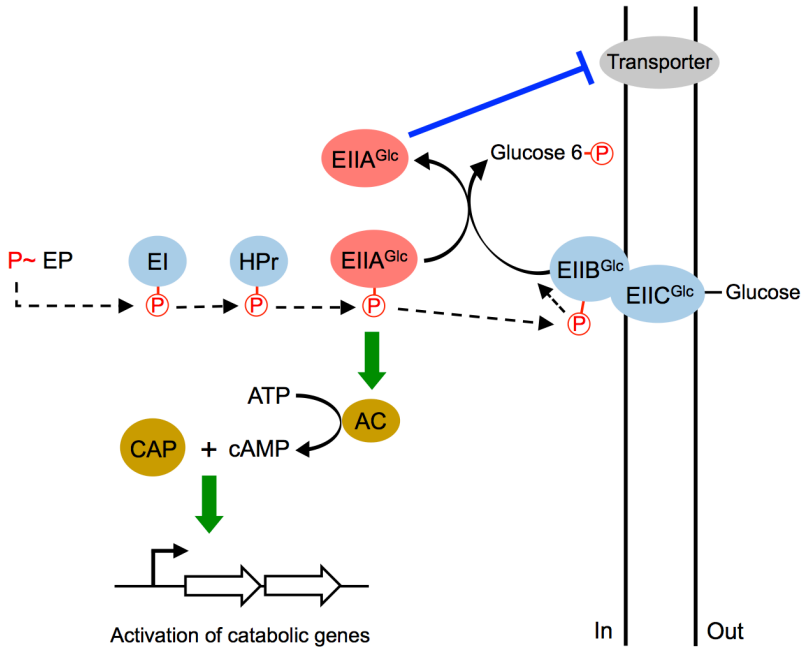

Figure 1.7. Carbon catabolite repression in *E. coli*. Phosphorylation state of EIIA^{Glc} primarily mediates CCR by two different regulatory mechanisms. In the presence of glucose, the phosphate group of phosphoenolpyruvate (PEP) is ultimately transferred to glucose, resulting in dephosphorylation of EIIA^{Glc}. The nonphosphorylated EIIA^{Glc} binds and inactivates the transporters for non-preferred carbon sources, thereby inhibiting their entry into the cell (inducer exclusion). Meanwhile, the nonphosphorylated EIIA^{Glc} impedes transcription of the genes for catabolism of non-preferred sugars, whose activation requires the CAP-cAMP complex. The activity of adenylate cyclase (AC) for producing cAMP depends on the phosphorylated EIIA^{Glc}.

1.5.2 Mechanisms of CCR in *Bacillus subtilis*

In *B. subtilis* and other related Gram-positive bacteria, glucose is also the preferred carbon source and enters into cells through the PTS system. Of note, the central regulator of CCR in *B. subtilis* is HPr, rather than EIIA^{Glc}, and CCR is achieved via transcriptional repression by the catabolite control protein A (CcpA) (Warner & Lolkema, 2003) (Figure 1.8). HPr of *B. subtilis* can be phosphorylated at two different residues: His-15 and Ser-46. In the presence of glucose, phosphoryl group of PEP is

transferred through EI to HPr at the His-15 residue, which then impart the phosphoryl group to EII^{Glc} and finally to glucose. Meanwhile, the HPr is phosphorylated by HPr kinase (HPrK) at the residue Ser-46 with the phosphoryl group from ATP. This HPr(Ser-P) interacts with CcpA, and the resultant HPr(Ser-P)-CcpA complex is able to bind to the *cre* (catabolite responsive element) site in the target genes, thereby inhibiting transcription of the genes for utilization of non-preferred carbon sources (Rojo, 2010; Warner & Lolkema, 2003). The formation of HPr(Ser-P)-CcpA complex and the interaction between the complex and *cre* site are enhanced in the presence of glycolytic intermediates fructose-1,6-biphosphate or glucose-6-phosphate, whose levels are high in the conditions with glucose being assimilated (Deutscher *et al.*, 1995; Schumacher *et al.*, 2007).

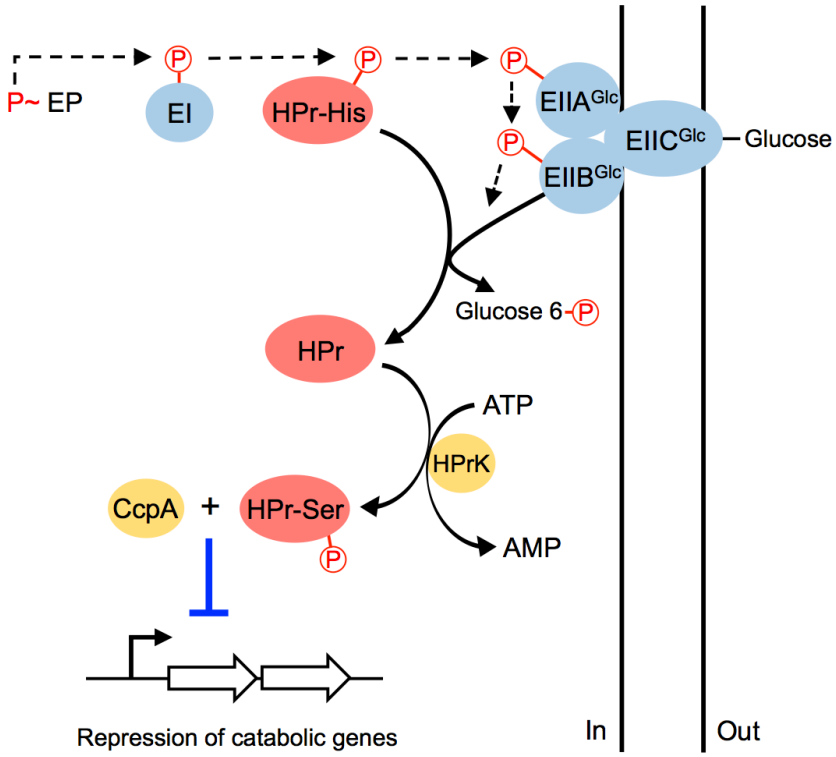

Figure 1.8. Carbon catabolite repression in *B. subtilis*. Phosphorylation state of HPr primarily determines CCR. HPr can be phosphorylated at either His-15 or Ser-46 residue. HPr acquires phosphate group from phosphoenolpyruvate (PEP) at the His-15 residue. HPr(His-P) then serves as the phosphate donor for incoming glucose, resulting in dephosphorylation of HPr protein. When glucose is being utilized, the HPr protein is phosphorylated by HPr kinase (HPrK) at the Ser-46 residue. HPr(Ser-P) interacts with catabolite control protein A (CcpA), forming HPr(Ser-P)-CcpA complex, which inhibits expression of the catabolic genes for non-preferred carbon sources by binding to the *cre* site.

1.5.3 Mechanism of CCR in *Pseudomonas*

It has long been known that the abovementioned mechanisms of CCR established in enteric bacteria and *B. subtilis* do not hold for *Pseudomonas*. *Pseudomonas* use succinate and other intermediates in the TCA cycle as the most preferred carbon source (Rojo, 2010). Importantly, glucose is not a preferred carbon source for *Pseudomonas*. Expression of enzymes for glucose catabolism is inhibited by the presence of succinate as shown in *P. aeruginosa* (Collier *et al.*, 1996). Glucose uptake in *Pseudomonas* is not carried out by PTS, and the cAMP level does not change in the presence of glucose (Li & Lu, 2007). Succinate-induced CCR was also observed for the utilization of gluconate, glycerol, histidine, mannitol and xylose, *etc*. (Hug *et al.*, 1968; Liu *et al.*, 2017; Rojo, 2010). Neither PTS nor CAP homologue is involved in the succinate-provoked CCR (Suh *et al.*, 2002). The key players of CCR in *Pseudomonas* are the two-component system CbrAB, ncRNAs CrcZ and CrcY, and Crc/Hfq protein complex (Garcia-Maurino *et al.*, 2013; Liu *et al.*, 2017; Valentini *et al.*, 2014) (Figure 1.9). In *Pseudomonas*, CCR occurs at the post-transcription level and is mediated by Crc, a RNA-binding protein, which is absent in *E. coli* and *B. subtilis* (Rojo, 2010). With the aid of a RNA chaperonic protein Hfq, the Crc/Hfq protein complex represses translation of the catabolic genes for non-preferred carbon sources via binding to an A-rich motif 'AAnAAnAA' at the 5-end of their mRNA transcripts. The Crc/Hfq-mediated repression is under the control of CbrAB. In the absence of succinate, CbrB activates the expression of CrcZ and CrcY, which sequester the Crc/Hfq complex from binding to the target mRNAs, thereby relieving the catabolite repression of the corresponding genes. Presence of succinate represses the expression of *crcY/Z* via the CbrAB system. Subsequently, the Crc/Hfq complex is free to target the mRNA transcripts. However, it is still unknown what signals trigger the activity of CbrAB.

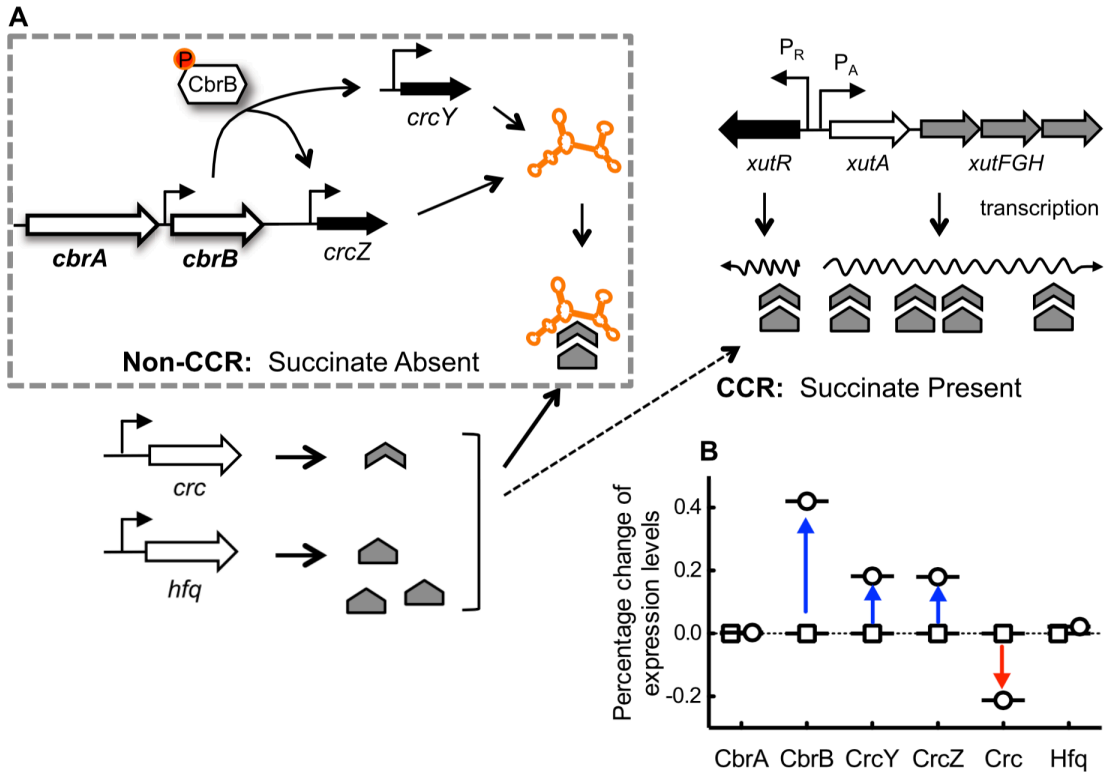

Figure 1.9. Carbon catabolite repression in *Pseudomonas*, using the CCR control of xylose utilization (*xut*) genes in *P. fluorescens* as an example (A). Xylose is a non-preferred carbon source, which is subject to the catabolite repression by succinate. In the presence of succinate, the Crc/Hfq complex binds to the *xut* mRNA transcripts, inhibiting their translation. When succinate is absent, the two-component system CbrAB activates the expression of ncRNAs CrcY and CrcZ, which relieve CCR via sequestration of the Crc/Hfq complex. (B) Percentage increase or decrease of expression levels of the CCR regulators during metabolic shift from CCR (square) to Non-CCR (circle) conditions. (Figure from Liu *et al.*, 2017)

1.6 Carbon and nitrogen regulation of histidine utilization

Histidine serves many bacteria as a good source of carbon and nitrogen. However, utilization of histidine is physiologically challenging as it contains excess nitrogen over carbon in its structure. Histidine catabolism has thus been used as a model system for studying the coordination between cellular carbon and nitrogen metabolisms. Here, I will describe how the expression of *hut* genes is positively regulated in model organisms of enteric bacteria (*K. pneumoniae* and *Salmonella enterica*), *B. subtilis* and *Pseudomonas*, representing three different types of gene regulation.

1.6.1 Carbon and Nitrogen regulation of Hut system in *K. pneumoniae*

In *K. pneumoniae*, expression of the *hut* genes is activated by CAP charged with cAMP, and it is thus subject to CCR control mediated by glucose. The rate of histidine degradation is repressed in the presence of glucose, one of the most preferred carbon sources for this bacterium (Magasanik, 1955). Addition of cAMP to the growth medium relieves the glucose-mediated repression of histidase synthesis (Prival & Magasanik, 1971). This led to the finding that cAMP and CAP play an important role in regulating the *hut* expression in response to carbon limitation. The cAMP-CAP complex activates transcription from the *hutU* promoter by binding to two operator sites, a strong site and a weak site, wherein the strong site is essential for the activation of transcription (Osuna *et al.*, 1991; Osuna, Janes*, et al.*, 1994) (Figure 1.10). The connection between glucose-mediated CCR and cAMP-CAP is very clear in *E. coli* as mentioned above. The formation of cAMP-CAP complex is impeded by the nonphosphorylated $EIIA^{Glc}$ of the sugar PTS, which is predominant in the presence of glucose.

In *K. pneumoniae*, the glucose-mediated repression of *hut* genes can be overcome if the cells are grown under conditions of nitrogen limitation (Bender, 2012), indicating the regulation of *hut* genes by the nitrogen signaling system. Transcription of the *hut* genes is activated by NAC, a LysR-type transcriptional regulator, in response to nitrogen limitation (Bender, 2010; Schwacha & Bender, 1993). NAC binds to the promoter region of *hutU* to activate the transcription in a σ^{70}-dependent manner (Goss & Bender, 1995) (Figure 1.10). Mutants devoid of NAC cannot activate the *hutU* expression in nitrogen-limited conditions, whereas the response of *hut* transcription to carbon limitation is unaffected (Bender *et al.*, 1983). It is suggested that NAC also activates the *hutIG* expression as *hutG* responds to nitrogen limitation (Magasanik *et al.*, 1965). The expression of *nac* is controlled by the Ntr system. NtrBC activates the transcription of *nac* from a σ^{54}-dependent promoter under nitrogen-limited conditions (Reitzer, 2003).

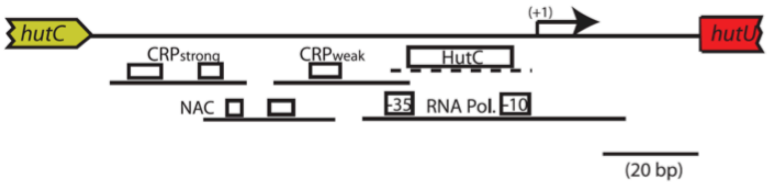

Figure 1.10. The *hut* promoter region of *K. pneumoniae* showing operator sites for the CAP and NAC activators. Boxes represent sequences that match to the consensus sequence of the CAP and NAC operator sites. Transcription start site of the *hutUHT* operon is marked by +1. Lines beneath the boxes indicate the regions of footprint of these regulators on DNA. (Figure from Bender, 2012)

1.6.2 Carbon and nitrogen regulation of Hut system in *B. subtilis*

Histidine utilization by *B. subtilis* is also subject to the glucose-mediated catabolite repression, and the underlying mechanisms differ between *B. subtilis* and enteric bacteria (Chasin & Magasanik, 1968). The key regulator of CCR in *B. subtilis* is CcpA, which blocks gene transcription by binding at a *cre* site (Henkin, 1996). A *cre* site was identified in the coding region of *hutP* and required for the glucose-induced repression of *hut* genes (Wray *et al.*, 1994) (Figure 1.11). HutP is a positive regulator for the downstream *hut* genes. It abolishes transcription termination caused by a stem-loop structure located between *hutP* and *hutH* (Kumarevel *et al.*, 2005). Although the direct binding of CcpA to the *hut cre* site has not been demonstrated, it is very likely that the glucose-induced CCR of *hut* operon is achieved by CcpA binding to the *cre* site (Bender, 2012). Thus, the *hutP* transcription is repressed by CcpA in CCR conditions, and consequently, the transcription of *hut* genes downstream is impeded.

In *B. subtilis*, expression of the genes responding to nitrogen availability are controlled by two global regulatory proteins, GlnR and TnrA. TnrA activates transcription of nitrogen-related genes in response to nitrogen limitation, whereas GlnR acts during nitrogen excess to repress gene transcription (Fisher, 1999). However, the expression of *hut* operon does not respond to nitrogen limitation, and the *hut* operon is not under the control of the GlnR/TnrA-mediated nitrogen regulation (Bender, 2012). The *hut* operon of *B. subtilis* is subject to amino acid repression mediated by the transcriptional repressor CodY. Expression of the *hut* genes is strongly repressed in the presence of a mixture of 11 different amino acids due to the molecular interaction between CodY and the operator site ($hutO_A$) located downstream of the *hut* promoter (M. R. Atkinson

et al., 1990; Wray & Fisher, 1994) (Figure 1.11). CodY is a global regulator in *B. subtilis*, whose activity responds to intracellular nutrient status and amino acid availability (Slack *et al.*, 1995; Sonenshein, 2007).

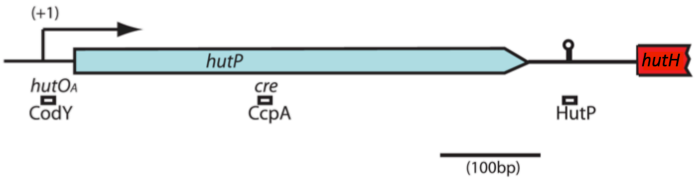

Figure 1.11. Regulatory sites in the *hut* operon of *B. subtilis*. Transcription start site of the *hut* operon is marked by +1. Boxes indicate the binding sites for the regulatory proteins of *hut* expression: CodY binds to the *hut*O_A site to repress the *hut* transcription; CcpA blocks the transcription by binding at a *cre* site; HutP acts at a stem-loop structure upstream *hutH* to prevent transcriptional termination. (Figure from Bender, 2012)

1.6.3 Carbon and Nitrogen regulation of Hut system in *Pseudomonas*

The *hut* genes in *Pseudomonas* species have been characterized decades ago, whereas little is known about how the Hut system is regulated in response to cellular carbon and nitrogen conditions. In *Pseudomonas*, the succinate-induced catabolite repression of histidine utilization was first described in 1960s. Activities of the Hut enzymes in *P. aeruginosa* were significantly reduced in the presence of succinate (Lessie & Neidhardt, 1967). In *P. putida*, histidase and urocanase were inhibited by succinate, and the rate of histidine degradation was reduced when succinate was added into the medium (Hug *et al.*, 1968).

The mechanism of CCR in *Pseudomonas* had not been known until recent years. The CbrAB-CrcYZ-Crc/Hfq regulatory cascade of CCR was identified in several *Pseudomonas* species, and many genes were found subject to the regulation by Crc/Hfq. However, CCR of the Hut system is still elusive. A proteomic analysis of *P. putida* observed no difference between wild type and *crc* mutant strains on the expression of Hut enzymes when cells were grown in LB medium (Moreno *et al.*, 2009). In *P. aeruginosa*, the succinate-mediated repression on histidase and urocanase activities was not relieved in *crc* mutants (Collier *et al.*, 1996). Data available so far suggest that the Crc protein plays no role in CCR control of histidine utilization.

Previous work in *P. fluorescens* and *P. aeruginosa* shows that both CbrAB and NtrBC are involved in the activation of *hut* genes. Deletion of *cbrA* or *cbrB* caused no growth on histidine as the sole carbon source, but the mutant was able to grow on histidine as the sole nitrogen source in the presence of succinate or glucose (Li & Lu, 2007; Nishijyo *et al.*, 2001; Zhang & Rainey, 2008). The expression of *hutU-G* operon of *P. fluorescens* requires CbrB when growing on histidine as the sole carbon source. The *hutU-G* operon is transcribed from a σ^{54}-dependent promoter in this condition, suggesting that CbrB may directly activate the *hut* transcription (Zhang & Rainey, 2008).

When histidine is the sole nitrogen source, expression of *hut* genes is subject to complex regulation by CbrAB and NtrBC. In *P. fluorescens* SBW25, deletion of *cbrB* reduced the expression level of *hutU*. The remaining *hutU* expression was maintained by NtrC as deletion of both *cbrB* and *ntrC* totally abolished the expression. Consistently, the Δ*cbrB*Δ*ntrC* mutant cannot grow on histidine as the sole nitrogen source. Either CbrB or NtrC is required for the growth in this condition (Zhang & Rainey, 2008). Therefore, CbrAB and NtrBC probably work coordinately to regulate the *hut* expression in response to the intracellular carbon and nitrogen metabolic status. However, the mode of regulation mediated by CbrB and NtrC is unclear. Whether the regulation is direct or indirect is to be determined.

Interestingly, ammonia augment the succinate-provoked repression of histidase synthesis in *P. aeruginosa* (Collier *et al.*, 1996). Ammonia is one of the most preferred nitrogen sources for *Pseudomonas* (Itoh *et al.*, 2007). Addition of ammonia causes a further 30% reduction of histidase expression, whereas ammonia only have a much weaker repressing effect on histidase in the absence of a preferred carbon source (Collier *et al.*, 1996). Moreover, the succinate-induced repression of Hut expression only occurs in the conditions with excess nitrogen. The CCR of Hut is relieved when cells are grown in nitrogen-limited conditions (Lessie & Neidhardt, 1967; Potts & Clarke, 1976). Together, the data indicate that expression of *hut* genes are positively controlled by a combination of both cellular carbon and nitrogen metabolisms, but the underlying mechanism remains elusive.

1.7 Previous work leading to this project

P. fluorescens SBW25 is a model plant-associated bacterium, which was originally isolated from field-grown sugar beet plant (Rainey & Bailey, 1996). It is a plant growth-promoting rhizobacterium and colonizes plant leaves and roots where it contributes to plant health by improving nutrients bioavailability and antagonizing plant pathogen *Pythium ultimum* (Alsohim *et al.*, 2014; Moon *et al.*, 2008; Naseby *et al.*, 2001). *P. fluorescens* is metabolically versatile, it can live in phytosphere and also other environments, including soil and water.

To gain insights into the molecular mechanisms that contributes to the ecological success of *P. fluorescens* SBW25 *in planta*, *in vivo* expression technology (IVET) was used to identify genes whose expression is elevated during bacterial colonization of sugar beet seedlings (Rainey, 1999). Among the 139 plant-inducible genes identified in total, twenty-two (16%) are involved in nutrient acquisition (Giddens *et al.*, 2007; Silby *et al.*, 2009). Of note, one of the identified genes shows 96% amino acid identity to *hutT* (encoding the histidine transporter) of *P. putida*, indicating that *hut* genes are expressed at elevated levels during the colonization of *P. fluorescens* SBW25 on the surface of sugar beet (Rainey, 1999; Zhang *et al.*, 2006). The data suggest that histidine utilization genes may contribute to the ecological success of *P. fluorescens* SBW25 in the plant environment.

Subsequent studies have identified genes involved in the enzymatic breakdown of histidine (Zhang & Rainey, 2007) and transporters for the specific uptake of histidine as well as urocanate (Zhang *et al.*, 2012). The role of HutC repressor in determining histidine and urocanate concentration-dependent expression of *hut* genes has been established (Zhang & Rainey, 2007), but the work has also suggested a yet-unknown global regulatory role beyond histidine metabolism (Zhang *et al.*, 2013).

The positive regulation of *hut* is complex in *Pseudomonas*. Two two-component systems CbrAB and NtrBC are required for *hut* activation, but their precise roles remain elusive. It is unknown whether CbrAB and NtrBC activate *hut* expression in direct manner or through the function of another yet-unknown activator, like NAC in enteric bacteria (Zhang & Rainey, 2008). Inhibition of *hut* enzymes by more preferred carbon

source, such as succinate and glucose, have been noted, but the underlying mechanism of CCR has remained mysterious for many years.

Using the xylose utilization (*xut*) genes as a model, significant progress has been made on the molecular mechanisms of CCR in *P. fluorescens* SBW25 (Liu *et al.*, 2017; Liu *et al.*, 2015). As shown in Figure 1.9, CbrAB resides at the top of the CCR regulatory hierarchy with the Crc/Hfq complex as key mediator of CCR via targeting mRNAs of catabolic genes. The Crc/Hfq-mediated repression is relieved through competitive binding by the CrcYZ ncRNAs, whose expression is controlled by the CbrAB system. This knowledge has laid the foundation for further investigation into the mysterious mechanisms of the positive control of *hut* expression in *Pseudomonas*.

1.8 Objectives of this study

The overall objective of this project is to elucidate the molecular mechanisms of *hut* gene regulation in *Pseudomonas*. My work will focus on dissecting the novel regulatory roles of HutC in global gene regulation, while gaining new insights into the molecular interactions between HutC and P_{hut} promoters. I also aim to define the yet-unknown mechanisms of positive regulation of *hut* genes for histidine utilization in nutrient-complex environments. The data will help integrate our current understanding of carbon catabolite repression into the cellular nitrogen metabolism of *Pseudomonas*.

This study has been conducted with *P. fluorescens* SBW25, a plant growth-promoting bacterium and a model organism for studying plant-microbe interactions. The specific aims of this work are listed below:

1. **Dissecting the regulatory roles of HutC in the expression of histidine utilization (*hut*) genes.**
    - Examining the molecular interactions between HutC and the *hut* promoters, and determining the stoichiometry of HutC interacting with the target DNAs.
    - Determining the HutC-recognized DNA sequence in the *hut* promoters, and analyzing the function of the HutC-binding sites by site-directed mutagenesis.
    - Elucidating the mode of HutC actions on transcriptional repression of the *hut* operons.

2. Investigating the global regulatory role of HutC in *P. fluorescens* SBW25.

- Identification of the putative HutC-binding sites in the genome of *P. fluorescens* SBW25 by *in silico* analysis and experimental verification.
- Analyzing the novel regulatory role of HutC in the expression of *ntrBC,* a newly identified HutC-regulated candidate.
- Phenotypic analysis of HutC in bacterial motility and biofilm formation.

3. Elucidating how cellular carbon and nitrogen metabolic balance is maintained for efficient utilization of histidine in *Pseudomonas*.

- Characterization of the positive regulation of *hut* genes by CbrAB and NtrBC both *in vitro* and *in vivo*.
- Determining the role of CbrAB and NtrBC in Hut expression in response to various carbon and nitrogen conditions.
- Elucidating the mechanism of succinate-mediated CCR of histidine utilization.
- Dissecting the novel regulatory role of HutC in maintaining the C/N balance for growth on histidine.
- Establishing the overall regulatory network for histidine utilization to coordinate the carbon and nitrogen metabolisms.

1.9 References

Achtman, M., Zurth, K., Morelli, G., Torrea, G., Guiyoule, A., & Carniel, E. (1999). Yersinia pestis, the cause of plague, is a recently emerged clone of *Yersinia pseudotuberculosis*. *Proc Natl Acad Sci U S A, 96*(24), 14043-14048.

Allison, S. L., & Phillips, A. T. (1990). Nucleotide sequence of the gene encoding the repressor for the histidine utilization genes of *Pseudomonas putida*. *J Bacteriol, 172*(9), 5470-5476.

Alsohim, A. S., Taylor, T. B., Barrett, G. A., Gallie, J., Zhang, X. X., Altamirano-Junqueira, A. E., . . . Jackson, R. W. (2014). The biosurfactant viscosin produced by *Pseudomonas fluorescens* SBW25 aids spreading motility and plant growth promotion. *Environ Microbiol, 16*(7), 2267-2281. doi: 10.1111/1462-2920.12469

Amador, C. I., Canosa, I., Govantes, F., & Santero, E. (2010). Lack of CbrB in *Pseudomonas putida* affects not only amino acids metabolism but also different stress responses and biofilm development. *Environ Microbiol, 12*(6), 1748-1761. doi: 10.1111/j.1462-2920.2010.02254.x

Aravind, L., & Anantharaman, V. (2003). HutC/FarR-like bacterial transcription factors of the GntR family contain a small molecule-binding domain of the chorismate lyase fold. *FEMS Microbiol Lett, 222*(1), 17-23.

Aravind, L., Anantharaman, V., Balaji, S., Babu, M. M., & Iyer, L. M. (2005). The many faces of the helix-turn-helix domain: transcription regulation and beyond. *FEMS Microbiol Rev, 29*(2), 231-262. doi: 10.1016/j.femsre.2004.12.008

Arcondeguy, T., Jack, R., & Merrick, M. (2001). P(II) signal transduction proteins, pivotal players in microbial nitrogen control. *Microbiol Mol Biol Rev, 65*(1), 80-105. doi: 10.1128/MMBR.65.1.80-105.2001

Arocena, G. M., Zorreguieta, A., & Sieira, R. (2012). Expression of VjbR under nutrient limitation conditions is regulated at the post-transcriptional level by specific acidic pH values and urocanic acid. *PLoS One, 7*(4), e35394. doi: 10.1371/journal.pone.0035394

Atkinson, M. R., Wray, L. V., Jr., & Fisher, S. H. (1990). Regulation of histidine and proline degradation enzymes by amino acid availability in *Bacillus subtilis*. *J Bacteriol, 172*(9), 4758-4765.

Atkinson, S., Chang, C. Y., Patrick, H. L., Buckley, C. M., Wang, Y., Sockett, R. E., . . . Williams, P. (2008). Functional interplay between the *Yersinia pseudotuberculosis* YpsRI and YtbRI quorum sensing systems modulates swimming motility by controlling expression of *flhDC* and *fliA*. *Mol Microbiol, 69*(1), 137-151. doi: 10.1111/j.1365-2958.2008.06268.x

Barroso, R., Garcia-Maurino, S. M., Tomas-Gallardo, L., Andujar, E., Perez-Alegre, M., Santero, E., & Canosa, I. (2018). The CbrB Regulon: Promoter dissection reveals novel insights into the CbrAB expression network in *Pseudomonas putida*. *PLoS One, 13*(12), e0209191. doi: 10.1371/journal.pone.0209191

Bender, R. A. (2010). A NAC for regulating metabolism: the nitrogen assimilation control protein (NAC) from *Klebsiella pneumoniae*. *J Bacteriol, 192*(19), 4801-4811. doi: 10.1128/JB.00266-10

Bender, R. A. (2012). Regulation of the histidine utilization (hut) system in bacteria. *Microbiol Mol Biol Rev, 76*(3), 565-584. doi: 10.1128/MMBR.00014-12

Bender, R. A., Snyder, P. M., Bueno, R., Quinto, M., & Magasanik, B. (1983). Nitrogen regulation system of *Klebsiella aerogenes*: the *nac* gene. *J Bacteriol, 156*(1), 444-446.

Bowden, G., Mothibeli, M. A., Robb, F. T., & Woods, D. R. (1982). Regulation of hut enzymes and intracellular protease activities in *Vibrio alginolyticus* hut mutants. *J Gen Microbiol, 128*(9), 2041-2045. doi: 10.1099/00221287-128-9-2041

Boylan, S. A., & Bender, R. A. (1984). Genetic and physical maps of *Klebsiella aerogenes* genes for histidine utilization (*hut*). *Mol Gen Genet, 193*(1), 99-103.

Bruckner, R., & Titgemeyer, F. (2002). Carbon catabolite repression in bacteria: choice of the carbon source and autoregulatory limitation of sugar utilization. *FEMS Microbiol Lett, 209*(2), 141-148. doi: 10.1111/j.1574-6968.2002.tb11123.x

Cabeen, M. T., Leiman, S. A., & Losick, R. (2016). Colony-morphology screening uncovers a role for the *Pseudomonas aeruginosa* nitrogen-related phosphotransferase system in biofilm formation. *Mol Microbiol, 99*(3), 557-570. doi: 10.1111/mmi.13250

Chasin, L. A., & Magasanik, B. (1968). Induction and repression of the histidine-degrading enzymes of *Bacillus subtilis*. *J Biol Chem, 243*(19), 5165-5178.

Chavarria, M., Fuhrer, T., Sauer, U., Pfluger-Grau, K., & de Lorenzo, V. (2013). Cra regulates the cross-talk between the two branches of the phosphoenolpyruvate : phosphotransferase system of *Pseudomonas putida*. *Environ Microbiol, 15*(1), 121-132. doi: 10.1111/j.1462-2920.2012.02808.x

Chavarria, M., Kleijn, R. J., Sauer, U., Pfluger-Grau, K., & de Lorenzo, V. (2012). Regulatory tasks of the phosphoenolpyruvate-phosphotransferase system of *Pseudomonas putida* in central carbon metabolism. *MBio, 3*(2). doi: 10.1128/mBio.00028-12

Chubukov, V., Gerosa, L., Kochanowski, K., & Sauer, U. (2014). Coordination of microbial metabolism. *Nat Rev Microbiol, 12*(5), 327-340. doi: 10.1038/nrmicro3238

Collier, D. N., Hager, P. W., & Phibbs, P. V., Jr. (1996). Catabolite repression control in the Pseudomonads. *Res Microbiol, 147*(6-7), 551-561.

Commichau, F. M., Forchhammer, K., & Stulke, J. (2006). Regulatory links between carbon and nitrogen metabolism. *Curr Opin Microbiol, 9*(2), 167-172. doi: 10.1016/j.mib.2006.01.001

Deutscher, J., Francke, C., & Postma, P. W. (2006). How phosphotransferase system-related protein phosphorylation regulates carbohydrate metabolism in bacteria. *Microbiol Mol Biol Rev, 70*(4), 939-1031. doi: 10.1128/MMBR.00024-06

Deutscher, J., Kuster, E., Bergstedt, U., Charrier, V., & Hillen, W. (1995). Protein kinase-dependent HPr/CcpA interaction links glycolytic activity to carbon catabolite repression in gram-positive bacteria. *Mol Microbiol, 15*(6), 1049-1053.

Dhakshnamoorthy, B., Mizuno, H., & Kumar, P. K. R. (2013). Alternative binding modes of l-histidine guided by metal ions for the activation of the antiterminator protein HutP of *Bacillus subtilis*. *J Struct Biol, 183*(3), 512-518. doi: 10.1016/j.jsb.2013.05.019

Doucette, C. D., Schwab, D. J., Wingreen, N. S., & Rabinowitz, J. D. (2011). alpha-Ketoglutarate coordinates carbon and nitrogen utilization via enzyme I inhibition. *Nat Chem Biol, 7*(12), 894-901. doi: 10.1038/nchembio.685

Fadi Aldehni, M., Sauer, J., Spielhaupter, C., Schmid, R., & Forchhammer, K. (2003). Signal transduction protein P(II) is required for NtcA-regulated gene expression during nitrogen deprivation in the cyanobacterium *Synechococcus elongatus* strain PCC 7942. *J Bacteriol, 185*(8), 2582-2591.

Fisher, S. H. (1999). Regulation of nitrogen metabolism in *Bacillus subtilis*: vive la difference! *Mol Microbiol, 32*(2), 223-232.

Forchhammer, K. (2004). Global carbon/nitrogen control by PII signal transduction in cyanobacteria: from signals to targets. *FEMS Microbiol Rev, 28*(3), 319-333. doi: 10.1016/j.femsre.2003.11.001

Garcia-Maurino, S. M., Perez-Martinez, I., Amador, C. I., Canosa, I., & Santero, E. (2013). Transcriptional activation of the CrcZ and CrcY regulatory RNAs by the CbrB response regulator in *Pseudomonas putida*. *Mol Microbiol, 89*(1), 189-205. doi: 10.1111/mmi.12270

Gerth, M. L., Ferla, M. P., & Rainey, P. B. (2012). The origin and ecological significance of multiple branches for histidine utilization in *Pseudomonas aeruginosa* PAO1. *Environ Microbiol, 14*(8), 1929-1940. doi: 10.1111/j.1462-2920.2011.02691.x

Gibbs, N. K., Tye, J., & Norval, M. (2008). Recent advances in urocanic acid photochemistry, photobiology and photoimmunology. *Photochem Photobiol Sci, 7*(6), 655-667. doi: 10.1039/b717398a

Giddens, S. R., Jackson, R. W., Moon, C. D., Jacobs, M. A., Zhang, X. X., Gehrig, S. M., & Rainey, P. B. (2007). Mutational activation of niche-specific genes provides insight into regulatory networks and bacterial function in a complex environment. *Proc Natl Acad Sci U S A, 104*(46), 18247-18252. doi: 10.1073/pnas.0706739104

Goldberg, R. B., & Magasanik, B. (1975). Gene order of the histidine utilization (hut) operons in *Klebsiella aerogenes*. *J Bacteriol, 122*(3), 1025-1031.

Gorke, B., & Stulke, J. (2008). Carbon catabolite repression in bacteria: many ways to make the most out of nutrients. *Nat Rev Microbiol, 6*(8), 613-624. doi: 10.1038/nrmicro1932

Goss, T. J., & Bender, R. A. (1995). The nitrogen assimilation control protein, NAC, is a DNA binding transcription activator in *Klebsiella aerogenes*. *J Bacteriol, 177*(12), 3546-3555.

Groisman, E. A. (2016). Feedback Control of Two-Component Regulatory Systems. *Annu Rev Microbiol, 70*, 103-124. doi: 10.1146/annurev-micro-102215-095331

Henkin, T. M. (1996). The role of CcpA transcriptional regulator in carbon metabolism in *Bacillus subtilis*. *FEMS Microbiol Lett, 135*(1), 9-15. doi: 10.1111/j.1574-6968.1996.tb07959.x

Hervas, A. B., Canosa, I., & Santero, E. (2008). Transcriptome analysis of *Pseudomonas putida* in response to nitrogen availability. *J Bacteriol, 190*(1), 416-420. doi: 10.1128/JB.01230-07

Hesketh, A., Fink, D., Gust, B., Rexer, H. U., Scheel, B., Chater, K., . . . Engels, A. (2002). The GlnD and GlnK homologues of *Streptomyces coelicolor* A3(2) are functionally dissimilar to their nitrogen regulatory system counterparts from enteric bacteria. *Mol Microbiol, 46*(2), 319-330.

Hu, L., Allison, S. L., & Phillips, A. T. (1989). Identification of multiple repressor recognition sites in the hut system of *Pseudomonas putida*. *J Bacteriol, 171*(8), 4189-4195.

Hu, L., & Phillips, A. T. (1988). Organization and multiple regulation of histidine utilization genes in *Pseudomonas putida*. *J Bacteriol, 170*(9), 4272-4279.

Huergo, L. F., Chandra, G., & Merrick, M. (2013). P(II) signal transduction proteins: nitrogen regulation and beyond. *FEMS Microbiol Rev, 37*(2), 251-283. doi: 10.1111/j.1574-6976.2012.00351.x

Huergo, L. F., & Dixon, R. (2015). The Emergence of 2-Oxoglutarate as a Master Regulator Metabolite. *Microbiol Mol Biol Rev, 79*(4), 419-435. doi: 10.1128/MMBR.00038-15

Hug, D. H., Roth, D., & Hunter, J. (1968). Regulation of histidine catabolism by succinate in *Pseudomonas putida*. *J Bacteriol, 96*(2), 396-402.

Itoh, Y. , Nishijyo, T. , & Nakada, Y. (2007). Histidine catabolism and catabolite regulation. *Pseudomonas. Springer, Berlin, Germany, 5*, 371-395.

Jiang, P., Peliska, J. A., & Ninfa, A. J. (1998). The regulation of Escherichia coli glutamine synthetase revisited: role of 2-ketoglutarate in the regulation of glutamine synthetase adenylylation state. *Biochemistry, 37*(37), 12802-12810. doi: 10.1021/bi980666u

Joshua, G. W., Atkinson, S., Goldstone, R. J., Patrick, H. L., Stabler, R. A., Purves, J., . . . Wren, B. W. (2015). Genome-wide evaluation of the interplay between *Caenorhabditis elegans* and *Yersinia pseudotuberculosis* during in vivo biofilm formation. *Infect Immun, 83*(1), 17-27. doi: 10.1128/IAI.00110-14

Kaminskas, E., & Magasanik, B. (1970). Sequential synthesis of histidine-degrading enzymes in *Bacillus subtilis*. *J Biol Chem, 245*(14), 3549-3555.

Kendrick, K. E., & Wheelis, M. L. (1982). Histidine dissimilation in *Streptomyces coelicolor*. *J Gen Microbiol, 128*(9), 2029-2040.

Kimhi, Y., & Magasanik, B. (1970). Genetic basis of histidine degradation in *Bacillus subtilis*. *J Biol Chem, 245*(14), 3545-3548.

Kumarevel, T., Mizuno, H., & Kumar, P. K. (2005). Structural basis of HutP-mediated anti-termination and roles of the Mg2+ ion and L-histidine ligand. *Nature, 434*(7030), 183-191. doi: 10.1038/nature03355

Lee, C. R., Cho, S. H., Yoon, M. J., Peterkofsky, A., & Seok, Y. J. (2007). *Escherichia coli* enzyme IIANtr regulates the K+ transporter TrkA. *Proc Natl Acad Sci U S A, 104*(10), 4124-4129. doi: 10.1073/pnas.0609897104

Lee, C. R., Park, Y. H., Kim, M., Kim, Y. R., Park, S., Peterkofsky, A., & Seok, Y. J. (2013). Reciprocal regulation of the autophosphorylation of enzyme INtr by glutamine and alpha-ketoglutarate in *Escherichia coli*. *Mol Microbiol, 88*(3), 473-485. doi: 10.1111/mmi.12196

Lenski, R. E. (1991). Quantifying fitness and gene stability in microorganisms. *Biotechnology, 15*, 173-192.

Lessie, T. G., & Neidhardt, F. C. (1967). Formation and operation of the histidine-degrading pathway in *Pseudomonas aeruginosa*. *J Bacteriol, 93*(6), 1800-1810.

Li, W., & Lu, C. D. (2007). Regulation of carbon and nitrogen utilization by CbrAB and NtrBC two-component systems in *Pseudomonas aeruginosa*. *J Bacteriol, 189*(15), 5413-5420. doi: 10.1128/JB.00432-07

Liang, X., Yu, X., Pan, X., Wu, J., Duan, Y., Wang, J., & Zhou, M. (2018). A thiadiazole reduces the virulence of *Xanthomonas oryzae pv. oryzae* by inhibiting the histidine utilization pathway and quorum sensing. *Mol Plant Pathol, 19*(1), 116-128. doi: 10.1111/mpp.12503

Liu, Y., Gokhale, C. S., Rainey, P. B., & Zhang, X. X. (2017). Unravelling the complexity and redundancy of carbon catabolic repression in *Pseudomonas fluorescens* SBW25. *Mol Microbiol, 105*(4), 589-605. doi: 10.1111/mmi.13720

Liu, Y., Rainey, P. B., & Zhang, X. X. (2015). Molecular mechanisms of xylose utilization by *Pseudomonas fluorescens*: overlapping genetic responses to

xylose, xylulose, ribose and mannitol. *Mol Microbiol, 98*(3), 553-570. doi: 10.1111/mmi.13142

Luttmann, D., Heermann, R., Zimmer, B., Hillmann, A., Rampp, I. S., Jung, K., & Gorke, B. (2009). Stimulation of the potassium sensor KdpD kinase activity by interaction with the phosphotransferase protein IIA(Ntr) in *Escherichia coli*. *Mol Microbiol, 72*(4), 978-994. doi: 10.1111/j.1365-2958.2009.06704.x

Magasanik, B. (1955). The metabolic control of histidine assimilation and dissimilation in *Aerobacter aerogenes*. *J Biol Chem, 213*(2), 557-569.

Magasanik, B., Lund, P., Neidhardt, F. C., & Schwartz, D. T. (1965). Induction and repression of the histidine-degrading enzymes in *Aerobacter aerogenes*. *J Biol Chem, 240*(11), 4320-4324.

Maheswaran, M., & Forchhammer, K. (2003). Carbon-source-dependent nitrogen regulation in *Escherichia coli* is mediated through glutamine-dependent GlnB signalling. *Microbiology, 149*(Pt 8), 2163-2172. doi: 10.1099/mic.0.26449-0

Martinez-Argudo, I., Little, R., & Dixon, R. (2004). Role of the amino-terminal GAF domain of the NifA activator in controlling the response to the antiactivator protein NifL. *Mol Microbiol, 52*(6), 1731-1744. doi: 10.1111/j.1365-2958.2004.04089.x

Merrick, M. J., & Edwards, R. A. (1995). Nitrogen control in bacteria. *Microbiol Rev, 59*(4), 604-622.

Moon, C. D., Zhang, X. X., Matthijs, S., Schafer, M., Budzikiewicz, H., & Rainey, P. B. (2008). Genomic, genetic and structural analysis of pyoverdine-mediated iron acquisition in the plant growth-promoting bacterium *Pseudomonas fluorescens* SBW25. *BMC Microbiol, 8*, 7. doi: 10.1186/1471-2180-8-7

Moreno, R., Martinez-Gomariz, M., Yuste, L., Gil, C., & Rojo, F. (2009). The *Pseudomonas putida* Crc global regulator controls the hierarchical assimilation of amino acids in a complete medium: evidence from proteomic and genomic analyses. *Proteomics, 9*(11), 2910-2928. doi: 10.1002/pmic.200800918

Naseby, D. C., Way, J. A., Bainton, N. J., & Lynch, J. M. (2001). Biocontrol of Pythium in the pea rhizosphere by antifungal metabolite producing and non-producing *Pseudomonas* strains. *J Appl Microbiol, 90*(3), 421-429.

Nieuwkoop, A. J., & Bender, R. A. (1988). RNA polymerase as a repressor of transcription in the hut(P) region of mutant *Klebsiella aerogenes* histidine utilization operons. *J Bacteriol, 170*(10), 4986-4990.

Nieuwkoop, A. J., Boylan, S. A., & Bender, R. A. (1984). Regulation of *hutUH* operon expression by the catabolite gene activator protein-cyclic AMP complex in *Klebsiella aerogenes*. *J Bacteriol, 159*(3), 934-939.

Ninfa, A. J., & Jiang, P. (2005). PII signal transduction proteins: sensors of alpha-ketoglutarate that regulate nitrogen metabolism. *Curr Opin Microbiol, 8*(2), 168-173. doi: 10.1016/j.mib.2005.02.011

Nishijyo, T., Haas, D., & Itoh, Y. (2001). The CbrA-CbrB two-component regulatory system controls the utilization of multiple carbon and nitrogen sources in *Pseudomonas aeruginosa*. *Mol Microbiol, 40*(4), 917-931.

Noguez, R., Segura, D., Moreno, S., Hernandez, A., Juarez, K., & Espin, G. (2008). Enzyme I NPr, NPr and IIA Ntr are involved in regulation of the poly-beta-

hydroxybutyrate biosynthetic genes in *Azotobacter vinelandii*. *J Mol Microbiol Biotechnol, 15*(4), 244-254. doi: 10.1159/000108658

Oda, M., Katagai, T., Tomura, D., Shoun, H., Hoshino, T., & Furukawa, K. (1992). Analysis of the transcriptional activity of the hut promoter in *Bacillus subtilis* and identification of a cis-acting regulatory region associated with catabolite repression downstream from the site of transcription. *Mol Microbiol, 6*(18), 2573-2582.

Oda, M., Sugishita, A., & Furukawa, K. (1988). Cloning and nucleotide sequences of histidase and regulatory genes in the *Bacillus subtilis* hut operon and positive regulation of the operon. *J Bacteriol, 170*(7), 3199-3205.

Osuna, R., Boylan, S. A., & Bender, R. A. (1991). In vitro transcription of the histidine utilization (*hutUH*) operon from *Klebsiella aerogenes*. *J Bacteriol, 173*(1), 116-123.

Osuna, R., Janes, B. K., & Bender, R. A. (1994). Roles of catabolite activator protein sites centered at -81.5 and -41.5 in the activation of the *Klebsiella aerogenes* histidine utilization operon *hutUH*. *J Bacteriol, 176*(17), 5513-5524.

Osuna, R., Schwacha, A., & Bender, R. A. (1994). Identification of the *hutUH* operator (hutUo) from *Klebsiella aerogenes* by DNA deletion analysis. *J Bacteriol, 176*(17), 5525-5529.

Patell, S., Gu, M., Davenport, P., Givskov, M., Waite, R. D., & Welch, M. (2010). Comparative microarray analysis reveals that the core biofilm-associated transcriptome of *Pseudomonas aeruginosa* comprises relatively few genes. *Environ Microbiol Rep, 2*(3), 440-448. doi: 10.1111/j.1758-2229.2010.00158.x

Pfluger, K., & de Lorenzo, V. (2008). Evidence of in vivo cross talk between the nitrogen-related and fructose-related branches of the carbohydrate phosphotransferase system of *Pseudomonas putida*. *J Bacteriol, 190*(9), 3374-3380. doi: 10.1128/JB.02002-07

Pfluger-Grau, K., & Gorke, B. (2010). Regulatory roles of the bacterial nitrogen-related phosphotransferase system. *Trends Microbiol, 18*(5), 205-214. doi: 10.1016/j.tim.2010.02.003

Pioszak, A. A., & Ninfa, A. J. (2004). Mutations altering the N-terminal receiver domain of NRI (NtrC) That prevent dephosphorylation by the NRII-PII complex in *Escherichia coli*. *J Bacteriol, 186*(17), 5730-5740. doi: 10.1128/JB.186.17.5730-5740.2004

Pomposiello, P. J., Janes, B. K., & Bender, R. A. (1998). Two roles for the DNA recognition site of the *Klebsiella aerogenes* nitrogen assimilation control protein. *J Bacteriol, 180*(3), 578-585.

Postma, P. W., & Lengeler, J. W. (1985). Phosphoenolpyruvate:carbohydrate phosphotransferase system of bacteria. *Microbiol Rev, 49*(3), 232-269.

Postma, P. W., Lengeler, J. W., & Jacobson, G. R. (1993). Phosphoenolpyruvate:carbohydrate phosphotransferase systems of bacteria. *Microbiol Rev, 57*(3), 543-594.

Potts, J. R., & Clarke, P. H. (1976). The effect of nitrogen limitation on catabolite repression of amidase, histidase and urocanase in *Pseudomonas aeruginosa*. *J Gen Microbiol, 93*(2), 377-387. doi: 10.1099/00221287-93-2-377

Powell, B. S., Court, D. L., Inada, T., Nakamura, Y., Michotey, V., Cui, X., . . . Reizer, J. (1995). Novel proteins of the phosphotransferase system encoded within the rpoN operon of *Escherichia coli*. Enzyme IIANtr affects growth on organic nitrogen and the conditional lethality of an erats mutant. *J Biol Chem, 270*(9), 4822-4839.

Prival, M. J., & Magasanik, B. (1971). Resistance to catabolite repression of histidase and proline oxidase during nitrogen-limited growth of *Klebsiella aerogenes*. *J Biol Chem, 246*(20), 6288-6296.

Rainey, P. B. (1999). Adaptation of *Pseudomonas fluorescens* to the plant rhizosphere. *Environ Microbiol, 1*(3), 243-257.

Rainey, P. B., & Bailey, M. J. (1996). Physical and genetic map of the *Pseudomonas fluorescens* SBW25 chromosome. *Mol Microbiol, 19*(3), 521-533.

Reitzer, L. (2003). Nitrogen assimilation and global regulation in *Escherichia coli*. *Annu Rev Microbiol, 57*, 155-176. doi: 10.1146/annurev.micro.57.030502.090820

Reizer, J., Reizer, A., Merrick, M. J., Plunkett, G., 3rd, Rose, D. J., & Saier, M. H., Jr. (1996). Novel phosphotransferase-encoding genes revealed by analysis of the *Escherichia coli* genome: a chimeric gene encoding an Enzyme I homologue that possesses a putative sensory transduction domain. *Gene, 181*(1-2), 103-108.

Resch, M., Schiltz, E., Titgemeyer, F., & Muller, Y. A. (2010). Insight into the induction mechanism of the GntR/HutC bacterial transcription regulator YvoA. *Nucleic Acids Res, 38*(7), 2485-2497. doi: 10.1093/nar/gkp1191

Rietsch, A., Wolfgang, M. C., & Mekalanos, J. J. (2004). Effect of metabolic imbalance on expression of type III secretion genes in *Pseudomonas aeruginosa*. *Infect Immun, 72*(3), 1383-1390.

Rigali, S., Derouaux, A., Giannotta, F., & Dusart, J. (2002). Subdivision of the helix-turn-helix GntR family of bacterial regulators in the FadR, HutC, MocR, and YtrA subfamilies. *J Biol Chem, 277*(15), 12507-12515. doi: 10.1074/jbc.M110968200

Rojo, F. (2010). Carbon catabolite repression in *Pseudomonas* : optimizing metabolic versatility and interactions with the environment. *FEMS Microbiol Rev, 34*(5), 658-684. doi: 10.1111/j.1574-6976.2010.00218.x

Romero-Rodriguez, A., Maldonado-Carmona, N., Ruiz-Villafan, B., Koirala, N., Rocha, D., & Sanchez, S. (2018). Interplay between carbon, nitrogen and phosphate utilization in the control of secondary metabolite production in *Streptomyces*. *Antonie Van Leeuwenhoek, 111*(5), 761-781. doi: 10.1007/s10482-018-1073-1

Schroder, J., Maus, I., Ostermann, A. L., Kogler, A. C., & Tauch, A. (2012). Binding of the IclR-type regulator HutR in the histidine utilization (*hut*) gene cluster of the human pathogen *Corynebacterium resistens* DSM 45100. *FEMS Microbiol Lett, 331*(2), 136-143. doi: 10.1111/j.1574-6968.2012.02564.x

Schumacher, M. A., Seidel, G., Hillen, W., & Brennan, R. G. (2007). Structural mechanism for the fine-tuning of CcpA function by the small molecule effectors glucose 6-phosphate and fructose 1,6-bisphosphate. *J Mol Biol, 368*(4), 1042-1050. doi: 10.1016/j.jmb.2007.02.054

Schwacha, A., & Bender, R. A. (1990). Nucleotide sequence of the gene encoding the repressor for the histidine utilization genes of *Klebsiella aerogenes*. *J Bacteriol, 172*(9), 5477-5481.

Schwacha, A., & Bender, R. A. (1993). The *nac* (nitrogen assimilation control) gene from *Klebsiella aerogenes*. *J Bacteriol, 175*(7), 2107-2115.

Schwacha, A., Cohen, J. A., Gehring, K. B., & Bender, R. A. (1990). Tn1000-mediated insertion mutagenesis of the histidine utilization (*hut*) gene cluster from *Klebsiella aerogenes*: genetic analysis of hut and unusual target specificity of Tn1000. *J Bacteriol, 172*(10), 5991-5998.

Shivers, R. P., Dineen, S. S., & Sonenshein, A. L. (2006). Positive regulation of *Bacillus subtilis* ackA by CodY and CcpA: establishing a potential hierarchy in carbon flow. *Mol Microbiol, 62*(3), 811-822. doi: 10.1111/j.1365-2958.2006.05410.x

Sieira, R., Arocena, G. M., Bukata, L., Comerci, D. J., & Ugalde, R. A. (2010). Metabolic control of virulence genes in *Brucella abortus*: HutC coordinates *virB* expression and the histidine utilization pathway by direct binding to both promoters. *J Bacteriol, 192*(1), 217-224. doi: 10.1128/jb.01124-09

Sieira, R., Arocena, G. M., Zorreguieta, A., Comerci, D. J., & Ugalde, R. A. (2012). A MarR-Type regulator directly activates transcription from the *Brucella abortus virB* promoter by sharing a redundant role with HutC. *J Bacteriol, 194*(23), 6431-6440. doi: 10.1128/JB.01007-12

Sieira, R., Bialer, M. G., Roset, M. S., Ruiz-Ranwez, V., Langer, T., Arocena, G. M., . . . Zorreguieta, A. (2017). Combinatorial control of adhesion of *Brucella abortus* 2308 to host cells by transcriptional rewiring of the trimeric autotransporter *btaE* gene. *Mol Microbiol, 103*(3), 553-565. doi: 10.1111/mmi.13576

Silby, M. W., Cerdeno-Tarraga, A. M., Vernikos, G. S., Giddens, S. R., Jackson, R. W., Preston, G. M., . . . Thomson, N. R. (2009). Genomic and genetic analyses of diversity and plant interactions of *Pseudomonas fluorescens*. *Genome Biol, 10*(5), R51. doi: 10.1186/gb-2009-10-5-r51

Slack, F. J., Serror, P., Joyce, E., & Sonenshein, A. L. (1995). A gene required for nutritional repression of the *Bacillus subtilis* dipeptide permease operon. *Mol Microbiol, 15*(4), 689-702.

Smith, G. R., & Magasanik, B. (1971). Nature and self-regulated synthesis of the repressor of the *hut* operons in *Salmonella typhimurium*. *Proc Natl Acad Sci U S A, 68*(7), 1493-1497.

Sonenshein, A. L. (2007). Control of key metabolic intersections in *Bacillus subtilis*. *Nat Rev Microbiol, 5*(12), 917-927. doi: 10.1038/nrmicro1772

Suh, S. J., Runyen-Janecky, L. J., Maleniak, T. C., Hager, P., MacGregor, C. H., Zielinski-Mozny, N. A., . . . West, S. E. (2002). Effect of vfr mutation on global gene expression and catabolite repression control of *Pseudomonas aeruginosa*. *Microbiology, 148*(Pt 5), 1561-1569. doi: 10.1099/00221287-148-5-1561

Suvorova, I. A., Korostelev, Y. D., & Gelfand, M. S. (2015). GntR Family of Bacterial Transcription Factors and Their DNA Binding Motifs: Structure, Positioning and Co-Evolution. *PLoS One, 10*(7), e0132618. doi: 10.1371/journal.pone.0132618

Ulrich, L. E., Koonin, E. V., & Zhulin, I. B. (2005). One-component systems dominate signal transduction in prokaryotes. *Trends Microbiol, 13*(2), 52-56. doi: 10.1016/j.tim.2004.12.006

Valentini, M., Garcia-Maurino, S. M., Perez-Martinez, I., Santero, E., Canosa, I., & Lapouge, K. (2014). Hierarchical management of carbon sources is regulated similarly by the CbrA/B systems in *Pseudomonas aeruginosa* and *Pseudomonas putida*. *Microbiology, 160*(Pt 10), 2243-2252. doi: 10.1099/mic.0.078873-0

Velazquez, F., Pfluger, K., Cases, I., De Eugenio, L. I., & de Lorenzo, V. (2007). The phosphotransferase system formed by PtsP, PtsO, and PtsN proteins controls production of polyhydroxyalkanoates in *Pseudomonas putida*. *J Bacteriol, 189*(12), 4529-4533. doi: 10.1128/JB.00033-07

Warner, J. B., & Lolkema, J. S. (2003). CcpA-dependent carbon catabolite repression in bacteria. *Microbiol Mol Biol Rev, 67*(4), 475-490.

Wray, L. V., Jr., & Fisher, S. H. (1994). Analysis of *Bacillus subtilis hut* operon expression indicates that histidine-dependent induction is mediated primarily by transcriptional antitermination and that amino acid repression is mediated by two mechanisms: regulation of transcription initiation and inhibition of histidine transport. *J Bacteriol, 176*(17), 5466-5473.

Wray, L. V., Jr., Pettengill, F. K., & Fisher, S. H. (1994). Catabolite repression of the *Bacillus subtilis hut* operon requires a cis-acting site located downstream of the transcription initiation site. *J Bacteriol, 176*(7), 1894-1902.

Xu, H., Lin, W., Xia, H., Xu, S., Li, Y., Yao, H., . . . Qiao, M. (2005). Influence of *ptsP* gene on pyocyanin production in *Pseudomonas aeruginosa*. *FEMS Microbiol Lett, 253*(1), 103-109. doi: 10.1016/j.femsle.2005.09.027

Yeung, A. T., Torfs, E. C., Jamshidi, F., Bains, M., Wiegand, I., Hancock, R. E., & Overhage, J. (2009). Swarming of *Pseudomonas aeruginosa* is controlled by a broad spectrum of transcriptional regulators, including MetR. *J Bacteriol, 191*(18), 5592-5602. doi: 10.1128/JB.00157-09

Yoshida, K., Sano, H., Seki, S., Oda, M., Fujimura, M., & Fujita, Y. (1995). Cloning and sequencing of a 29 kb region of the *Bacillus subtilis* genome containing the hut and wapA loci. *Microbiology, 141 (Pt 2)*, 337-343. doi: 10.1099/13500872-141-2-337

Zhang, C. C., Zhou, C. Z., Burnap, R. L., & Peng, L. (2018). Carbon/Nitrogen Metabolic Balance: Lessons from *Cyanobacteria*. *Trends Plant Sci, 23*(12), 1116-1130. doi: 10.1016/j.tplants.2018.09.008

Zhang, X. X., Chang, H., Tran, S. L., Gauntlett, J. C., Cook, G. M., & Rainey, P. B. (2012). Variation in transport explains polymorphism of histidine and urocanate utilization in a natural *Pseudomonas* population. *Environ Microbiol, 14*(8), 1941-1951. doi: 10.1111/j.1462-2920.2011.02692.x

Zhang, X. X., George, A., Bailey, M. J., & Rainey, P. B. (2006). The histidine utilization (*hut*) genes of *Pseudomonas fluorescens* SBW25 are active on plant surfaces, but are not required for competitive colonization of sugar beet seedlings. *Microbiology, 152*(Pt 6), 1867-1875. doi: 10.1099/mic.0.28731-0

Zhang, X. X., & Rainey, P. B. (2007). Genetic analysis of the histidine utilization (*hut*) genes in *Pseudomonas fluorescens* SBW25. *Genetics, 176*(4), 2165-2176. doi: 10.1534/genetics.107.075713

Zhang, X. X., & Rainey, P. B. (2008). Dual involvement of CbrAB and NtrBC in the regulation of histidine utilization in *Pseudomonas fluorescens* SBW25. *Genetics, 178*(1), 185-195. doi: 10.1534/genetics.107.081984

Zhang, X. X., Ritchie, S. R., & Rainey, P. B. (2013). Urocanate as a potential signaling molecule for bacterial recognition of eukaryotic hosts. *Cellular and Molecular Life Sciences, 71*(4), 541-547. doi: 10.1007/s00018-013-1527-6

Zimmer, B., Hillmann, A., & Gorke, B. (2008). Requirements for the phosphorylation of the *Escherichia coli* EIIANtr protein in vivo. *FEMS Microbiol Lett, 286*(1), 96-102. doi: 10.1111/j.1574-6968.2008.01262.x

Zschiedrich, C. P., Keidel, V., & Szurmant, H. (2016). Molecular Mechanisms of Two-Component Signal Transduction. *J Mol Biol, 428*(19), 3752-3775. doi: 10.1016/j.jmb.2016.08.003

Chapter 2

Dissecting the regulatory roles of HutC in the expression of histidine utilization (*hut*) genes

2.1 Preamble

HutC has been known as the regulator of *hut* genes for the utilization of histidine and its derivative, urocanate. It represses the expression of *hut* genes by binding to a Phut site in the *hut* promoters - repression is relieved via interaction between HutC and urocanate (Allison & Phillips, 1990; Hu *et al.*, 1989; Newell & Lessie, 1970). However, the knowledge was based on research conducted in the late 1980s and early 1990s prior to the genomic era. Electrophoretic mobility shift assay (EMSA) and DNase I footprinting assays had been used to examine the molecular interactions between HutC and its target DNAs in the *hut* operon of *P. putida* (Hu *et al.*, 1989). However, the work was performed with crude cell lysates instead of purified HutC protein. This left gaps in our understanding with regards to the DNA sequences that HutC recognizes and interacts with.

In a previous work, histidine utilization genes have been genetically characterized in a plant growth-promoting bacterium *Pseudomonas fluorescens* SBW25, using a combination of site-directed mutagenesis analysis and chromosomally integrated *lacZ* fusions (Zhang & Rainey, 2007). The genetic data confirmed the predicted role of HutC in repression of the *hut* operons with urocanate (and not histidine) as the effector molecule. HutC possesses a domain structure that is typical for bacterial one-component signal transduction systems: a N-terminal winged helix-turn-helix (wHTH) DNA-binding domain plus a C-terminal effector-binding regulatory domain (Gorelik *et al.*, 2006). However, the mechanisms of HutC action have received little research attention until recently. Recent work on the opportunistic human pathogen *Pseudomonas aeruginosa* and zoonotic pathogen *Brucella abortus* shows that HutC plays a significant role in global control of cellular metabolism, cell motility and expression of virulence factors such as the type IV pili (reviewed in Zhang *et al.*, 2013).

For the plant-associated bacterium *P. fluorescens* SBW25, relative fitness of the derived Δ*hutC* mutant have been examined in both laboratory media and plant environments (Zhang & Rainey, 2007). Relative fitness was calculated in terms of the selection rate constant (SRC) (Lenski, 1991). A fitness of zero indicates that the mutant and wild type are equally fit (a negative or positive value indicates a reduction or increase in fitness relative to wild type). *hutC* inactivation results in constitutive expression of the *hut* operons, which is detrimental in the absence of histidine. Consequently, a slight decrease of fitness (-0.71 ± 0.16 of the selection rate constant) was observed in M9 medium with glucose and ammonium as the sole source of carbon and nitrogen, respectively. However, a large significant reduction in competitive colonization was detected on the surfaces of sugar beet plants. The measured fitness of the Δ*hutC* mutant relative to wild-type SBW25 was -2.28 ± 0.30 and -1.9 ± 0.39 in the shoot and rhizosphere, respectively (Figure 5, Zhang & Rainey, 2007). This result was surprising because plant surfaces do contain histidine albeit it is at low concentrations (~3.87 μM) (Zhang *et al.*, 2006). Therefore, the observed severe fitness reduction of Δ*hutC in planta* cannot be explained by its effect on *hut* expression alone. Moreover, a primary search of putative Phut sites revealed numerous candidate genes beyond histidine catabolism, including *ntrBC*, a global regulator for nitrogen metabolism. Together, evidence available to date strongly implicates that HutC plays a significant role in global gene regulation and contributes to the ecological success of *P. fluorescens* SBW25 in the plant environments.

The primary goal of this work is to determine the global gene regulation mediated by HutC with a specific focus on genes beyond histidine metabolism. However, to this end, we first need to advance the understanding of HutC interacting with the P_{hut} promoters in the *hut* locus. In this Chapter, we report the purification of His_6-tagged HutC protein from *P. fluorescens* SBW25 in *E. coli*, and the subsequent comprehensive analysis of the molecular interactions between $HutC_{His6}$ and its target DNAs in the *hut* locus (specifically, the P_{hutU} and P_{hutFC} promoters). The data enable us to propose an updated model of HutC function, which involves complex protein oligomerization in response to varying concentrations of urocanate. More importantly, we have identified a novel HutC-binding site, termed Pntr, which is located adjacent to the normal Phut site in the P_{hutFC} promoter of *P. fluorescens* SBW25. The biological significance of the Pntr site on *hut* regulation will be discussed (and subject to further functional characterization in Chapter 3).

2.2 Results

2.2.1 Purification of HutC protein from *P. fluorescens* SBW25

To investigate the detailed molecular interactions between HutC and its target DNAs, a pair of primers HutC-ProF and HutC-ProR was designed to amplify the *hutC* coding region, with incorporation of a hexa-histidine (His6) tag at the N-terminal. The resultant 800-bp PCR product was then cloned into the expression vector pTrc99A. IPTG (1 mM) was used to induce the expression of $HutC_{His6}$ in *E. coli* BL21 (DE3). The results showing HutC protein induction and solubility are in Figure S2.1 (Page 79) and Figure S2.2 (Page 80), respectively. The HutC protein was subsequently purified using immobilized metal affinity chromatography (TALON metal affinity resin). Purity of the obtained $HutC_{His6}$ was confirmed by 12% SDS-PAGE analysis. A typical gel image is shown in Figure 2.1. Only one band with the expected molecular weight of 28.6 kDa was present in the $HutC_{His6}$ protein samples (lanes 4-9).

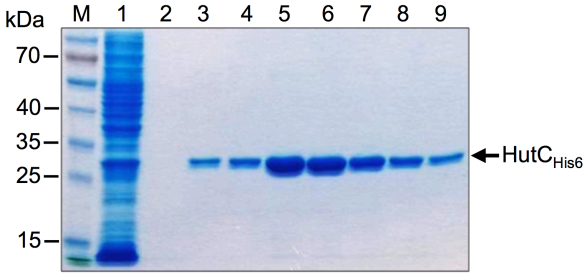

Figure 2.1. SDS-PAGE analysis of the purified $HutC_{His6}$ protein. Lane 1, IPTG-induced whole cell lysate. Lane 2, flow-through fraction with lysis buffer containing 5 mM imidazole. Lane 3, flow-through fraction with washing buffer containing 70 mM imidazole. Lane 4 - 9, elution fractions by elution buffer containing 200 mM imidazole. Lane M, protein molecular weight marker.

2.2.2 Mode of HutC-mediated regulation of the P_{hutU} promoter in *P. fluorescens* SBW25

2.2.2.1 Molecular interactions between HutC and the P_{hutU} promoter DNA

The DNA binding properties of $HutC_{His6}$ to P_{hutU} was first examined using EMSA. The specific DNA probe named PhutU-325, a 325-bp DNA fragment of the P_{hutU} promoter region, was prepared by PCR using forward primer PhutU_D and biotin-labelled

reverse primer Bio-UR (Figure 2.2A). As shown in Figure 2.2B, one band was observed in EMSA for the free probe DNA (lane 1). However, the addition of $HutC_{His6}$ at increasing concentrations from lane 2 to 8 resulted in four shifted bands, which are labelled 'a', 'b', 'c' and 'd' from low to high molecular weights. Along with the increase of $HutC_{His6}$, the dominant shifted band was gradually shifted from 'a' and 'b' to 'c' and 'd'; and only the largest shifted band 'd' was present when $HutC_{His6}$ was added at the highest concentration of 2.1 μM (lane 8). Together, the data confirmed the predicted function of HutC binding to P_{hutU} promoter, and suggested that HutC possesses at least four oligomeric states upon binding with the P_{hutU} promoter DNA *in vitro*.

Next, we sought to determine the effects of urocanate on the molecular interaction between $HutC_{His6}$ and the P_{hutU} promoter. EMSA was performed with the PhutU-325 DNA probe, $HutC_{His6}$ and varying concentrations of urocanate (Figure 2.2C). In the absence of urocanate, $HutC_{His6}$ bound to the P_{hutU} promoter, forming four retarded protein-DNA complexes (lane 1). As the concentration of urocanate was increased from lane 2 to 6, there was a decrease of shifted bands along with an increase of the free probe DNA. Hence, the data confirmed the predicted role of urocanate in disassociation of the HutC-P_{hutU} complex. Interestingly, the dissociation of HutC from P_{hutU} caused by increasing concentrations of urocanate (Figure 2.2C) showed a reverse process of the HutC-P_{hutU} complexes formation observed with the addition of HutC at increasing concentrations (Figure 2.2B). A comparison of the DNA retardation profiles in Figure 2.2B and Figure 2.2C consistently suggest that the HutC-P_{hutU} complexes in bands 'b' and 'd' are relatively more stable than those in bands 'a' and 'c'.

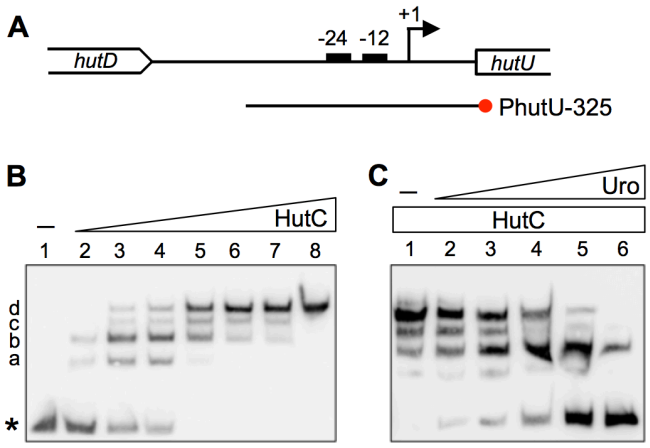

Figure 2.2. Molecular interactions between HutC and P_{hutU} *in vitro*.
(A) Genetic map of the P_{hutU} promoter. -24/-12 consensus of the putative σ^{54}-binding site is marked. The transcription start site of *hutU* is indicated by +1 (Zhang & Rainey, 2007). The red circle on the PhutU-325 probe indicates the end labelled by biotin.
(B) EMSA showing the HutC-P_{hutU} interactions. The concentrations of $HutC_{His6}$ from lane 1 to 8 were 0, 35, 70, 140, 210, 315, 525 and 2100 nM, respectively. The position of free DNA probe is denoted by asterisk. The HutC-P_{hutU} complexes are indicated as 'a', 'b', 'c' and 'd'.
(C) EMSA showing the effects of urocanate on the HutC-P_{hutU} interaction. Lane 1 - 6, $HutC_{His6}$ was added at the concentration of 280 nM for all lanes, and urocanate was added at the concentrations of 0, 125, 250, 500, 1000 and 1500 µM, respectively. The concentration of DNA probe used was 20 nM.

2.2.2.2 Using formaldehyde cross-linking to determine HutC oligomerization *in vitro*

The finding that HutC-P_{hutU} can form at least four protein-DNA complexes prompted further investigation into the oligomerization of $HutC_{His6}$ *in vitro*. To this end, a cross-linking experiment was performed with purified $HutC_{His6}$ using formaldehyde as the cross-linking reagent. Formaldehyde causes the formation of a methylene bridge between interacting proteins, thereby maintaining the subunit interactions within a protein oligomer (Nadeau & Carlson, 2007). Briefly, in a 20-µl reaction $HutC_{His}$ (19 µM) was incubated with 25 mM formaldehyde, and the reaction was stopped with the addition of SDS buffer (see Materials and Methods) at three different time points. The protein samples were then subject to 12% SDS-PAGE analysis. Results shown in Figure 2.3 clearly indicate that HutC is capable of forming a dimer, trimer and tetramer. Of note, a weak band of HutC dimer was also found in the protein reaction without formaldehyde (lane 1). This was likely due to incomplete denaturation of HutC during SDS-PAGE.

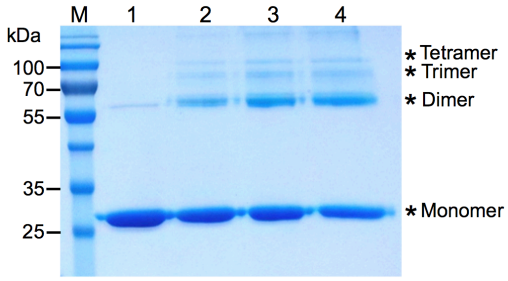

Figure 2.3. Formaldehyde cross-linking showing HutC oligomerization *in vitro*. $HutC_{His6}$ was treated with 25 mM formaldehyde for 1, 2.5 and 4 hrs in lanes 2 to 4, respectively. Lane 1 was the control for $HutC_{His6}$ (19 μM) without formaldehyde treatment. The molecular weight of $HutC_{His6}$ is 28.6 kDa.

2.2.2.3 Stoichiometric analysis of HutC-P_{hutU} interactions

The method of continuous variation analysis (also called Job plot) was applied to determine the stoichiometry of specific $HutC_{His6}$ and P_{hutU} interactions. In this method, the total molar concentration of protein and DNA remains constant in a series of reactions but varies in their relative composition. The binding stoichiometry of a specific protein-DNA complex is then determined by the protein/DNA ratio when the amount of this complex reaches its maximum (Beno *et al.*, 2011; Huang, 1982).

In this work, ten $HutC_{His6}$-P_{hutU} binding reactions were set up and each contained a total protein-DNA concentration at 100 nM (Figure 2.4A). Intensity of the shifted bands was measured by ImageJ software and each complex was plotted against the HutC fractions. Complex 'a' produced a stoichiometry of 1:0.96, suggesting the presence of a HutC monomer binding to the DNA probe. Complex 'd' is most likely formed by a HutC tetramer as it produced a stoichiometry of 1:3.64. The calculated stoichiometry for complex 'b' was 1:1.48. However, the stoichiometry of complex 'c' could not be determined due to the smearing and weak bands. Given that complex 'a' was estimated to be a monomer and 'd' a tetramer, complexes 'b' and 'c' are most likely the intermediate dimer and trimer, respectively.

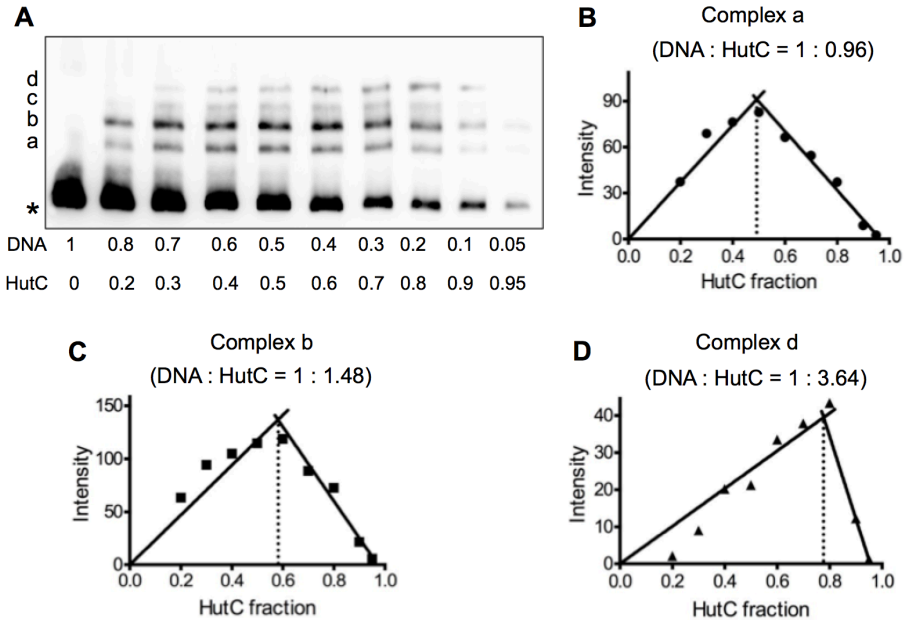

Figure 2.4. Job plot analysis determining the stoichiometry of HutC-P_{hutU} interactions. (A) EMSA of $HutC_{His6}$ and P_{hutU} DNA (PhutU-325). The total molar concentration of protein and DNA was maintained at 100 nM and the molar fractions of protein and DNA are indicated below. (B) (C) (D) Job plot of the DNA to protein ratio in complex 'a', 'b' and 'd', respectively. The intersection of the lines that are least square fitted to the rising and falling subsets of the data yields the binding stoichiometry for each complex.

Additionally, the EMSA data presented in Figure 2.4A was subject to stoichiometric analysis using the method introduced by Hilmar Bading (1988). The molecular weights of DNA-binding proteins were calculated on the basis of their migration distance in the native polyacrylamide gel (see details in Materials and Methods). Results suggest that complex 'a', 'b', 'c' and 'd' corresponds to a $HutC_{His6}$ monomer, dimer, trimer and tetramer binding to the P_{hutU} probe DNA, respectively (Table 2.1).

Taken together, both Job plot and stoichiometric analysis using the Hilmar Bading's method consistently suggest that HutC possesses four oligomeric states, forming a monomer, dimer, trimer and tetramer in a sequential manner along with the increase of HutC concentrations. Furthermore, a cross-examination of the DNA retardation profiles presented in Figure 2.2 and 2.4 consistently suggests that the HutC dimer (band 'b') and tetramer (band 'd') are more stable compared with monomer (band 'a') and trimer (band 'c').

Table 2.1. Calculation of the molecular weight of HutC protein(s) in the HutC-P_{hutU} complexes by Hilmar Bading's method

	Migration distance (cm)	Molecular weight of HutC protein(s) (KDa)	Number of HutC protein(s)
Complex 4	4.75	119.74	4.19
Complex 3	5.25	91.67	3.21
Complex 2	5.80	66.38	2.32
Complex 1	6.50	40.38	1.41
Free DNA	8.00	--	--

2.2.2.4 Determining HutC binding sequence in the P_{hutU} promoter

Next, we sought to determine the precise HutC binding site in the P_{hutU} promoter. To this end, DNase I footprinting was conducted with the purified $HutC_{His6}$ protein and the same biotin-labelled P_{hutU} DNA probe (PhutU-325) used in the above EMSAs. A representative gel image is shown in Figure 2.5A, and the result indicates a 49-bp region being protected by $HutC_{His6}$ from DNase I digestion (Figure 2.5C). Notably, the HutC-protected region overlaps with the putative σ^{54}-binding site of the P_{hutU} promoter. A short inverted repeat sequence TGTA-N2-TACA was identified at the center of the HutC-protected region. This inverted repeat is highly conserved in P_{hut} promoters from different *Pseudomonas* species, which is termed Phut site hereafter (see details in section 2.2.2.5). Accordingly, the two half sites TGTA and TACA are designated as Phut-I and Phut-II, respectively, on the basis of the functional characterization described below.

To further determine the effects of urocanate on HutC-P_{hutU} interaction, DNase I footprinting was conducted for HutC-P_{hutU} with the addition of urocanate at varying concentrations. The results are shown in Figure 2.5B. Parallel to our expectation, the 49-bp region was protected by $HutC_{His6}$ in the absence of urocanate (lanes 1-3). However, when urocanate was added at increasing concentrations from lane 4 to 8, regions at the two ends of the HutC-protected DNA region gradually lost protections. This result clearly indicates that HutC binds to the central region more tightly than the DNA regions at the two ends. A close examination of the sequence of HutC-protected region revealed that the weak HutC-protected regions show no similarity to the conserved inverted repeat (TGTA-N2-TACA), suggesting that the weak protected DNA

regions at the ends are not involved in direct interactions with the HutC protein.

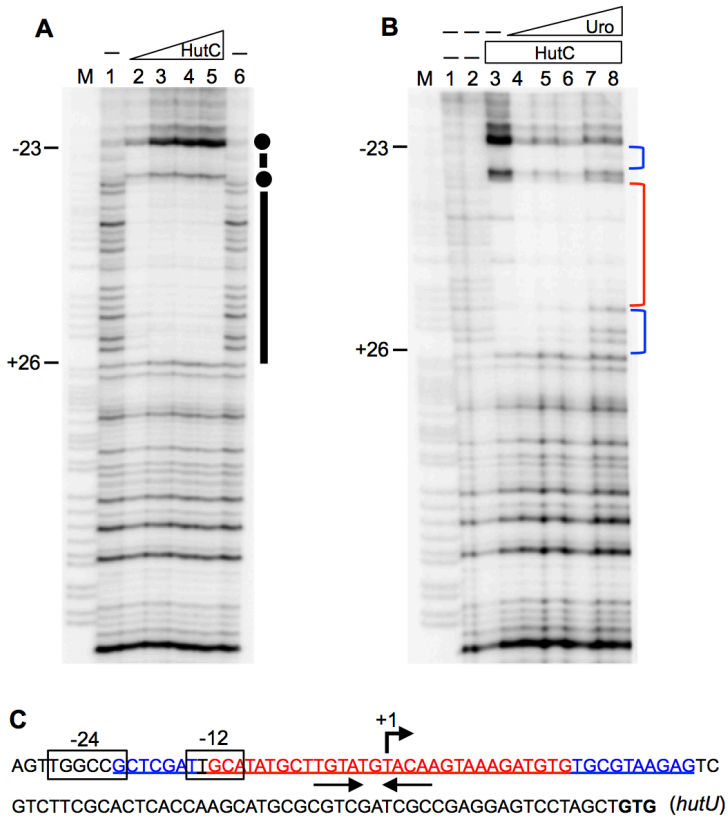

Figure 2.5. Determination of HutC-binding site in the P_{hutU} promoter.
(A) DNase I footprinting of $HutC_{His6}$ and P_{hutU} DNA probe. Lane 1 and 6 are negative controls without $HutC_{His6}$. In lanes 2 to 5, $HutC_{His6}$ was added at 0.68, 2.39, 4.08 and 5.78 μM, respectively. Lane M is a G+A marker. HutC-protected region is indicated by black bars on the right, and black dots denote hypersensitive DNase I cleavage sites.
(B) DNase I footprinting of $HutC_{His6}$-P_{hutU} with the addition of urocanate (Uro). Lane 1 and 2 are negative controls without $HutC_{His6}$ and urocanate. $HutC_{His6}$ was added at the same concentration of 2.8 μM for lanes 3 to 8. Urocanate was added at 0.2, 0.5, 1, 2 and 3 mM in lanes 4 to 8, respectively. The strong and weak HutC-protected regions are shown by red and blue brackets, respectively.
(C) DNA sequence of the P_{hutU} promoter region. The HutC-protected region is underlined and the strong and weak HutC-protected sequences are shown in red and blue font, respectively. The conserved inverted repeat is indicated by arrows. -24/-12 consensus of the putative σ^{54}-binding site is boxed. GTG start codon of *hutU* is marked in boldface type. The transcription start site of *hutU* is indicated by +1 (Zhang & Rainey, 2007).

2.2.2.5 *In silico* analysis of the HutC-binding sequence among *Pseudomonas* species

A multiple sequence alignment was performed with P_{hutU} and P_{hutF} promoter regions (~50 bp in length) from 40 representative *Pseudomonas* strains (from 13 *Pseudomonas* species). A logo was then generated on the basis of the 80 aligned DNA sequences

(Figure 2.6). The result clearly indicates that all P_{hutU} and P_{hutFC} promoters in *Pseudomonas* possess the identical 8-bp inverted repeat (Phut), which is located at the centre of the strong HutC-protected region of P_{hutU} in *P. fluorescens* SBW25 (Figure 2.5C). In contrast, the two weak HutC-protected regions in the P_{hutU} promoter identified above are not conserved among different species of *Pseudomonas*.

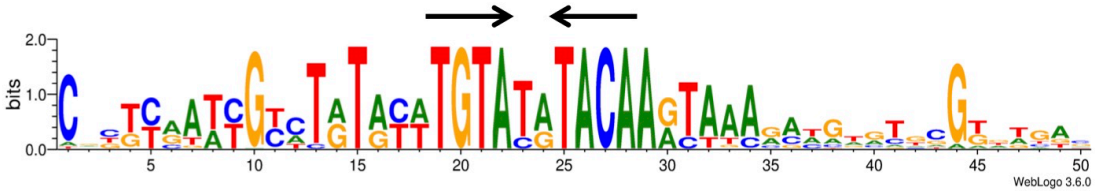

Figure 2.6. Sequence logo representation of the HutC binding site (Phut) in *Pseudomonas*. A total of 80 P_{hutU} and P_{hutF} promoter sequences were aligned from 40 *Pseudomonas* genomes (http://www.pseudomonas.com/). The sequence logo was generated using the WebLogo 3 server (http://weblogo.threeplusone.com/). The inverted repeat sequences are indicated by arrows.

2.2.2.6 Functional analysis of the HutC targeting site (Phut) of the P_{hutU} promoter

To test the functionality of the Phut site in the P_{hutU} promoter, three P_{hutU} variants ($P_{hutU\text{-}M1}$, $P_{hutU\text{-}M2}$ and $P_{hutU\text{-}M1\&2}$) were constructed, each carrying a mutant allele of either Phut-I or Phut-II or both. Specifically, the conserved Phut-I (TGTA) and Phut-II (TACA) half sites were substituted with a 4-bp sequence of CCGG and GGCC, respectively. Hence, three variant DNA probes (PhutU-M1, PhutU-M2 and PhutU-M1&2) were prepared, which have the same length of 325 bp as the wild-type PhutU-325 probe, but differ in the Phut-I or Phut-II half site sequences (Figure 2.7B). EMSA was performed with purified $HutC_{His6}$ and the representative gel images are shown in Figure 2.7. The wild-type PhutU-325 probe produced four shifted bands with a dissociation constant (Kd) of 44.6 nM (Figure 2.7A & 2.7F). However, only one shifted band was observed for variant probes PhutU-M1 and PhutU-M2 (Figure 2.7C & 2.7D), and their calculated Kd values were 472.1 and 478.1 nM, respectively. The one shifted band is most likely a $HutC_{His6}$ monomer binding to the remaining half site in the probe DNA. This result indicates that disruption of either Phut-I or Phut-II caused a significant reduction of the binding affinity with $HutC_{His6}$. Significantly, disruption of both Phut-I and Phut-II completely abolished the $HutC_{His6}$ binding activities as observed for the variant probe PhutU-M1&2 (Figure 2.7E). Together, the EMSA data strongly suggest that simultaneous

binding to both half sites (Phut-I and Phut-II) is crucial for HutC-mediated gene repression.

Next, the functionality of the Phut site was investigated *in vivo* using transcriptional *lacZ* fusions to wild-type P_{hutU} promoter and its derived variants $P_{hutU\text{-}M1}$ and $P_{hutU\text{-}M2}$ with the disruption of Phut-I and Phut-II, respectively. To do this, the three 325-bp DNA fragments (same as the DNA probes) were cloned into pUC18-mini-Tn7T-Gm-lacZ, and the resulting *lacZ* fusions were introduced into wild-type SBW25 and its derived Δ*hutC* mutant (MU60-1). Results of the β-galactosidase activities are shown in Figure 2.7B. Consistent with expectation, in the absence of histidine, the P_{hutU} promoter activity was very low in wild-type SBW25 due to the HutC-mediated repression, and increased significantly in the Δ*hutC* mutant. However, the promoter activities of $P_{hutU\text{-}M1}$ and $P_{hutU\text{-}M2}$ were remarkably high in both Δ*hutC* mutant and wild-type strains, indicating that the HutC-mediated repression was completely abolished on these two P_{hutU} variants. Together, the data led us to conclude that HutC represses the expression of *hutU* by simultaneously binding to both two Phut half sites.

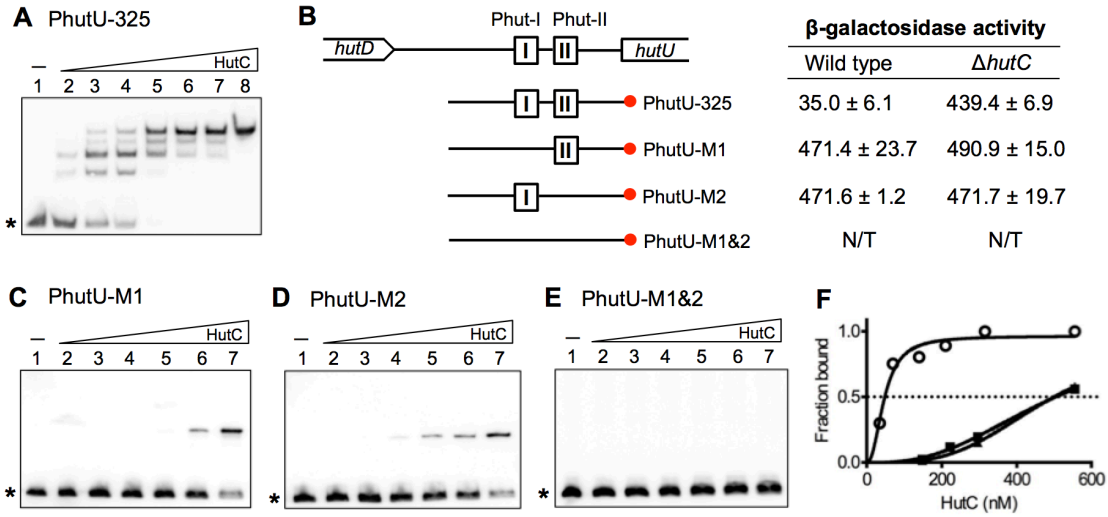

Figure 2.7. Functional analysis of the HutC targeting site in the P_{hutU} promoter.
(A) EMSA of $HutC_{His6}$ and P_{hutU} DNA probe. The concentrations of $HutC_{His6}$ from lane 1 to 8 were 0, 35, 70, 140, 210, 315, 525 nM and 2.1 μM, respectively. Position of free DNA probe is denoted by an asterisk.
(B) DNA fragment of the variant P_{hutU} DNA probes is indicated. Red circle on DNA probes indicates the end labelled by biotin. For the β-galactosidase assays, bacteria were grown in minimal salts medium supplemented with 20 mM succinate and 1 mg/ml NH_4Cl. β-galactosidase activities (μM 4MU min^{-1} OD_{600}^{-1}) were measured at 6 hours after inoculation. Values are means and standard errors of three biological repeats. N/T stands for 'not tested'.
(C) EMSA of $HutC_{His6}$ and $P_{hutU\text{-}M1}$ DNA probe. The concentrations of $HutC_{His6}$ from lane 1 to 7 were 0, 11, 37, 74, 148, 296 and 555 nM, respectively.
(D) EMSA of $HutC_{His6}$ and $P_{hutU\text{-}M2}$ DNA probe. The concentrations of $HutC_{His6}$ from lane 1 to 7 were 0, 37, 74, 148, 222, 296 and 555 nM, respectively.
(E) EMSA of $HutC_{His6}$ and $P_{hutU\text{-}M1\&2}$ DNA probe. The concentrations of $HutC_{His6}$ from lane 1 to 7 were 0, 37, 74, 148, 222, 333 and 555 nM, respectively.
(F) Determination of the equilibrium dissociation constant (Kd) of $HutC_{His6}$ binding to PhutU-325 (open circles), PhutU-M1 (solid triangles) and PhutU-M2 (solid squares) DNA probes.

2.2.2.7 Deciphering the mode of action of HutC-mediated regulation of the P_{hutU} promoter

Taking all data together, we are able to propose an updated model of HutC in regulating the P_{hutU} promoter activities in response to the presence/absence of histidine (or urocanate) in the environment (Figure 2.8). The model involves specific interactions between a HutC monomer and its cognate operator site Phut-I or Phut-II, which compose the highly conserved inverted repeat (TGTA-N2-TACA). The model also involves HutC oligomerization via specific protein-protein interactions. Both the specific protein-DNA interaction and the protein-protein interaction can be disrupted by the *hut* inducer urocanate.

As summarized in Figure 2.8, on the decrease of urocanate, the apo-HutC monomer is capable of binding to either the Phut-I site or Phut-II site in the P_{hutU} promoter region. However, efficient repression is achieved only when HutC forms a dimer and simultaneously binds to the two half sites (Figure 2.8 b). As urocanate concentration further decreases, HutC eventually forms a tetramer, which tightly binds to the Phut site and causes stronger repression of the P_{hutU} promoter (Figure 2.8 d). This dynamic process is reversed on the increase of urocanate.

Of note, HutC represses its own transcription in parallel with structural genes in the *hutU-G and hutF* operons. Negative autoregulation is a common phenomenon for prokaryotic transcription factors. It enables bacterial cells to homeostatically maintain regulatory proteins at desired levels. Specific for HutC, more HutC proteins will be produced along with the increase of urocanate concentration. This will ensure that the HutC-mediated *hut* gene repression reaches saturation at higher urocanate levels.

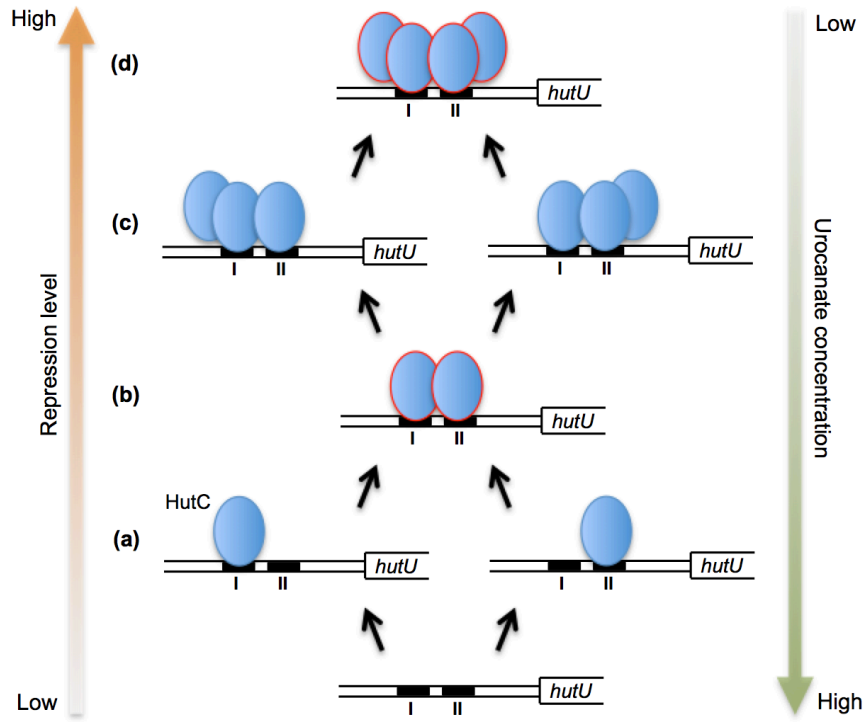

Figure 2.8. Model of HutC function in regulating the P_{hutU} promoter activities. In the presence of histidine (or urocanate) at a high concentration, HutC is dissociated from the P_{hutU} promoter region. On the decrease of urocanate, the apo-HutC monomer binds to either Phut-I site or Phut-II site in the P_{hutU} promoter (a). Efficient repression is achieved only when HutC forms a dimer and simultaneously binds to the two half sites (b). As further decrease of urocanate, HutC forms a trimer (c), and eventually a tetramer, which tightly binds to the Phut site and causes stronger repression of the P_{hutU} promoter (d). HutC dimer and tetramer binding to the P_{hutU} promoter are more stable than HutC monomer and trimer. This dynamic process is reversed on the increase of urocanate.

2.2.3 Mode of HutC-mediated regulation of the P_{hutFC} promoter

2.2.3.1 Molecular interactions between HutC and the P_{hutFC} promoter DNA in *P. fluorescens* SBW25

The *hutF* and *hutCD* operons are divergently transcribed and their expression is also subject to HutC-mediated repression, like the *hutU-G* operon (Figure 1.2 for the *hut* operon). *In silico* analysis indicated the presence of only one Phut site located in the intergenic region between *hutF* and *hutC* (Figure 2.9A). It is thus expected that this Phut site is responsible for the urocanate-induced expression of both *hutF* and *hutCD*. Indeed, EMSA analysis with a 256-nt probe DNA (PhutFC-256, spanning -142 to +114 of *hutF*) showed that $HutC_{His6}$ is capable of binding to the P_{hutFC} probe DNA. However, three major protein-DNA complexes were observed, instead of four for the P_{hutU} probe

describe above (Figure 2.9B).

Next, we examined the effects of urocanate on HutC binding to the P_{hutFC} DNA probe. Result shown in Figure 2.9C confirmed the predicted role of urocanate in dissociation of the HutC-P_{hutFC} binding. A comparison of the effects observed for the HutC concentration (Figure 2.9B) and the urocanate concentration (Figure 2.9C) indicates that HutC and P_{hutFC} DNA are able to form three stable complexes; or in other words, all three shifted bands dominate the interactions at certain HutC and urocanate concentrations. Together, the EMSA data strongly suggest that HutC interacts with the P_{hutFC} promoter in a different manner as with the P_{hutU} promoter.

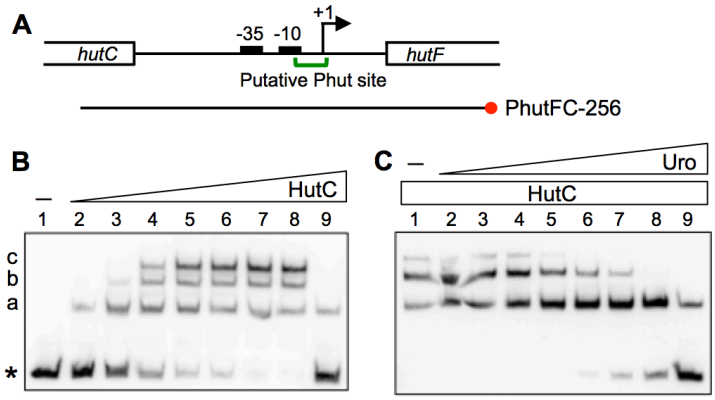

Figure 2.9. Molecular interactions between HutC and P_{hutFC} *in vitro*.
(A) Genetic map of the P_{hutFC} promoter region. -35/-10 consensus of the putative σ^{70}-binding site is marked. The transcription start site of *hutF* is indicated by +1 (Zhang & Rainey, 2007). The red circle on the PhutFC-256 probe indicates the end labelled by biotin.
(B) EMSA showing the HutC-P_{hutFC} interactions. The concentrations of $HutC_{His6}$ from lane 1 to 9 were 0, 35, 70, 140, 210, 280, 350, 455 and 455 nM, respectively. A 200-fold molar excess of unlabelled PhutFC-256 DNA probe (specific competitor) was added in lane 9. The position of free DNA probe is denoted by asterisk. The HutC-P_{hutFC} complexes are indicated as 'a', 'b' and 'c'.
(C) EMSA showing the effects of urocanate on the HutC-P_{hutFC} interaction. Lane 1 - 9, $HutC_{His6}$ was added at the concentration of 350 nM for all lanes, and urocanate was added at the concentrations of 0, 50, 500 nM, 5, 50, 125, 250, 750 uM and 2.5 mM, respectively. The concentration of DNA probe used was 20 nM.

2.2.3.2 Determining the HutC binding sequence of the P_{hutFC} promoter

DNase I footprinting assays were performed using the PhutFC-256 probe and purified $HutC_{His6}$ with and without the addition of urocanate effector (Figure 2.10). Results showed that HutC protected a 28-bp DNA region with high affinity. It contains the

highly conserved inverted repeat TGTA-N2-TACA at the center. Interestingly, HutC was capable of additionally binding to a 40-bp DNA region at relatively low affinity. Specifically, this protection was evidenced only when HutC was added at higher concentrations, and was eliminated by lower concentrations of urocanate compared to the 28-bp strong Phut site. Thus, a total of 68 bp sequence was protected by HutC in the P_{hutFC} promoter, which is much longer than the 49 bp sequence detected in the P_{hutU} promoter (Figure 2.5). More importantly, there appear to be two HutC-binding sites organized in tandem in P_{hutFC} with different binding affinities. This is different from the P_{hutU} promoter, which contains only one HutC-binding site (i.e. Phut) flanked by two weak protected regions at both ends.

Additionally, an imperfect inverted repeat (ACACGACCGGGGTGC), very similar to the consensus sequence of NtrC-binding site (GCACCA-N3-TGGTGC) (Hervas *et al.*, 2008), was identified in the 40-bp weak HutC-protected region (Figure 2.10C). It was subject to further functional characterization presented in Section 2.2.3.4 below.

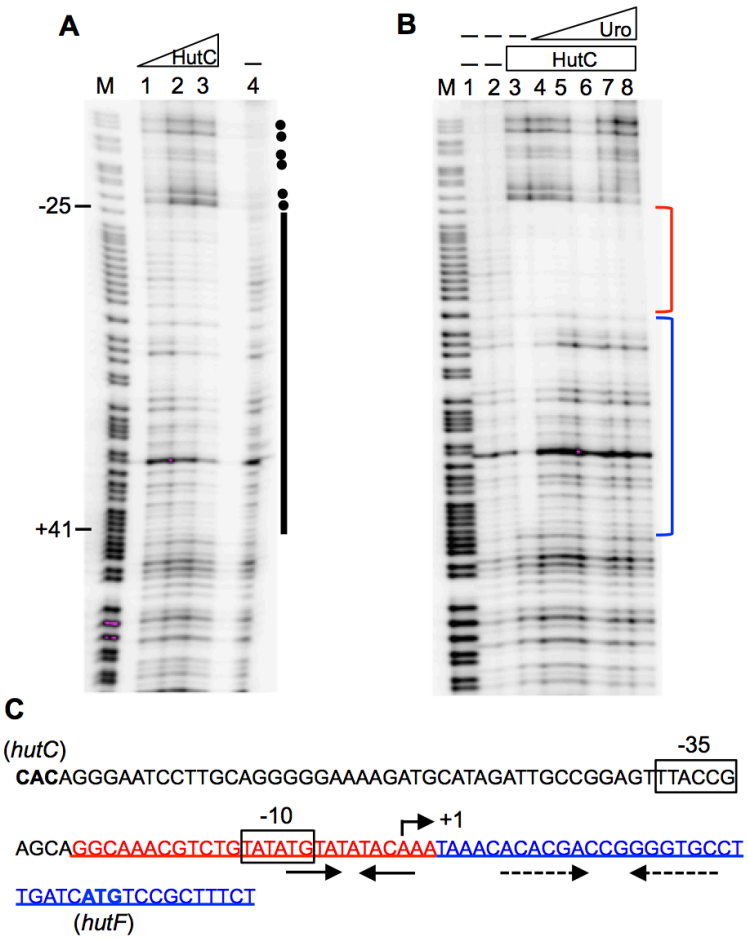

Figure 2.10. Determination of HutC-binding site in the P_{hutFC} promoter.
(A) DNase I footprinting of $HutC_{His6}$ and P_{hutFC} DNA probe. In lanes 1 to 3, $HutC_{His6}$ was added at 1.4, 2.8 and 4.2 μM, respectively. Lane 4 was negative control without $HutC_{His6}$. Lane M, G+A marker. HutC-protected region is indicated by a black bar on the right, and black dots denote hypersensitive DNase I cleavage sites.
(B) DNase I footprinting of $HutC_{His6}$-P_{hutFC} with the addition of urocanate (Uro). Lane 1 and 2 were negative controls without $HutC_{His6}$ and urocanate. $HutC_{His6}$ was added at the same concentration of 2.8 μM at lanes 3 to 8. Urocanate was added at 0.5, 1, 2, 3 and 5 mM in lanes 4 to 8, respectively. The strong and weak HutC-protected regions are shown by red and blue brackets, respectively.
(C) DNA sequence of the P_{hutFC} promoter region. The HutC-protected region is underlined and the strong and weak HutC-protected sequences are shown in red and blue font, respectively. The HutC-binding inverted repeat is indicated by arrows. Dashed arrows denote the sequence showing similarity to the consensus NtrC-binding site. -35/-10 consensus of the putative σ^{70}-binding site is boxed. Start codon of *hutF* and the reversed start codon of *hutC* are marked in boldface type. The transcription start site of *hutF* is indicated by +1 (Zhang & Rainey, 2007).

2.2.3.3 Investigating the molecular interactions between HutC and P_{hutFC} in *P. aeruginosa* PAO1

In a separate work, the regulatory role of HutC has been examined in parallel in the human pathogenic bacterium *Pseudomonas aeruginosa* PAO1, and the experimental work was conducted by Kiran Jayan, a PhD candidate student in Zhang's lab.

Histidine-tagged fusion protein $HutC_{His6}$ from *P. aeruginosa* PAO1 was expressed in *E. coli* and subject to purification using cobalt affinity chromatography as described above. EMSA analysis was performed with a 176-bp biotin-labelled probe (PhutFC-176) containing the P_{hutFC} promoter region of *P. aeruginosa* PAO1 (Figure 2.11A). Surprisingly, EMSA analysis repeatedly revealed only one retarded band instead of three as observed in *P. fluorescens* SBW25 (Figure 2.11B). This data implicated significant difference in the modes of HutC-P_{hutFC} interactions between *P. aeruginosa* and *P. fluorescens*.

To determine whether the different EMSA profiles were attributable to the HutC proteins or probe DNAs or both, we examined the reciprocal interactions using $HutC_{His6}$ and biotin-labelled P_{hutFC} probes from both *P. aeruginosa* PAO1 and *P. fluorescens* SBW25. The resultant four DNA retardation gel images are shown in Figure 2.11. Only one shifted band was obtained for the PAO1 DNA probe, whereas three strong shifted bands (plus one weak band) were detected for the SBW25 DNA probe, regardless of the HutC proteins. The data thus clearly indicated that *P. aeruginosa* and *P. fluorescens* have evolved different operator DNA sites for HutC-mediated regulation of the P_{hutFC} promoter.

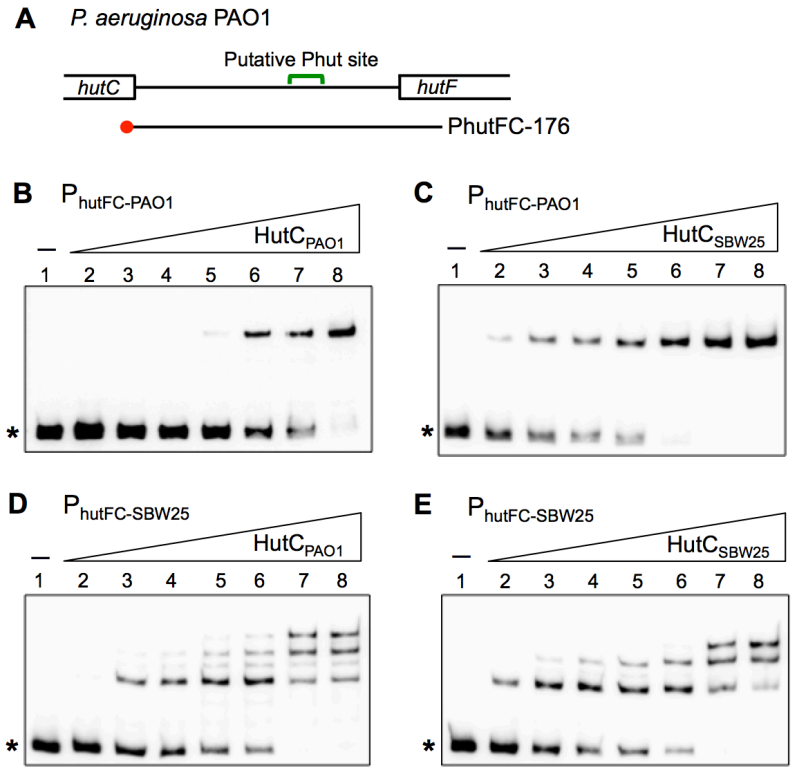

Figure 2.11. EMSA analyses of the reciprocal interactions of HutC protein with P_{hutFC} DNA from both *P. aeruginosa* PAO1 and *P. fluorescens* SBW25.
(A) Genetic map of the P_{hutFC} promoter region of *P. aeruginosa* PAO1. The red circle on the PhutFC-176 probe indicates the end labelled by biotin.
(B-E) Representative EMSA gel images. Lane 1 was negative control without $HutC_{His6}$. In lanes 2 to 8, $HutC_{His6}$ was added at 70, 140, 200, 300, 400, 600 and 800 nM, respectively. DNA probe and $HutC_{His6}$ protein used for each assay are as indicated. The position of free DNA probe is denoted by asterisk. (Kiran Jayan, unpublished data)

Next, DNase I footprinting was performed with $HutC_{His6}$ and P_{hutFC} DNA probe from *P. aeruginosa* PAO1 (Figure 2.12). The result showed that $HutC_{His6}$ protected a 32-bp DNA region with the conserved inverted repeat TGTA-N2-TACA at the center. No obvious weak HutC-protected region was evidenced. Thus, the data indicate that the P_{hutFC} promoter of *P. aeruginosa* PAO1 possesses only the typical Phut site, and consistently it does not contain sequence homolog to the 40-bp weak binding site identified in the P_{hutFC} promoter of *P. fluorescens* SBW25. Together, the multiple retarded bands observed in the EMSA analysis of P_{hutFC} DNA of *P. fluorescens* SBW25 was most likely due to the presence of the weak HutC-binding site.

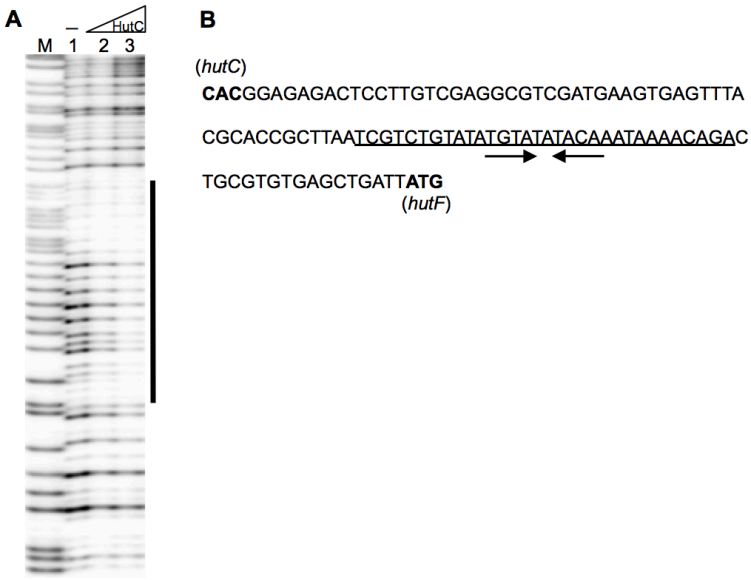

Figure 2.12. Determination of HutC-binding site in the P_{hutFC} promoter of *P. aeruginosa* PAO1.
(A) DNase I footprinting of $HutC_{His6}$ and P_{hutFC} DNA from *P. aeruginosa* PAO1. Lane 1 was negative control without $HutC_{His6}$. In lanes 2 and 3, $HutC_{His6}$ was added at 0.5 and 2.0 μM, respectively. Lane M, G+A marker. HutC-protected region is indicated by a black bar. (Kiran Jayan, unpublished data)
(B) DNA sequence of the P_{hutFC} promoter region of *P. aeruginosa* PAO1. HutC-protected region is underlined. The conserved inverted repeat is indicated by arrows. Start codon of *hutF* and the reversed start codon of *hutC* are marked in boldface type.

Finally, to estimate the oligomeric states of HutC interacting with the P_{hutFC} promoter, Job plot analysis was performed using the PhutFC-176 DNA probe from *P. aeruginosa* PAO1. The single band was shifted due to binding of a HutC dimer (Figure S2.3, Page 80). This is consistent with the result of estimation using the Hilmar Bading's method (Table S2.1, Page 80). Moreover, we have also used the Hilmar Bading's method to calculate the molecular weights of HutC forming the three dominant shifted bands observed in EMSA with the PhutFC-256 DNA probe from *P. fluorescens* SBW25 (Table 2.2). Results suggest that the retarded bands from low to high molecular weights are a HutC dimer, tetramer and hexamer, respectively. The weak retarded band occasionally detected in EMSA is most likely a trimer, as it is positioned between the dimer and tetramer.

Table 2.2. Calculation of the molecular weight of HutC protein(s) in the HutC-P_{hutFC} complexes of *P. fluorescens* SBW25 by Hilmar Bading's method

	Migration distance (cm)	Molecular weight of HutC protein(s) (KDa)	Number of HutC protein(s)
Complex 3	4.40	153.13	5.53
Complex 2	5.00	113.75	4.11
Complex 1	6.00	65.63	2.37
Free DNA	8.25	--	--

2.2.3.4 Identification of a novel HutC-binding site in the P_{hutFC} promoter of *P. fluorescens* SBW25

The data presented thus far indicate that the P_{hutFC} promoter of *P. fluorescens* SBW25 contains a weak HutC-binding site, which is absent in the corresponding P_{hutFC} promoter of *P. aeruginosa* PAO1. A closer inspection of the 40-bp weak HutC-binding sequence led to identification of an imperfect inverted repeat sequence (ACACGACCGGGGTGC), which is very similar to the consensus sequence of the NtrC binding sites (GCACCA-N3-TGGTGC) (shown in Figure 2.10). Hence, this novel HutC-binding site was designated Pntr on the basis of the functional characterization described below. Of note, a search of putative Pntr site in the P_{hutFC} promoter among *Pseudomonas* genomes showed that Pntr site is species-specific; it is conservatively present in *P. fluorescens*, *P. chlororaphis*, *P. orientalis* and *P. simiae*, but absent in most other *Pseudomonas* species (Figure 2.13).

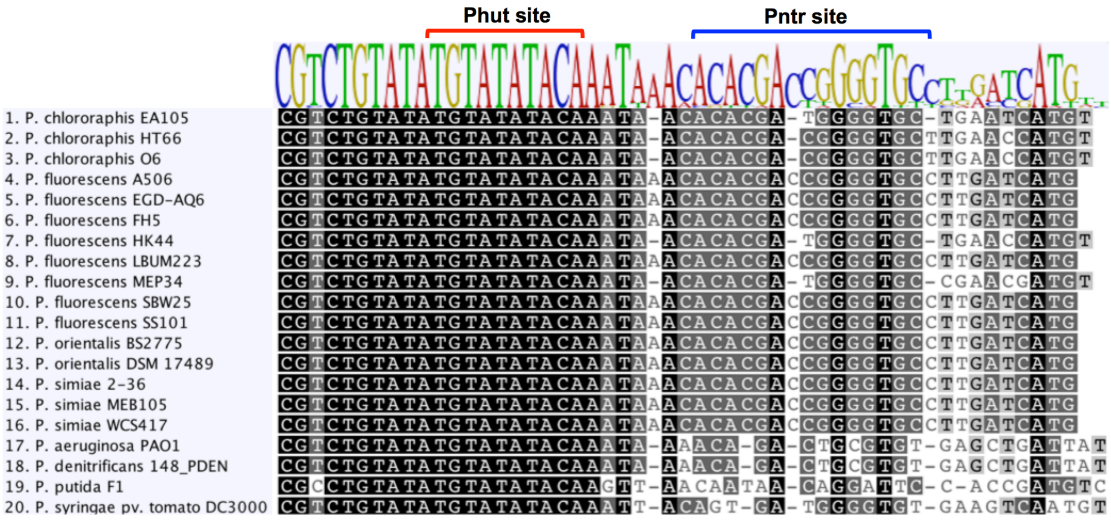

Figure 2.13. *In silico* analysis of the HutC-binding Pntr site in the P_{hutFC} promoter of *Pseudomonas* species. The sequence logo and alignment were generated by Geneious 9.0.5.

To test the functionality of the Pntr site in *P. fluorescens* SBW25, a 256-bp P_{hutFC} promoter DNA was subject to site-directed mutagenesis whereby the putative critical residues (ACACGACCGGGGTGC) were substituted with random sequences (ATGAGCCCGGCAGAA). The resultant DNA variant $P_{hutFC\text{-}Mut1}$ was used for EMSA analysis *in vitro*, together with the wild-type DNA fragment as a control (Figure 2.14). Consistent with our expectation, only one shifted band was observed with the purified $HutC_{His6}$, and it had the similar migration distance with the lowest protein/DNA complex for the wild-type P_{hutFC} predicted to be formed by a HutC dimer.

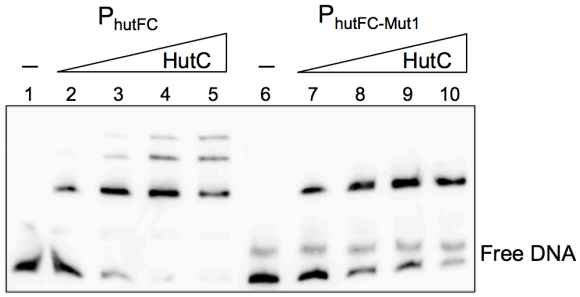

Figure 2.14. EMSA analysis showing Pntr site is involved in HutC binding. In lanes 1 to 10, $HutC_{His6}$ was added at the concentrations of 0, 73, 219, 365, 584, 0, 73, 219, 365 and 584 nM, respectively. An extra band for free $P_{hutFC\text{-}Mut1}$ DNA probe was formed, which could be caused by DNA tertiary structure. This band is absent in denatured agarose gel.

2.2.3.5 The proposed model for HutC interaction with the P_{hutFC} promoter of *P. fluorescens* SBW25

Data presented in this work indicate that HutC mediates the histidine-induced expression of *hutF* and *hutC* by targeting two sites, Phut and Pntr, in the overlapping promoter region. As shown in Figure 2.15, on the decrease of urocanate, HutC first forms a stable dimer, with each monomer binding to one half site of the strong Phut site; next, HutC binds to the adjacent Pntr site as a dimer, giving rise to two dimers binding to the operator site. Finally, a HutC hexamer is formed when urocanate is absent (or present at extremely low concentrations), ensuring a tight repression of both *hutF* and *hutC*. The dynamic process of HutC interacting with the Phut and Pntr sites is complex, and it certainly involves multiple transition steps. However, it becomes clear from our data that dimer, tetramer and hexamer are the most stable oligomeric states for HutC acting on the P_{hutF} and P_{hutC} promoters.

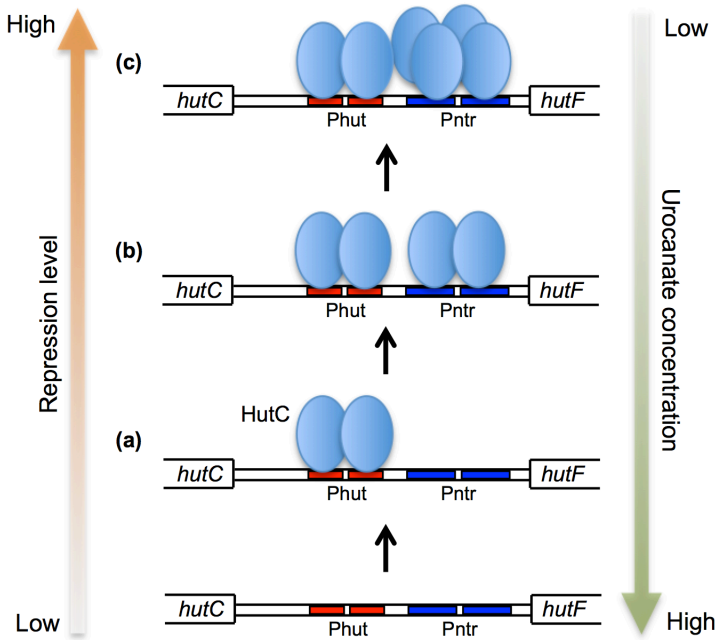

Figure 2.15. Model of HutC function in regulating promoter activities of P_{hutF} and P_{hutC} of *P. fluorescens* SBW25. In the presence of histidine (or urocanate) at a high concentration, HutC is dissociated from the P_{hutFC} promoter region. On the decrease of urocanate, HutC forms a stable dimer, with each monomer binding to one half site of the strong Phut site (a). Next, HutC binds to the adjacent Pntr site as a dimer (b), giving rise to two dimers binding to the operator site (c) when urocanate is absent or present at extremely low concentrations. This dynamic process is reversed on the increase of urocanate.

Finally, we compared the HutC binding affinities between P_{hutU} and P_{hutFC} promoters. To do this, equilibrium dissociation constant (Kd) was calculated on the basis of the EMSA gel images presented in Figures 2.2B and 2.9B. Results showed that HutC binds to P_{hutU} promoter at a higher affinity (Kd=44.6 nM) than that of the P_{hutFC} promoters (Kd=90.6 nM) (Figure 2.16). The underlying physiological reasons are not very clear. However, a relatively lower binding affinity for the P_{hutC} promoter is likely necessary for the expression of a sufficient amount of HutC when histidine concentration fluctuates at low levels.

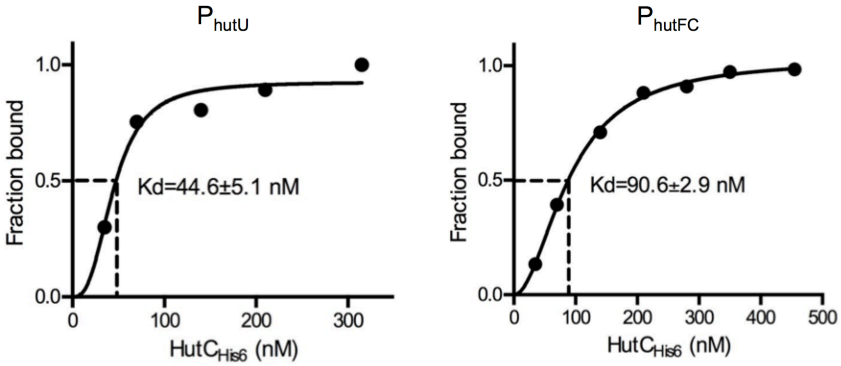

Figure 2.16. Determination of the equilibrium dissociation constant (Kd) of HutC binding to the P_{hutU} and P_{hutFC} promoters.

2.3 Discussion

In this chapter, we examined the molecular interactions between the HutC repressor and its targeting promoter DNAs (P_{hutU} and P_{hutF}) in *hut* operons of *P. fluorescens* SBW25. Results indicate complex oligomerization of the HutC protein determined by varying levels of the urocanate effector. The conserved HutC-binding inverted repeat (TGTA-N_2-TACA) was identified in the P_{hutU} and P_{hutFC} promoters, whereas the modes of HutC interacting with these two DNA targets are different. These differences imply the coordination of HutC in regulating the expression of the three *hut* operons. Moreover, our research found that it is the DNA sequences, not HutC protein, to determine the oligomeric state of HutC when interacting with target DNAs. Importantly, a newfound Pntr site for HutC binding was identified in the P_{hutFC} promoter, which is distinct to the Phut site recognized by HutC. That HutC can bind to two distinct DNA sequences reveals complexity of the molecular mechanisms of HutC interacting with the targeting DNA sites.

In *P. fluorescens* SBW25, oligomerization of HutC was observed when binding to both P_{hutU} and P_{hutFC} promoters. However, the case is different in some other bacteria. In *Brucella abortus*, only one HutC-P_{hut} complex was observed in EMSA, and the HutC-protected region in the *hut* promoter is only 20 bp centered by a short inverted repeat sequence (Sieira *et al.*, 2010). Similar results were also obtained in a study on *Klebsiella pneumoniae*, which identified a 20-bp dyad symmetric sequence critical for HutC binding in *hut* promoter (Osuna *et al.*, 1994). These results suggest that a HutC dimer binds to a dyad symmetric sequence of its target DNA, without involving complex oligomerization. Additionally, the effector-binding domain (UTRA domain) of members from the GntR/HutC subfamily also serves as a dimerization domain, and the mode of protein dimerization is conserved throughout the GntR/HutC subfamily (Fillenberg *et al.*, 2016). Our research found that HutC forms oligomers of different levels when interacting with its target DNAs, and we evidenced that the operator DNA sequences play a decisive role in the oligomerization of HutC.

It is not uncommon for transcriptional regulators to form protein oligomers when regulating gene expression. Oligomerization of repressor proteins is beneficial for tight control of regulated genes. First, multiple repressor molecules lengthen the occupancy of operator DNA by increasing the local concentration of repressor, which ultimately increases the repression efficiency (Lloyd *et al.*, 2001; Rojo, 1999). In *P. fluorescens* SBW25, due to formation of higher-order oligomers the HutC-mediated repression can be fully relieved only when the concentration of urocanate is high and stable. Second, for some repressors, oligomerization of repressor molecules causing a large protein-protected region on target DNA is critical for transcriptional repression. The auto-regulation of DnaA protein from *E. coli* is an example. A DnaA monomer specifically binds to the DnaA box located between the two promoters of *dnaA*. Subsequently, oligomerizaiton of DnaA protein proceeds to the two promoters from the DnaA box, thereby occluding RNA polymerase binding to both two promoters (Lee & Hwang, 1997). Third, oligomerization is required for some repressors to achieve maximal repression on target genes, e.g., LacI of *E. coli*. Tetramer assembly by self-association of LacI is essential for the formation of looped DNA structure that plays a pivotal role in maximizing repression of the *lac* operon (Chakerian & Matthews, 1992).

Oligomerization of DNA-binding proteins can be achieved by different mechanisms. The DnaA oligomerization is caused either by protein intrinsic aggregation property or by nonspecific binding of DnaA to DNA surrounding the first DnaA protein (Lee & Hwang, 1997). Oligomerization of regulatory proteins can also be caused by presence of multiple binding sites in the regulated promoter, and cooperative binding of proteins to DNA is commonly involved to increase binding affinity (Porter *et al.*, 1993; Sieira *et al.*, 2016). Additionally, cofactors of a regulator can also affect its oligomeric state. An example is the well-studied TyrR protein of *E. coli*, which is able to interact with three aromatic amino acids, tyrosine, phenylalanine and tryptophan. TyrR forms dimers in solution, while in the conditions with tyrosine and ATP the TyrR dimers associate to hexamers. TyrR proteins with different oligomeric states vary in binding affinities to certain operator sites (Pittard *et al.*, 2005). It should be stressed that DNA sequence of the operator sites in the P_{hut} promoters determine the oligomeric state of HutC. The protein-DNA binding assays performed with HutC proteins from *P. fluorescens* SBW25 and *P. aeruginosa* PAO1 showed that HutC proteins from different *Pseudomonas* species share the same DNA binding properties, whereas the variations in DNA sequence of the operators modify the mode of HutC action.

HutC is involved in coordinated expression of the three *hut* operons, which is crucial for bacteria to adapt to the environmental changes of histidine availability. First, the modes of HutC-DNA interactions are different between the P_{hutU} and P_{hutFC} promoters. In addition, the affinity of HutC binding to the P_{hutU} promoter is higher than the P_{hutFC} promoter. Thus, when histidine is absent or present at extremely low concentrations, the structural operon *hutU-G* is repressed while *hutC* can still express at a certain level to bind to the P_{hut} promoters. A previous study on *P. putida* showed that HutC has similar binding affinities for P_{hutU} and P_{hutFC} promoters, and same amount of urocanate is required for equivalent inhibition of binding, suggesting that HutC-DNA interactions are identical for these two promoters (Hu *et al.*, 1989). Our findings in *P. fluorescens* SBW25 extended the knowledge of HutC-P_{hut} interactions. Second, the HutC-binding site in the P_{hutFC} promoter is closer to the *hutF* coding region than the *hutC* coding region, which might provide a tighter control on the expression of *hutF* over *hutC*. By this way, the auto-regulation of transcriptional factor (TF) is slightly weaker than the regulation of structural genes. It is also widely observed in members of the GntR family that when transcription factors regulate divergently transcribed operons by binding to a single operator site in between, the operator site is slightly closer to the structural

operon, not the operon with TF genes (Suvorova *et al.*, 2015). Importantly, identification of the Pntr site in the P_{hutFC} promoter deepened our understanding on the HutC-mediated regulation of *hut* genes. By binding to both the Phut and Pntr sites HutC forms a hexamer on the P_{hutFC} promoter and consequently extends the protein-protected region into the *hutF* coding region. Accordingly, the HutC-mediated repression on *hutF* could be further strengthened in the absence of histidine.

2.4 Materials and Methods

2.4.1 Bacterial strains and growth conditions

One Shot® TOP10 (Invitrogen) chemically competent *E. coli* was used for transferring pCR™8/GW/TOPO® vector (Invitrogen, Auckland) with cloning PCR products for subsequent sequencing. *E. coli* DH5αλ_{pir} was used for general gene cloning and tri-parental conjugation of *P. fluorescens* SBW25. *E. coli* BL21 (DE3) was used for protein purification. Other bacterial strains and plasmids used in this work are listed in Table 2.3. Luria-Bertani (LB) medium was routinely used to grow *P. fluorescens* and *E. coli* strains at 28°C and 37°C, respectively. Strains for β-galactosidase assays were grown in minimal M9 salt medium (Sambrook *et al.*, 1989) with 20 mM succinate and 1 mg/ml NH_4Cl as the sole carbon and nitrogen sources. When required, antibiotics were used at the following concentrations: ampicillin (Ap), 100 μg/ml; tetracycline (Tc), 15 μg/ml; spectinomycin (Sp), 100 μg/ml; kanamycin (Km), 50 μg/ml; gentamicin (Gm), 25 μg/ml; nitrofurantoin (NF), 100 μg/ml.

Table 2.3. Bacterial strains and plasmids used in this work

P. fluorescens strain	Genotype and characteristics	Source or reference
SBW25	Wild-type strain isolated from phyllosphere of sugar beet	(Bailey *et al.*, 1995)
MU60-1	Δ*hutC*, SBW25 devoid of *pflu0359*	This work
MU60-2	SBW25 carrying mini-Tn*7*T-Gm-lacZ::PhutU	This work
MU60-3	SBW25Δ*hutC* carrying mini-Tn*7*T-Gm-lacZ::PhutU	This work
MU60-4	SBW25 carrying mini-Tn*7*T-Gm-lacZ::PhutU-M1	This work
MU60-5	SBW25Δ*hutC* carrying mini-Tn*7*T-Gm-lacZ::PhutU-M1	This work

MU60-6	SBW25 carrying mini-Tn7T-Gm-lacZ::PhutU-M2	This work
MU60-7	SBW25Δ*hutC* carrying mini-Tn7T-Gm-lacZ::PhutU-M2	This work
Plasmid		
pCR2.1-TOPO	Cloning vector, Km^r, Ap^r	Invitrogen
pCR8/GW/TOPO	Cloning vector, Sp^r	Invitrogen
pCR8-PhutU-M1	Recombinant plasmid for amplifying PhutU-M1 probe DNA	This work
pCR8-PhutU-M2	Recombinant plasmid for amplifying PhutU-M2 probe DNA	This work
pCR2.1-PhutU-MW	Recombinant plasmid for amplifying PhutU-M1&2 probe DNA	This work
pTrc99A	Protein expression vector, P_{tac} promoter, Ap^r	(Amann *et al.*, 1988)
pTrc99A-hutC	pTrc99A carrying $HutC_{His6}$ from SBW25, Ap^r	This work
pET14b-hutC (PAO1)	pET14b carrying $HutC_{His6}$ from PAO1, Ap^r	M.L. Gerth
pUX-BF13	Helper plasmid for transposition of mini-Tn7 element, Ap^r	(Bao *et al.*, 1991)
pUC18-mini-Tn7T-Gm-lacZ	Mini-Tn7 vector for transcriptional fusion to promoterless lacZ, Ap^r, Gm^r	(Choi *et al.*, 2005)
pUC18-Tn7T-lacZ-PhutU	pUC18-mini-Tn7T-Gm-lacZ containing *lacZ* fusion to P_{hutU} promoter	This work
pUC18-Tn7T-lacZ-PhutU-M1	pUC18-mini-Tn7T-Gm-lacZ containing *lacZ* fusion to $P_{hutU-M1}$ promoter	This work
pUC18-Tn7T-lacZ-PhutU-M2	pUC18-mini-Tn7T-Gm-lacZ containing *lacZ* fusion to $P_{hutU-M2}$ promoter	This work
pCR2.1-PhutFC-Mut	Recombinant plasmid for amplifying PhutFC-Mut1 probe DNA	This work

2.4.2 Strains construction

Standard protocols were used for plasmid DNA isolation, restriction endonuclease digestion, ligation and PCR reaction. Restriction enzymes were obtained from New England Biolabs. Ligation reactions were conducted using T4 DNA ligase from Invitrogen (Auckland, New Zealand). PCR reactions were performed using *Taq* DNA polymerase from Invitrogen. Oligonucleotide primers used in this chapter are listed in Table 2.4. pCR8/GW/TOPO® Cloning Kit (Invitrogen) was used for TA cloning. For gene cloning from the genomic DNA of *P. fluorescens* SBW25, PCR product was first cloned into pCR8/GW/TOPO vector for DNA sequencing (Macrogen, South Korea).

Then the desired insert DNA was subcloned into destination vectors and transferred into *P. fluorescens* strains by electroporation.

Site-directed mutagenesis of *hutC* gene was achieved by a previously established procedure of SOE-PCR (splicing by overlapping extension PCR) (Horton *et al.*, 1989) in conjunction with a two-step allelic-exchange strategy using the suicide-integration vector pUIC3 (Rainey, 1999). Briefly, two pairs of primers were designed to amplify the flanking regions (~500 bp) of *hutC* gene, wherein the two primers closer to *hutC* are complementary for 20-23 bp at the join site. The two PCR products were used as DNA templates in the second-round PCR whereby the two DNA fragments were joined together. The resultant single DNA fragment was cloned into plasmid pUIC3. Next, the recombinant pUIC3 plasmid was transferred into *P. fluorescens* through conjugation with the helper plasmid pRK2013 (Ditta *et al.*, 1980). The desired allelic exchange mutants were selected by a previously described procedure of D-cycloserine enrichment (Zhang & Rainey, 2007).

Site-directed mutagenesis of the operator sites Phut-I, Phut-II or both in the P_{hutU} promoter region and the Pntr site in the P_{hutFC} promoter region was performed using SOE-PCR mentioned above. The resultant mutated DNA fragments were cloned into pCR8/GW/TOPO or pCR2.1-TOPO® (Invitrogen) as DNA template for PCR amplification of DNA probes in EMSA or as intert fragment subcloned into another destination vector such as pUC18-mini-Tn7T-Gm-lacZ.

Table 2.4. Oligonucleotides used in this work

Primer	Sequence (5′ - 3′)[a]	Application
HutC-ProF	aaatttaccatgggccatcatcatcatcatCCGACTCCGCCCGCCAAGTCTC	Expression of HutC protein from SBW25
HutC-ProR	aaatttgaagcttGCGCCAGACGCTTATTGCACTCAT	
PhutU_D	aaatttactagtATTTGTTACCGAATGCCCCAGC	Amplifying DNA probe PhutU-325
Bio-UR[b]	GCTTGTTACCGTGGGCGGCACGGAT	
PhutU_B	aaatttactagtGTCGGTACATCTATGACTGAAAC	Mutagenizing Phut-I site in P_{hutU} promoter
PhutU-mut1	cttgtacaccggAGCATATGCAATCGAG	
PhutU-mut2	catatgctccggTGTACAAGTAAAGATGTG	
hutU-T7R2	TGTTCATCAGCATGCGCAGC	

PhutU-mut3	atctttacggccACATACAAGCATATGCAA	Mutagenizing Phut-II site in P_{hutU} promoter with primers PhutU_B and hutU-T7R2
PhutU-mut4	ttgtatgtggccGTAAAGATGTGTGCGTAA	
hutU-M1	ttacggccacaccggAGCATATGCAATCG AGCGGCCA	Mutagenizing Phut-I and Phut-II site in P_{hutU} promoter with primers PhutU_B and hutU-T7R2
hutU-M2	atgctccggtgtggccGTAAAGATGTGTGC GTAAGAG	
PhutU_Rev	aaatttctgcagAGCTTGTTACCGTGGGC GGC	P_{hutU} transcriptional fusion to lacZ with primer PhutU_D
Bio-F-new2[b]	CAGCCCATCGGCGCTGACTT	Amplifying DNA probe PhutFC-256
hutF-F	aactagtACAAGGGCGCCGGACTTTCG	
PAO1-hutCF	aactagtGGACATTTCGCGCCCAGCCT	Amplifying DNA probe PhutFC-176
PhutFC-bio1[b]	GGAGGAAGAGGACGTCAC	
hutF1	gaagatcTGATCTGACGCGACAGTTC	Mutagenizing Pntr site in P_{hutFC} promoter
hutF-M1	aacatgagcccggcagaaCTTGATCATGTC CGCTTTCTT	
hutF-M2	aagttctgccgggctcatGTTTATTTGTATAT ACATATAC	
hutC5	cgggatcCTCTTGGGCTCGGCGACGA	

[a] Artificial sequences integrated into the primers are shown in lowercase with restriction sites underlined.
[b] Primers are labeled by biotin at the 5′ end.

2.4.3 β-galactosidase Assay

To construct transcriptional fusions to the promoterless *lacZ* the promoter region (~500 bp) of genes was cloned into plasmid pUC18-mini-Tn*7*T-Gm-*lacZ*. The *lacZ* fusion in the plasmid was introduced into *P. fluorescens* together with plasmid pUX-BF13 by electroporation. The mini-Tn*7* element carrying transcriptional fusion integrates into the chromosome at a single attTn*7* site downstream of the *glmS* gene (Choi *et al.*, 2005).

β-galactosidase assays for measuring the expression of *lacZ* fusions were performed following a standard protocol with 4-methylumbelliferyl-β-D-galactoside (4MUG) as the enzymatic substrate (Zhang *et al.*, 2006). Enzymatic reactions were performed using bacterial cells grown in the tested media for 2-8 hours after inoculation. The fluorescent product, 7-hydroxy-4-methylcoumarin (4MU), was measured at 460 nm with an excitation wavelength of 365 nm on a Synergy 2 plate reader (Bio-Tek). β-

galactosidase activity was expressed as the amount of 4MU (μM) produced per minute per cell (OD_{600}).

2.4.4 Electrophoretic mobility shift assays

The coding region of HutC was amplified by PCR from the genomic DNA of *P. fluorescens* SBW25 and subsequently cloned into the protein expression vector pTrc99A (Amann *et al.*, 1988) with the integration of six histidine residues at the N-terminal. The recombinant plasmid pTrc99A-hutC was transformed into *E. coli* BL21(DE3) for protein overexpression (Studier & Moffatt, 1986). IPTG was added at the final concentration of 1 mM to the *E. coli* culture (OD_{600}, 0.5~0.7) to induce protein expression for 4 hours at 37°C. Cells were lysed by sonication using the Sonicator S-4000 (Misonix, Inc). The His6-tagged protein was purified using TALON® metal affinity resin (Clontech laboratories, Inc.) according to the manufacturer's instructions. The type of buffer solution and pH for protein preparation were adjusted based on the properties of protein. Twenty mM HEPES buffer (pH 7.4) was used for the purification of HutC. Concentration of the purified protein was determined by the Bradford method (Bradford, 1976).

DNA probes for EMSA were amplified by PCR using primers listed in Table 2.4. One of each pair of primers is labeled by biotin at the 5′ end. DNA probes were purified by phenol-chloroform extraction. The DNA probes used in this work are summarized in Table 2.5. EMSA reactions were set up by mixing 20 nM DNA probe, varying concentrations of protein, 1 μg salmon sperm DNA (Invitrogen) in EMSA binding buffer (10 mM HEPES, 50 mM KCl, 5 mM $MgCl_2$ and 1 mM DTT, pH 7.5) to a final volume of 20 μl. After incubation at room temperature for 30 minutes, reactions were electrophoresed on 6% native polyacrylamide gel in 0.5x TBE buffer at 120V at 4°C. The DNA in gel was transferred to positively charged Whatman® Nytran™ SuPerCharge nylon membrane (Sigma-Aldrich) by electroblotting and immobilized by incubating the membrane at 80°C for 30 minutes. LightShift™ chemiluminescent EMSA kit (Thermo Fisher Scientific) was used to detect the biotin-labelled DNA probes, and the image was visualized by LAS-4000 Luminescent Imager equipped with ImageQuant™ LAS 4000 software (FujiFilm).

Table 2.5. DNA probes used in this work

DNA probe	Primers used for PCR amplification	Length (bp)	Labeling	Application
PhutU-325	PhutU_D & Bio-UR	325	5′ end labeled by biotin	EMSA and DNase I footprinting of HutC and P_{hutU} promoter DNA
PhutU-M1	PhutU_D & Bio-UR	325	5′ end labeled by biotin	EMSA of HutC and P_{hutU} promoter DNA carrying a mutant allele of Phut-I site
PhutU-M2	PhutU_D & Bio-UR	325	5′ end labeled by biotin	EMSA of HutC and P_{hutU} promoter DNA carrying a mutant allele of Phut-II site
PhutU-M1&2	PhutU_D & Bio-UR	325	5′ end labeled by biotin	EMSA of HutC and P_{hutU} promoter DNA carrying a mutant allele of Phut-I and Phut-II sites
PhutFC-256	Bio-F-new2 & hutF-F	256	5′ end labeled by biotin	EMSA and DNase I footprinting of HutC and P_{hutFC} promoter DNA
PhutFC-176	PAO1-hutCF & PhutFC-bio1	176	5′ end labeled by biotin	EMSA and DNase I footprinting of HutC and P_{hutFC} promoter DNA from PAO1
PhutFC-Mut1	Bio-F-new2 & hutF-F	256	5′ end labeled by biotin	EMSA of HutC and P_{hutFC} promoter DNA carrying a mutant allele of Pntr site

2.4.5 DNase I footprinting assays

Reactions were set up under the same condition described for EMSA but in a larger volume of 50 µl, wherein 2 µM DNA probe was used. After incubation at room temperature for 30 minutes, 50 µl of cofactor solution (5 mM $CaCl_2$ and 10 mM $MgCl_2$) was added. Then the samples were treated with 0.02 U of DNase I (Invitrogen) for 5 min at room temperature. After termination of the reactions with 100 µl of DNase I stop solution (200 mM NaCl, 20 mM EDTA and 1% SDS), DNA was extracted with an equal volume of 1:1 phenol/chloroform mixture and precipitated by adding 1 µl of glycogen (20 mg/ml, Fermentas), $1/10^{th}$ volume of 3 M sodium acetate (pH 5.2) and three volumes of ethanol. Following incubation at -20°C for at least 1 hour, DNA was pelleted by centrifugation and resuspended in 8 µl of loading buffer (95% formamide, 0.05% bromophenol blue and 20 mM EDTA). After denaturing at 95°C for 10 min, the samples were electrophoresed on a 6% denaturing urea-polyacrylamide gel (21 x 40 cm) in 1x TBE buffer using the Sequi-Gen® GT electrophoresis system (Bio-Rad

Laboratories Pty). Then DNA was transferred from the gel to positively charged nylon membrane by contact blotting (Petersen *et al.*, 1996). Detection of the DNA fragments was conducted as described above in EMSA. A G+A marker showing the sequence of DNA fragments was included in the gel. It was produced with the same biotin-labelled DNA probe by Maxam-Gilbert chemical sequencing reactions (Maxam & Gilbert, 1980).

2.4.6 Determination of protein binding affinity

HutC binding affinities to the target DNAs were presented as equilibrium dissociation constant (Kd), which was calculated on the basis of EMSA gel images. Fractions of free DNA probe and protein-bound DNA probe were quantitated based on the intensity of DNA bands by using ImageJ software. The fraction of protein-bound probe was plotted against concentrations of protein using Prism 6 software. Kd value was presented as the concentration of protein added by which 50% of probes are bound by the protein.

2.4.7 Cross-linking with formaldehyde

Oligomerization of HutC *in vitro* was determined by cross-linking with formaldehyde (Nadeau & Carlson, 2007). Five hundred mM formaldehyde stock solution was prepared and incubated at 100°C for 24 hours in a heating block, then stored at 4°C. Reactions were set up by mixing 19 μM HutC protein, 20 mM HEPES (pH 8.2), 100 mM NaCl, 0.1 mM EDTA (pH 8.0) and 25 mM formaldehyde to a total volume of 20 μl and incubated at 25°C for 1, 2.5 and 4 hours, respectively. An equal volume of SDS buffer (20% glycerol, 5% β-mercaptoethanol, 4% SDS, 0.003% coomassie blue and 0.125 M Tris-HCl, pH6.8) was added to terminate the reactions. 25 μl of each sample was subject to SDS-PAGE analysis.

2.4.8 Stoichiometric analysis of protein-DNA interactions

Continuous variation analysis (Job plot)

Job plot (Beno *et al.*, 2011; Huang, 1982) was used to determine the stoichiometry of HutC-P_{hutU} interactions. EMSA was first performed with $HutC_{His6}$ and P_{hutU} DNA probe (PhutU-325), wherein the total molar concentration of protein and DNA remained constant in a series of reactions but varied in their relative composition. The reactions were set up as shown in Table 2.6. The procedure of EMSA was the same as previously described. Intensity of each protein/DNA complex in the EMSA gel image was quantitated using ImageJ software and plotted against the fractions of protein by Prism 6 software. The binding stoichiometry of each HutC-P_{hutU} complex was determined by the protein/DNA ratio when the amount of this complex reached its maximum.

Table 2.6. Components of EMSA reactions for Job plot

Reactions	R1	R2	R3	R4	R5	R6	R7	R8	R9	R10
10x EMSA binding buffer (µl)	2	2	2	2	2	2	2	2	2	2
1 µg/µl salmon sperm DNA (µl)	1	1	1	1	1	1	1	1	1	1
200 nM PhutU-325 (µl)	10	8	7	6	5	4	3	2	1	0.5
200 nM $HutC_{His6}$ (µl)	0	2	3	4	5	6	7	8	9	9.5
MilliQ H_2O (µl)	7	7	7	7	7	7	7	7	7	7

Hilmar Bading's method

Stoichiometry of protein-DNA interactions was also evaluated by a method based on mobility difference between free DNA and protein-bound DNA during EMSA, which was introduced by Hilmar Bading (Bading, 1988). The principle of this method is the quotient of the migration distances of free DNA (m) and protein-DNA complex (m') is a function of the molecular weight (MW) of the protein(s) bound to the DNA. The equation for calculating the molecular weight of the protein(s) was deduced:

$$MW = (m/m' - 1)\ K$$

The proportionality factor K shows a negatively correlated linear relationship with the acrylamide concentration of EMSA gel. K value for a 6% native polyacrylamide gel is approximately 175 according to a plot of K value against acrylamide concentrations by a known protein-DNA interaction. Migration distances of free DNA (m) and protein-bound DNA (m') in the EMSA gel were measured and the molecular weight of protein(s) in each complex was calculated using the equation shown above.

2.5 References

Allison, S. L., & Phillips, A. T. (1990). Nucleotide sequence of the gene encoding the repressor for the histidine utilization genes of *Pseudomonas putida*. *J Bacteriol, 172*(9), 5470-5476.

Amann, E., Ochs, B., & Abel, K. J. (1988). Tightly regulated tac promoter vectors useful for the expression of unfused and fused proteins in *Escherichia coli*. *Gene, 69*(2), 301-315.

Bading, H. (1988). Determination of the molecular weight of DNA-bound protein(s) responsible for gel electrophoretic mobility shift of linear DNA fragments examplified with purified viral myb protein. *Nucleic Acids Res, 16*(12), 5241-5248.

Bailey, M. J., Lilley, A. K., Thompson, I. P., Rainey, P. B., & Ellis, R. J. (1995). Site directed chromosomal marking of a fluorescent pseudomonad isolated from the phytosphere of sugar beet; stability and potential for marker gene transfer. *Mol Ecol, 4*(6), 755-763.

Bao, Y., Lies, D. P., Fu, H., & Roberts, G. P. (1991). An improved Tn7-based system for the single-copy insertion of cloned genes into chromosomes of gram-negative bacteria. *Gene, 109*(1), 167-168.

Beno, I., Rosenthal, K., Levitine, M., Shaulov, L., & Haran, T. E. (2011). Sequence-dependent cooperative binding of p53 to DNA targets and its relationship to the structural properties of the DNA targets. *Nucleic Acids Res, 39*(5), 1919-1932. doi: 10.1093/nar/gkq1044

Bradford, M. M. (1976). A rapid and sensitive method for the quantitation of microgram quantities of protein utilizing the principle of protein-dye binding. *Anal Biochem, 72*, 248-254.

Chakerian, A. E., & Matthews, K. S. (1992). Effect of *lac* repressor oligomerization on regulatory outcome. *Mol Microbiol, 6*(8), 963-968.

Choi, K. H., Gaynor, J. B., White, K. G., Lopez, C., Bosio, C. M., Karkhoff-Schweizer, R. R., & Schweizer, H. P. (2005). A Tn7-based broad-range bacterial cloning and expression system. *Nat Methods, 2*(6), 443-448. doi: 10.1038/nmeth765

Ditta, G., Stanfield, S., Corbin, D., & Helinski, D. R. (1980). Broad host range DNA cloning system for gram-negative bacteria: construction of a gene bank of *Rhizobium meliloti*. *Proc Natl Acad Sci U S A, 77*(12), 7347-7351.

Fillenberg, S. B., Friess, M. D., Korner, S., Bockmann, R. A., & Muller, Y. A. (2016). Crystal Structures of the Global Regulator DasR from *Streptomyces coelicolor*: Implications for the Allosteric Regulation of GntR/HutC Repressors. *PLoS One, 11*(6), e0157691. doi: 10.1371/journal.pone.0157691

Gorelik, M., Lunin, V. V., Skarina, T., & Savchenko, A. (2006). Structural characterization of GntR/HutC family signaling domain. *Protein Sci, 15*(6), 1506-1511. doi: 10.1110/ps.062146906

Hervas, A. B., Canosa, I., & Santero, E. (2008). Transcriptome analysis of *Pseudomonas putida* in response to nitrogen availability. *J Bacteriol, 190*(1), 416-420. doi: 10.1128/JB.01230-07

Horton, R. M., Hunt, H. D., Ho, S. N., Pullen, J. K., & Pease, L. R. (1989). Engineering hybrid genes without the use of restriction enzymes: gene splicing by overlap extension. *Gene, 77*(1), 61-68.

Hu, L., Allison, S. L., & Phillips, A. T. (1989). Identification of multiple repressor recognition sites in the *hut* system of *Pseudomonas putida*. *J Bacteriol, 171*(8), 4189-4195.

Huang, C. Y. (1982). Determination of binding stoichiometry by the continuous variation method: the Job plot. *Methods Enzymol, 87*, 509-525.

Lee, Y. S., & Hwang, D. S. (1997). Occlusion of RNA polymerase by oligomerization of DnaA protein over the *dnaA* promoter of *Escherichia coli*. *J Biol Chem, 272*(1), 83-88.

Lenski, R. E. (1991). Quantifying fitness and gene stability in microorganisms. *Biotechnology, 15*, 173-192.

Lloyd, G., Landini, P., & Busby, S. (2001). Activation and repression of transcription initiation in bacteria. *Essays Biochem, 37*, 17-31.

Maxam, A. M., & Gilbert, W. (1980). Sequencing end-labeled DNA with base-specific chemical cleavages. *Methods Enzymol, 65*(1), 499-560.

Nadeau, O. W., & Carlson, G. M. (2007). Protein Interactions Captured by Chemical Cross-linking: One-Step Cross-linking with Formaldehyde. *CSH Protoc, 2007*, pdb prot4634. doi: 10.1101/pdb.prot4634

Newell, C. P., & Lessie, T. G. (1970). Induction of histidine-degrading enzymes in *Pseudomonas aeruginosa*. *J Bacteriol, 104*(1), 596-598.

Osuna, R., Schwacha, A., & Bender, R. A. (1994). Identification of the *hutUH* operator (hutUo) from *Klebsiella aerogenes* by DNA deletion analysis. *J Bacteriol, 176*(17), 5525-5529.

Petersen, I., Reichel, M. B., & Dietel, M. (1996). Use of non-radioactive detection in SSCP, direct DNA sequencing and LOH analysis. *Clin Mol Pathol, 49*(2), M118-121.

Pittard, J., Camakaris, H., & Yang, J. (2005). The TyrR regulon. *Mol Microbiol, 55*(1), 16-26. doi: 10.1111/j.1365-2958.2004.04385.x

Porter, S. C., North, A. K., Wedel, A. B., & Kustu, S. (1993). Oligomerization of NTRC at the *glnA* enhancer is required for transcriptional activation. *Genes Dev, 7*(11), 2258-2273.

Rainey, P. B. (1999). Adaptation of *Pseudomonas fluorescens* to the plant rhizosphere. *Environ Microbiol, 1*(3), 243-257.

Rojo, F. (1999). Repression of transcription initiation in bacteria. *J Bacteriol, 181*(10), 2987-2991.

Sambrook, J., Fritsch, E.F., & Maniatis, T. (1989). Molecular Cloning: A Laboratory Manual. *Cold Spring Harbor Laboratory Press, New York, USA*.

Sieira, R., Arocena, G. M., Bukata, L., Comerci, D. J., & Ugalde, R. A. (2010). Metabolic control of virulence genes in *Brucella abortus*: HutC coordinates *virB* expression and the histidine utilization pathway by direct binding to both promoters. *J Bacteriol, 192*(1), 217-224. doi: 10.1128/jb.01124-09

Sieira, R., Bialer, M. G., Roset, M. S., Ruiz-Ranwez, V., Langer, T., Arocena, G. M., . . . Zorreguieta, A. (2016). Combinatorial control of adhesion of *Brucella abortus*

2308 to host cells by transcriptional rewiring of the trimeric autotransporter *btaE* gene. *Mol Microbiol, 103*(3), 553-565. doi: 10.1111/mmi.13576

Studier, F. W., & Moffatt, B. A. (1986). Use of bacteriophage T7 RNA polymerase to direct selective high-level expression of cloned genes. *J Mol Biol, 189*(1), 113-130.

Suvorova, I. A., Korostelev, Y. D., & Gelfand, M. S. (2015). GntR Family of Bacterial Transcription Factors and Their DNA Binding Motifs: Structure, Positioning and Co-Evolution. *PLoS One, 10*(7), e0132618. doi: 10.1371/journal.pone.0132618

Zhang, X. X., George, A., Bailey, M. J., & Rainey, P. B. (2006). The histidine utilization (*hut*) genes of *Pseudomonas fluorescens* SBW25 are active on plant surfaces, but are not required for competitive colonization of sugar beet seedlings. *Microbiology, 152*(Pt 6), 1867-1875. doi: 10.1099/mic.0.28731-0

Zhang, X. X., & Rainey, P. B. (2007). Genetic analysis of the histidine utilization (*hut*) genes in *Pseudomonas fluorescens* SBW25. *Genetics, 176*(4), 2165-2176. doi: 10.1534/genetics.107.075713

Zhang, X. X., Ritchie, S. R., & Rainey, P. B. (2013). Urocanate as a potential signaling molecule for bacterial recognition of eukaryotic hosts. *Cellular and Molecular Life Sciences, 71*(4), 541-547. doi: 10.1007/s00018-013-1527-6

2.6 Supplementary data

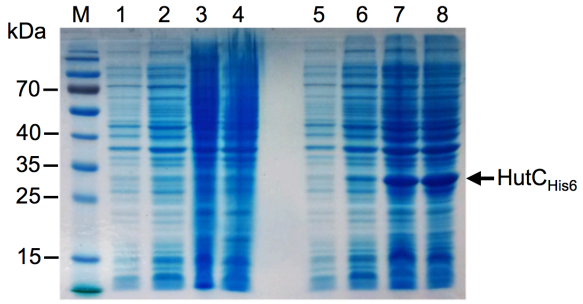

Figure S2.1. SDS-PAGE analysis of HutC expression.

To test the HutC expression on pTrc99A via IPTG induction, a small-scale expression was conducted by growing the *E. coli* BL21 (DE3) in 20 ml LB broth to OD_{600} of 0.5 - 0.7. After addition of IPTG (1.0 mM), 1-ml aliquots of the bacterial culture were taken after 1, 2, 4 hours and over-night induction at 37°C and subject to 12% SDS-PAGE analysis with Coomassie blue staining. Lane 1 - 4, Protein expression of *E. coli* BL21 (DE3) cells containing vector pTrc99A induced for 1h, 2h, 4h and overnight, respectively. Lane 5 - 8, Protein expression of *E. coli* BL21 (DE3) cells containing pTrc99A-hutC induced for 1h, 2h, 4h and overnight, respectively. Lane M, protein molecular weight marker.

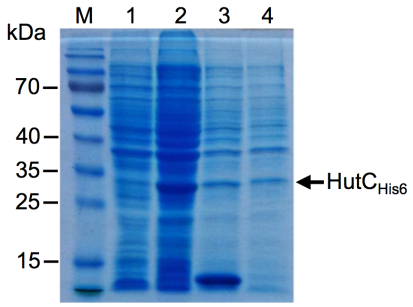

Figure S2.2. SDS-PAGE analysis of the solubility of expressed HutC protein.

E. coli BL21 (DE3) cells containing pTrc99A-hutC were induced with IPTG (1.0 mM) at 37°C for 4 hours. The cells were lysed by addition of lysozyme and sonication. The supernatant soluble fraction and the precipitated insoluble fraction were separated by centrifugation and analyzed by 12% SDS-PAGE. The result showed that more than 50% of the induced HutC protein is in the soluble fraction. Lane 1, whole cell lysate without IPTG induction. Lane 2, IPTG-induced whole cell lysate. Lane 3, soluble fraction of the induced cell lysate. Lane 4, insoluble fraction of the induced cell lysate. Lane M, protein molecular weight marker.

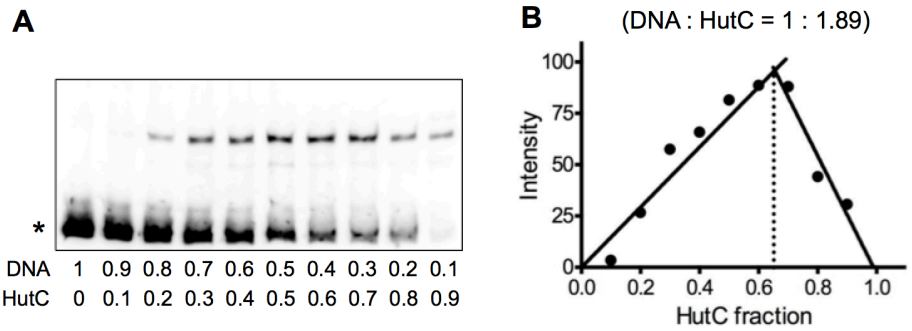

Figure S2.3. Job plot analysis determining the stoichiometry of HutC-P_{hutFC} interactions of *P. aeruginosa* PAO1.
(A) EMSA of $HutC_{His6}$ and P_{hutFC} promoter DNA (PhutFC-176). The total molar concentration of protein and DNA was maintained at 400 nM and the molar fractions of protein and DNA are indicated below. (Kiran Jayan, unpublished data)
(B) Job plot showing the DNA to protein ratio. The intersection of the lines that are least square fitted to the rising and falling subsets of the data yields the binding stoichiometry for the complex.

Table S2.1. Calculation of the molecular weight of HutC protein(s) in the HutC-$P_{hutFC\text{-}PAO1}$ complex by Hilmar Bading's method

	Migration distance (cm)	Molecular weight of HutC protein(s) (KDa)	Number of HutC protein(s)
Complex	5.40	71.30	2.49
Free DNA	7.60	--	--

Chapter 3

The HutC repressor for histidine utilization play a global regulatory role in *Pseudomonas fluorescens* SBW25

3.1 Preamble

HutC is a transcriptional repressor of histidine utilization (*hut*) genes in many Gram-negative bacteria, including *Pseudomonas fluorescens* SBW25. It regulates histidine-induced expression of *hut* genes by binding to operator sites of the *hut* operons. The HutC-mediated repression is relieved by urocanate, the first intermediate of the histidine degradation pathway. In Chapter 2, we examined the detailed molecular interactions between HutC and its operator DNA in the P_{hutU} and P_{hutFC} promoters. Results showed that HutC binds to the P_{hutU} promoter as a dimer, and the repression is strengthened via the formation of a HutC tetramer whereby higher levels of *hut* repression is achieved. Significantly, we also showed that HutC functions at the *hutF* and *hutC* promoter region by binding to two distinct sites: the canonical Phut site and a newly discovered Pntr site. The two operator sites exhibit little sequence similarity, suggesting the complexity of HutC-mediated gene regulation.

Recent progress indicates that HutC plays a surprising role in global regulation of cellular metabolism, cell motility and production of virulence factors. In a zoonotic pathogen *Brucella abortus*, HutC regulates the bacterial attachment to host cell surface by directly activating the *btaE* gene. *btaE* encodes an adhesin that translocates across the bacterial outer membrane (Sieira *et al.*, 2016). HutC is also involved in the regulation of Type IV secretion system (T4SS) by acting as a coactivator for transcription of the *virB* operon, and consequently, deletion of *hutC* causes a reduced bacterial resistance to intracellular host defences (Sieira *et al.*, 2010). Thus, all evidence showed that HutC is a master regulator of cellular metabolism and it determines the virulence of *B. abortus*. In *Yersinia pseudotuberculosis*, deletion of *hutC* abrogates biofilm formation on the host *Caenorhabditis elegans*, but enhances swimming motility in laboratory medium (Joshua *et al.*, 2015). Moreover, a transcriptomic analysis of

Pseudomonas aeruginosa PAO1 (a human opportunistic pathogen) showed that the expression of *hutC* is significantly altered during biofilm formation, suggesting a regulatory role of HutC in controlling planktonic-biofilm transition (Patell *et al.*, 2010). A separate study with *P. aeruginosa* PA14 showed that Δ*hutC* mutant has an increased ability to form biofilm and displays a strong defect in swimming motility (Yeung *et al.*, 2009). Significantly, a recent study by Zhang's group showed that the Δ*hutC* mutant of *P. aeruginosa* PAO1 is defective in the type IV pili-mediated twitching motility (X.-X. Zhang, unpublished data).

Primary data suggest that HutC also plays a global regulatory role beyond histidine catabolism in the plant growth-promoting bacterium *P. fluorescens* SBW25. Deletion of *hutC* caused a significant reduction in its ability to colonize the surface of sugar beet plants, which cannot be explained by the established role of HutC in the *hut* gene expression (Zhang & Rainey, 2007).

Research in this chapter aims to determine the specific global regulatory role of HutC in *P. fluorescens* SBW25. First, we performed a genome-scale bioinformatic analysis of putative HutC-binding sites, and their ability of binding HutC was confirmed by electrophoretic mobility shift assay (EMSA) with a selected panel of eight candidate promoters. Next, we focused on the roles of HutC in regulating the expression of the *ntrBC* operon, which encodes a two-component regulatory system for global control of cellular nitrogen metabolism. This led to the identification of two distinct HutC-binding sites in the P_{ntrBC} promoter, the Phut site and Pntr site. Furthermore, HutC and NtrC bind to the same Pntr site in the P_{ntrBC} promoter. NtrBC is self-regulated as its expression requires its own response regulator, NtrC (Schumacher *et al.*, 2013). We speculate that HutC negatively affects the expression of *ntrBC* via competing the operator site of the transcriptional activator NtrC. The physiological function of HutC in the regulation of *ntrBC* expression will be described in details in Chapter 4. We also show that HutC is involved in the regulation of swimming and swarming motilities, but not biofilm formation in *P. fluorescens* SBW25.

3.2 Results

3.2.1 Identification of putative HutC-binding sites in the genome of *P. fluorescens* SBW25

Putative HutC-binding sites were determined in the *P. fluorescens* SBW25 genome by using the matrix-based motif-scanning tool FIMO (Grant *et al.*, 2011). Briefly, a motif discovery tool MEME (http://meme-suite.org/tools/meme) was first used to generate a position-dependent letter-probability matrix on the basis of ~60 bp DNA sequence of P_{hutU} and P_{hutFC} promoters from 40 different *Pseudomonas* species currently deposited in the *Pseudomonas* database (http://www.pseudomonas.com). Then the matrix of HutC-binding motif was inputted into FIMO programme (version 4.11.2) to search for occurrences of this motif in the SBW25 genome. This resulted in 143 motif occurrences with a p-value of less than 10^{-4}. The results are summarized in Table S3.1 (Page 117), which is sorted by increasing p-value. The p-value of a motif occurrence is defined as the probability of a random sequence of the same length as the motif matching that position of the sequence with as good or better score (Grant *et al.*, 2011). Eighty-eight out of the 143 predicted HutC-binding sites (62%) are located within 500 bp upstream of a gene, which likely contains a promoter. The rest are located in a region where there is no potential regulated gene downstream.

Among the potential HutC-regulated genes, ten are likely involved in amino acid metabolism, including *hisB* in histidine biosynthesis, *argA* in arginine biosynthesis, genes involved in aspartate and arginine catabolic processes and also several genes encoding amino acid transport proteins. Five candidate genes take part in energy metabolism, i.e., *aceE* and *glcB* in pyruvate metabolism, *gcl* in glyoxylate catabolism, an enzymatic gene for D-glucarate degradation and transporter genes for glucarate and trehalose. Moreover, the candidate genes also include *glnE* and *ntrBC*, which play an important role in cellular nitrogen metabolism. Genes involved in the catabolic processes of phosphatidylcholine and peptidoglycan were also identified. Furthermore, three candidate genes are likely involved in the type IV pili assembly.

3.2.2 Experimental verification of the putative HutC-binding sites

Subsequently, eight putative HutC-binding sites were subjected to experimental verification using the standard technique EMSA. They were selected because the potential regulated genes encode functions of our interests and also show relatively higher levels of similarity with the consensus HutC-binding sequence. Sequence features of the predicted HutC-binding sites and the predicted functions of the eight genetic loci are summarized in Table 3.1.

Table 3.1. Information of the experimentally tested candidate HutC-binding sites

Putative HutC-binding palindrome		Adjacent gene(s)	
Sequence	Location	Locus tag	Putative or established function
TGTATATACA [a]	PFLU0848 ■ PFLU0849 [b]	PFLU0848	Plc (phosphatidylcholine-hydrolyzing phospholipase C)
		PFLU0849	5-dehydro-4-deoxyglucarate dehydratase
TGTATAAACA	PFLU2466 ■ PFLU2467	PFLU2466	Hypothetical protein
		PFLU2467	AraC family transcriptional regulator
CGTATATACA	PFLU0461 ■ PFLU0460	PFLU0460	AceE (pyruvate dehydrogenase subunit E1)
		PFLU0461	GlnE (Bifunctional glutamine-synthetase adenylyltransferase/deadenyltransferase)
TGTATGCACA	PFLU0325 ■ PFLU0327	PFLU0327	HisB (imidazoleglycerol-phosphate dehydratase)
TGTATGCACA	PFLU6088 ■ PFLU6087	PFLU6087	N-acetylmuramoyl-L-alanine amidase
		PFLU6088	Putative GTP cyclohydrolase
CGTTTGTACA	PFLU4948 ■ PFLU4947	PFLU4947	PilZ (type IV pilus assembly protein)
TGTATATACG	PFLU2987 ■ PFLU2988	PFLU2987	Putative phage cointegrase resolution protein
		PFLU2988	TnpS, cointegrase
TGTCCGAACA	PFLU0345 ■ PFLU0344	PFLU0344	NtrB (nitrogen-specific signal transduction histidine kinase)

a. The putative HutC-binding inverted repeats are underlined. Nucleotides in red are mismatches to the consensus HutC-binding inverted repeat.
b. The black rectangle denotes the putative HutC-binding site.

3.2.2.1 Molecular interactions between HutC and the P_{plc} promoter DNA

A putative HutC-binding site was identified in the promoter region of *plc* and *pflu0849*. The *plc* gene encodes a phosphatidylcholine-hydrolyzing phospholipase C (PC-PLC), which participates in the breakdown of phosphatidylcholine (PC) (Dehghan-Noodeh *et*

al., 2014). Phosphatidylcholine is a major phospholipid of the plasma membrane of eukaryotic cells and a component of the mammalian pulmonary surfactant (Sanchez *et al.*, 2017). It is also present in the plasma membrane of a small number of bacteria (Geiger *et al.*, 2013). PC-PLCs participate in bacteria-host interactions and contribute to bacterial virulence of some pathogens (Le Moigne *et al.*, 2015; Wargo *et al.*, 2011). Moreover, it was reported in *P. fluorescens* MFN1032 that the *plc* gene is involved in bacterial cell motility and biofilm formation. The Δ*plc* mutant showed defect in swarming motility, loss of biosurfactant production, low level of flagellin but increased ability of biofilm formation (Rossignol *et al.*, 2008). The divergently transcribed gene *pflu0849* encodes a 5-dehydro-4-deoxyglucarate dehydratase, which is an enzyme involved in D-glucarate degradation (Aghaie *et al.*, 2008).

EMSA analysis was conducted with a 290-bp probe DNA (Pplc-290), which was prepared by PCR using primers Bio-plc (biotin-labeled) and plc-R (Figure 3.1E). The result showed that $HutC_{His6}$ with increasing concentrations (lanes 2 to 7) induced the formation of three protein-DNA complexes, and DNA retardation was abolished with the addition of an excess amount of the same unlabeled probe DNA (lane 8), indicating specific protein-DNA interactions between $HutC_{His6}$ and the P_{plc} promoter DNA (Figure 3.1A). In addition, the DNA probe Pplc-Mut carrying a mutant allele of the putative Phut site (TGTATATACA was substituted with AAGCGGACTT) was unable to bind $HutC_{His6}$ (Figure 3.1C). The equilibrium dissociation constant (Kd) of $HutC_{His6}$ binding to the P_{plc} promoter was calculated to be 824.5 nM (Figure 3.1D), suggesting a low-affinity binding compared with the P_{hutU} promoter (Kd=44.6 nM). Of note, the P_{plc} promoter contains a precise inverted repeat sequence (TGTA-N_2-TACA) for the Phut site. Therefore, the data suggest that DNA sequences flanking the conserved Phut inverted repeat are also involved in determining HutC binding affinity. As expected, urocanate was able to dissociate the interaction between $HutC_{His6}$ and the P_{plc} promoter DNA (Figure 3.1B).

As the putative Phut site is conserved in the promoter region of *plc*, but not the *pflu0849* homologs, among *Pseudomonas* species, the effect of HutC on the promoter activity of *plc* was subsequently examined by β-galactosidase assays. A 290-bp DNA fragment of *plc* promoter region (268 bp upstream and 22 bp downstream of the start codon) was fused to the *lacZ* reporter gene on the plasmid pUC18-mini-Tn7T-Gm-lacZ (Figure 3.1E). β-galactosidase activities were measured for cells grown in LB, MSM

supplemented with succinate plus ammonia and succinate plus histidine. As shown in Figure 3.1F, in LB medium and MSM with succinate plus ammonia, no significant difference in the *plc* expression was observed between the wild-type SBW25 and Δ*hutC* mutant (MU60-1). However, in the medium with succinate plus histidine, the expression of *plc* was higher compared with that in the above two media, and the expression level was reduced by the *hutC* deletion. The results suggest that HutC activates the *plc* expression in certain nutrient conditions, and consequently, may be involved in the regulation of cell motility and biofilm formation.

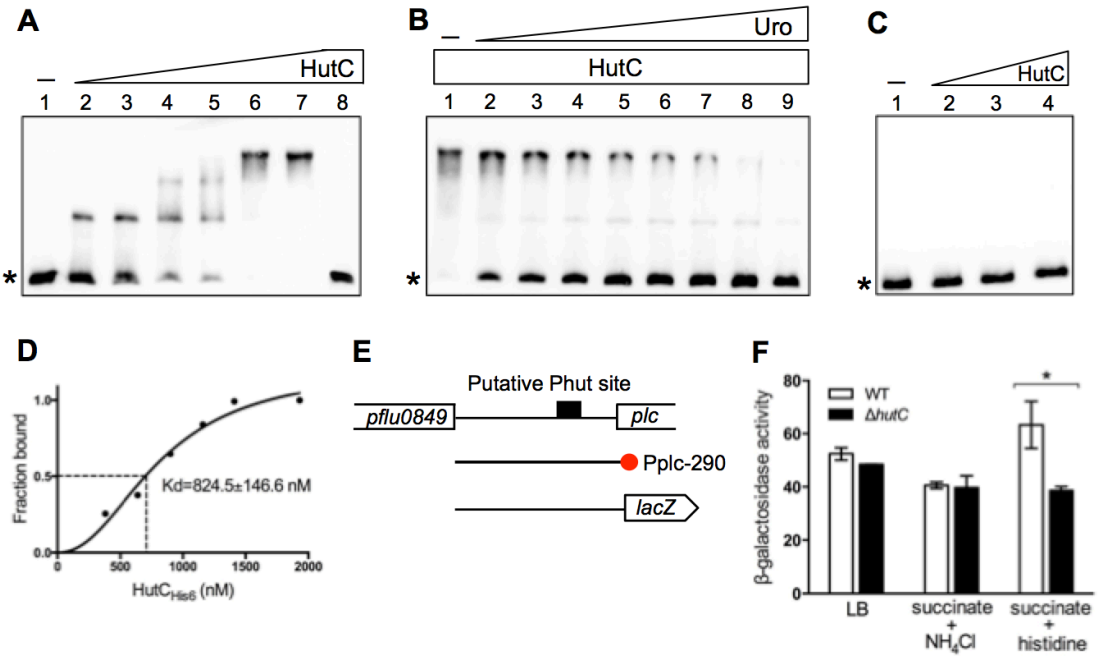

Figure 3.1. Characterization of the putative Phut site in the P_{plc} promoter.
(A) EMSA of $HutC_{His6}$ and P_{plc} DNA probe. Concentrations of $HutC_{His6}$ from lane 1 to 8 were 0, 0.38, 0.64, 0.9, 1.16, 1.41, 1.93 and 1.93 μM, respectively. A 200-fold molar excess of unlabelled P_{plc} probe DNA (specific competitor) was added in lane 8. Position of free DNA probe is indicated by asterisk. **(B)** Effect of urocanate on the HutC-P_{plc} interaction. Lane 1-9, $HutC_{His6}$ was added at the concentration of 1.5 μM for all lanes, and urocanate was added at the concentrations of 0, 0.125, 0.25, 0.5, 1, 1.5, 2.25, 3 and 5 mM, respectively. **(C)** EMSA of $HutC_{His6}$ and Pplc-Mut DNA probe. Concentrations of $HutC_{His6}$ from lane 1 to 4 were 0, 0.64, 1.16 and 1.93 μM, respectively. **(D)** Determination of the equilibrium dissociation constant (Kd) of $HutC_{His6}$ binding to the P_{plc} promoter. **(E)** DNA fragment of Pplc-290 probe and for P_{plc}-*lacZ* fusion construct. The red circle on probe indicates the end labelled by biotin. **(F)** Expression of the P_{plc}-*lacZ* fusion in wild-type SBW25 and Δ*hutC* mutant. Bacteria were grown in LB, MSM supplemented with succinate (20 mM) plus histidine (10 mM) or succinate (20 mM) plus NH_4Cl (1 mg/ml). β-galactosidase activities (μM 4MU min^{-1} OD_{600}^{-1}) were measured at 6 hours after inoculation. Values are means and standard errors of three biological repeats. Bars connected are significantly different ($P < 0.05$) by Tukey's HSD test.

3.2.2.2 Examining molecular interactions between HutC and six other candidate HutC-binding sites

The molecular interactions between HutC and another six predicted HutC-binding sites were examined by EMSA. The six DNA probes for EMSA were amplified by PCR and labeled by digoxigenin (DIG) at the 3′-ends. The information of the primers for DNA probe amplification is listed in Table 3.3. DNA fragment and length of the DNA probes are shown in Figure 3.2A. The EMSA results showed that $HutC_{His6}$ is capable to bind to the promoter DNA of P_{2467}, P_{aceE}, P_{hisB}, P_{4947} and P_{tnpS} (Figure 3.2B&C). Smeared retarded band of protein-DNA complexes was formed by $HutC_{His6}$ and the P_{6088} DNA probe, indicating unstable protein-DNA interactions (Lane 3, Figure 3.2C).

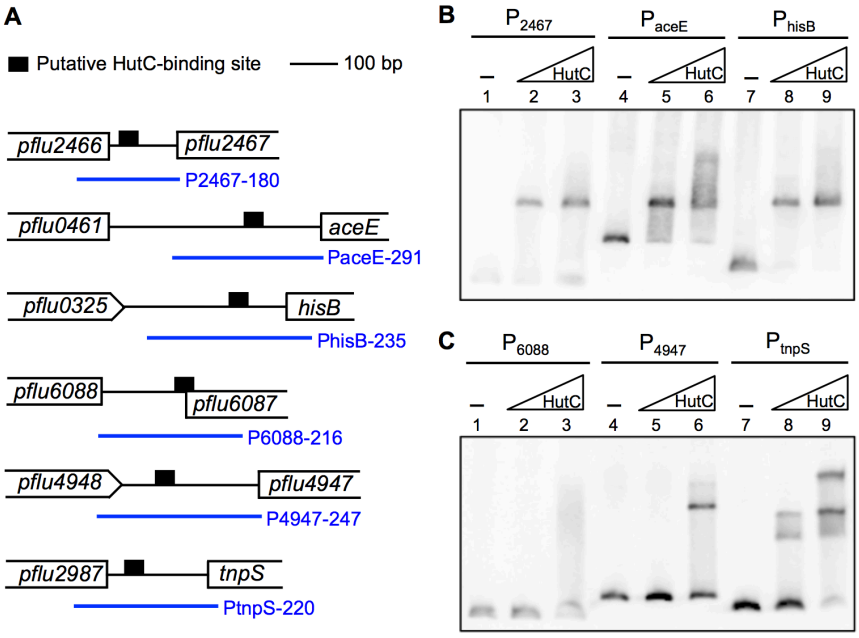

Figure 3.2. EMSAs examining the molecular interactions between HutC and the candidate promoter DNAs.
(A) DNA fragment of the probes used for EMSA are shown as blue lines.
(B) EMSA of $HutC_{His6}$ with P_{2467}, P_{aceE} and P_{hisB} promoter DNAs. Concentrations of $HutC_{His6}$ from lane 1 to 9 were 0, 0.73, 2.2, 0, 0.73, 2.2, 0, 0.73 and 2.2 μM, respectively.
(C) EMSA of $HutC_{His6}$ with P_{6088}, P_{4947} and P_{tnpS} promoter DNAs. Concentrations of $HutC_{His6}$ from lane 1 to 9 were 0, 0.37, 1.8, 0, 0.37, 1.8, 0, 0.37 and 1.8 μM, respectively.

aceE (*pflu0460*) encodes the pyruvate dehydrogenase subunit E1, which composes pyruvate dehydrogenase complex (PDC) with another two enzymes, dihydrolipoamide acetyltransferase E2 (AceF) and dihydrolipoamide dehydrogenase E3. PDC catalyzes the overall conversion of pyruvate to acetyl-CoA and CO_2, and acetyl-CoA will be used

in TCA (de Kok *et al.*, 1998; Sugden & Holness, 2011). *aceE* and *aceF* (*pflu0459*) are likely organized as an operon as the intergenic region between these two genes is only 11 bp, and *pflu0461* is transcribed divergently to *aceE*. Thus, the predicted HutC-binding site in the *aceE* promoter region is possibly involved in the transcriptional regulation of these three genes. The molecular interaction between HutC and P_{aceE} promoter raise the possibility that HutC coordinates histidine metabolism with the crucial central metabolism by regulating both the *hut* genes and genes for pyruvate catabolism. *pflu0461* encodes the bifunctional glutamine-synthetase adenylyltransferase/deadenyltransferase (GlnE), which catalyzes adenylation and deadenylation of glutamine synthetase. Glutamine synthetase is an essential enzyme involved in cellular nitrogen metabolism, which catalyzes the condensation of glutamate and ammonia to form glutamine. Adenylation (inactive form) and deadenylation (active form) of glutamine synthetase subunits is important for the regulation of this enzyme (Carroll *et al.*, 2008; Jiang *et al.*, 2007; Rhee *et al.*, 1985). Two of the predicted HutC-regulated candidates, *ntrBC* and *pflu0461* (*glnE*), are related to cellular nitrogen metabolism. It is interesting to further investigate whether HutC plays a role in bacterial nitrogen metabolism.

hisB (*pflu0327*) encodes the imidazoleglycerol-phosphate dehydratase, which catalyzes the sixth step of histidine biosynthesis in microorganisms (Busch *et al.*, 2001; Chiariotti *et al.*, 1986). In SBW25 genome, *hisB* probably forms an operon with the downstream genes (*hisH*, *pflu0329*, *hisA* and *hisF*), which are also involved in histidine biosynthesis. The molecular interaction between HutC and the P_{hisB} promoter suggests that HutC may regulate histidine catabolism and biosynthesis simultaneously. A hypothetical model for the dual functions of HutC is that in the conditions of histidine limitation, HutC binds to the *hut* promoters to repress expression, meanwhile, HutC binds to the *his* promoter to activate gene transcription; in the conditions of histidine abundance, HutC dissociates from both the *hut* and *his* promoters, thereby derepressing the *hut* genes and inactivating the *his* genes.

pflu2467 encodes an AraC family transcriptional regulator with unknown function. The function of the divergently transcribed gene *pflu2466* is also unknown. The putative HutC-binding site in their promoter region was selected for experimental verification as it shows the best p-value apart from the P_{hut} promoters.

pflu6088 encodes a putative GTP cyclohydrolase and the divergently transcribed gene *pflu6087* encodes a putative N-acetylmuramoyl-L-alanine amidase, an enzyme participating in peptidoglycan catabolism (Gelius *et al.*, 2003; Lazarevic *et al.*, 1992). The predicted HutC-binding site in the P_{6088} promoter has the identical inverted repeat sequence with the one in P_{hisB} promoter. However, EMSA result showed that HutC cannot bind to the P_{6088} promoter as stably as the P_{hisB} promoter (lane 3, Figure 3.2C). The reason probably lies in the differences in DNA sequences flank the HutC-binding inverted repeat. The flanking nucleotides could play a role in stabilizing HutC-DNA interactions.

The product of *pflu4947* is the homologue of pilus assembly protein PilZ, which is a c-di-GMP binding protein essential for type IV pili biogenesis (Alm *et al.*, 1996; Amikam & Galperin, 2006). Studies on PilZ mainly focused on its function and signal transduction, while the regulation of its expression is largely not understood (Burrows, 2012). That HutC is able to bind to the promoter region of *pilZ* suggests the involvement of HutC in the transcriptional regulation of *pilZ*. Additionally, the *in silico* analysis also identified a putative HutC-binding site in the promoter region of *pflu0772* and *pflu0773*, which encode a type IV pilus-like protein and a pilus assembly protein PilV, respectively. Importantly, it was observed that a Δ*hutC* mutant of *P. aeruginosa* PAO1 is defective in the type IV pili-mediated twitching motility (X.-X. Zhang, unpublished data). Together, these findings imply the possible participation of HutC in cell motility.

pflu2988 and the divergently transcribed gene *pflu2987* were also identified as the HutC-regulated candidate genes. They encode a cointegrase TnpS and a cointegrase resolution protein TnpT, respectively, which are proteins involved in the recombination process of transposable elements, playing an important role in shaping the bacterial genome (Yano *et al.*, 2013).

3.2.3 Determining the role of HutC in *ntrBC* expression

As shown in Table 3.1, a putative HutC-binding site was predicted in the *ntrBC* locus of *P. fluorescens* SBW25. The two genes are overlapped by four nucleotides (ATGA), suggesting that they are co-transcribed. NtrBC plays a global regulatory role in bacterial

nitrogen metabolism and also participates in the regulation of *hut* genes. It is required for *P. fluorescens* SBW25 to grow on histidine as the nitrogen source (Zhang & Rainey, 2008). These prompted further investigation into the mechanisms of HutC-mediated regulation of *ntrBC*.

3.2.3.1 Investigating the predicted molecular interactions between HutC and the P_{ntrBC} promoter DNA

To test the molecular interaction between HutC and P_{ntrBC} promoter, EMSA was performed with $HutC_{His6}$ and a 387-bp probe DNA 'PntrBC-387', which was produced by PCR using primers ntrB-SpeI and Bio-ntrR (biotin-labeled) (Figure 3.3A). The result presented in Figure 3.3B clearly indicates that $HutC_{His6}$ was capable of binding to the P_{ntrBC} DNA probe, forming only one HutC-DNA complex unlike the cases of P_{hut} and P_{plc} promoters. The equilibrium dissociation constant (Kd) of $HutC_{His6}$ binding to the P_{ntrBC} promoter is shown in Figure 3.3D. The binding affinity of HutC with the P_{ntrBC} promoter (Kd=1381 nM) is much lower than that of P_{hutU} promoter. This was not surprising as the Phut site in the P_{ntrBC} promoter contains two mismatches to the 8-bp Phut inverted repeat (Table 3.4). As expected, the observed HutC binding with the P_{ntrBC} promoter DNA was disrupted by the addition of urocanate (Figure 3.3C).

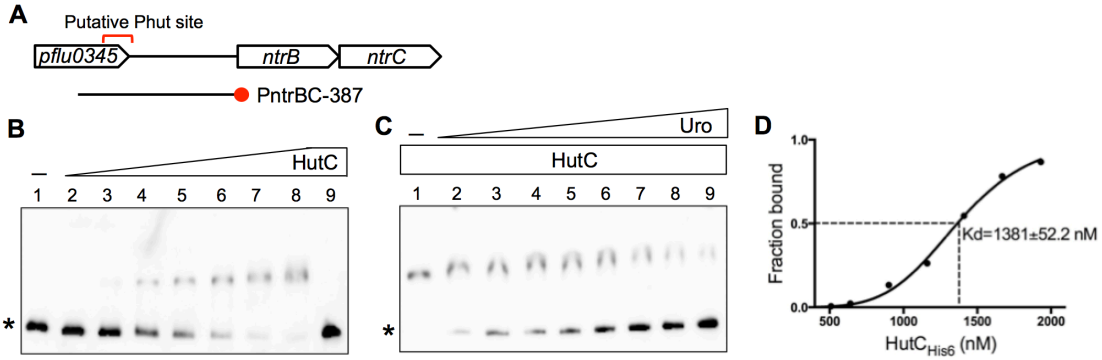

Figure 3.3. Molecular interactions between HutC and P_{ntrBC} promoter DNA *in vitro*.
(A) DNA fragment of PntrBC-387 probe used in EMSA. The red circle on probe indicates the end labelled by biotin.
(B) EMSA of $HutC_{His6}$ and the P_{ntrBC} probe DNA. Concentrations of $HutC_{His6}$ from lane 1 to 9 were 0, 0.51, 0.64, 0.9, 1.16, 1.41, 1.67, 1.93 and 1.93 μM, respectively. A 200-fold molar excess of unlabelled P_{ntrBC} probe DNA (specific competitor) was added in lane 9. Position of free P_{ntrBC} DNA probe is indicated by asterisk.
(C) Effect of urocanate on the HutC-P_{ntrBC} interaction. Lane 1-9, $HutC_{His6}$ was added at the concentration of 1.9 μM for all lanes, and urocanate was added at the concentrations of 0, 0.125, 0.25, 0.5, 1, 1.5, 2.25, 3 and 5 mM, respectively.
(D) Determination of the equilibrium dissociation constant (Kd) of $HutC_{His6}$ binding to the P_{ntrBC} promoter.

3.2.3.2 Determining the HutC binding sequence in the P_{ntrBC} promoter: identification of the Pntr site

To determine the HutC binding sequence in the P_{ntrBC} promoter, DNase I footprinting was performed with $HutC_{His6}$ and a 300-bp P_{ntrBC} DNA probe 'PntrBC-300', which was amplified by primers ntrB-SpeI and Bio-ntrR1 (biotin-labeled) (Figure 3.4D). The result of DNase I footprinting showed that $HutC_{His6}$ protected a 28-bp region (TAAAACCGCACTATATTGGTGCGATAGG) in the P_{ntrBC} promoter (Figure 3.4A&D). However, we were surprised to find that this identified HutC-binding site is not the predicted Phut site shown above, but located 80 bp downstream. This HutC-protected region is centered by an inverted repeat sequence, which exhibits high similarity to the consensus of NtrC-binding site (GCACCA-N3-TGGTGC) (Hervas *et al.*, 2008). The promoter region of *ntrBC* contains a typical σ^{54}-binding site downstream of the putative NtrC-binding site, suggesting that the expression of *ntrBC* is subject to self-regulation by NtrC. Notably, this HutC-P_{ntrBC} interaction is consistent with the findings in Chapter 2 that HutC is able to bind to the Pntr site in the P_{hutFC} promoter, which shows sequence similarity to the NtrC-binding site. The data suggest that HutC and NtrC bind to the

same site in the P_{ntrBC} promoter. This identified HutC-binding Pntr site was named as O_{HutC1}.

Next, to experimentally verify the putative NtrC-binding site in the P_{ntrBC} promoter, molecular interaction between NtrC protein and the P_{ntrBC} promoter DNA was examined *in vitro*. First, to overexpress NtrC protein, a 1434-bp DNA fragment of *ntrC* coding region of *P. fluorescens* SBW25 was amplified by PCR using primers NtrC-ProF and NtrC-ProR and cloned into plasmid pTrc99A. A N-terminal hexa-histidine tag was introduced for purification of the NtrC protein. The recombinant plasmid designated pTrc99A-ntrC was then transferred into *E. coli* BL21 (DE3) for protein expression. The protein was purified as described above. The SDS-PAGE analysis showing purity of the $NtrC_{His6}$ protein is presented in Figure S3.1 (Page 117). Next, EMSA analysis of $NtrC_{His6}$ and the probe DNA 'PntrBC-300' showed that $NtrC_{His6}$ specifically binds to the P_{ntrBC} promoter DNA (Figure 3.4C).

To determine the precise NtrC binding site in the P_{ntrBC} promoter, DNase I footprinting of $NtrC_{His6}$ and PntrBC-300 probe DNA was performed. The result demonstrated two NtrC-protected regions in the P_{ntrBC} promoter (Figure 3.4B). One is a 25-bp region including the predicted NtrC binding site (TAAAACCGCACTATATTGGTGCGAT). The other one downstream is a 23-bp region (CTGGCCAGCCCATTTTGGTTCGA), which includes an imperfect inverted repeat with lower similarity to the consensus of NtrC binding site. Location and sequence of the NtrC-protected regions are presented in Figure 3.4D. These two NtrC binding sites were named as O_{NtrC1} and O_{NtrC2}, respectively. Of note, NtrC binds stronger to O_{NtrC1} site than to O_{NtrC2} as the protection by NtrC to O_{NtrC1} was more evident than the latter.

The DNase I footprinting assays clearly showed that HutC and NtrC are able to bind to the same site in the P_{ntrBC} promoter. However, the modes of protein-DNA interactions differ between HutC and NtrC, which is supported by two pieces of evidence. First, the length of protein-protected regions are slightly different between HutC and NtrC. A longer DNA region is protected by HutC. Second, a hypersensitive site in the protected region was observed for NtrC, but not HutC, suggesting that this nucleotide was exposed as a result of NtrC-DNA interaction. Of note, the binding affinity of HutC to the Pntr site is lower compared to that of NtrC as much higher concentrations of HutC

were required for DNase I footprinting than NtrC. The O_{NtrC2} site was not protected by HutC probably due to the lower binding affinity.

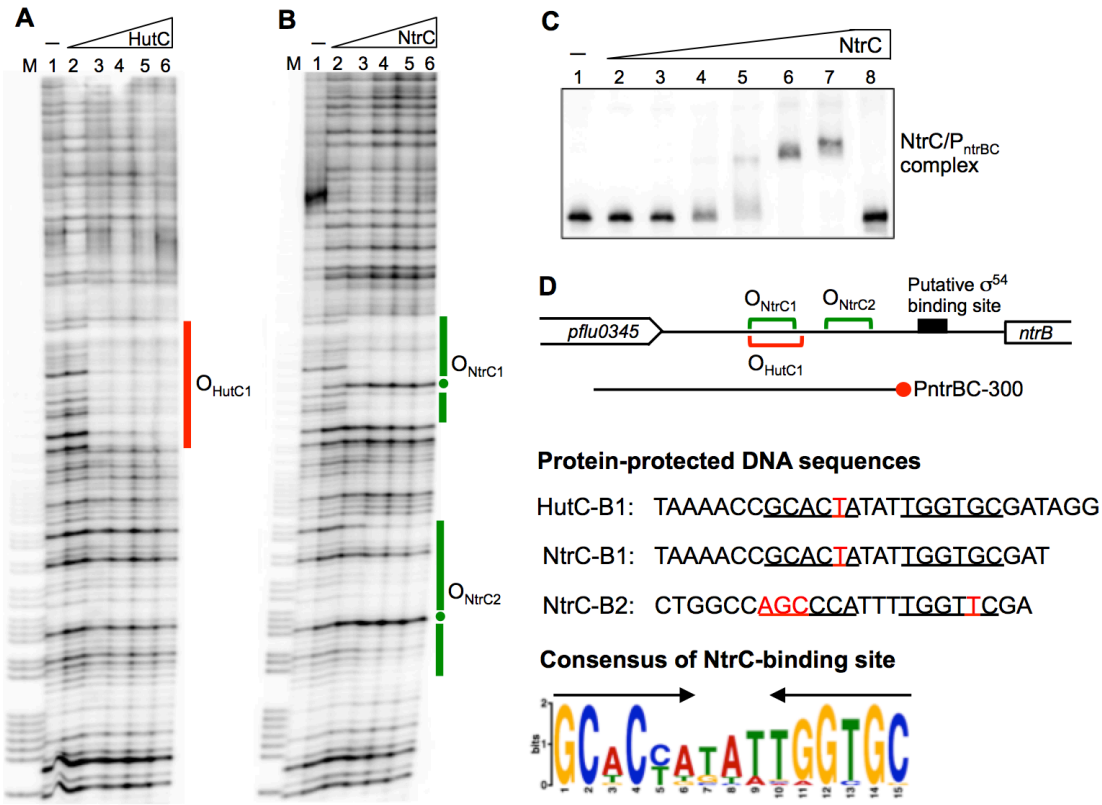

Figure 3.4. Characterization of HutC and NtrC binding sites in the P_{ntrBC} promoter.
(A) DNase I footprinting of $HutC_{His6}$ and P_{ntrBC} promoter DNA (PntrBC-300). Concentrations of $HutC_{His6}$ from lane 1 to 6 were 0, 1.16, 2.32, 4.64, 7.54 and 10.44 μM, respectively. Lane M, G+A marker. HutC-protected region is marked by a red bar.
(B) DNase I footprinting of $NtrC_{His6}$ and P_{ntrBC} promoter DNA (PntrBC-300). Concentrations of $NtrC_{His6}$ from lane 1 to 6 were 0, 0.07, 0.2, 0.54, 1.1 and 1.7 μM, respectively. NtrC-protected regions are indicated by green bars. Hypersensitive residues are marked with filled circles.
(C) EMSA of $NtrC_{His6}$ and PntrBC-300. Concentrations of $NtrC_{His6}$ from lane 1 to 8 were 0, 0.1, 0.3, 0.8, 1.5, 3, 5 and 5 μM, respectively. A 200-fold molar excess of unlabeled PntrBC-300 probe (specific competitor) was added in lane 8.
(D) DNA sequence of the HutC- and NtrC-protected regions in the P_{ntrBC} promoter. The NtrC-binding sites are underlined, and red font denotes mismatch to the consensus of NtrC-binding site. DNA fragment of the probe PntrBC-300 is indicated and the red circle on probe indicates the end labelled by biotin. Sequence logo representing the concensus NtrC-binding site was generated by WebLogo 3 server (http://weblogo.threeplusone.com/) using *ntrBC* promoter homologs from 30 *Pseudomonas* strains. The inverted repeat sequence is indicated by arrows.

Furthermore, the protein-DNA interaction between $HutC_{His6}$ and the PntrBC-300 probe DNA was disrupted by addition of urocanate, and substitution of the Pntr site with random sequence eliminated the $HutC_{His6}$ binding activity (Figure 3.5A&B). Together,

the *in vitro* data consistently indicate that HutC is capable of binding to the dominant NtrC operator site (O_{NtrC1}), hence HutC has a potential to modulate *ntrBC* expression via competitive binding with the NtrC activator.

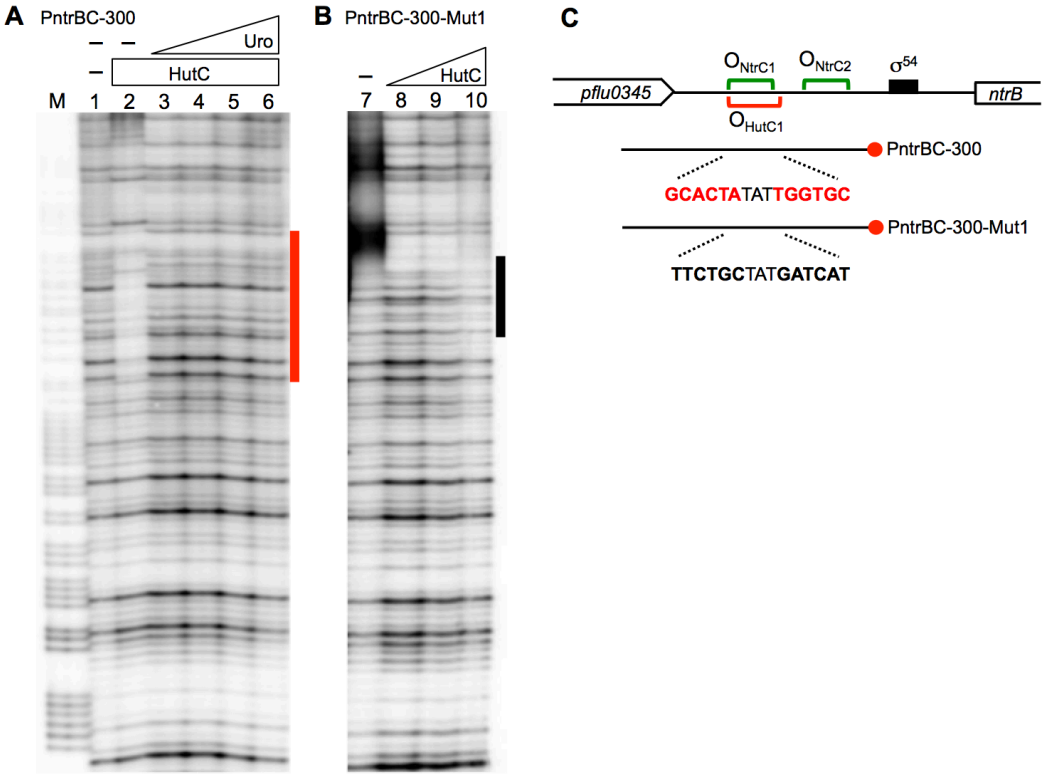

Figure 3.5. Effects of urocanate and Pntr site mutation on the protein-DNA interactions between HutC and its targeting P_{ntrBC} promoter DNA.
DNase I footprinting was performed using $HutC_{His6}$ and DNA probe PntrBC-300 **(A)** or PntrBC-300-Mut1 **(B)**. The two probes differ in sequence only at the Pntr site for HutC (and NtrC) binding, which is marked by a red bar. The wild-type Pntr site in the PntrBC-300 probe highlighted in red colour was changed to random sequence in the mutant probe PntrBC-300-Mut1 shown in boldface type **(C)**. Lane 1, no $HutC_{His6}$ or urocanate added; Lanes 2-6, $HutC_{His6}$ was added at 7.2 μM, urocanate was added at increasing concentrations from 0, 0.5, 1.5, 3.6 to 8 mM; Lanes 7-10, $HutC_{His6}$ was added at 0, 2.32, 4.64 and 7.54 μM, respectively. The HutC-protected region in the wild-type probe PntrBC-300 is indicated by a red bar, and position of the altered Pntr site is marked by a black bar for the PntrBC-300-Mut1 probe.

3.2.3.3 Identification of the O_{HutC2} site in the *ntrBC* promoter region

Next, we asked whether the originally predicted HutC binding site by *in silico* analysis is able to bind HutC protein. To this end, a 154-bp DNA probe 'PntrBC-154', containing this predicted HutC binding site alone, was amplified by PCR using primers ntrB-SpeI and Bio-ntrR3 (biotin-labeled) (Figure 3.6D). EMSA performed with $HutC_{His6}$

and the PntrBC-154 probe DNA confirmed the HutC-DNA interaction (Figure 3.6C). Moreover, the result of DNase I footprinting showed a 38-bp region in the PntrBC-154 probe protected by $HutC_{His6}$, which includes the predicted HutC-binding site (termed O_{HutC2}) (Figure 3.6A&D). As expected, addition of urocanate dissociated $HutC_{His6}$ from the O_{HutC2} site (Figure 3.6B). Together, the data indicate that HutC binds to two distinct operator sites (O_{HutC1} and O_{HutC2}) in the promoter region of *ntrBC*.

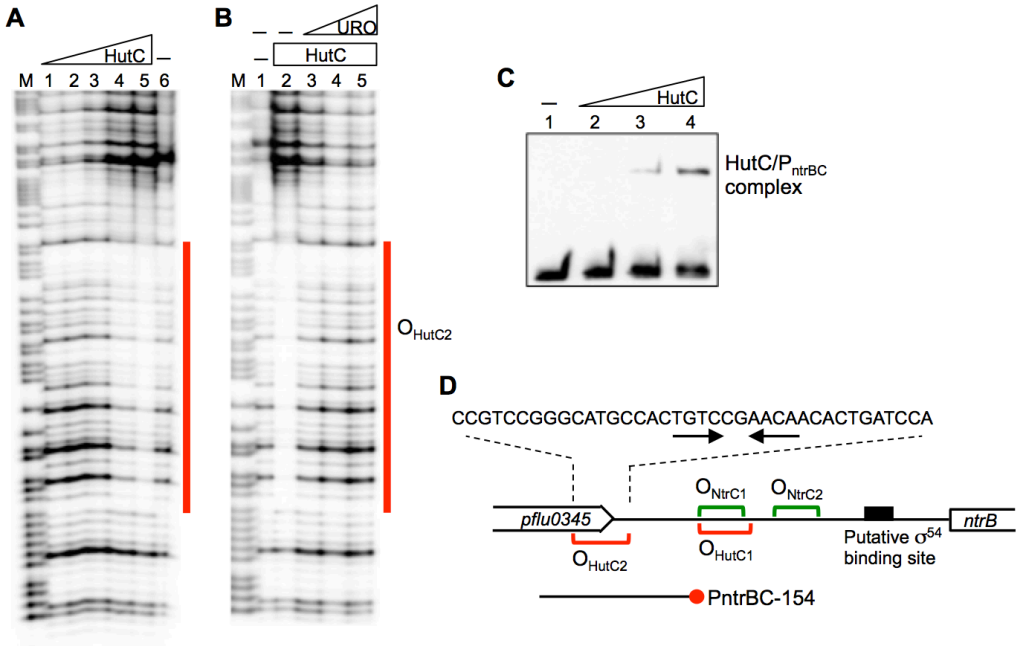

Figure 3.6. Determining the HutC-binding site (O_{HutC2}) in the P_{ntrBC} promoter.
(A) DNase I footprinting of $HutC_{His6}$ and the probe DNA PntrBC-154. Concentrations of $HutC_{His6}$ from lane 1 to 5 were 0.26, 0.77, 1.8, 3.34 and 5.14 μM, respectively. Lane 6, no $HutC_{His6}$ added. Lane M, G+A marker. HutC-protected region is indicated by a red bar.
(B) Effect of urocanate on the molecular interaction between $HutC_{His6}$ and PntrBC-154. Lane 1, no HutC or urocanate added. Lane 2-5, 5.14 μM HutC was added, and urocanate was added at the concentrations of 0, 0.2, 0.5 and 2 mM, respectively.
(C) EMSA showing the molecular interaction between $HutC_{His6}$ and PntrBC-154. Concentrations of HutC from lane 1 to 4 were 0, 0.64, 1.28 and 1.92 μM, respectively.
(D) DNA sequence of the HutC-protected region in the P_{ntrBC} promoter. The Phut site is indicated by arrows. DNA fragment of the probe PntrBC-154 is as indicated, and the red circle on probe indicates the end labelled by biotin.

3.2.3.4 Mutational analysis of the HutC-binding sites in P_{ntrBC} promoter

Two HutC binding sites were identified in the P_{ntrBC} promoter by DNase I footprinting assays, whereas only one retarded band for the HutC/P_{ntrBC} complex was observed in EMSA. Next, to further understand the profile of HutC binding to the P_{ntrBC} promoter,

site-directed mutagenesis of the two HutC-binding sites was conducted. Accordingly, three variant P_{ntrBC} DNA probes were constructed: PntrBC-Mut1 and PntrBC-Mut2 carrying a mutant allele of the O_{HutC1} and O_{HutC2} site, respectively, and PntrBC-Mut3 with both HutC-binding sites mutated (Figure 3.8). Specifically, the O_{HutC1} site (GCACTATATTGGTGC) was substituted by TTCTGCTATGATCAT (same as the altered Pntr site in Figure 3.5C), and the O_{HutC2} site (TGTCCGAACA) was changed into CACTTAGGTC. The ability of HutC to bind to the P_{ntrBC} variants was examined by EMSA. The results showed that $HutC_{His6}$ is capable to bind to PntrBC-Mut1, and weakly bind to PntrBC-Mut2 given that a smeared band of free DNA was formed by addition of $HutC_{His6}$ with higher concentrations, whereas PntrBC-Mut3 is not able to bind $HutC_{His6}$ (Figure 3.7). The data indicate that HutC binds to the O_{HutC2} site more stably than to the O_{HutC1} site, and the retarded band of HutC-DNA complex in EMSA is dominated by the interaction between HutC and O_{HutC2}.

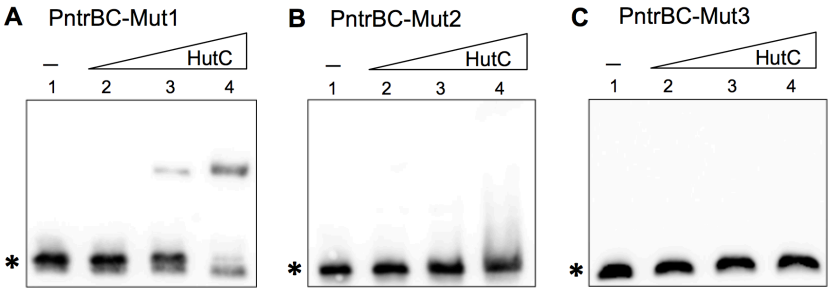

Figure 3.7. EMSA experiments examining the molecular interactions between $HutC_{His6}$ and the P_{ntrBC} variants. Concentrations of $HutC_{His6}$ from lane 1 to 4 were 0, 0.64, 1.28 and 1.92 μM, respectively. Position of free DNA probe is denoted by an asterisk.

Next, we sought to clarify if HutC binding to the O_{HutC1} site requires the presence of the O_{HutC2} site. To this end, DNase I footprinting was performed with $HutC_{His6}$ and the probe DNA 'PntrBC-196', which excludes the O_{HutC2} site. A HutC-protected region corresponding to the O_{HutC1} site was also identified in PntrBC-196 (data not shown), which demonstrates that HutC binding to the O_{HutC1} site is independent of the O_{HutC2} presence. Results of all the binding assays performed with $HutC_{His6}$ and P_{ntrBC} promoter DNA are summarized in Figure 3.8.

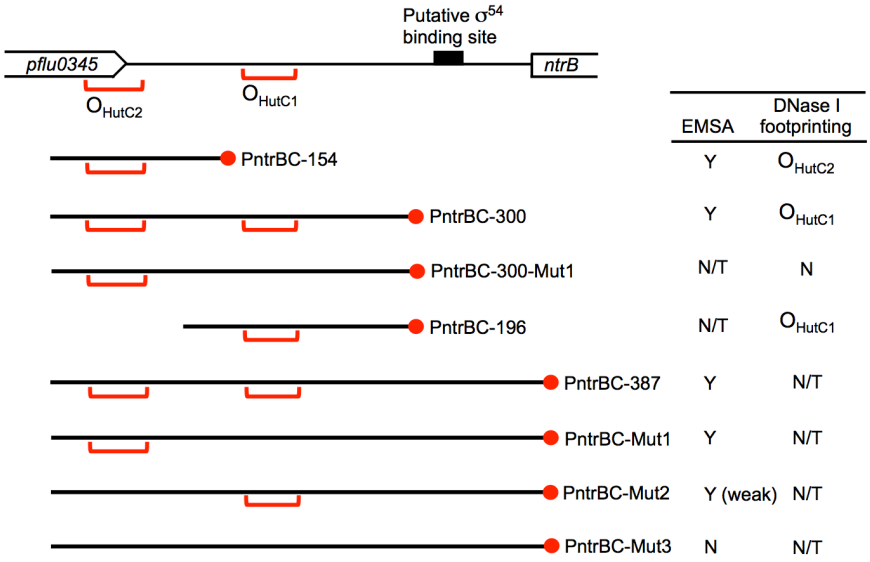

Figure 3.8. A summary of protein-DNA binding assays between $HutC_{His6}$ and various P_{ntrBC} probe DNAs. The DNA probes used are as indicated, and the red circle on probes indicates the end labelled by biotin. 'Y' denotes HutC-DNA interaction detected, 'N' denotes no HutC-DNA interaction, and 'N/T' stands for "not tested". HutC-binding site identified by DNase I footprinting is indicated.

3.2.3.5 *In silico* analysis of the operator sites of HutC and NtrC in P_{ntrBC} promoter

An alignment of the P_{ntrBC} promoter homologues from 30 *Pseudomonas* genomes shows that the O_{HutC1}/O_{NtrC1} site and O_{NtrC2} site in the P_{ntrBC} promoter are conserved among the *Pseudomonas* species analyzed (Figure 3.9). However, the O_{HutC2} site was not identified in the promoter region of *ntrBC* in these *Pseudomonas* species except for *P. fluorescens* SBW25. Consistently, no effect of O_{HutC2} mutation was observed on the expression of *ntrBC* (data not shown). This operator site might be involved in the regulation of the upstream gene *pflu0345*. Therefore, our study will not address the O_{HutC2} site with regard to the HutC-mediated regulation of *ntrBC*. The physiological significance of HutC-mediated *ntrBC* expression is further analyzed in Chapter 4, and results show that HutC acts as a governor, providing a negative feedback for the positive auto-regulation of NtrBC.

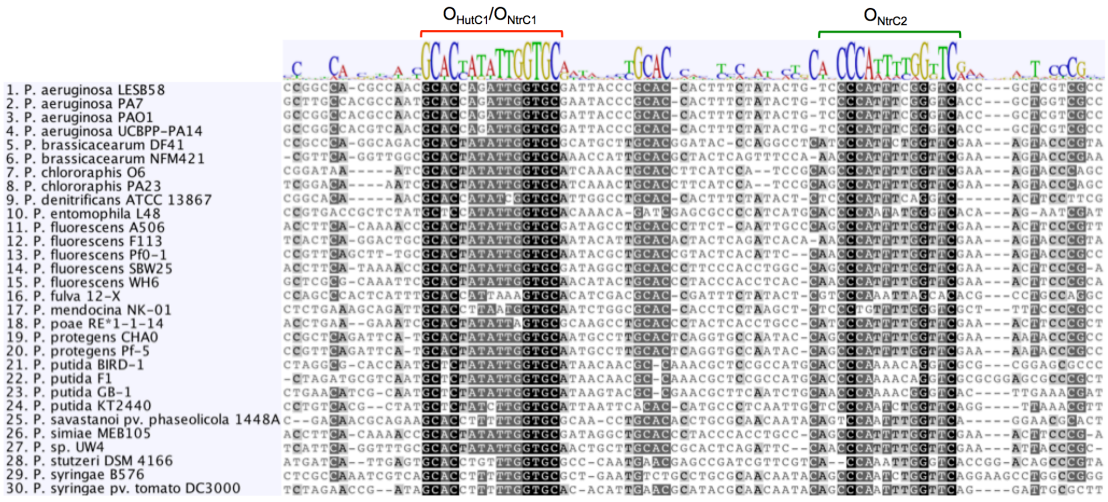

Figure 3.9. *In silico* analysis of the HutC and NtrC operator sites in the P_{ntrBC} promoter among *Pseudomonas*. The alignment and sequence logo were generated by Geneious 9.0.5.

3.2.4 Phenotypic analyses of HutC

3.2.4.1 Effects of HutC on *P. fluorescens* SBW25 motility

One of the identified HutC-regulated candidate genes is *pflu4947* encoding a homologue of the pilus assembly protein PilZ, which raises the possibility that HutC is involved in the regulation of type IV pili synthesis. Moreover, a parallel project in our lab found that a Δ*hutC* mutant of *P. aeruginosa* PAO1 is defective in the type IV pili-mediated twitching motility. These findings necessitated the examination of the effect of HutC on bacterial motility. Motility assays were performed with the wild-type SBW25 and Δ*hutC* mutant (MU60-1) in three different media, LB, MSM supplemented with succinate and urocanate or succinate and histidine (as carbon and nitrogen sources). Agar plates with 1%, 0.5% and 0.3% agar were prepared to test twitching, swarming and swimming motilities, respectively. No twitching phenotype was observed for both the wild-type SBW25 and Δ*hutC* mutant in all the media tested. For swimming and swarming motilities, Δ*hutC* mutant showed increased motility compared to the wild type in MSM plus succinate and histidine. Intriguingly, this difference between the wild type and Δ*hutC* mutant were not observed in LB or MSM plus succinate and urocanate (Figure 3.10A). Diameter of the colonies spread in MSM plus succinate and histidine were significantly different (P<0.05) between the wild type and Δ*hutC* mutant for both swimming and swarming motilities (Figure 3.10B). To rule out the possibility that the difference in cell motility was caused by difference in growth

phenotype between the two strains, growth assay was performed in MSM broth plus succinate and histidine. As shown in Figure 3.10C, the growth phenotype of these two strains was similar. Together, the data indicate that HutC negatively regulates swimming and swarming motilities of *P. fluorescens* SBW25 in certain nutrient conditions. However, the mechanisms of HutC-mediated regulation of bacterial motilities still need further study.

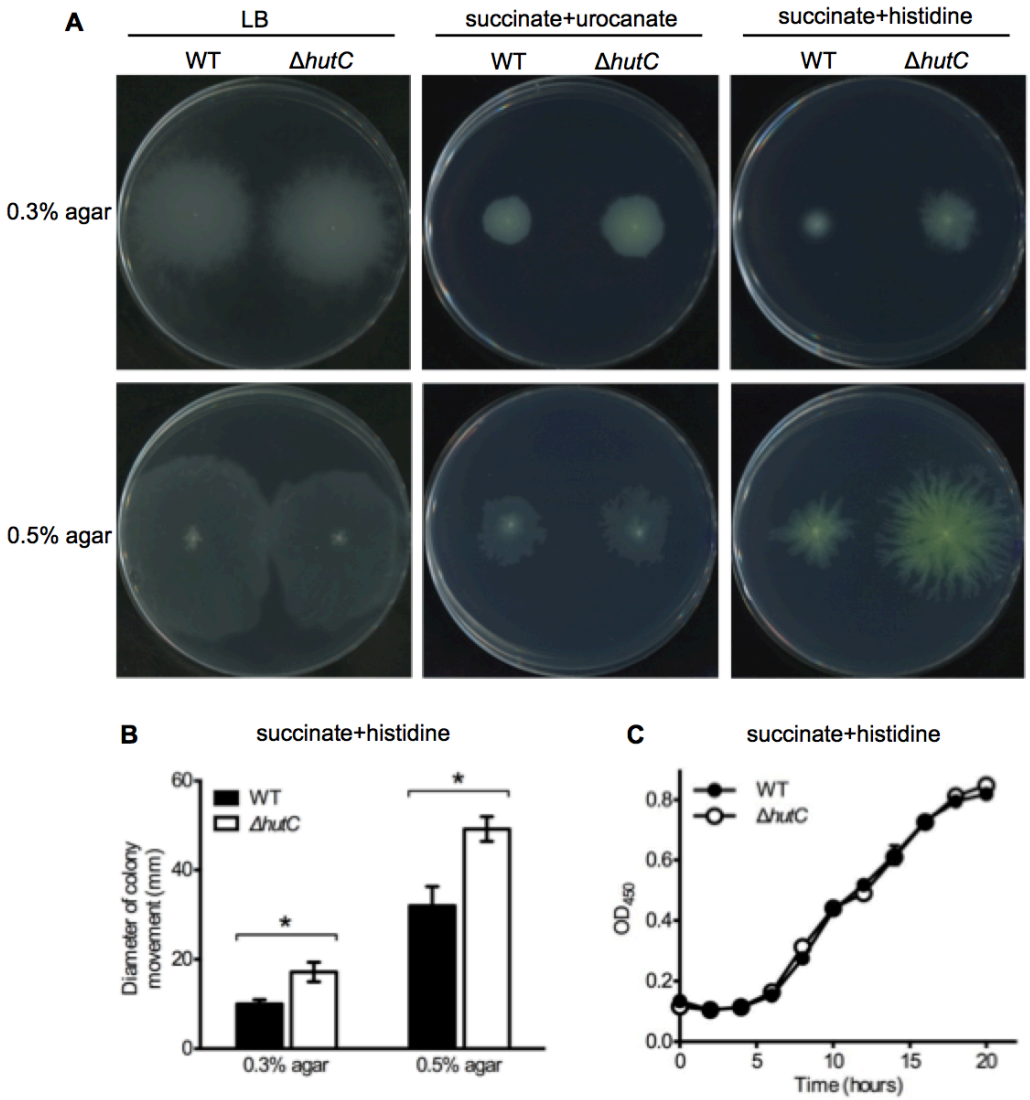

Figure 3.10. Effects of HutC on cell motility of *P. fluorescens* SBW25.
(A) Swimming (0.3% agar) and swarming (0.5% agar) motilities were examined in LB, MSM with succinate (20 mM) plus urocanate (10 mM) and MSM with succinate (20 mM) plus histidine (10 mM). Photos were taken after incubated the plates for 16 hours at 28 °C. The 0.5% agar plate of MSM with succinate plus histidine was incubated for 36 hours due to slow growth.
(B) Diameters of colony movements. Results presented are means with standard errors from five independent plates. Asterisk denotes significant difference between means as revealed by the Student's t-test ($P < 0.05$).
(C) Growth dynamics measured in MSM with succinate (20 mM) plus histidine (10 mM). Data are means and standard errors of four independent cultures.

3.2.4.2 Examining the effects of HutC on biofilm formation of *P. fluorescens* SBW25

Biofilm formation is an essential physiological process for bacterial survival and overall adaptation to the living environment. It has been reported in *Yersinia pseudotuberculosis* and *P. aeruginosa* that HutC plays a role in regulation of biofilm formation (Joshua *et al.*, 2015; Patell *et al.*, 2010; Yeung *et al.*, 2009). It is significant to know if HutC is involved in biofilm formation of *P. fluorescens* SBW25. Biofilm assays of the wild-type SBW25 and Δ*hutC* mutant were conducted in two types of environment, 96-well microtiter plates (plastic surface) and glass microcosms (glass surface) using crystal violet staining after O'Toole *et al.* (2011). On microtiter plates, four different media were inoculated with the strains and statically incubated for two or three days. Biofilms formed on the wall and/or bottom of the wells were then quantified by crystal violet staining. The results showed no significant difference among the wild type, Δ*hutC* mutant (MU60-1) and *hutC* overexpression strain (MU60-10, carrying pME6010-hutC) in the four media tested (Figure 3.11). Of note, biofilm was produced at a higher level in the medium supplemented with histidine or urocanate than in another two nutrient conditions.

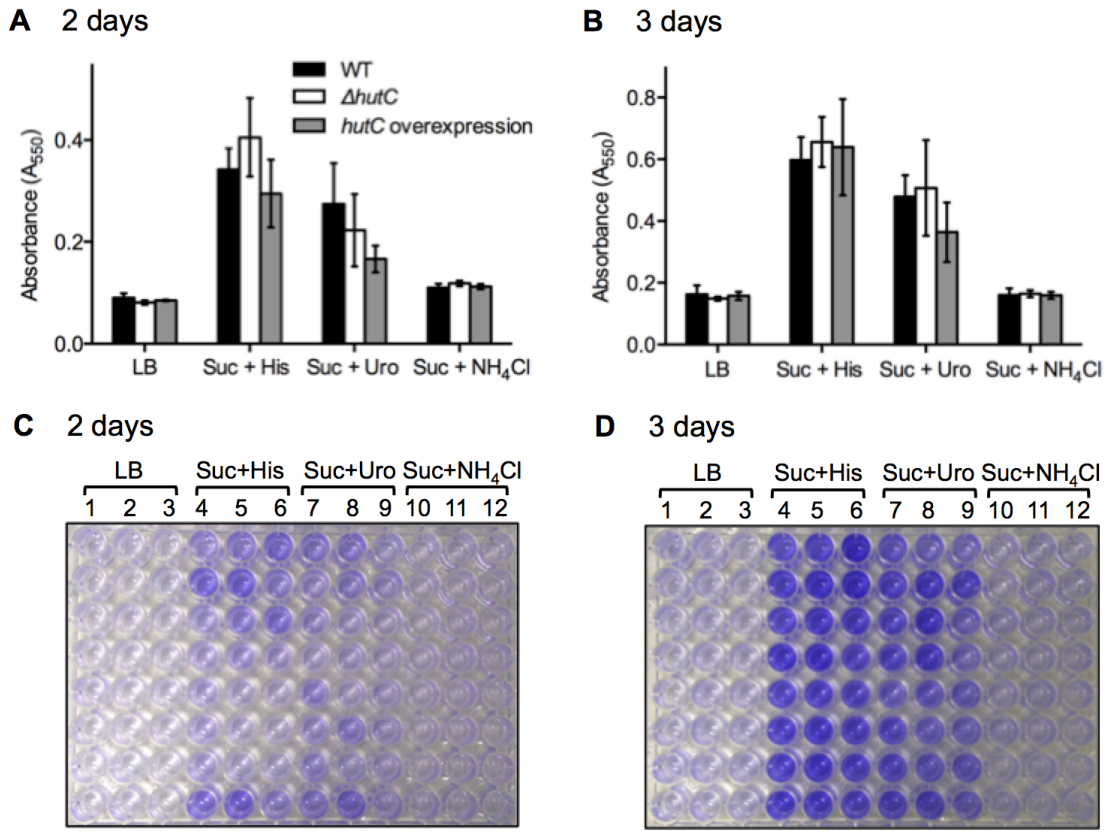

Figure 3.11. Biofilm assays on 96-well microtiter plates. Biofilms were quantified by crystal violet staining after incubation for two **(A)** or three **(B)** days. Data shown are means and standard errors of eight independent cultures. **(C, D)** Representative images showing the results of crystal violet staining after solubilized by 30% acetic acid. The wild-type SBW25 was inoculated in lanes 1, 4, 7 and 10. Δ*hutC* mutant was inoculated in lanes 2, 5, 8 and 11. *hutC* overexpression strain was inoculated in lanes 3, 6, 9 and 12. Succinate supplemented as the carbon source was added at 20 mM. Histidine, urocanate and NH_4Cl as the nitrogen source were added at 10 mM, 10 mM and 1 mg/ml, respectively.

Biofilm formation on glass microcosms of the wild-type SBW25 and Δ*hutC* mutant was measured in LB and MSM plus succinate and histidine. Biofilms were mainly formed at the air-liquid interface. As shown in Figure 3.12, no significant difference on biofilm formation was observed between the wild type and Δ*hutC* mutant. Together, the data indicate that HutC is not involved in the regulation of biofilm formation of *P. fluorescens* SBW25 under the conditions tested.

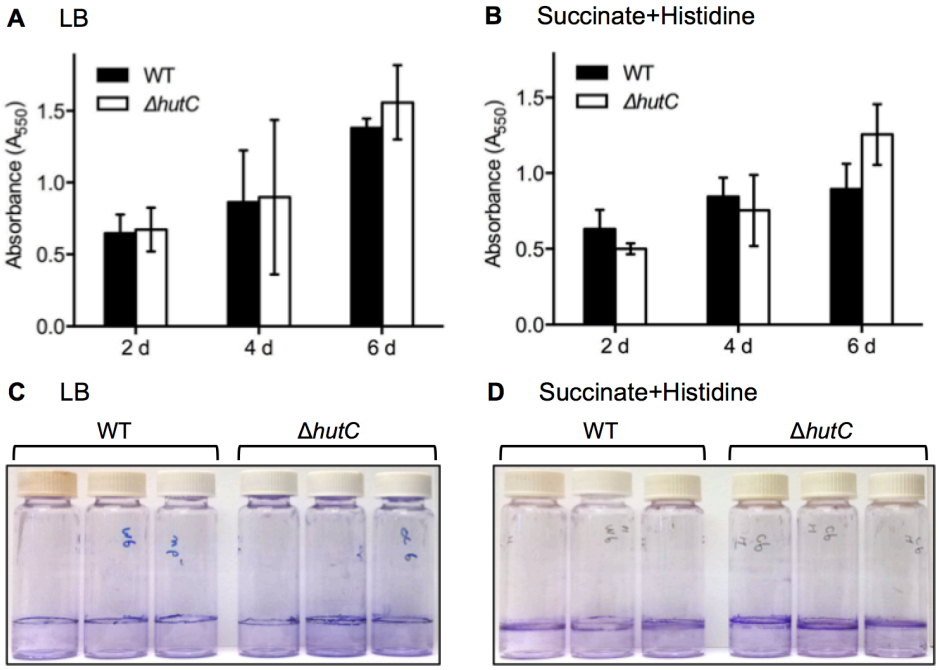

Figure 3.12. Biofilm assays on glass microcosms. Biofilm formation in LB **(A)** and MSM supplemented with succinate (20 mM) and histidine (10 mM) **(B)** were quantified by crystal violet staining after incubation for 2, 4 and 6 days. Data shown are means and standard errors of three independent cultures. **(C, D)** Representative images of the crystal violet-stained biofilms after incubation for 6 days.

3.3 Discussion

In this chapter, we examined the global regulatory role of HutC in *P. fluorescens* SBW25. The work led to the identification of 88 putative HutC binding sites, eight of which have been subject to further verification by EMSA analysis and/or DNase I footprinting. Results confirmed the ability of *plc*, *pflu2467*, *aceE*, *hisB*, *pflu6088*, *pflu4947*, *tnpS* and *ntrB* promoter DNAs to specifically bind with the purified $HutC_{His6}$ protein *in vitro*. Of particular note is a putative HutC binding site located in the *ntrBC* locus. However, data presented here show that the canonical HutC binding site (O_{HutC2}) is not involved in the expression of *ntrBC*. Instead we accidently found that HutC is capable of binding to the NtrC binding site in the *ntrBC* promoter, which is targeted by NtrC to activate its own expression.

Transcription factors (TFs) regulate gene expression by binding to *cis*-regulatory regions of DNA in a sequence-specific manner (Charoensawan *et al.*, 2010). Each transcription factor recognizes a single consensus DNA sequence (or binding-site motif) (Lodish *et*

al., 2016; Todeschini *et al.*, 2014). However, this paradigm has been challenged by the findings that some eukaryotic TFs have evolved the ability to recognize multiple DNA binding-site motifs (Nakagawa *et al.*, 2013; Siggers & Gordan, 2014). Eukaryotic TFs can potentially read the shape of the DNA molecule (not just the base sequence) as a major source of information for specific site recognition (Inukai *et al.*, 2017; Slattery *et al.*, 2014).

Some TFs can recognize multiple DNA sites as they have two DNA-binding domains. The mouse transcription factor Oct-1 is a typical example in this category. The two DNA-binding domains of Oct-1 can recognize two distinct DNA sequences, and the combination of these two DNA-binding domains recognizes a third type of operator site (Klemm *et al.*, 1994). Another mechanism of recognizing different DNA sequences is that proteins adopt alternate structural conformations when interacting with different operator sites (Kim *et al.*, 1995).

Recognition of multiple binding-site motifs by one protein is also reported in bacteriophage. The integrase protein of bacteriophage λ interacts with two types of DNA site via two DNA-binding domains (Moitoso de Vargas *et al.*, 1988). In contrast, the CI protein of coliphage 186 recognizes two distinct DNA sequences by its single helix-turn-helix DNA-binding domain (Shearwin *et al.*, 2002). However, this recognition of multiple DNA sequences by one TF in prokaryotes is largely unexplored.

Here, we found, for the first time, that a prokaryotic TF (i.e. HutC) recognizes two distinct binding sites (Phut and Pntr). Given that HutC contains only one wHTH DNA-binding domain, we speculate that HutC may adopt different conformations when interacting with the two types of binding site. Moreover, residues outside DNA-binding domain of transcriptional regulators can also contribute to alternative binding site recognition (Siggers & Gordan, 2014). Some particular residues outside the DNA-binding domain of HutC may also play a role in recognition of the different operator sites. In future work, a combination of X-ray crystallography of HutC interacting with each binding site and site-directed mutagenesis of critical residues in both protein and DNA will unravel the mechanism basis of the dual site recognition by HutC.

In Chapter 2, the Pntr site was identified in the P_{hutF} promoter, which is responsible for HutC binding to the weak protected region. In this chapter, we also found that HutC

binds to the same DNA operator site of NtrC in the P_{ntrBC} promoter. HutC belongs to the GntR protein family, members of which share similar wHTH DNA-binding domain in the N-terminus (Gorelik *et al.*, 2006). NtrC is a member of NtrC family with a C-terminal helix-turn-helix (HTH) DNA-binding domain (Twerdochlib *et al.*, 2003). These two regulatory proteins possess distinct DNA-binding domains and carry out different regulatory tasks. Significantly, HutC and NtrC can specifically bind to the same DNA sequence (the O_{NtrC1}/O_{HutC1} site). The modes of protein-DNA interactions differ between HutC and NtrC. This was evidenced by two experimental findings: first, the length of protein-protected regions are slightly different between HutC and NtrC; second, a hyposensitive site of DNase I cleavage in the protected region was observed for NtrC, but not HutC. Thus, these two proteins could possibly interact with different nucleotides within the shared binding site.

3.4 Materials and Methods

3.4.1 Bacterial strains and growth conditions

One Shot® TOP10 (Invitrogen, Auckland) chemically competent *E. coli* was used for transferring pCR™8/GW/TOPO® vector (Invitrogen, Auckland) with cloning PCR products for subsequent sequencing. *E. coli* DH5αλ_{pir} was used for general gene cloning and tri-parental conjugation of *P. fluorescens* SBW25. *E. coli* BL21 (DE3) was used for protein purification. Other bacterial strains and plasmids used in this work are listed in Table 3.2. Luria-Bertani (LB) medium was routinely used to grow *P. fluorescens* and *E. coli* strains at 28°C and 37°C, respectively. When bacteria were grown in the mininal M9 salt medium (Sambrook *et al.*, 1989), the components and concentrations of carbon and nitrogen sources were supplemented as indicated in each assay. When required, antibiotics were used at the following concentrations: ampicillin (Ap), 100 μg/ml; tetracycline (Tc), 15 μg/ml; spectinomycin (Sp), 100 μg/ml; kanamycin (Km), 50 μg/ml; gentamicin (Gm), 25 μg/ml; nitrofurantoin (NF), 100 μg/ml.

Table 3.2. Bacterial strains and plasmids used in this work

P. fluorescens strain	Genotypes and characteristics	Reference
SBW25	Wild-type strain isolated from phyllosphere of	(Bailey *et al.*,

	sugar beet	1995)
MU60-1	Δ*hutC*, SBW25 devoid of *pflu0359*	This work
MU60-8	SBW25 carrying mini-Tn*7*T-Gm-lacZ::Pplc	This work
MU60-9	SBW25Δ*hutC* carrying mini-Tn*7*T-Gm-lacZ::Pplc	This work
MU60-10	SBW25 *hutC* overexpression strain carrying pME6010-hutC	This work
Plasmid		
pCR2.1-TOPO	Cloning vector, Km^r, Ap^r	Invitrogen
pCR8/GW/TOPO	Cloning vector, Sp^r	Invitrogen
pUX-BF13	Helper plasmid for transposition of mini-Tn*7* element, Ap^r	(Bao *et al.*, 1991)
pUC18-mini-Tn7T-Gm-lacZ	Mini-Tn*7* vector for transcriptional fusion to promoterless lacZ, Ap^r, Gm^r	(Choi *et al.*, 2005)
pUC18-Tn7T-lacZ-Pplc	pUC18-mini-Tn*7*T-Gm-lacZ containing *lacZ* fusion to P_{plc} promoter	This work
pTrc99A	Protein expression vector, P_{tac} promoter, Ap^r	(Amann *et al.*, 1988)
pTrc99A-hutC	pTrc99A carrying $HutC_{His6}$, Ap^r	This work
pTrc99A-ntrC	pTrc99A carrying $NtrC_{His6}$, Ap^r	This work
pCR2.1-Pplc-Mut	Recombinant plasmid for amplifying Pplc-Mut probe DNA	This work
pCR8-PntrB-Mut1	Recombinant plasmid for amplifying PntrBC-Mut1 probe DNA	This work
pCR2.1-PntrB-Mut2	Recombinant plasmid for amplifying PntrBC-Mut2 probe DNA	This work
pCR2.1-PntrB-Mut3	Recombinant plasmid for amplifying PntrBC-Mut3 probe DNA	This work
pME6010	Broad-host-range vector, Tc^r	(Heeb *et al.*, 2000)
pME6010-hutC	Recombinant plasmid for *hutC* overexpression	This work

3.4.2 Growth assays in laboratory media

P. fluorescens strains from -80°C stock were initially grown in 5 ml of LB broth at 28°C overnight. One ml of the cell culture was spun down and washed twice with MSM salt solution. The cells were starved in MSM salt solution at 28°C for 2 hours and then mixed with fresh tested media by 1:100 folds dilution. Two hundred µl aliquots of the cell culture were placed onto a 96-well microplate. Growth kinetics were monitored at 28°C by a Synergy 2 plate reader installed with Gen5 software (Bio-Tek). Absorbance at 450 nm was recorded every 5 minutes for a period of 24 or 48 hours.

3.4.3 Strain construction

Standard protocols were used for isolation of plasmid DNA, restriction endonuclease digestion, ligation and PCR reaction. Restriction enzymes were obtained from New England Biolabs. Ligation reactions were conducted using T4 DNA ligase from Invitrogen (Auckland, New Zealand). PCR reactions were performed using *Taq* DNA polymerase from Invitrogen. Oligonucleotide primers used in this chapter are listed in Table 3.3. pCR8/GW/TOPO® Cloning Kit (Invitrogen) was used for TA cloning. For gene cloning from the genomic DNA of *P. fluorescens* SBW25, PCR product was first cloned into pCR8/GW/TOPO vector for DNA sequencing (Macrogen, South Korea). Then the desired insert DNA was subcloned into destination vectors and transferred into *P. fluorescens* strains by electroporation.

Site-directed mutagenesis of *hutC* gene was achieved by a previously established procedure of SOE-PCR (splicing by overlapping extension PCR) (Horton *et al.*, 1989) in conjunction with a two-step allelic-exchange strategy using the suicide-integration vector pUIC3 (Rainey, 1999). Briefly, two pairs of primers were designed to PCR amplify flanking regions (~500 bp) of the target gene, wherein the two primers closer to the gene are complementary for 20-23 bp at the join site. The two PCR products were used as DNA templates in the second-round PCR whereby the two DNA fragments were joined together. The resultant single DNA fragment was cloned into plasmid pUIC3. Next, the recombinant pUIC3 plasmid was transferred into *P. fluorescens* through conjugation with the helper plasmid pRK2013 (Ditta *et al.*, 1980). The desired allelic exchange mutants were selected by a previously described procedure of D-cycloserine enrichment (Zhang & Rainey, 2007).

Site-directed mutagenesis of the HutC operator sites in the P_{ntrBC} and P_{plc} promoters was performed using SOE-PCR mentioned above. The resultant mutated DNA fragments were cloned into pCR8/GW/TOPO or pCR2.1-TOPO® (Invitrogen) as DNA template for PCR amplification of DNA probes in electrophoretic mobility shift assay (EMSA) or DNase I footprinting assay. The multi-copy shuttle vector pME6010 was used for *hutC* overexpression from a constitutive P_k promoter (Heeb *et al.*, 2000). The coding region of *hutC* was cloned into pME6010, and the recombinant plasmid pME6010-hutC was introduced into the wild-type SBW25 by electroporation. The resultant strain carrying pME6010-hutC was used for biofilm assays.

Table 3.3. Oligonucleotides used in this work

Primer	Sequence (5′ - 3′)[a]	Application
Bio-plc[b]	CTGCGAGTTCAAGACCTGACAT	Amplifying DNA probe Pplc-290
plc-R	ggactagtGGACTTCAGTTCTTGTGGATTC	
plc-Mut1	gctgtaaagtccgcttGCTTTAGCGAGCATAGAGG	Mutagenizing HutC binding site in P_{plc} promoter with primer plc-R
plc-Mut2	taaagcaagcggacttTACAGCATTTAAGGAAGATTC	
plc-Mut3	CAGGGCGATGACTTGGCCATAC	
plc-F	ggaagcttCTGCGAGTTCAAGACCTGACAT	P_{plc} transcriptional fusion to *lacZ* with primer plc-R
P2467-F	GAAGGACTTGGGTTCACCGT	Amplifying DNA probe P2467-180
P2467-R	CATGGGCATGCACATCGATC	
PaceE-F	CATAGTTGTTGGCAGGGAAC	Amplifying DNA probe PaceE-291
PaceE-R	TCTTGCATGGCTTGCTCCAG	
PhisB-F	AGCCACCTCGTTCTTTCAGT	Amplifying DNA probe PhisB-235
PhisB-R	TTACGTTCGGCCATCACCAG	
P6088-F	TTGCGTATCTGTGTGGCGTG	Amplifying DNA probe P6088-216
P6088-R	CATGAGCAGGTCCATCGTTG	
P4947-F	GCGTCCAGCTTCGTTATGATG	Amplifying DNA probe P4947-247
P4947-R	CATGGTGAGATCGCCATCCA	
P2987-F	CATGGGAGGCCTTTGTGTAC	Amplifying DNA probe PtnpS-220
P2987-R	AGGCGTGCCGTTTGAACTAC	
ntrB-SpeI	gactaGTATTACCGGCAACACCCCGGTCGA	Amplifying DNA probe PntrBC-387
Bio-ntrR[b]	GCTGATGGTCATTGGGACCTCTT	
Bio-ntrR1[b]	CTCCGAAAAGAAGCGTGCAAGC	Amplifying DNA probe PntrBC-300 with primer ntrB-SpeI
HutC-ProF	aaatttaccatgggccatcatcatcatcatcatCCGACTCCGCCCGCCAAGTCTC	HutC protein expression
HutC-ProR	aaatttgaagcttGCGCCAGACGCTTATTGCACTCAT	
NtrC-ProF	accatgggccatcatcatcatcatcatAGCCGTAGTGAAACCGTCTGGAT	NtrC protein expression
NtrC-ProR	gaagcttTCAGCCTTCATCGCCCTCGTCAT	
Bio-ntrR3[b]	ATGAAGGTTGTTCAGGAAGTGG	Amplifying DNA probe PntrBC-154 with primer ntrB-SpeI
PntrB-mut3	atcatgatcatagcagaaGGTTTTATGAAGGTTGT	Mutagenizing O_{HutC1} site in P_{ntrBC} promoter with primers ntrB-SpeI and ntrB-HindIII
PntrB-mut4	accttctgctatgatcatGATAGGCTGCACCCTTC	
ntrB-HindIII	gaagcttGCTGATGGTCATTGGGACCTCTT	Mutagenizing O_{HutC2} site in P_{ntrBC} promoter
PntrBM2-1	TCATGGGATGGCACACCTTAC	
PntrBM2-2	tgccaccacttaggtcACACTGATCCATCCCCCACT	

PntrBM2-3	agtgtgacctaagtgGTGGCATGCCCGGACGGCCCGCGT	
PntrB-2	TCAACCCGCCCTGAAAACGAT	Amplifying DNA probe PntrBC-196 with primer Bio-ntrR1
hutF1	gaagatCTGATCTGACGCGACAGTTC	*hutC* deletion
hutC-del2	aagctatgacGCACAGGGAATCCTTGCAG	
hutC-del3	attccctgtgCGTCATAGCTTGGAAGGAC	
hutD1	gaagatctTGGGTCAGTTCGATCAGGC	
hutC7	gaagatCTGCAAGGATTCCCTGTGCC	*hutC* overexpression with primer HutC-ProR

[a] Artificial sequences integrated into the primers are presented in lowercase with restriction sites underlined.
[b] Primers are labeled by biotin at the 5′-end.

3.4.4 β-galactosidase Assay

To construct transcriptional fusions to the promoterless *lacZ* the promoter region (~500 bp) of genes was cloned into plasmid pUC18-mini-Tn7T-Gm-*lacZ*. The *lacZ* fusion in the plasmid was introduced into *P. fluorescens* together with plasmid pUX-BF13 by electroporation. The mini-Tn7 element carrying transcriptional fusion integrates into the chromosome at a single attTn7 site downstream of the *glmS* gene (Choi *et al.*, 2005).

β-galactosidase assays for measuring expression of the *lacZ* fusions were performed following a standard protocol with 4-methylumbelliferyl-β-D-galactoside (4MUG) as the enzymatic substrate (Zhang *et al.*, 2006). Enzymatic reactions were performed using bacterial cells grown in the tested media for 2-8 hours after inoculation. The fluorescent product, 7-hydroxy-4-methylcoumarin (4MU), was measured at 460 nm with an excitation wavelength of 365 nm on a Synergy 2 plate reader (Bio-Tek). β-galactosidase activity was expressed as the amount of 4MU (μM) produced per minute per cell (OD_{600}).

3.4.5 Electrophoretic mobility shift assays

The coding regions of HutC and NtrC were amplified by PCR from the genomic DNA of *P. fluorescens* SBW25 and subsequently cloned into the protein expression vector pTrc99A (Amann *et al.*, 1988) with the integration of six histidine residues at the N-terminal. The recombinant plasmid pTrc99A-hutC and pTrc99A-ntrC was transformed into *E. coli* BL21(DE3) for protein overexpression (Studier & Moffatt, 1986). IPTG was added at the final concentration of 1 mM to the *E. coli* culture (OD_{600}, 0.5~0.7) to induce protein expression for 4 hours at 37°C. Cells were lysed by sonication using the Sonicator S-4000 (Misonix, Inc). The His6-tagged protein was purified using TALON® metal affinity resin (Clontech laboratories, Inc.) according to the manufacturer's instructions. The type of buffer solution and pH for protein preparation were adjusted based on the properties of protein. Twenty mM HEPES buffer (pH 7.4) was used for the purification of HutC and NtrC. Concentration of the purified proteins was determined by the Bradford method (Bradford, 1976).

DNA probes for EMSA were amplified by PCR using primers listed in Table 3.3. For the biotin-labeled DNA probes, one primer of each pair was labeled by biotin at the 5'–end. The DNA probes were purified by phenol-chloroform extraction. The DIG (digoxigenin)-labeled DNA probes were first amplified by PCR and then labeled using DIG Oligonucleotide 3'-End Labeling Kit, 2nd Generation (Roche) following the manufacturer's instruction. The DNA probes used in this work are summarized in Table 3.4.

EMSA reactions were set up by mixing 20 nM DNA probe, designated concentrations of protein, 1 µg salmon sperm DNA (Invitrogen) in EMSA binding buffer (10 mM HEPES, 50 mM KCl, 5 mM $MgCl_2$ and 1 mM DTT, pH 7.5) to a final volume of 20 µl. After incubation at room temperature for 30 minutes, reactions were electrophoresed on 6% native polyacrylamide gel in 0.5x TBE buffer at 120V at 4°C. The DNA in gel was transferred to positively charged Whatman® Nytran™ SuPerCharge nylon membrane (Sigma-Aldrich) by electroblotting and immobilized by incubating the membrane at 80°C for 30 minutes. LightShift™ chemiluminescent EMSA kit (Thermo Fisher Scientific) was used to detect the biotin-labelled DNA probes and DIG Nucleic Acid Detection Kit (Roche) was used for the DIG-labelled DNA probes. The images were visualized by LAS-4000 Luminescent Imager equipped with ImageQuant™ LAS

4000 software (FujiFilm). HutC binding affinities to the target DNAs were presented as equilibrium dissociation constant (Kd), which was calculated as previously described in Chapter 2.

Table 3.4. DNA probes used in this work

DNA probe	Primers used for PCR amplification	Length (bp)	Labeling	Application
Pplc-290	Bio-plc & plc-R	290	5′ end labeled by biotin	EMSA of HutC and P_{plc} promoter DNA
Pplc-Mut	Bio-plc & plc-R	290	5′ end labeled by biotin	EMSA of HutC and P_{plc} promoter DNA carrying a mutant allele of Phut site
P2467-180	P2467-F & P2467-R	180	3′ end labeled by DIG	EMSA of HutC and *pflu2467* promoter DNA
PaceE-291	PaceE-F & PaceE-R	291	3′ end labeled by DIG	EMSA of HutC and *aceE* promoter DNA
PhisB-235	PhisB-F & PhisB-R	235	3′ end labeled by DIG	EMSA of HutC and *hisB* promoter DNA
P6088-216	P6088-F & P6088-R	216	3′ end labeled by DIG	EMSA of HutC and *pflu6088* promoter DNA
P4947-247	P4947-F & P4947-R	247	3′ end labeled by DIG	EMSA of HutC and *pflu4947* promoter DNA
PtnpS-220	P2987-F & P2987-R	220	3′ end labeled by DIG	EMSA of HutC and *tnpS* promoter DNA
PntrBC-387	ntrB-SpeI & Bio-ntrR	387	5′ end labeled by biotin	EMSA of HutC and P_{ntrBC} promoter DNA
PntrBC-300	ntrB-SpeI & Bio-ntrR1	300	5′ end labeled by biotin	DNase I footprinting of HutC and P_{ntrBC} promoter DNA
PntrBC-300-Mut1	ntrB-SpeI & Bio-ntrR1	300	5′ end labeled by biotin	DNase I footprinting of HutC and P_{ntrBC} promoter DNA carrying a mutant allele of O_{HutC1} site
PntrBC-154	ntrB-SpeI & Bio-ntrR3	154	5′ end labeled by biotin	DNase I footprinting of HutC and P_{ntrBC} promoter DNA
PntrBC-Mut1	ntrB-SpeI & Bio-ntrR	387	5′ end labeled by biotin	EMSA of HutC and P_{ntrBC} promoter DNA carrying a mutant allele of O_{HutC1} site
PntrBC-Mut2	ntrB-SpeI & Bio-ntrR	387	5′ end labeled by	EMSA of HutC and P_{ntrBC} promoter DNA carrying a

			biotin	mutant allele of O_{HutC2} site
PntrBC-Mut3	ntrB-SpeI & Bio-ntrR	387	5′ end labeled by biotin	EMSA of HutC and P_{ntrBC} promoter DNA carrying a mutant allele of O_{HutC1} and O_{HutC2} sites
PntrBC-196	PntrB-2 & Bio-ntrR1	196	5′ end labeled by biotin	DNase I footprinting of HutC and P_{ntrBC} promoter DNA

3.4.6 DNase I footprinting assays

Reactions were set up under the same condition described for EMSA but in a larger volume of 50 µl with 2 µM DNA probe. After incubation at room temperature for 30 minutes, 50 µl of cofactor solution (5 mM $CaCl_2$ and 10 mM $MgCl_2$) was added. Then the samples were treated with 0.02 U of DNase I (Invitrogen) for 5 min at room temperature. After the termination of reactions with 100 µl of DNase I stop solution (200 mM NaCl, 20 mM EDTA and 1% SDS), DNA was extracted with an equal volume of 1:1 phenol/chloroform mixture and precipitated by adding 1 µl of glycogen (20 mg/ml, Fermentas), 1/10th volume of 3 M sodium acetate (pH 5.2) and three volumes of ethanol. Following incubation at -20°C for at least 1 hour, DNA was pelleted by centrifugation and resuspended in 8 µl of loading buffer (95% formamide, 0.05% bromophenol blue and 20 mM EDTA). After denaturing at 95°C for 10 min, the samples were electrophoresed on a 6% denaturing urea-polyacrylamide gel (21 x 40 cm) in 1x TBE buffer using the Sequi-Gen® GT electrophoresis system (Bio-Rad Laboratories Pty). Then DNA was transferred from the gel to positively charged nylon membrane by contact blotting (Petersen *et al.*, 1996). Detection of the DNA fragments was conducted as described above in EMSA. A G+A marker showing the sequence of DNA fragments was included in the gel. It was produced with the same biotin-labeled DNA probe by Maxam-Gilbert chemical sequencing reactions (Maxam & Gilbert, 1980).

3.4.7 Motility assay

Bacterial motility was examined on 0.3% and 0.5% agar plates of different media. The agar plates were prepared and incubated at 23°C for 24 hours before use. Wild-type SBW25 and Δ*hutC* mutant were first grown on 0.3% LB agar plates overnight. Assays

were conducted by dipping the overnight bacterial culture and stabbing into the surface of agar plates tested using inoculation needles. After inoculation, the plates were incubated at 28ºC for at least 16 hours.

3.4.8 Biofilm assays

Bacterial biofilm formation was determined quantitatively using the method of crystal violet staining (O'Toole, 2011). For the biofilm assay conducted on 96-well microtiter plates, overnight bacterial culture was washed with sterile water twice and diluted 1:100 into fresh medium for assay. One hundred µl aliquots of diluted culture were added onto a 96-well microtiter plate and incubated at 28ºC for 2 to 3 days. Cells were dumped out and the wells were gently washed with water. One hundred and twenty five µl of 0.1% crystal violet (CV) was added and incubated at room temperature for 15 minutes. The plate was washed 3 times with water and allowed to dry overnight. One hundred and twenty five µl of 30% acetic acid was added to solubilize CV followed by incubation at room temperature for 15 minutes. Absorbance at 550 nm was measured using a Synergy 2 plate reader (Bio-Tek). The biofilm assay performed in microcosms followed the same procedure with a large-scale usage of bacterial culture and reagents.

3.5 References

Aghaie, A., Lechaplais, C., Sirven, P., Tricot, S., Besnard-Gonnet, M., Muselet, D., . . . Perret, A. (2008). New insights into the alternative D-glucarate degradation pathway. *J Biol Chem, 283*(23), 15638-15646. doi: 10.1074/jbc.M800487200

Alm, R. A., Bodero, A. J., Free, P. D., & Mattick, J. S. (1996). Identification of a novel gene, *pilZ*, essential for type 4 fimbrial biogenesis in *Pseudomonas aeruginosa*. *J Bacteriol, 178*(1), 46-53.

Amann, E., Ochs, B., & Abel, K. J. (1988). Tightly regulated tac promoter vectors useful for the expression of unfused and fused proteins in *Escherichia coli*. *Gene, 69*(2), 301-315.

Amikam, D., & Galperin, M. Y. (2006). PilZ domain is part of the bacterial c-di-GMP binding protein. *Bioinformatics, 22*(1), 3-6. doi: 10.1093/bioinformatics/bti739

Bailey, M. J., Lilley, A. K., Thompson, I. P., Rainey, P. B., & Ellis, R. J. (1995). Site directed chromosomal marking of a fluorescent pseudomonad isolated from the

phytosphere of sugar beet; stability and potential for marker gene transfer. *Mol Ecol, 4*(6), 755-763.

Bao, Y., Lies, D. P., Fu, H., & Roberts, G. P. (1991). An improved Tn7-based system for the single-copy insertion of cloned genes into chromosomes of gram-negative bacteria. *Gene, 109*(1), 167-168.

Bradford, M. M. (1976). A rapid and sensitive method for the quantitation of microgram quantities of protein utilizing the principle of protein-dye binding. *Anal Biochem, 72*, 248-254.

Burrows, L. L. (2012). *Pseudomonas aeruginosa* twitching motility: type IV pili in action. *Annu Rev Microbiol, 66*, 493-520. doi: 10.1146/annurev-micro-092611-150055

Busch, S., Hoffmann, B., Valerius, O., Starke, K., Duvel, K., & Braus, G. H. (2001). Regulation of the *Aspergillus nidulans hisB* gene by histidine starvation. *Curr Genet, 38*(6), 314-322.

Carroll, P., Pashley, C. A., & Parish, T. (2008). Functional analysis of GlnE, an essential adenylyl transferase in *Mycobacterium tuberculosis*. *J Bacteriol, 190*(14), 4894-4902. doi: 10.1128/JB.00166-08

Charoensawan, V., Wilson, D., & Teichmann, S. A. (2010). Genomic repertoires of DNA-binding transcription factors across the tree of life. *Nucleic acids research, 38*(21), 7364-7377. doi: 10.1093/nar/gkq617

Chiariotti, L., Nappo, A. G., Carlomagno, M. S., & Bruni, C. B. (1986). Gene structure in the histidine operon of *Escherichia coli*. Identification and nucleotide sequence of the *hisB* gene. *Mol Gen Genet, 202*(1), 42-47.

Choi, K. H., Gaynor, J. B., White, K. G., Lopez, C., Bosio, C. M., Karkhoff-Schweizer, R. R., & Schweizer, H. P. (2005). A Tn7-based broad-range bacterial cloning and expression system. *Nat Methods, 2*(6), 443-448. doi: 10.1038/nmeth765

de Kok, A., Hengeveld, A. F., Martin, A., & Westphal, A. H. (1998). The pyruvate dehydrogenase multi-enzyme complex from Gram-negative bacteria. *Biochim Biophys Acta, 1385*(2), 353-366.

Dehghan-Noodeh, A., Nasir, A., & Robson, G. D. (2014). Effect of phosphatidylcholine on the level expression of *plc* genes of *Aspergillus fumigatus* by real time PCR method and investigation of these genes using bioinformatics analysis. *Iran J Microbiol, 6*(2), 104-111.

Ditta, G., Stanfield, S., Corbin, D., & Helinski, D. R. (1980). Broad host range DNA cloning system for gram-negative bacteria: construction of a gene bank of *Rhizobium meliloti*. *Proc Natl Acad Sci U S A, 77*(12), 7347-7351.

Geiger, O., Lopez-Lara, I. M., & Sohlenkamp, C. (2013). Phosphatidylcholine biosynthesis and function in bacteria. *Biochim Biophys Acta, 1831*(3), 503-513. doi: 10.1016/j.bbalip.2012.08.009

Gelius, E., Persson, C., Karlsson, J., & Steiner, H. (2003). A mammalian peptidoglycan recognition protein with N-acetylmuramoyl-L-alanine amidase activity. *Biochem Biophys Res Commun, 306*(4), 988-994.

Gorelik, M., Lunin, V. V., Skarina, T., & Savchenko, A. (2006). Structural characterization of GntR/HutC family signaling domain. *Protein Sci, 15*(6), 1506-1511. doi: 10.1110/ps.062146906

Grant, C. E., Bailey, T. L., & Noble, W. S. (2011). FIMO: scanning for occurrences of a given motif. *Bioinformatics, 27*(7), 1017-1018. doi: 10.1093/bioinformatics/btr064

Heeb, S., Itoh, Y., Nishijyo, T., Schnider, U., Keel, C., Wade, J., . . . Haas, D. (2000). Small, stable shuttle vectors based on the minimal pVS1 replicon for use in gram-negative, plant-associated bacteria. *Mol Plant Microbe Interact, 13*(2), 232-237. doi: 10.1094/MPMI.2000.13.2.232

Hervas, A. B., Canosa, I., & Santero, E. (2008). Transcriptome analysis of *Pseudomonas putida* in response to nitrogen availability. *J Bacteriol, 190*(1), 416-420. doi: 10.1128/JB.01230-07

Horton, R. M., Hunt, H. D., Ho, S. N., Pullen, J. K., & Pease, L. R. (1989). Engineering hybrid genes without the use of restriction enzymes: gene splicing by overlap extension. *Gene, 77*(1), 61-68.

Inukai, S., Kock, K. H., & Bulyk, M. L. (2017). Transcription factor-DNA binding: beyond binding site motifs. *Current Opinion in Genetics & Development, 43*, 110-119. doi: 10.1016/j.gde.2017.02.007

Jiang, P., Pioszak, A. A., & Ninfa, A. J. (2007). Structure-function analysis of glutamine synthetase adenylyltransferase (ATase, EC 2.7.7.49) of *Escherichia coli*. *Biochemistry, 46*(13), 4117-4132. doi: 10.1021/bi0620508

Joshua, G. W., Atkinson, S., Goldstone, R. J., Patrick, H. L., Stabler, R. A., Purves, J., . . . Wren, B. W. (2015). Genome-wide evaluation of the interplay between *Caenorhabditis elegans* and *Yersinia pseudotuberculosis* during *in vivo* biofilm formation. *Infect Immun, 83*(1), 17-27. doi: 10.1128/IAI.00110-14

Kim, J. B., Spotts, G. D., Halvorsen, Y. D., Shih, H. M., Ellenberger, T., Towle, H. C., & Spiegelman, B. M. (1995). Dual DNA binding specificity of ADD1/SREBP1 controlled by a single amino acid in the basic helix-loop-helix domain. *Mol Cell Biol, 15*(5), 2582-2588.

Klemm, J. D., Rould, M. A., Aurora, R., Herr, W., & Pabo, C. O. (1994). Crystal structure of the Oct-1 POU domain bound to an octamer site: DNA recognition with tethered DNA-binding modules. *Cell, 77*(1), 21-32.

Lazarevic, V., Margot, P., Soldo, B., & Karamata, D. (1992). Sequencing and analysis of the *Bacillus subtilis lytRABC* divergon: a regulatory unit encompassing the structural genes of the N-acetylmuramoyl-L-alanine amidase and its modifier. *J Gen Microbiol, 138*(9), 1949-1961. doi: 10.1099/00221287-138-9-1949

Le Moigne, V., Rottman, M., Goulard, C., Barteau, B., Poncin, I., Soismier, N., . . . Herrmann, J. L. (2015). Bacterial phospholipases C as vaccine candidate antigens against cystic fibrosis respiratory pathogens: the *Mycobacterium abscessus* model. *Vaccine, 33*(18), 2118-2124. doi: 10.1016/j.vaccine.2015.03.030

Lodish, H, Berk, A, Kaiser, C, Krieger, M, Bretscher, A, Ploegh, H, . . . K.C., Martin. (2016). *Molecular Cell Biology*: Freeman, W.H. & Company.

Maxam, A. M., & Gilbert, W. (1980). Sequencing end-labeled DNA with base-specific chemical cleavages. *Methods Enzymol, 65*(1), 499-560.

Moitoso de Vargas, L., Pargellis, C. A., Hasan, N. M., Bushman, E. W., & Landy, A. (1988). Autonomous DNA binding domains of lambda integrase recognize two different sequence families. *Cell, 54*(7), 923-929.

Nakagawa, S., Gisselbrecht, S. S., Rogers, J. M., Hartl, D. L., & Bulyk, M. L. (2013). DNA-binding specificity changes in the evolution of forkhead transcription factors. *Proceedings of the National Academy of Sciences of the United States of America, 110*(30), 12349-12354. doi: 10.1073/pnas.1310430110

O'Toole, G. A. (2011). Microtiter dish biofilm formation assay. *J Vis Exp*(47). doi: 10.3791/2437

Patell, S., Gu, M., Davenport, P., Givskov, M., Waite, R. D., & Welch, M. (2010). Comparative microarray analysis reveals that the core biofilm-associated transcriptome of *Pseudomonas aeruginosa* comprises relatively few genes. *Environ Microbiol Rep, 2*(3), 440-448. doi: 10.1111/j.1758-2229.2010.00158.x

Petersen, I., Reichel, M. B., & Dietel, M. (1996). Use of non-radioactive detection in SSCP, direct DNA sequencing and LOH analysis. *Clin Mol Pathol, 49*(2), M118-121.

Rainey, P. B. (1999). Adaptation of Pseudomonas fluorescens to the plant rhizosphere. *Environ Microbiol, 1*(3), 243-257.

Rhee, S. G., Park, S. C., & Koo, J. H. (1985). The role of adenylyltransferase and uridylyltransferase in the regulation of glutamine synthetase in *Escherichia coli*. *Curr Top Cell Regul, 27*, 221-232.

Rossignol, G., Merieau, A., Guerillon, J., Veron, W., Lesouhaitier, O., Feuilloley, M. G., & Orange, N. (2008). Involvement of a phospholipase C in the hemolytic activity of a clinical strain of *Pseudomonas fluorescens*. *BMC Microbiol, 8*, 189. doi: 10.1186/1471-2180-8-189

Sambrook, J., Fritsch, E.F., & Maniatis, T. (1989). Molecular Cloning: A Laboratory Manual. *Cold Spring Harbor Laboratory Press, New York, USA*.

Sanchez, D. G., Primo, E. D., Damiani, M. T., & Lisa, A. T. (2017). *Pseudomonas aeruginosa gbdR* gene is transcribed from a sigma54-dependent promoter under the control of NtrC/CbrB, IHF and BetI. *Microbiology, 163*(9), 1343-1354. doi: 10.1099/mic.0.000502

Schumacher, J., Behrends, V., Pan, Z., Brown, D. R., Heydenreich, F., Lewis, M. R., . . . Buck, M. (2013). Nitrogen and carbon status are integrated at the transcriptional level by the nitrogen regulator NtrC *in vivo*. *MBio, 4*(6), e00881-00813. doi: 10.1128/mBio.00881-13

Shearwin, K. E., Dodd, I. B., & Egan, J. B. (2002). The helix-turn-helix motif of the coliphage 186 immunity repressor binds to two distinct recognition sequences. *J Biol Chem, 277*(5), 3186-3194. doi: 10.1074/jbc.M107740200

Sieira, R., Arocena, G. M., Bukata, L., Comerci, D. J., & Ugalde, R. A. (2010). Metabolic control of virulence genes in *Brucella abortus*: HutC coordinates *virB* expression and the histidine utilization pathway by direct binding to both promoters. *J Bacteriol, 192*(1), 217-224. doi: 10.1128/jb.01124-09

Sieira, R., Bialer, M. G., Roset, M. S., Ruiz-Ranwez, V., Langer, T., Arocena, G. M., . . . Zorreguieta, A. (2016). Combinatorial control of adhesion of *Brucella abortus*

2308 to host cells by transcriptional rewiring of the trimeric autotransporter *btaE* gene. *Mol Microbiol, 103*(3), 553-565. doi: 10.1111/mmi.13576

Siggers, T., & Gordan, R. (2014). Protein-DNA binding: complexities and multi-protein codes. *Nucleic acids research, 42*(4), 2099-2111. doi: 10.1093/nar/gkt1112

Slattery, M., Zhou, T. Y., Yang, L., Machado, A. C. D., Gordan, R., & Rohs, R. (2014). Absence of a simple code: how transcription factors read the genome. *Trends in Biochemical Sciences, 39*(9), 381-399. doi: 10.1016/j.tibs.2014.07.002

Studier, F. W., & Moffatt, B. A. (1986). Use of bacteriophage T7 RNA polymerase to direct selective high-level expression of cloned genes. *J Mol Biol, 189*(1), 113-130.

Sugden, M. C., & Holness, M. J. (2011). The pyruvate carboxylase-pyruvate dehydrogenase axis in islet pyruvate metabolism: Going round in circles? *Islets, 3*(6), 302-319. doi: 10.4161/isl.3.6.17806

Todeschini, A. L., Georges, A., & Veitia, R. A. (2014). Transcription factors: specific DNA binding and specific gene regulation. *Trends in Genetics, 30*(6), 211-219. doi: 10.1016/j.tig.2014.04.002

Twerdochlib, A. L., Chubatsu, L. S., Souza, E. M., Pedrosa, F. O., Steffens, M. B., Yates, M. G., & Rigo, L. U. (2003). Expression, purification, and DNA-binding activity of the solubilized NtrC protein of *Herbaspirillum seropedicae*. *Protein Expr Purif, 30*(1), 117-123.

Wargo, M. J., Gross, M. J., Rajamani, S., Allard, J. L., Lundblad, L. K., Allen, G. B., . . . Hogan, D. A. (2011). Hemolytic phospholipase C inhibition protects lung function during *Pseudomonas aeruginosa* infection. *Am J Respir Crit Care Med, 184*(3), 345-354. doi: 10.1164/rccm.201103-0374OC

Yano, H., Genka, H., Ohtsubo, Y., Nagata, Y., Top, E. M., & Tsuda, M. (2013). Cointegrate-resolution of toluene-catabolic transposon Tn4651: determination of crossover site and the segment required for full resolution activity. *Plasmid, 69*(1), 24-35. doi: 10.1016/j.plasmid.2012.07.004

Yeung, A. T., Torfs, E. C., Jamshidi, F., Bains, M., Wiegand, I., Hancock, R. E., & Overhage, J. (2009). Swarming of *Pseudomonas aeruginosa* is controlled by a broad spectrum of transcriptional regulators, including MetR. *J Bacteriol, 191*(18), 5592-5602. doi: 10.1128/JB.00157-09

Zhang, X. X., George, A., Bailey, M. J., & Rainey, P. B. (2006). The histidine utilization (hut) genes of *Pseudomonas fluorescens* SBW25 are active on plant surfaces, but are not required for competitive colonization of sugar beet seedlings. *Microbiology, 152*(Pt 6), 1867-1875. doi: 10.1099/mic.0.28731-0

Zhang, X. X., & Rainey, P. B. (2007). Genetic analysis of the histidine utilization (*hut*) genes in *Pseudomonas fluorescens* SBW25. *Genetics, 176*(4), 2165-2176. doi: 10.1534/genetics.107.075713

Zhang, X. X., & Rainey, P. B. (2008). Dual involvement of CbrAB and NtrBC in the regulation of histidine utilization in *Pseudomonas fluorescens* SBW25. *Genetics, 178*(1), 185-195. doi: 10.1534/genetics.107.081984

3.6 Supplementary data

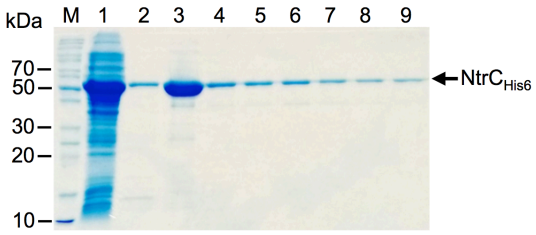

Figure S3.1. SDS-PAGE analysis of the purified $NtrC_{His6}$ protein. Lane 1, IPTG-induced whole cell lysate. Lane 2, flow-through fraction with washing buffer containing 70 mM imidazole. Lane 3 - 9, elution fractions by elution buffer containing 200 mM imidazole. Lane M, protein molecular weight marker. $NtrC_{His6}$ protein with molecular weight of 54 kDa is indicated by an arrow.

Table S3.1. Predicted HutC-binding sites in *P. fluorescens* SBW25

p-value	Matched Sequence [a]	Motif Location		Putative or established function of candidate genes [b]
		Start	End	
8.49E-09	TATA**TGTA**TA**TACA**AA	396038	396053	PFLU0358: HutF
9.13E-09	TGCT**TGTA**TG**TACA**AG	397745	397760	PFLU0361: HutU
1.21E-06	TCCA**TGTA**TA**AACA**AG*	2682811	2682826	PFLU2466: hypothetical protein. PFLU2467: AraC family transcriptional regulator.
2.49E-06	TATT**TGTA**TA**CAAA**AG	4800553	4800568	PFLU4355: Xanthine/uracil permeases family protein.
3.69E-06	TATT**TGTA**TG**CACA**GA*	6665739	6665754	PFLU6087: putative N-acetylmuramoyl-L-alanine amidase, an enzyme participates in peptidoglycan catabolic process. PFLU6088: putative GTP cyclohydrolase.
4.59E-06	GATA**TGTT**TG**TACA**AG	3934565	3934580	
6.34E-06	TGTA**TGTA**TA**TACA**GC*	957430	957445	PFLU0848: Plc, phosphatidylcholine-hydrolyzing phospholipase C. PFLU0849: 5-dehydro-4-deoxyglucarate dehydratase, an enzyme involved in D-glucarate degradation.
6.47E-06	TGTT**TGAA**TA**TTCA**AA	5361498	5361513	PFLU4885: hypothetical protein. A LTXXQ domain-containing protein, which shows similarity to a pilus assembly protein.
7.22E-06	TGTA**TGCA**AA**TACA**AA	2875177	2875192	PFLU2604: hypothetical protein, which shows similarity to the GCN5 family acetyltransferase.
8.74E-06	TGCT**TGTT**TA**TATA**AG	3019426	3019441	PFLU2736: hypothetical protein.
8.93E-06	TGTT**TGCA**TG**TTCA**AA	1819996	1820011	PFLU1658: Fnl2, NAD dependent epimerase/dehydratase.
9.06E-06	TGTT**CGTT**TG**TACA**AG*	5428854	5428869	PFLU4947: hypothetical protein. Its identified ortholog is pilus assembly protein PilZ.
9.13E-06	TGCA**TGTA**TG**TGCA**TG	5770150	5770165	PFLU5255: Hypothetical protein. Its ortholog is ribosome maturation protein RimP, which is important for maturation of the 30S ribosomal subunit.
1.14E-05	TATG**TGGA**TA**TAAA**AA	3125190	3125205	
1.15E-05	TATA**TCAA**TT**TACA**AG	1851392	1851407	
1.23E-05	CATA**TATA**TA**TAAA**AA	192404	192419	PFLU0172: hypothetical protein.
1.56E-05	TATT**TATT**TA**TATA**AA	817631	817646	PFLU0709: RspL, alternate sigma factor. PFLU0710: No information.
1.57E-05	TATT**TGTA**TG**TAGG**AC	4575786	4575801	

1.79E-05	GATT**TTTA**TA**TAGA**AG	4674453	4674468	
2.36E-05	TTTA**TGTT**TA**TAAA**AA	5295164	5295179	PFLU4815: putative glutathione S-transferase like protein.
2.36E-05	TTTT**TGCA**TG**TACA**AC	3711537	3711552	PFLU3353: putative amidase, its ortholog is acyl-homoserine lactone acylase subunit beta, which is involved in quorum sensing. PFLU3354: hypothetical protein.
2.36E-05	TACC**TATA**TA**TACC**AG	5252378	5252393	
2.62E-05	TACT**CGTA**TT**TAGA**AG	3126232	3126247	
2.97E-05	TACT**CGTA**TA**TACA**TT*	520016	520031	PFLU0460: AceE, pyruvate dehydrogenase subunit E1. PFLU0461: bifunctional glutamine-synthetase adenylyltransferase/deadenyltransferase.
3.04E-05	TATT**TCGA**TA**CACA**AA	4779233	4779248	PFLU4327: putative sulfatase.
3.17E-05	TATT**TGAC**TA**TAAA**AA	3433087	3433102	PFLU3141: LipB, lipase.
3.19E-05	CAGT**TGTA**TG**CACA**TG*	360518	360533	PFLU0327: HisB, imidazoleglycerol-phosphate dehydratase.
3.29E-05	TATT**TATA**TG**AATA**AA	4501472	4501487	PFLU4069: hypothetical protein.
3.37E-05	GATT**TGTA**TA**ATA**AG	2182043	2182058	PFLU2013: CycA, D-serine/D-alanine/glycine transporter.
3.43E-05	TATA**TCGA**TA**TTCA**AG	4573285	4573300	
3.43E-05	TATT**CGTA**CA**TAGA**AG	6418864	6418879	PFLU5862: ArgA, N-acetylglutamate synthase involved in arginine biosynthesis pathway.
3.54E-05	TATT**TTTT**TG**TAAA**AG	2045361	2045376	PFLU1874: putative transporter-like acyltransferase protein. Its ortholog is glycerol acyltransferase.
3.54E-05	TATC**TGTC**TG**TACG**AA	4678701	4678716	
3.54E-05	TATG**TGTA**TG**AGCA**AG	1584681	1584696	
3.63E-05	TAAT**TGGT**TG**TACA**AG	3192681	3192696	
3.67E-05	TAAT**TGTG**AG**TACA**AG	6160944	6160959	PFLU5623: GlcB, malate synthase G.
3.68E-05	TTTT**TGTA**GG**TAAA**AG	3761310	3761325	
3.79E-05	TATA**TGTC**GA**TCCA**AA	1060899	1060914	
3.79E-05	TATA**TGTG**AA**TACA**GA	3527700	3527715	PFLU3218: putative TonB-dependent outer membrane receptor. PFLU3219: SyrP-like protein. SyrP is a regulatory protein involved in syringomycin production and virulence in *P. syringae*.
3.93E-05	GATA**TGCA**TA**TTCA**AA	4101662	4101677	PFLU3705: hypothetical protein.
4.04E-05	TATA**TGAA**CA**TTCA**AA	4570067	4570082	PFLU4126B: hypothetical protein.
4.14E-05	TATA**GGTA**TG**TTAA**AA	1818852	1818867	
4.18E-05	TATA**TTTA**CG**TGCA**AA	2720248	2720263	
4.37E-05	TATT**TGGA**TG**TAAC**AA	3164038	3164053	PFLU2900: hypothetical protein.
4.45E-05	CACT**TTTA**TG**TAAA**AA	3431252	3431267	PFLU3139: hypothetical protein. PFLU3140: putative lipoprotein.
4.45E-05	CCAC**TGTC**CG**AACA**AC*	377028	377043	PFLU0344: NtrB, nitrogen-specific signal transduction histidine kinase.
4.45E-05	TATA**TGGA**TG**CAAA**AA	3468310	3468325	PFLU3176: aspartate aminotransferase, which catalyzes the interconversion of aspartate and α-ketoglutarate to oxaloacetate and glutamate. PFLU3177: hypothetical protein. Its ortholog is NAD-dependent dehydratase.
4.45E-05	TATA**TTTA**TG**ACCA**AA	4101101	4101116	
4.56E-05	TATA**TCTT**TG**TCCA**AA	5824380	5824395	PFLU5305: putative plasmid partitioning protein.
4.56E-05	TACA**TATT**TG**TAGA**AA	6297047	6297062	
4.61E-05	TATT**TCCA**TG**TACA**CA	6639456	6639471	PFLU6064: GntR family transcriptional regulator. PFLU6065: putative regulatory protein.
4.71E-05	TACT**TCTA**GA**TGCA**AG	960179	960194	PFLU0851: putative sugar ABC transporter membrane protein.

				Its ortholog is glucarate transporter.
4.81E-05	TACT**AGTA**TA**TAGA**GG	1612714	1612729	PFLU1465: NadB, L-aspartate oxidase, which participates in alanine and aspartate metabolism. PFLU1467: AlgU, a sigma factor, which regulates genes involved in alginate biosynthesis.
4.95E-05	TATT**TGTA**CA**CACG**AG	2357140	2357155	PFLU2175: hypothetical protein.
5.15E-05	TATT**GGTC**AA**TACA**AG	3188737	3188752	
5.28E-05	TATA**GGTA**CA**AACA**AG	4575654	4575669	
5.47E-05	TATT**TCTG**TG**TACA**CG	202548	202563	
5.74E-05	TATA**TGTA**CG**TATA**CG	2930280	2930295	PFLU2657: putative sulfite reductase. PFLU2658: hypothetical protein.
5.89E-05	TTCA**TGTC**TA**AACA**AA	2052141	2052156	PFLU1879: hypothetical protein.
5.89E-05	TCTA**TGCA**TG**TCCA**AA	2691737	2691752	PFLU2477: hypothetical protein.
5.99E-05	CACA**TGTA**CA**TACA**GA	2409875	2409890	PFLU2222: putative ABC transporter membrane protein.
5.99E-05	TACA**TGTA**GA**TACT**CA	3192340	3192355	PFLU2927: hypothetical protein.
5.99E-05	TACT**TGGA**GA**TACA**CA	5654723	5654738	PFLU5155: putative MerR family transcriptional regulator. PFLU5156: hypothetical protein with very high similarity to antibiotic biosynthesis monooxygenase.
5.99E-05	AATA**CGTA**TG**TTCA**AA	2065013	2065028	PFLU1890: hypothetical protein.
6.05E-05	TATT**TGGA**TG**AACC**AA	2069374	2069389	
6.05E-05	TATT**GGTA**TG**TGCA**TA	3168701	3168716	
6.17E-05	TACA**TGGA**AA**TCCA**AG	2730579	2730594	PFLU2516: hypothetical protein, a TetR family transcriptional regulator.
6.17E-05	TATT**TGTT**TG**ATCA**AG	1968004	1968019	PFLU1803: Gcl, glyoxylate carboligase, which participates in glycolate degradation. PFLU1804: hypothetical protein. Its ortholog is GlcG protein with unknown function.
6.21E-05	TATT**CGTA**AG**TACA**CG	2958127	2958142	PFLU2681: PepN, aminopeptidase.
6.24E-05	AATT**TGTA**GG**TTCA**AG	4649122	4649137	PFLUt63: tRNA-Glu.
6.25E-05	TACT**CGTA**TG**AAGA**AG	5761130	5761145	PFLU5248: osmotically inducible protein Y.
6.32E-05	TGTT**TTTA**TA**TACA**GT	54429	54444	PFLU0054: hypothetical protein with very high similarity to DNA repair photolyase.
6.32E-05	TGAT**CGTA**TC**TACA**AG	4367523	4367538	
6.37E-05	TGCG**TTTA**TC**TACA**AG	5381873	5381888	
6.37E-05	TTCA**TGTA**TG**TACT**GG	5604071	5604086	PFLU5103: hypothetical protein.
6.43E-05	TGCA**TGGA**TT**TACA**AT	829311	829326	PFLU0727: RspB, putative type III secretion protein.
6.43E-05	TGTA**TGTA**TT**AATA**AA	2164052	2164067	PFLU1992: hypothetical protein, showing high similarity to amidase. PFLU1993: GntR family transcriptional regulator.
6.49E-05	CACA**TGGA**TG**TACA**CA	4109407	4109422	
6.52E-05	TGTT**TTTT**TC**TACA**AG	5256428	5256443	
6.62E-05	TACT**CGTC**TG**TACG**AG	5539401	5539416	PFLU5040: PTS system sucrose-specific transporter subunit IIBC. PFLU5041: trehalose operon transcriptional repressor.
6.68E-05	TGTT**TGTA**TA**GACA**GT	1303654	1303669	PFLU1166: hypothetical protein. PFLU1167: putative regulatory protein, its ortholog is transcriptional repressor PrtR which regulates pyocin-producing genes.
6.78E-05	TGTA**TGCA**TA**TACA**GT	1304632	1304647	PFLU1169: hypothetical protein.
6.79E-05	TGAA**TGTG**TA**AACA**AA	3336181	3336196	
6.86E-05	TGTA**CGTA**TT**TACC**AA	3708943	3708958	PFLUt50: tRNA-Cys.
6.86E-05	TGTC**TGTA**TG**CAAA**AA	3777730	3777745	

6.95E-05	TGTC**GGTA**TA**AACA**AG	4334862	4334877	PFLU3927: DNA-binding ATP-dependent protease La; heat shock K-protein.
6.99E-05	GGCA**TATA**TC**TACA**AG	3832062	3832077	
7.03E-05	AGCA**TGGA**TA**TACA**AC	6590392	6590407	PFLU6027: hypothetical protein.
7.04E-05	TGTT**TATA**AA**TGCA**AA	5351550	5351565	PFLU4870: aromatic amino acid transport protein. PFLU4872: hypothetical protein with high similarity to leucyl aminopeptidase (aminopeptidase T).
7.04E-05	TGTA**TGTT**TG**TACA**GC	1918052	1918067	PFLU1750: hypothetical protein, a highly conserved transcriptional regulator in *Pseudomonas*.
7.13E-05	TGTA**TGGA**TG**TACA**GC	2337963	2337978	PFLU2157: TopB, DNA topoisomerase III.
7.16E-05	TGTA**TGTA**TG**AACA**GT	3123864	3123879	PFLU2842: hypothetical protein. Its ortholog is ATP-dependent hsl protease ATP-binding subunit hslU.
7.18E-05	TGTA**ATTG**TA**TACA**AG	1967841	1967856	PFLU1803: Gcl, glyoxylate carboligase, which participates in glycolate degradation. PFLU1804: hypothetical protein. Its ortholog is GlcG protein with unknown function.
7.24E-05	TGCG**TGAA**TA**TCCA**AA	5683522	5683537	PFLU5187: putative amino acid transporter membrane protein.
7.24E-05	CGAA**TGTT**TG**TACA**AA	127586	127601	
7.27E-05	TGGT**TGTC**TG**TTCA**AA	2366894	2366909	
7.27E-05	GGAT**TGCA**TG**TACA**AG	4094071	4094086	PFLU3698: putative TonB-dependent outer membrane receptor protein. PFLU3699: putative GGDEF domain signaling protein.
7.29E-05	TGCT**TGTA**AA**GATA**AA	445895	445910	PFLU0402: PriA, primosome assembly protein. PFLU0403: RpmE, 50S ribosomal protein L31.
7.39E-05	TGCA**TTTA**TA**TCCA**CA	2201527	2201542	
7.44E-05	TGCT**TATC**GA**TACA**AA	2574931	2574946	PFLU2365: putative TonB-dependent siderophore receptor.
7.52E-05	GGTA**GGGA**TA**TACA**AA	3018076	3018091	PFLU2734: hypothetical protein.
7.61E-05	GGTA**TGTA**TA**TACG**TA*	3255865	3255880	PFLU2987: putative phage cointegrase resolution protein. PFLU2988: TnpS, cointegrase.
7.87E-05	CGTA**GGTA**TA**TACA**CA	5503929	5503944	PFLU5008: XerD, site-specific tyrosine recombinase.
7.87E-05	TGCA**TGAA**TA**GATA**AA	5540677	5540692	PFLU5042: putative regulatory protein.
7.92E-05	TGCA**GGTC**TG**TACA**AC	2315111	2315126	
7.98E-05	TGCT**GGTC**TG**TACA**AT	4750305	4750320	PFLU4307: TenA family transcriptional regulator.
7.98E-05	TGTT**TGTC**TG**AAAA**AA	2489624	2489639	PFLU2290: putative acetyl-CoA synthetase.
8.08E-05	TGTT**TGTC**TG**AAAA**AA	2490009	2490024	
8.14E-05	TGCA**TCTA**TG**TAAA**TA	3330114	3330129	
8.25E-05	TGTT**TGTC**TG**TGAA**AA	3391717	3391732	
8.32E-05	TGCA**TCAA**TG**TAAA**AA	792973	792988	
8.35E-05	TGCA**TGTA**TA**CCGA**AG	2443235	2443250	
8.38E-05	AGCT**TTTA**TA**TTCA**AG	3752558	3752573	
8.49E-05	GGCT**TCTA**TA**AACA**AG	4361503	4361518	
8.57E-05	TGCA**TGTA**TA**TAAT**GG	5544003	5544018	PFLU5044: inosine 5'-monophosphate dehydrogenase.
8.57E-05	CGTA**TCTA**TG**CACA**AG	1513619	1513634	
8.67E-05	TGTT**TCGG**TG**TACA**AG	4620202	4620217	
8.67E-05	TGCG**TGTG**TG**TACA**CG	2550391	2550406	
8.87E-05	TGCT**TGTA**GA**AACC**AA	5013760	5013775	
8.99E-05	TGCT**TGCA**TA**GCCA**AA	1627083	1627098	
8.99E-05	TGCA**TGTT**TA**TCCA**CA	5014262	5014277	
9.14E-05	TGCT**TCTG**TG**TACA**TA	1360685	1360700	
9.23E-05	CGCA**TGTT**TG**TAGA**AA	2011553	2011568	

9.23E-05	TGCA**TTTA**TG**TCCC**AA	6232815	6232830	PFLU5686: BetA, choline dehydrogenase.
9.23E-05	CGCA**AATA**TG**TACA**AA	935972	935987	PFLU0826: DppA3, dipeptide ABC transporter substrate-binding protein.
9.26E-05	TGTT**TGTC**TG**TACG**TA	3251963	3251978	PFLU2983: putative lipoprotein.
9.28E-05	TGCT**TGTA**AG**TTTA**AA	6251444	6251459	PFLU5700: hypothetical protein.
9.32E-05	TGCA**GGTA**GA**GACA**AG	3028964	3028979	PFLU2745: putative ABC transporter mannitol-binding protein.
9.39E-05	TGCT**TTTT**TG**TTCA**AG	75295	75310	PFLU0074: ZnuC, high-affinity zinc ABC transporter ATP-binding protein.
9.39E-05	TGTT**TGCA**GG**TACA**CG	709299	709314	PFLU0626: SpeA, arginine decarboxylase.
9.46E-05	TGTT**TGTG**TG**AACA**GG	2914511	2914526	PFLU2640: putative substrate-binding transport protein.
9.46E-05	TGCT**TGTA**AG**AAAA**AG	6506555	6506570	
9.46E-05	TGCA**TATA**TG**ACCA**AG	6578846	6578861	PFLU6017: hypothetical protein with high similarity to a type VI secretion protein. PFLU6018: hypothetical protein with high similarity to the type VI secretion protein ImpA.
9.48E-05	TGCT**GGGA**TG**TACA**CA	52910	52925	PFLU0053: AdhB, alcohol dehydrogenase cytochrome C subunit.
9.57E-05	TGCT**TGTC**TG**CACG**AA	875808	875823	PFLU0772: putative type IV pilus-like protein. PFLU0773: hypothetical protein. Its ortholog is pilus assembly protein PilV.
9.57E-05	GGCA**AGTA**GG**TACA**AA	1909814	1909829	PFLU1740: putative two-component system response regulator, LuxR family transcriptional regulator.
9.57E-05	TGCA**GGTA**CG**TGCA**AA	3122089	3122104	PFLU2839: hypothetical protein.
9.57E-05	TGCA**TGGA**TG**AACG**AG	486244	486259	PFLU0438: hypothetical protein, shows similarity to 3-oxoacyl-ACP synthase, which is involved in fatty acid biosynthesis. PFLU0439: putative chromosome partitioning ParA-like protein.
9.64E-05	CGCA**TGGA**TG**TGCA**AG	1174625	1174640	PFLU1062: RecO, DNA repair protein.
9.72E-05	TGCT**TGTA**CG**TCCA**GG	3067587	3067602	PFLU2774: putative 3-phosphoshikimate 1-carboxyvinyltransferase, which is involved in aromatic amino acid biosynthesis.
9.75E-05	TGCA**TGCC**AG**TACA**AG	3799694	3799709	PFLU3431: hypothetical protein.
9.82E-05	GGCT**TGAA**TG**TGCA**AG	4276360	4276375	
9.93E-05	GGCA**TGGA**TG**TACA**TG	6436208	6436223	PFLU5879: 2-octaprenyl-6-methoxyphenyl hydroxylase, which is involved in ubiquinone biosynthesis and oxidation-reduction process.

[a] The putative HutC-binding Phut site is highlighted in boldface type.

[b] Genes harboring a predicted HutC-binding site in their regulatory region (from 500 bp upstream to 100bp downstream of the start codon).

* The predicted HutC-binding sites verified by EMSA with purified $HutC_{His6}$.

Chapter 4

How carbon/nitrogen metabolic balance is maintained for histidine utilization by *Pseudomonas*

Abstract

Histidine is a good source of nutrients for *Pseudomonas fluorescens* SBW25, but its utilization poses a significant challenge as it produces excess nitrogen over carbon. The rate of histidine utilization (*hut*) thus must be carefully regulated. Here we show, for the first time, that expression of *hut* genes is positively regulated by two global regulators CbrAB and NtrBC in a *direct* manner, while subjecting to histidine concentration-dependent negative control by the HutC repressor. *hut* expression is further regulated at the post-transcriptional level by the CbrAB-CrcYZ-Crc/Hfq cascade in response to the presence of succinate (the most preferred carbon source). When growing in nutrient-complex conditions such as a minimal medium supplemented with succinate and histidine, wherein histidine is the sole nitrogen but less-preferred carbon source, CbrAB is involved in directly activating *hut* transcription but indirectly repressing *hut* translation. Under this condition, NtrBC plays the dominant role in transcriptional activation of *hut*, but it requires assistance of the HutC repressor. A combination of genetic and biochemical analysis show that HutC acts as a governor to monitor and control histidine catabolic rate, preventing production of excess ammonium and subsequent inactivation of the NtrBC system. HutC can additionally recognise the NtrC binding site responsible for *ntrBC* expression, which provides a negative feedback for NtrBC autoregulation. Together, our data show that carbon/nitrogen metabolic balance is maintained by the interplay of CbrAB and NtrBC at the *hut* operator site, and it requires the local regulator HutC to prevent *hut* expression from exceeding a critical upper limit.

4.1 Introduction

Carbon catabolite repression (CCR) enables bacteria to preferentially utilize certain carbon and energy sources over others to maximize their growth rate and competitive fitness in nutrient-complex environments (Gorke & Stulke, 2008; Romero-Rodriguez *et al.*, 2018). The phenomenon of CCR was first proposed by Magasanik (1955) on the basis of the observation that glucose represses expression of enzymes for the utilization of histidine and lactose in enteric bacteria (Magasanik, 1955). The molecular mechanisms driving CCR have been extensively studied in *E. coli*, which preferentially utilize glucose over less preferred carbon sources such as lactose (Bruckner & Titgemeyer, 2002). The catabolite-activating protein (CAP) charged with cAMP is required for transcriptional activation of the lactose utilization (*lac*) genes. The activity of adenylate cyclase for cAMP synthesis and the transporter of lactose are inhibited in the presence of glucose (Deutscher, 2008; Gorke & Stulke, 2008). However, this well-defined mechanism does not hold for many non-enteric bacteria, including *Pseudomonas*.

Succinate is the most preferred carbon source for *Pseudomonas*, and it represses the expression of enzymatic genes and transporters for the utilization of glucose, mannitol, histidine, *etc.* (Collier *et al.*, 1996; Rojo, 2010). Recent work shows that CCR in *Pseudomonas*, including *P. fluorescens* SBW25, occurs at the post-transcription level via the CbrAB-CrcYZ-Crc/Hfq regulatory cascade. Translation of the substrate-specific catabolic genes is repressed by the RNA-binding Crc/Hfq protein complex in the presence of succinate. When succinate is consumed, CbrAB activates expression of the ncRNAs (CrcY and CrcZ), which prevents the Crc/Hfq protein from binding to the mRNA transcripts (Hernandez-Arranz *et al.*, 2013; Liu *et al.*, 2017; Sonnleitner *et al.*, 2009).

Histidine serves as a source of carbon and nitrogen for many bacteria. Historically, the pathway of histidine utilization (*hut*) has been an important model in bacterial genetics, particularly for the coordination of cellular carbon and nitrogen metabolisms (Bender, 2012). Early studies on histidine utilization in *Klebsiella pneumoniae* has led to the concept of catabolite repression (Magasanik, 1961). In *K. pneumoniae*, histidine degradation is inhibited in the presence of glucose (Magasanik, 1955). Transcription of *hut* genes is activated by CAP charged with cAMP in response to carbon limitation. Glucose reduces the intracellular cAMP levels, thereby repressing the *hut* expression (Osuna *et al.*, 1991; Osuna *et al.*, 1994; Prival & Magasanik, 1971).

However, the mechanisms of CCR involved in histidine utilization in *Pseudomonas* is not known. The CAP homolog and cAMP play no role in *hut* regulation and catabolite repression in *Pseudomonas* (Phillips & Mulfinger, 1981; Suh *et al.*, 2002). The succinate-provoked CCR of histidine utilization has been reported in different *Pseudomonas* species (Hug *et al.*, 1968; Lessie & Neidhardt, 1967). Previous work in other *Pseudomonas* species revealed no significant role of Crc in the CCR control of *hut* genes (Collier *et al.*, 1996; Moreno *et al.*, 2009). The CbrAB two-component system is required for activation of *hut* genes in response to carbon limitation (Li & Lu, 2007; Nishijyo *et al.*, 2001; Zhang & Rainey, 2008). When growing on histidine as the sole carbon source, the *hutU-G* operon of *P. fluorescens* is transcribed from a σ^{54}-dependent promoter (Zhang & Rainey, 2008). These data suggest that CbrAB likely activate *hut* transcription in a direct manner.

Histidine is a source of both carbon and nitrogen, and thus, the expression of *hut* genes is also subject to nitrogen regulation. In enteric bacteria, transcription of the *hut* genes is activated by the nitrogen assimilation control protein (NAC) from a σ^{70}-promoter when histidine is used as a nitrogen source (Bender, 2010; Goss & Bender, 1995; Schwacha & Bender, 1993). The expression of *nac* is activated by the two-component system NtrBC in a σ^{54}-dependent manner. The activity of NtrBC is controlled by the PII signaling system in response to nitrogen limitation (Itoh *et al.*, 2007; Reitzer, 2003). However, the homolog of NAC in *Pseudomonas* plays no role in the nitrogen regulation of *hut* genes (Hervas *et al.*, 2008; Zhang & Rainey, 2008). In *P. fluorescens*, both CbrAB and NtrBC contribute to the activation of *hut* genes when histidine is utilized as a nitrogen source. Deletion of *cbrB* reduces expression level of the *hutU-G* operon. The remaining *hutU-G* expression was maintained by NtrC as deletion of both *cbrB* and *ntrC* totally abolished the expression (Zhang & Rainey, 2008). However, the precise regulatory role of CbrB and NtrC in *hut* regulation is unclear, and it remains unknown whether the regulation is direct or indirect.

A major challenging task for efficient histidine utilization is to maintain carbon/nitrogen metabolic balance. When growing in nutrient-complex environment such as minimal salt medium supplemented with succinate and histidine, bacteria face a physiological dilemma to maximize *hut* expression as histidine is the sole source of nitrogen, meanwhile repressing *hut* activities as histidine is a less preferred carbon source. Therefore, defining the underlying mechanisms of *hut* regulation can provide insights into the coordination of cellular carbon and nitrogen metabolisms.

In this study, we report the positive regulatory mechanisms of *hut* gene expression in the plant growth-promoting bacterium *P. fluorescens* SBW25. Using a combination of genetic and biochemical analysis, we show that CbrAB directly activates transcription of the *hut* genes, but represses their expression at the translational level via the CbrAB-CrcYZ-Crc/Hfq cascade. However, under nitrogen-starved conditions, *hut* expression is directly activated by the NtrBC system. Metabolic balance for carbon and nitrogen is thus maintained through interplay between CbrAB and NtrBC at the *hut* operator sites. Furthermore, our data reveal a novel regulatory role of HutC in the autoregulation of NtrBC. The physiological significance of a local regulator functioning as a governor will be discussed.

4.2 Results

4.2.1 Identifying P_{hutU} as the major promoter of positive regulation by CbrAB and NtrBC

The *hut* genes of *P. fluorescens* SBW25 are organized in three transcriptional units (*hutF*, *hutCD* and *hutUT$_u$XWVH$_1$H$_2$T$_h$IG*), which are subject to negative regulation mediated by the HutC repressor (Zhang & Rainey, 2007) (Figure 4.1). In the absence of histidine, HutC binds to the operator sites of P_{hutF}, P_{hutC} and P_{hutU}, causing repression of *hut*; however, in the presence of histidine, the repression is relieved through molecular interactions between HutC and urocanate (the first intermediate of the histidine degradation pathway). In previous work we showed that CbrAB is required for bacterial growth on histidine as the sole carbon source; when histidine is used as the sole nitrogen source, either CbrB or NtrC can activate *hut* genes (Zhang & Rainey, 2008).

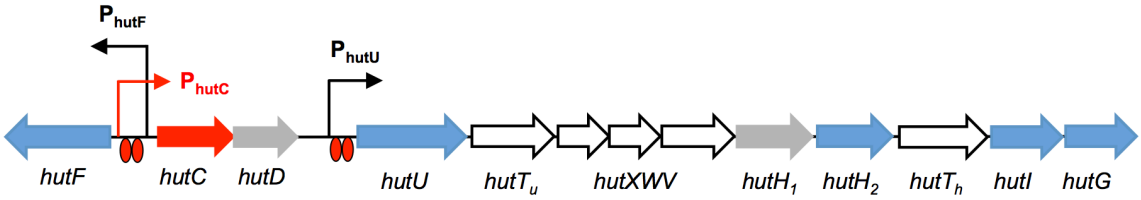

Figure 4.1. Structure of the *P. fluorescens* SBW25 *hut* locus. The *hut* genes are organized in three transcriptional units *hutF*, *hutCD* and *hutU-G*. Their expression is induced by the presence of histidine or urocanate, and the induction is mediated by the HutC repressor targeting two operator sites located in the front of *hutU* and the *hutFC* intergenic region. $hutT_u$ and $hutT_h$ encode the high-affinity transporter for urocanate and histidine, respectively. *hutXWV* encodes an ABC-type transporter that plays a minor role in histidine uptake. The *hut* locus contains two *hutH* homologues, but *hutH1* was not required for bacterial growth on histidine. *hutD* is located downstream of *hutC* in an overlapped manner, but its precise function remains unknown.

First, we sought to determine which *hut* promoters are subject to positive regulation by CbrAB and NtrBC. To this end, transcriptional *lacZ*-fusions to P_{hutU}, P_{hutF} and P_{hutC} were made separately in the genetic background of wild-type SBW25 and three derived mutants Δ*cbrB*, Δ*ntrC* and Δ*cbrB*Δ*ntrC*. β-galactosidase activities were measured for cells grown on minimal salts medium (MSM) supplemented with either histidine + NH_4Cl or succinate + histidine as the sole source of carbon and nitrogen, respectively. When histidine is the sole carbon source, expression of *hutU-G* was abolished in the Δ*cbrB* background, and no effect was observed for *ntrC* deletion (Fig. 4.2A). However, when histidine is the sole nitrogen source, deletion of *cbrB* and *ntrC* significantly reduced the P_{hutU} promoter activity by 50.2% and 65.4%, respectively. More importantly, none or minor effects were observed for P_{hutF} and P_{hutC} promoter activities (Fig. 4.2B&C). Together, the data indicate that positive regulation of *hut* is predominantly mediated by CbrAB and NtrBC through the P_{hutU} promoter activities, and further investigation has thus focused on the characterization of P_{hutU}.

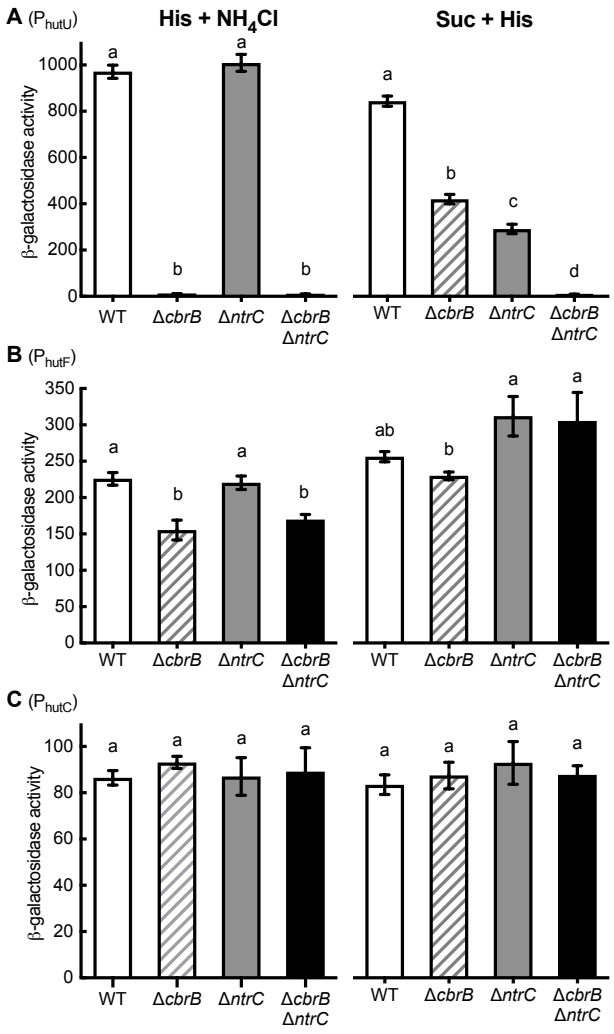

Figure 4.2. Expression of the P_{hutU} promoter, not P_{hutF} and P_{hutC}, is subject to positive regulation by CbrAB and NtrBC. β-galactosidase activities were measured for P_{hutU} **(A)**, P_{hutF} **(B)** and P_{hutC} **(C)** in wild-type SBW25 (WT) and three mutants devoid of *cbrB* and/or *ntrC*. Bacteria were grown in minimal salts medium supplemented with histidine (10 mM) + NH_4Cl (18.7 mM) or succinate (20 mM) + histidine (10 mM). Data are means and standard errors of four independent cultures. Bars that are not connected by the same letter (shown above each) are significantly different ($P < 0.05$) by Tukey's HSD test.

4.2.2 Genetic identification of NtrC and CbrB target sites in the P_{hutU} promoter

Two putative NtrC binding sites (namely NtrC-I/II and NtrC-III/IV, Fig. 4.3A) were identified by searching the intergenic region of *hutD* and *hutU* for the previously identified consensus sequence of NtrC binding site (GCACCA-N_3-TGGTGC). However, at the time this work was performed the CbrB binding sequence was not determined. To map the P_{hutU} promoter, a total of eleven P_{hutU} variants with the same 3′-end (+136) but variable 5′-ends were thus constructed in the plasmid vector pUC18-mini-Tn7T-lacZ (Fig. 4.3A). The

resulting transcriptional *lacZ* fusions were integrated into the mini-Tn7 site of wild-type SBW25. β-galactosidase activities were first compared for cells grown in minimal medium supplemented with succinate and histidine. Parallel to our expectation, P_{hutU} expression was reduced by half with the deletion of the NtrC-I half site (P_{hutU}D vs. P_{hutU}E), and the promoter activity was completely abolished when the second NtrC site (NtrC-III and NtrC-IV) was further deleted (P_{hutU}F vs. P_{hutU}G).

Of note, a small but significant reduction between P_{hutU}E and P_{hutU}F was observed with the deletion of the NtrC-II half site (Fig. 4.3A). This result was initially surprising, as NtrC-II was predicted to play a minor role in assisting NtrC-binding to its primary target site of NtrC-I. However, the data was consistent with the predicted role of CbrB in activating P_{hutU} when histidine is the sole nitrogen source (Fig. 4.2A). To test the involvement of CbrB, we compared the expression levels of three P_{hutU} variants (P_{hutU}D, P_{hutU}E and P_{hutU}F) in mutants devoid of *cbrB* and/or *ntrC* (Fig. 4.3B). Consistent with our expectation, the difference between P_{hutU}E and P_{hutU}F detected in wild type was not observed in the Δ*cbrB* mutant background (the remaining activity in Δ*cbrB* was clearly attributable to the second NtrC binding with NtrC-III/IV, as P_{hutU}F expression was abolished in the Δ*ntrC* mutant). The data thus suggest that NtrC and CbrB target the same DNA region to activate P_{hutU} for histidine utilization under N-starved conditions.

Next, we measured promoter activities of the eleven P_{hutU} variants in medium with histidine as the sole carbon source (Fig. 4.3A). Results clearly indicate that the 11 nt sequence present in P_{hutU}E but absent in P_{hutU}F was functionally required for P_{hutU} expression. The NtrC-II site (TGTTAC) was identical to the CbrB half site experimentally identified in the P_{crcZ} promoter of *P. aeruginosa* (Abdou *et al.*, 2011) and the P_{crcY} and P_{crcZ} promoters of *P. putida* (Garcia-Maurino *et al.*, 2013). A second CbrB half site (CbrB-II) was subsequently predicted in the P_{hutU} promoter region (Fig. 4.3A). Together, the genetic data strongly implicate that NtrBC and CbrAB regulate the P_{hutU} promoter activities in a direct manner.

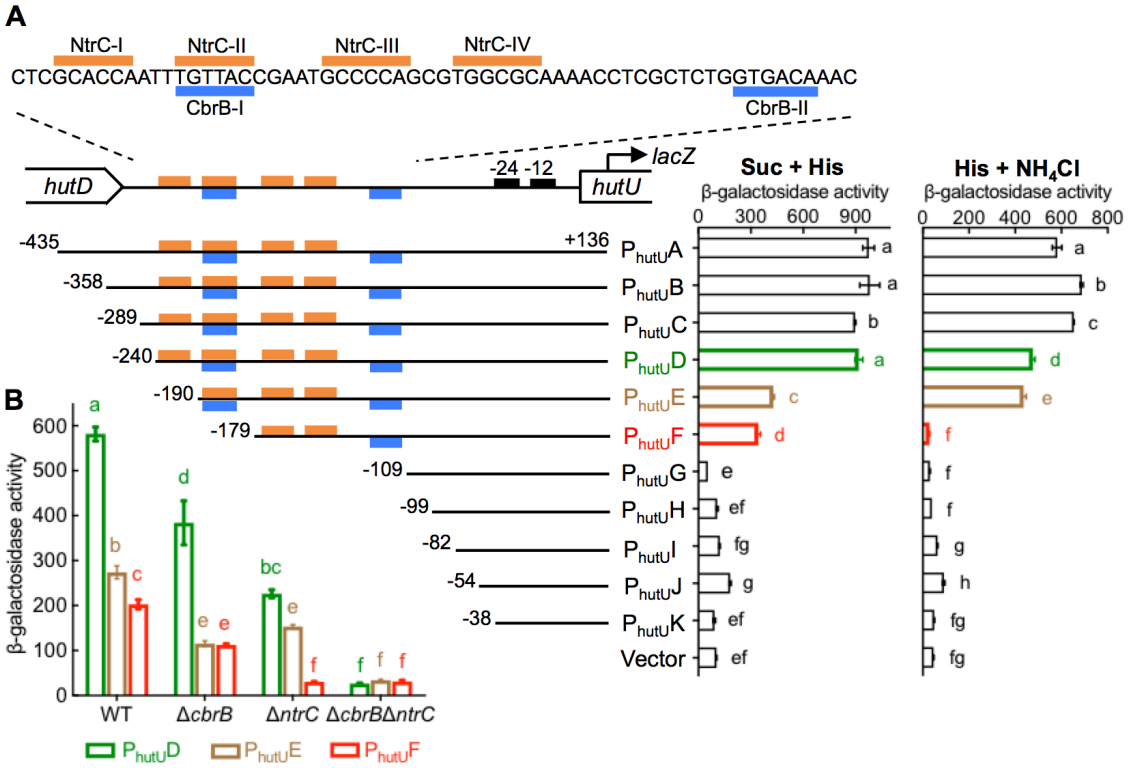

Figure 4.3. Genetic mapping of the P_{hutU} promoter showing the direct roles of CbrAB and NtrBC in *hut* expression.

(A) Levels of *hutU* expression in wild-type *P. fluorescens* SBW25 were compared using promoterless *lacZ* fusions to different P_{hutU} variants. Bacteria were grown in minimal salts medium supplemented with either succinate plus histidine (Suc + His) or histidine (His) plus NH_4Cl. Histidine, succinate and NH_4Cl were added at 10 mM, 20 mM and 18.7 mM, respectively.

(B) Expression levels of three P_{hutU}-*lacZ* variants were compared in wild-type (WT) and three mutant backgrounds (Δ*cbrB*, Δ*ntrC*, Δ*cbrB*Δ*ntrC*). Data are means and standard errors of four independent cultures. Bars that are not connected by the same letter (shown above each) are significantly different ($P < 0.05$) by Tukey's HSD test.

4.2.3 NtrC and CbrB bind *in vitro* with the P_{hutU} promoter DNA

To determine the direct interactions between NtrC and the P_{hutU} promoter, His_6-tagged NtrC from *P. fluorescens* SBW25 was expressed in *E. coli*, and the purified protein was first subject to DNase I footprinting analysis using a biotin-labelled P_{hutU} probe (PC-WT). Results show that a 44-bp DNA region was protected by $NtrC_{His6}$ from DNase I digestion, and it contains the two NtrC binding sites genetically identified above (Fig. 4.4A). Next, we subjected the purified $NtrC_{His6}$ protein to EMSA analysis with the wild-type P_{hutU} probe and three variants with substitutions of the NtrC-I, NtrC-II and NtrC-III/IV sites with random sequences. As shown in Figure 4.4C, a significant shift of the wild-type probe DNA (PC-

WT) was observed in the presence of increasing concentrations of $NtrC_{His6}$. However, for the three mutant probes DNA retardation was greatly reduced but was not completely abolished: although shifted bands were hardly visible, there was a significant reduction of the free probe DNAs with the addition of high concentrations of $NtrC_{His6}$ (Fig. 4.4C). The data thus suggest that NtrC-I, NtrC-II and NtrC-III/IV sites are all functionally required for stable binding of NtrC to the P_{hutU} promoter.

When EMSA was performed with purified $CbrB_{His6}$, a weak but significant shift was observed with wild-type P_{hutU} probe PE-WT, and DNA retardation was abolished with mutant probe PE-CbrB1 lacking the CbrB-I half site. While this result essentially confirmed the direct interaction between CbrB and P_{hutU}, we were unable to increase the proportion of shifted probe DNAs. This was initially surprising as we had no problem to achieve a ~60% DNA shift in a parallel EMSA assay with a P_{crcZ} probe (PcrcZ171, Fig. 4.4D). P_{crcZ} is a well-characterized promoter under the direct control of CbrB in *Pseudomonas*, including *P. fluorescens* SBW25 (Liu *et al.*, 2017). Interestingly, a comparative analysis of P_{crcZ} and P_{hutU} promoters from different *Pseudomonas* species revealed the presence of a third CbrB half site (designated CbrB-III, located in the middle between CbrB-I and CbrB-II) in all P_{crcZ} promoters (Fig. 4.5), but it is absent in the P_{hutU} promoters (Fig. 4.6). Notably, the P_{hutU} promoter of *P. brassicacearum* DF41 and *P. brassicacearum* NFM421 does contain three putative CbrB half sites. These suggest that the CbrB-III site is likely required for high-affinity CbrB binding. To test this, we performed EMSA with a mutant probe containing an introduced CbrB-III site (PE+CbrB3, Fig. 4.4D). Indeed, CbrB-binding was remarkably increased with a maximum of 51.3% probe DNA being shifted, whereas only 8.7% was shifted for the wild-type probe under the same assay conditions. Together, the data implicate that CbrB directly binds to P_{hutU} in relatively lower affinity when compared with the P_{crcZ} promoter.

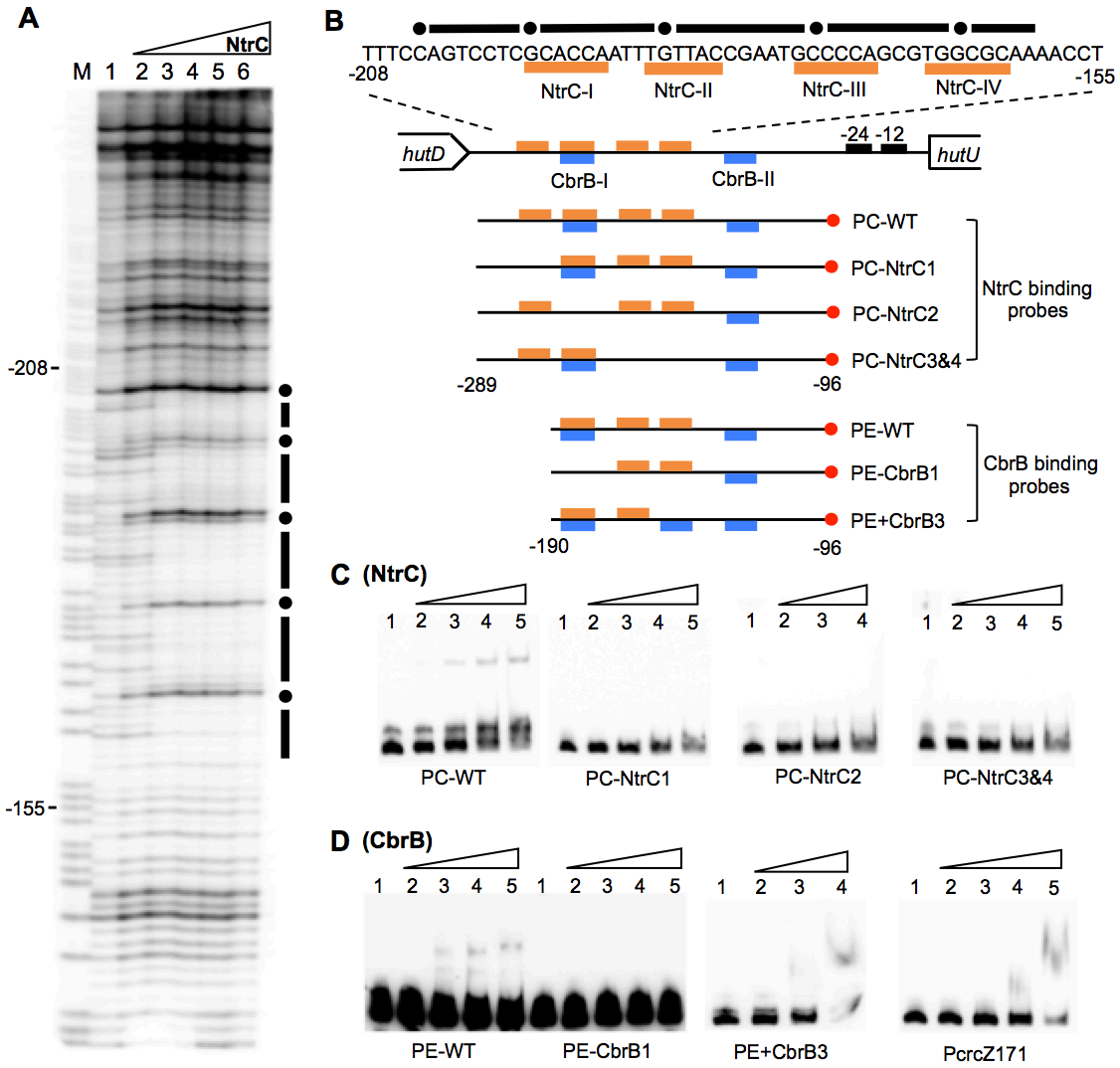

Figure 4.4. The protein-DNA interactions *in vitro* between NtrC/CbrB and their target P_{hutU} promoter.
(A) DNase I footprinting was performed using purified $NtrC_{His6}$ and a 194 bp biotin-labelled DNA probe PC-WT. Lane M is G+A marker; Lane 1, no $NtrC_{His6}$; Lane 2-6, $NtrC_{His6}$ added at an increasing concentration of 0.2, 0.6, 1.6, 3.2 and 5 μM, respectively. The protected region is indicated by black bars with hypersensitive residues being marked with filled circles.
(B) The intergenic region between *hutD* and *hutU* showing the DNA sequence protected by NtrC and locations of the DNA probes used for NtrC and CbrB binding assays. The biotin-labelled ends are marked with red circles.
(C) EMSA was performed using $NtrC_{His6}$ and biotin-labelled DNA probes containing wild-type (PC-WT) or mutant alleles devoid of NtrC-I, NtrC-II or NtrC-III/IV sites. Lane 1-5, $NtrC_{His6}$ was added at the concentrations of 0, 5, 15, 25 and 37.5 μM, respectively.
(D) EMSA analysis of $CbrB_{His6}$ was performed with a 95 bp probe DNA containing wild-type (PE-WT) or mutant alleles with elimination of the CbrB-I site (PE-CbrB1) or with incorporation of the CbrB-III site (PE+CbrB3). The two EMSA assays with PE-WT and PE-CbrB1 were performed in parallel and $CbrB_{His6}$ was added at 0, 1.1, 5.5, 11 and 16.5 μM in lanes 1-5, respectively. For the PE+CbrB3 probe, $CbrB_{His6}$ was added at the concentration of 0, 4.6, 9.2 and 16.5 μM, respectively. Additionally, a 171 bp probe DNA for the P_{crcZ} promoter (PcrcZ171) was used as a positive control for CbrB binding, and $CbrB_{His6}$ was added in lanes 1-5 at 0, 1.1, 5.5, 11.0 and 16.5 μM, respectively. Of note, the NtrC-I, NtrC-II/CbrB-I, NtrC-III and NtrC-IV sites were altered to random sequences of TTCAAG, AACCGT, TAAAGC and AACCGT, respectively. The CbrB-III artificial site "GTAACA" was introduced into the PE+CbrB3 probe sequence at the original NtrC-IV site.

	CbrB-I	CbrB-III	CbrB-II
***P. fluorescens* SBW25**	GTGAAAAAACTGTTACCGCGGATATTTCGCGTAACAAAGCCGGGGCTTACGGTAACgAAGCCCCGGC		
P. aeruginosa PAO1	CCCTGCAACCTGTTACCGCGGACGTACCGCGTAACAGAAACCGGGTTCATCGGTAACgGGAACCCGGT		
P. brassicacearum DF41	GTGAAAAAACTGTTACCTCAGCTTTTTCACGTAACAGAAGCCGGGGTTTACGGTAACgAAACCCCGGC		
P. chlororaphis PA23	GTGAAAAAACTGTTACCTCAGTCATTTCACGTAACAAAAGCCGGGGCTTACGGTAACgAAGCCCCGGC		
P. deceptionensis DSM 26521	CGCGCAAAACTGTTACCGCAGATTAAATACGTAACAAAAGCCGGGTCTTACGGTAACgATGACCCGGC		
P. entomophila L48	CGCAAAAATCTGTTACCCCTGCCCGATGGCGTAACAGCCTTCGAGGCATACGGTAACgAAATTTCTA		
P. protegens Pf-5	TGAAAAAAACTGTTACCTGCTCCATCGCACGTAACAGGAACCGGGGCTAAAGGTAACgAAGCCCCGGT		
P. putida KT2440	CGTAAAAATCTGTTACCCAAGCTTTCCGCCGTAACAGTCCCCGAGGCGTACGGTAACgAAATTGCGA		
P. simiae MEB105	GTGAAAAAACTGTTACCGCGGATATTTCGCGTAACAAAAGCCGGGGCTTACGGTAACgAAGCCCCGGC		
P. syringae DC3000	GCGTGCAAACTGTTACCGCAAGCACTTCACGTAACAAAAGCCGGGTCTTACGGTAACgCAGGCCCGG		

Figure 4.5. Alignment of the P_{crcZ} promoter sequences in *Pseudomonas*. The P_{crcZ} promoter region in ten representative *Pseudomonas* species was derived from the *Pseudomonas* Genome Database (http://beta.pseudomonas.com), showing corresponding regions from -161 to -94 to the previously identified *crcZ* transcriptional start site in *P. fluorescens* SBW25.

	NtrC-I	NtrC-II CbrB-I	NtrC-III	NtrC-IV	CbrB-II	
***P. fluorescens* SBW25**	TCCAGTCCTCGCACCAATTTGTTACCGAATGCcCCAGCGTGGcGCAAAACCTCGCTCTGGTgACAAACCTCCCTC					(208)
P. aeruginosa PAO1	CCGCAATTGCGCtgaACGGTGTTACCGAAGGCcCCAAACcGGTGCGCGCACGCTTcgAtCACGTGCACCCAGGGC					(265)
P. aeruginosa 19BR	CCGCAATTGCGCtgaACGGTGTTACCGAAGGCcCCAAACcGGTGCGCGCACGCTTcgAtCACGTGCACCCAGGGC					(265)
P. aeruginosa LESB58	CCGCAATTGCGCtgaACGGTGTTACCGAAGGCcCCAAACcGGTGCGCGCACGCTTcgAtCACGTGCACCCAGGGC					(265)
P. aeruginosa PA7	CCACATTTGCGCtgagCGGTGTTACCGAATGCcCCATTCgGGgGCGTGGATACcTgcCAGGAGAATGTGCGCGAT					(263)
P. aeruginosa UCBPP-PA14	CCGCAATTGCGCtgaACGGTGTTACCGAAGGCcCCAAACcGGTGCGCGCACGCTTcgAACACGTGCATCCAGGGC					(264)
P. brassicacearum DF41	TCCTCTTTGCGCACCAATTTGTTACCGAATGCcCCAGCGTGGcGCAATACCATGCTTCTGTgACcCTCCGATTGC					(241)
P. brassicacearum NFM421	TTTCTTCTGCGCACCAACTTGTTACCGAATGCcCCAGTGTGGcGCAACACCACGCTTCTGTgACcCTCCGATTTC					(241)
P. chlororaphis EA105	TTCCATCCACGCACCAACTTGTTACCGAACGCcCCAGCGTGGcGCAAAACTACGCTCATCtgAcCAAACCCCGAC					(269)
P. chlororaphis O6	TTTCCCTCGCGCACCAATTTGTTACCGAACGCcCCAGCGTGGcGCAAGGCTCAGCCGAAGTAACAGCGCTCACAT					(271)
P. chlororaphis PA23	TTTCCCTCGCGCACCAATTTGTTACCGAACGCcCCAGCGTGGcGCAAAGCTCAGCCGAAGTAACAGCGCTCACAT					(271)
P. deceptionensis DSM 26521	CGCGATCAGCACCcCCTCCTGTTACCGAACGCcCCAAAAaGacGCAAAACCCCCTCCCAGTAACATTCCCGCGCT					(200)
P. denitrificans ATCC 13867	GTTCCTTCGTAACGAGCGGTGTTACCGAATGCtaCgAAAaGGTGCAGGGCAGCCCGTTTCTGgggCATGACTCTG					(241)
P. fluorescens A506	TCCACTCCGCGCACCAATTTGTTACCGAATGCcCCAGCGTGacGCAAAGCTTCGCTGCCGTgACAAATTCCCCGC					(203)
P. fluorescens F113	CCCTACCCGCGCACCAACTTGTTACCGAACGCcCCAGCGTGGcGCAATACCACGCTTCTGTgACcCTCCGATTTC					(241)
P. fluorescens HK44	TTCCCTGTGCGCACCAGTTTGTTACCGAACGCcCCAGCGTGGcGCAAAACCGCGCTCAGGTAACATCTGTCACTC					(268)
P. fluorescens Pf0-1	CCCGAAATGCGCACCAACTTGTTACCGAACGCcCCAGCGTGGcGCAAAACCGCGCTTCCGTAACAACCTCTCGCC					(269)
P. orientalis BS2775	TCCAGATCGCGCACCAATTTGTTACCGAATGCcCCAGCGTGacGCAAAGTCGTGCTGCCGTgACtATATTTCTCC					(207)
P. poae DSM 14936	ACAAAACGGCGCACCAATTTGTTACCGAATGCcCCAGCGTGaTGCAGCTCCAGTGTttCgCCCTCGTTAAAAACA					(194)
P. protegens CHA0	TTTCTTGCGCGCACTcATTTGTTACCGAACGCcCCAGCTcGGcGCAAAAGCCCATCCTGGTAACAGCCGCGCGCG					(204)
P. protegens Pf-5	TTTCTTGCGCGCACTcATTTGTTACCGAACGCcCCAGCTcGGcGCAAAAGCCCATCCTGGTAACAGCCGCGCGCG					(204)
P. savastanoi 1448A	CACATTTACCGCACCATTCTGTTACCTGCCGCcCCAAAgcGcGCAAATCACGCTTCAGGTAACACGCCTGACCT					(245)
P. simiae 2-36	CCTGCCCCTCGCACCAATTTGTTACCAAATGCcCCAGCGTGGcGCAAAACCCCGCTGTCGTgACAAACCTTTCGC					(208)
P. simiae MEB105	CCTGCCCCTCGCACCAATTTGTTACCAAATGCcCCAGCGTGGcGCAAAACCCCGCTGTCGTgACAAACCTTTCGC					(207)
P. syringae B576	CACCCTCCTCGCACCAATCTGTTACCTGCCGCcCCAAActGcGCAAAAAGTCATTCAGGTAACAGAACAGCGCT					(245)
P. syringae DSM 10604	CACCCTCCTCGCACCAATCTGTTACCTGCCGCcCCAAActGcGCAAAAAGTCATTCAGGTAACAGAACAGCGCT					(244)
P. syringae DC3000	CACATTTCCCGCACCATTCTGTTACCTGCTGCcCCAAAgcGcGCAAGCCACGCCTCAGGTAACAATGCTCACCT					(245)

Figure 4.6. Alignment of the P_{hutU} promoter regions containing the NtrC- and CbrB-binding sites from 27 representative *Pseudomonas* species. DNA sequences were derived from the *Pseudomonas* Genome Database (http://beta.pseudomonas.com) and position is marked by the number in parenthesis at the end of each sequence counted from the GTG start codon of *hutU*. The predicted binding sites for NtrC and CbrB are marked with orange and blue colors, respectively. The third putative CbrB half site of *P. brassicacearum* DF41 and *P. brassicacearum* NFM421 is underlined.

4.2.4 Histidine utilization is subject to CCR control mediated by the CbrAB-CrcYZ-Crc/Hfq cascade

Interrogation of DNA sequence at the *hut* locus using the consensus sequence of "AAnAAnAA" revealed the presence of six putative Crc/Hfq-binding sites carrying four different sequence variants (Fig. 4.7A). "AACAACAA" is the CA motif used by the CrcY and CrcZ small regulatory RNAs for modulating Crc/Hfq activities (Garcia-Maurino *et al.*, 2013; Sonnleitner *et al.*, 2009), and it is present in $hutT_u$, a gene encoding urocanate-specific transporter (and also in *hutH1*, a non-functional histidase gene). The other target genes encode the histidine-specific transporter $HutT_h$ plus histidase (HutH2) and urocanase (HutU), which are involved in enzymatic breakdown of histidine and urocanate, respectively. The *in silico* data suggest that CCR acts on *hut* by targeting substrate uptake as well as the first one step of the catabolic pathway.

To test the predicted molecular interactions *in vitro*, EMSA was performed using purified Hfq_{His6} protein and four representative oligoribonucleotide probes (25 nt) centred by the predicted target sequence. As shown in Figure 4.7B, a significant shift of biotin-labelled RNA was observed for all four probes (1U, 3U, 5H and 6H) in the presence of increasing concentrations of Hfq_{His6} (lanes 2-8). RNA retardation was abolished by addition of excess competitor RNA, i.e., the same but unlabelled probe RNA (lane 9). Thus, the data confirm the specific binding of Hfq with mRNA transcripts of *hutU*, $hutT_u$, *hutH2* and $hutT_h$ genes.

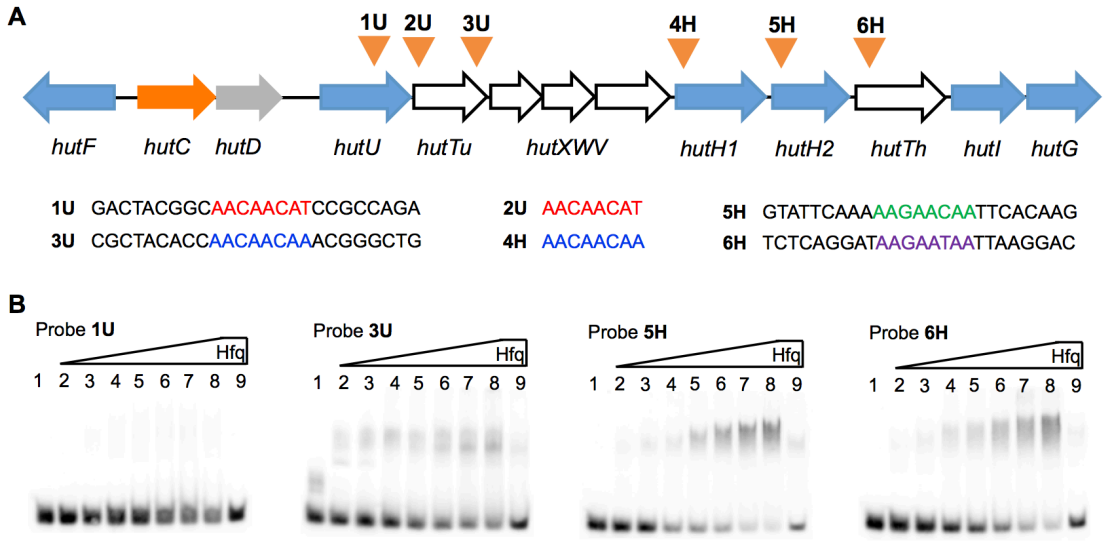

Figure 4.7. Specific interactions between Hfq and its target *hut* mRNAs.
(A) Locations of the six putative Crc/Hfq-binding sites are indicated by inverted triangles above the *hut* genes. The four oligoribonucleotide probes (1U, 3U, 5H and 6H) are 25 nt in length centred by the predicted Crc/Hfq-binding sequences.
(B) EMSA was performed using purified Hfq_{His6} and each of the four RNA probes labelled with biotin at the 5'-ends. Hfq_{His6} was added at 0, 55, 110, 220, 330, 440, 550, 660 and 660 nM in lanes 1 to 9, respectively. A 200-fold molar excess of the same unlabelled probe was added in lane 9 as a specific competitor for RNA binding.

4.2.5 Determining the role of CbrAB and NtrBC in carbon and nitrogen catabolite repression of *hut*

Armed with the knowledge of CbrAB- and NtrBC-mediated *hut* regulation, we proceeded to seek direct evidence of CCR and NCR of histidine utilization. To this end, we took advantage of the fluorescence property of urocanate and photometrically measured the rates of urocanate consumption by growing the wild-type strain in four minimal media containing urocanate (5 mM) with and without the preferred carbon and nitrogen sources, i.e. succinate and ammonium (NH_4Cl). Consistent with our expectation, the presence of succinate (20 mM) caused a decrease of urocanate consumption rate (Fig. 4.8A) and a reduction of P_{hutU} activity (Fig. 4.8B), while increasing the bacterial growth rate (Fig. S4.2, Page 164). Ammonium produced a minor but significant reduction of urocanate utilization (Fig. 4.8A, urocanate + succinate with and without NH_4Cl). However, the predicted ammonium-mediated NCR was more pronouncedly observed when the assay was performed at lower urocanate concentrations (Fig. S4.1, Page 163).

Intriguingly, in the 'urocanate + succinate + NH_4Cl' medium (urocanate as an alternative and less-preferred source of carbon and nitrogen) urocanate utilization was reduced but not abolished. The NtrBC system was inactive due to the presence of ammonium, and P_{ntrB} was expressed at the basal level (Fig. 4.9B). Thus, only the CbrAB system was expected to operate at the level of *hut* transcription and translation. Indeed, deletion of *cbrB* caused no urocanate uptake and the Δ*cbrB* mutant showed the same phenotype as the Δ*cbrB*Δ*ntrC* double deletion mutant (Fig. 4.8C). Similarly, NtrC was also inactive in the other two media 'urocanate' and 'urocanate + NH_4Cl' (Fig. 4.9B).

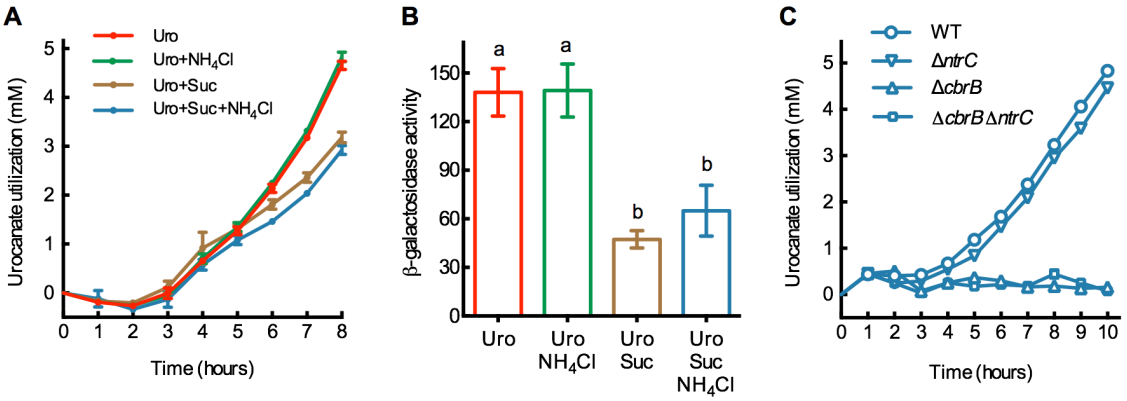

Figure 4.8. Inhibition of urocanate utilization by succinate and ammonium.
(A) Rate of urocanate consumption for wild-type cells grown in four minimal salts media supplemented with urocanate (Uro, 5 mM), succinate (Suc, 20 mM) or NH_4Cl (18.7 mM). Data are means and standard errors of six independent cultures. Two-way ANOVA revealed significant difference among medium treatments ($F_{3,180}$ = 299, $P < 0.0001$). The differences between Uro and Uro + Suc were highly significant at the three time points of 6, 7 and 8 hours ($P < 0.001$). Significant difference was also found between Uro + Suc and Uro + Suc + NH_4Cl ($P < 0.001$) at 6, 7 and 8 hours after inoculation.
(B) P_{hutU} promoter activity measured in the wild-type genetic background at 5 hours after inoculation. Bars that are not connected by the same letter (shown above each) are significantly different ($P < 0.05$) by Tukey's HSD test.
(C) A comparison of urocanate consumption rates between wild-type SBW25 (WT) and three isogenic mutants grown on urocanate (5 mM), succinate (20 mM) and NH_4Cl (18.7 mM). Multiple *t*-tests revealed no significant difference between wild type (WT) and Δ*ntrC* mutant.

However, in the 'succinate + urocanate' medium CbrAB and NtrBC coordinate in regulating *hut* expression to ensure that C/N balance is maintained for rapid utilization of urocanate. When compared with urocanate only medium, P_{crc} was expressed at higher levels, whereas P_{crcZ} expression was reduced, albeit no significant difference was observed for P_{cbrB} promoter activities (Fig. 4.9). The data thus implicate that CCR was operating as we would expect for this medium. Significantly, the P_{ntrB} promoter was highly expressed in

'urocanate + succinate' (Fig. 4.9B). Deletion of *ntrC* caused more severe effects on bacterial growth (Fig. 4.10) and P_{hutU} promoter activity (Fig. 4.2A) when compared with *cbrB* deletion. Given the overlapping nature of the NtrC and CbrB operator sites in the P_{hutU} promoter, data available so far consistently indicate that NtrBC plays a dominant role over CbrAB in activating the *hut* operon when growing on 'succinate + urocanate (or histidine)'.

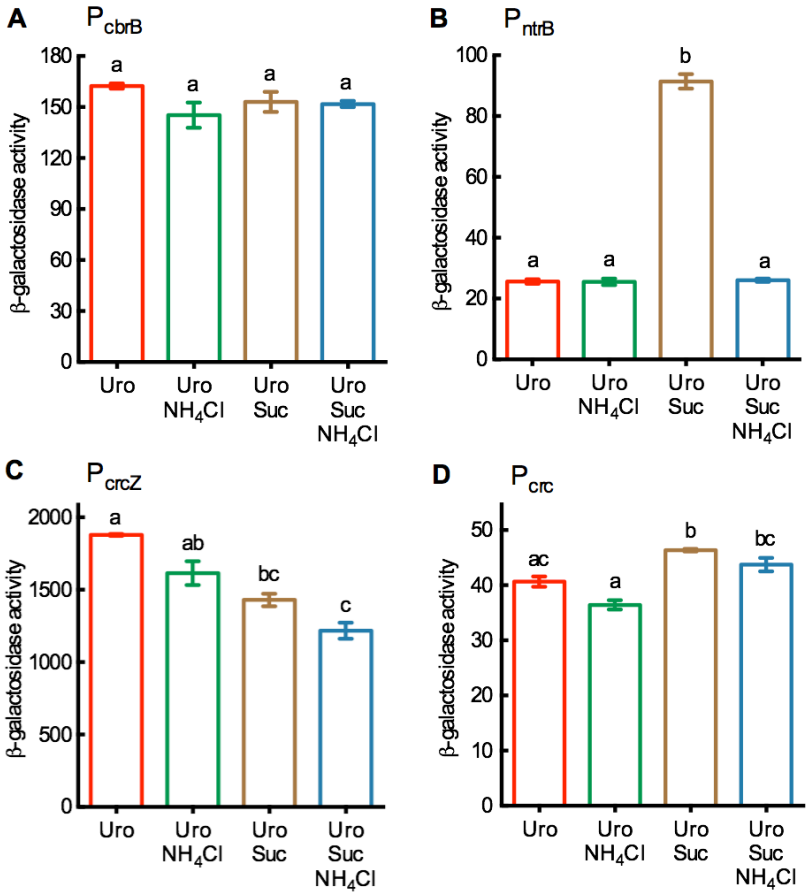

Figure 4.9. Expression of *hut* regulators in minimal salts medium containing urocanate with and without succinate and ammonium. Promoter activities of *cbrB* **(A)**, *ntrB* **(B)**, *crcZ* **(C)** and *crc* **(D)** genes were measured using cells at 5 hours after inoculation. Urocanate (Uro), succinate (Suc) and ammonium (NH_4Cl) were added at 5 mM, 20 mM and 18.7 mM, respectively. Data are means and standard errors of six independent cultures. Bars that are not connected by the same letter (shown above each) are significantly different ($P < 0.05$) by Tukey's HSD test.

Next, we compared the growth of seven isogenic mutants (Δ*cbrB*, Δ*ntrC*, Δ*cbrB*Δ*ntrC*, Δ*crc*, Δ*cbrB*Δ*crc*, Δ*crcYZ* and Δ*crc*Δ*crcYZ*) together with the wild-type strain in urocanate- and histidine-containing media supplemented with and without succinate and NH_4Cl. This time succinate was added at a low concentration of 5 mM, and it was consumed within ~8 hours after inoculation. The results summarized in Figure 4.10 and Table 4.1 are generally

consistent with the role of CbrAB in activating *hut* transcription but repressing *hut* translation via the CrcYZ-Crc/Hfq cascade. For example, the wild-type strain displayed a typical diauxic growth on succinate + urocanate, implicating a metabolic shift from succinate + urocanate to urocanate only (Fig. 4.10E); the Δ*cbrB* mutant was unable to continue to grow after succinate was consumed, as NtrBC was unable to activate *hut* because of its excess nitrogen. The diauxic growth disappeared for the Δ*crcYZ* mutant on succinate + urocanate, a likely consequence of the resultant constant and strong mRNA-binding activities of Crc/Hfq. Interestingly, the effects of CCR were much stronger for the utilization of histidine than urocanate (Fig. 4.10). This is consistent with the fact that one enzyme, i.e. histidase ($HutH_2$), is additionally targeted during the process of histidine utilization.

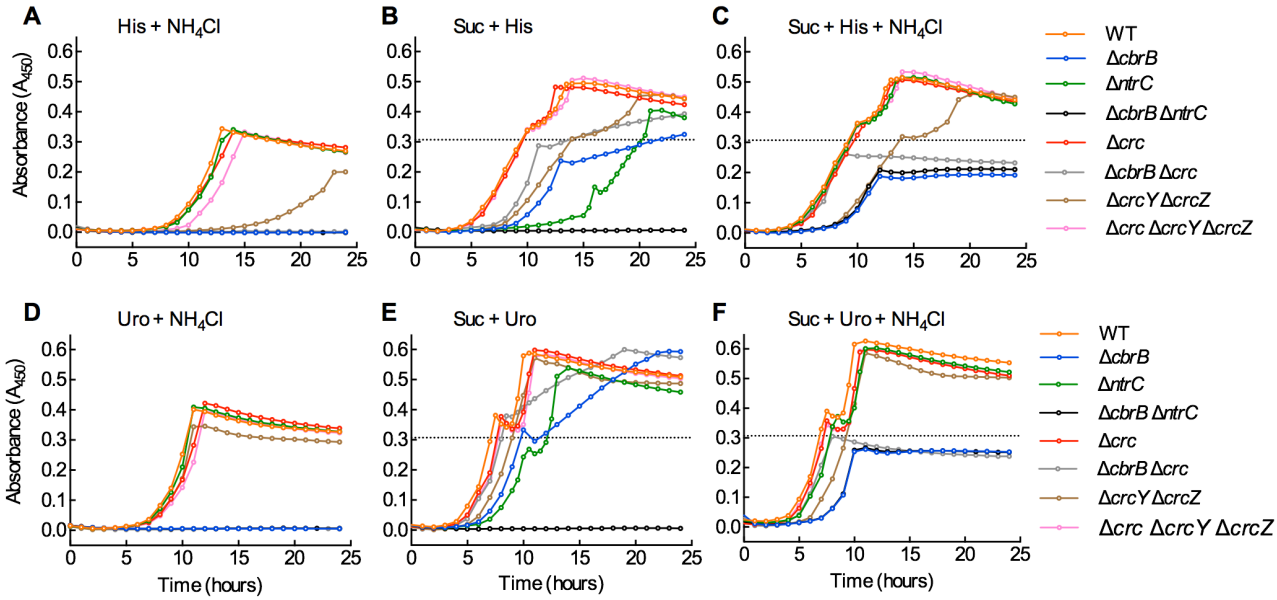

Figure 4.10. Growth dynamics of wild-type SBW25 and isogenic mutants devoid of regulators involved in *hut* gene expression. Growth was determined in 96-well microtiter plates containing 200 µl minimal salts medium per well. Succinate (Suc), histidine (His) and urocanate (Uro) were supplemented at the final concentration of 5 mM, and NH_4Cl was added at 18.7 mM. Absorbance (A_{450}) was measured every 5 min over a period of 24 hours, but only hourly (or half-hourly during transition) time points are shown for clarity. Data are means of six independent cultures. Standard errors are small and thus not shown for clarity. The dashed line denotes maximum absorbance value for the wild-type strain grown on succinate + NH_4Cl.

Table 4.1. Phenotypic interpretation of the CCR mutants grown on minimal salts medium containing histidine with and without succinate and ammonium on the basis of the data presented in Figure 4.10A-C.

	His + NH_4Cl	**Suc + His**	**Suc + His + NH_4Cl**
Wild type	Growth well with maximum absorbance (A_{450}) 0.35	It shows a typical diauxic growth: first grew on succinate + histidine, then the growth was shifted to histidine after succinate was consumed. Expression of *hut* was mediated by CbrAB and NtrBC in a coordinated manner.	The NtrBC system was repressed in this N-replete medium. Hence, *hut* expression was regulated by CbrAB only at both the transcriptional and translational levels. CCR & NCR were operating during the first growing phase on succinate + histidine + NH_4Cl. Then CCR would be relieved in the second phase after succinate was consumed.
Δ*cbrB*	No growth	Shows a reduced growth on succinate + histidine (and the *hut* genes were activated by NtrBC). However, when succinate concentration was reduced, growth ceased after 13 hours, suggesting the buildup of ammonium and consequent inactivation of NtrBC.	*hut* genes were not expressed, so the mutant grew on succinate + NH_4Cl. However, it grew slowly and did not reach the same yield as the wild-type strain. This was likely caused by the influences of *cbrAB* on succinate utilization and global effects of strong CCR.
Δ*ntrC*	Growth comparable with wild type	A severe growth reduction comparing with wild type. Unlike the Δ*cbrB* mutant, it showed a diauxic growth but the transition apparently occurred before succinate was consumed.	Growth was comparable with the wild-type strain. This is consistent with the fact that NtrBC is inactive in this medium.
Δ*cbrB* Δ*ntrC*	No growth	No growth	Like Δ*cbrB* mutant, this mutant cannot use histidine, and it grew on succinate and ammonium.
Δ*crc*	Growth slightly slower than the wild type	Growth comparable with the wild type	Similar growth as the wild-type strain
Δ*cbrB* Δ*crc*	No growth	Growth was improved when compared with the Δ*cbrB* mutant. This is consistent with strong CCR associated with *cbrB* deletion.	Growth was greatly improved when compared with the Δ*cbr*B mutant, suggesting the global influences of *crc* on bacterial growth on succinate and ammonium.
Δ*crcYZ*	A great growth reduction as a result of strong CCR	Show a diauxic growth at lower rates in both phases. This is a predicted result of constant and strong CCR.	Show a diauxic growth at lower rates in both phases, which is consistent with the constant and strong CCR.
Δ*crcYZ* Δ*crc*	Growth improved comparing with Δ*crcYZ* mutant.	Show similar diauxic growth as the wild-type strain.	Further deletion of *crc* eliminated the growth defects of Δ*crcYZ* mutant. This triple deletion mutant grew normally as the wild type.

4.2.6 Identifying HutC as a new regulator directly targeting the P_{ntrBC} promoter for *ntrBC* expression

The *ntrB* and *ntrC* genes are overlapped by 4 nucleotides (ATGA), and the promoter region contains a typical σ^{54}-binding site and a NtrC-binding site (O_{NtrC1}), suggesting that *ntrBC* are co-transcribed and their expression is subject to self-regulation by NtrC (Fig. 4.11C). Then, the above-described finding that HutC is capable of binding to a Pntr site in the P_{hutFC} promoter led to a hypothesis that HutC may play a novel role in modulating the *ntrBC* expression level, thereby fine-tuning *hut* expression. To test this hypothesis, DNase I footprinting analysis was first performed using purified $NtrC_{His6}$ and a 300-bp P_{ntrBC} probe DNA (PntrBC-300). Representative gel image shown in Figure 4.11A indicates that the P_{ntrBC} promoter possesses two NtrC operator sites O_{NtrC1} and O_{NtrC2}, which differ in $NtrC_{His6}$-binding affinities. Importantly, DNase I footprinting performed with the same P_{ntrBC} probe DNA and $HutC_{His6}$ clearly indicates that HutC is capable of binding to one of the NtrC operator sites in the P_{ntrBC} promoter (Fig. 4.11B, refer to Chapter 3 for a detailed description of protein-DNA binding assays of P_{ntrBC} promoter DNA and HutC/NtrC protein). The $HutC_{His6}$-protected region was 3 bp longer than that of $NtrC_{His6}$, and it did not show the hypersensitive bands observed with $NtrC_{His6}$, highlighting the structural difference when the same probe DNA was bound with NtrC and HutC. Furthermore, we showed that the protein-DNA interaction between $HutC_{His6}$ and the PntrBC-300 probe was disrupted by urocanate addition, and substitution of the Pntr site with random sequence eliminated the $HutC_{His6}$ binding activity (shown in Figure 3.5 of Chapter 3). Together, the *in vitro* data consistently indicate that HutC is capable of binding to the dominant NtrC operator site (O_{NtrC1}) in the P_{ntrBC} promoter, hence HutC has a potential to modulate *ntrBC* expression via competitive binding with the NtrC activator.

4.2.7 HutC is functionally required for *ntrBC* expression in an indirect manner

To determine the physiological role of HutC in *ntrBC* expression, we first compared P_{ntrBC}-*lacZ* promoter activities between wild type and Δ*hutC* for cells grown on succinate (20 mM) + histidine (10 mM). Given that HutC is a DNA-binding repressor protein, *hutC* deletion should cause a significant increase of P_{ntrBC} promoter activity. To our surprise, P_{ntrBC} expression was completely abolished in the Δ*hutC* mutant background, and a base-level expression was detected in the genetic backgrounds of both Δ*hutC* and Δ*ntrC* (Fig. 4.11F).

This result essentially indicates that NtrC and HutC are functionally required for *ntrBC* expression. However, this phenomenon cannot be mechanically explained by the known function of HutC as a transcriptional repressor.

To gain insights into the functional requirement of *hutC* for *ntrBC* expression, we examined the P_{ntrBC} promoter activities in wild-type strain grown separately on seven different carbon sources (succinate, glycerol, glucose, citrate, arabinose, mannitol and galactose) and five nitrogen sources (histidine, urocanate, proline, glutamate and NH_4Cl). Consistent with our expectation, P_{ntrBC} was not expressed in media containing NH_4Cl (data not shown). Interestingly, P_{ntrBC} was expressed at high levels on proline regardless of the carbon sources (Fig. 4.11E). When histidine was the sole N source, only succinate can greatly enhance P_{ntrBC} expression. Despite the fact that histidine breakdown generates one more ammonium than urocanate, P_{ntrBC} was generally expressed at higher levels on histidine than on urocanate (Fig. 4.11E).

Next, we proceeded to determine P_{ntrBC} expression in wild type and mutants devoid of *hutC* and *ntrC* when they were grown in succinate-containing medium using histidine, urocanate or proline as the sole N source (Fig. 4.11F). P_{ntrBC} was not expressed in the Δ*ntrC* background when growing on the three N-sources. This is consistent with the established role of NtrC in direct activation of P_{ntrBC} expression. In the Δ*hutC* background P_{ntrBC} was not expressed on histidine, but it was expressed on urocanate albeit at reduced levels when compared with wild type. More importantly, P_{ntrBC} was expressed at comparable levels in wild type and Δ*hutC* in the medium of succinate + proline (Fig. 4.11F). From these data we conclude that HutC is not directly involved in P_{ntrBC} activation. It is functionally required for *ntrBC* expression in the succinate + histidine medium, but the influence must be exerted indirectly through the NtrC activator.

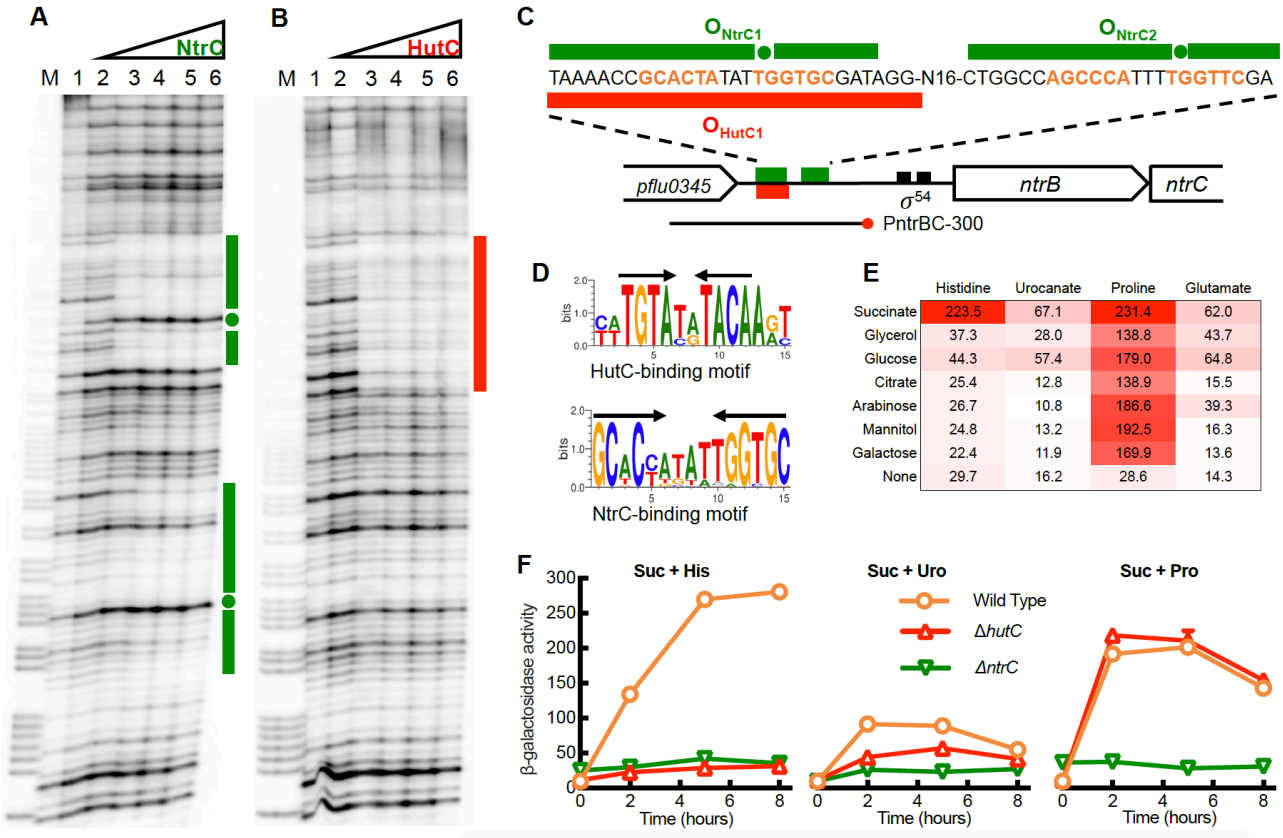

Figure 4.11. Biochemical and genetic characterization of the *ntrBC* promoter.

(A) Identification of NtrC target sites by DNase I footprinting. Lane M, G+A marker; Lanes 1-6, $NtrC_{His6}$ added at an increasing concentration from 0, 0.07, 0.2, 0.54, 1.1 to 1.7 μM. NtrC-protected regions are indicated by green bars, and hypersensitive residues are marked with filled circles.

(B) DNase I footprinting showing specific interactions between HutC and P_{ntrBC} promoter. Lane M, G+A marker; Lanes 1-6, $HutC_{His6}$ added at an increasing amount from 0, 1.16, 2.32, 4.64, 7.54 to 10.44 μM. HutC-protected region is marked by a red bar.

(C) A schematic map of the P_{ntrBC} promoter showing DNA sequences that were protected by NtrC and HutC from DNase I cleavage. The footprinting assays were conducted by using the PntrBC-300 probe with a biotin-labelled 3'-end.

(D) Sequence logos were generated from separate comparative analysis of P_{hutU} and P_{ntrBC} promoter regions across 30 *Pseudomonas* species. Inverted repeats are marked with arrows.

(E) A heat map showing variation in P_{ntrBC} promoter activities when bacteria were grown in minimal salts medium supplemented separately with seven carbon substrates (20 mM) using an amino acid (10 mM) as the sole N source. β-galactosidase activity (μM 4MU min^{-1} OD_{600}^{-1}) was measured at 0, 2, 5 and 8 hours after inoculation, but only mean values at 5 hours are shown here for clarity.

(F) Levels of P_{ntrBC} expression in wild-type, Δ*hutC* and Δ*ntrC* backgrounds for cells grown on succinate (20 mM) plus histidine, urocanate or proline (10 mM). Data are means and standard errors of six independent cultures.

4.2.8 HutC acts as a governor for histidine catabolism

Data presented above show that HutC directly binds to the P_{ntrBC} promoter DNA, but it indirectly influences *ntrBC* transcription through the NtrC activator. This finding led to a hypothesis that HutC functions as a governor that helps monitor and control the speed of histidine catabolism, ensuring that bacterial cells maintain N-starved, a physiological condition required for NtrC to activate its own expression (and the subsequent transcription of *hut* genes) (Fig. 4.12). Hence, HutC is a crucial part of the molecular mechanism for *P. fluorescens* SBW25 to maintain cellular C/N balance for efficient histidine utilization. By directly binding to the P_{ntrBC} promoter HutC is capable of fine-tuning the expression levels of the NtrBC activator to prevent over-production of the *hut* enzymes and the consequent excess ammonium.

It is important to note that *hutC* is subject to self-regulation (Fig. 4.12), the intracellular concentration of HutC is thus determined by histidine availability. Given the low-affinity of HutC-P_{ntrBC} interactions, HutC is expected to play a significant governor's role only when histidine is present at relatively higher concentrations (i.e. a lot of HutC are made). When there is little or none histidine in the environment, the HutC-P_{ntrBC} interaction will be negligible and it should not produce any significant effects on the expression of other nitrogen substrate utilization genes in the NtrBC regulon. Indeed, deletion of *hutC* did not affect P_{ntrBC} expression when bacteria were grown on succinate and proline (Fig. 4.11F).

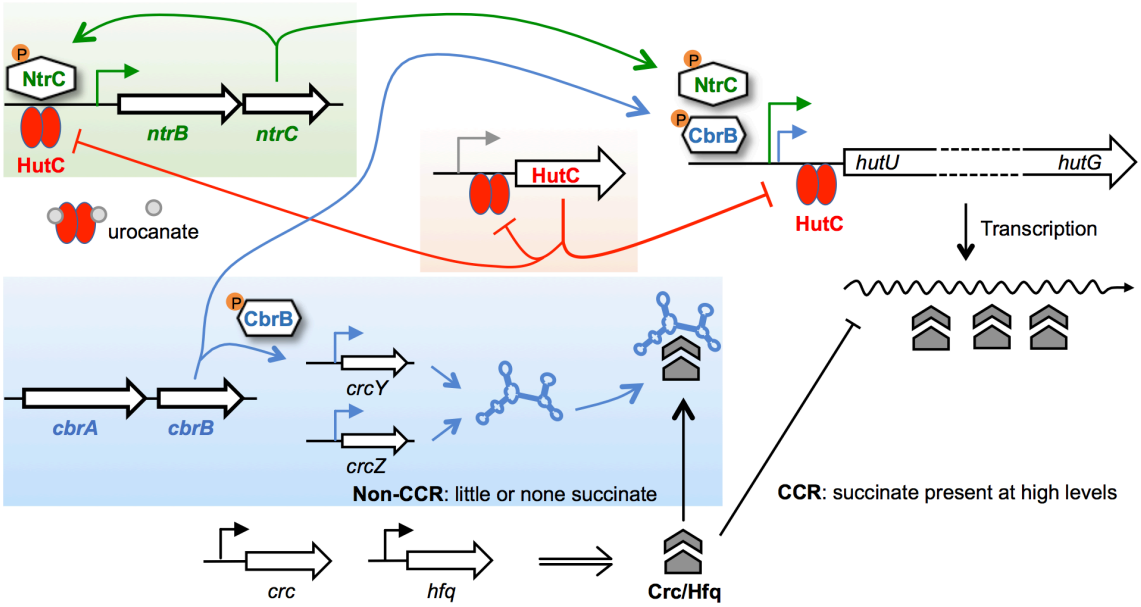

Figure 4.12. Expression of *hut* genes is coordinated by the two two-component systems CbrAB and NtrBC with assistance of the HutC governor. When there is little or none succinate in the medium, CbrAB plays a major role in activating *hut* transcription, and the Crc/Hfq-mediated translational repression of *hut* is also relieved as a result of high-level expression of the antagonistic ncRNAs CrcY and CrcZ whose expression is controlled by CbrAB. Conversely, when succinate is abundant, CbrAB mediates weak transcription of *hut* and *crcYZ* gene; hence, *hut* expression is repressed at the translational level. However, if the repression is too strong, cells will end up without sufficient nitrogen, causing growth limitation. Under this condition, the NtrBC system kicks in and plays the dominant role in activating *hut* transcription to meet the cellular demand for nitrogen. However, CCR is operating at the translational level, and it is not under the direct control of NtrBC. Hence, there is a high risk that *hut* genes are over-expressed, and produce excess ammonium, causing the NtrBC system to stall (and the NtrC-mediated *hut* transcription stops). To prevent this from occurring, HutC acts as a governor to monitor and control *hut* catabolic rate by directly targeting the P_{ntrBC} promoter. This will ensure that *ntrBC* is expressed at precise levels directly in response to histidine availability, and no buildup of excess ammonium during the process of bacterial growth on succinate and histidine.

To further test the governor model, we first show that P_{ntrBC} promoter activity varies in response to change of the C/N ratios in the medium. This was done by manipulating the relative abundance of succinate and histidine (and separately urocanate). Data presented in Figure 4.13 indicate that P_{ntrBC} was highly expressed at high C/N environments, and the expression levels declined along with the decrease of C/N (i.e. relatively less succinate and more histidine or urocanate). Next, we tested P_{ntrBC} expression in responses to *hut* catabolic changes when bacteria are grown on succinate (20 mM) and histidine (10 mM). From the results described above, P_{ntrBC} was expressed at the highest levels under this nutrient condition. However, the expression was abolished in the Δ*hutC* mutant, and the governor

model posits that this was caused by over-expression of *hut* genes, and the resulting excess ammonium inactivated the NtrBC system. Therefore, if we introduce a second *cbrB* mutation into the Δ*hutC* mutant background, *hut* expression will be greatly reduced as a result of strong CCR; and consequently, P_{ntrBC} expression should be restored in the double deletion mutant (Δ*cbrB*Δ*hutC*). Indeed, P_{ntrBC} was expressed at 5 hours after inoculation (Fig. 4.14A). However, it is interesting to note that no expression was detected at 2 hours after inoculation, whereas P_{ntrBC} was expressed at an expected lower level than the wild type. Thus, the data suggest that NtrBC system was struggling to activate its own expression (and the expression of *hut* genes) in the Δ*cbrB*Δ*hutC* mutant. Furthermore, the *hut* catabolism was abolished in the double deletion mutant Δ*hutC*Δ*hutH*$_2$ (His^-); but consistent with our expectation, P_{ntrBC} was expressed at the wild-type level on succinate + histidine (Fig. 4.14B). In this extreme case, cells were N-starved and P_{ntrBC} was fully induced independent of the HutC functionality.

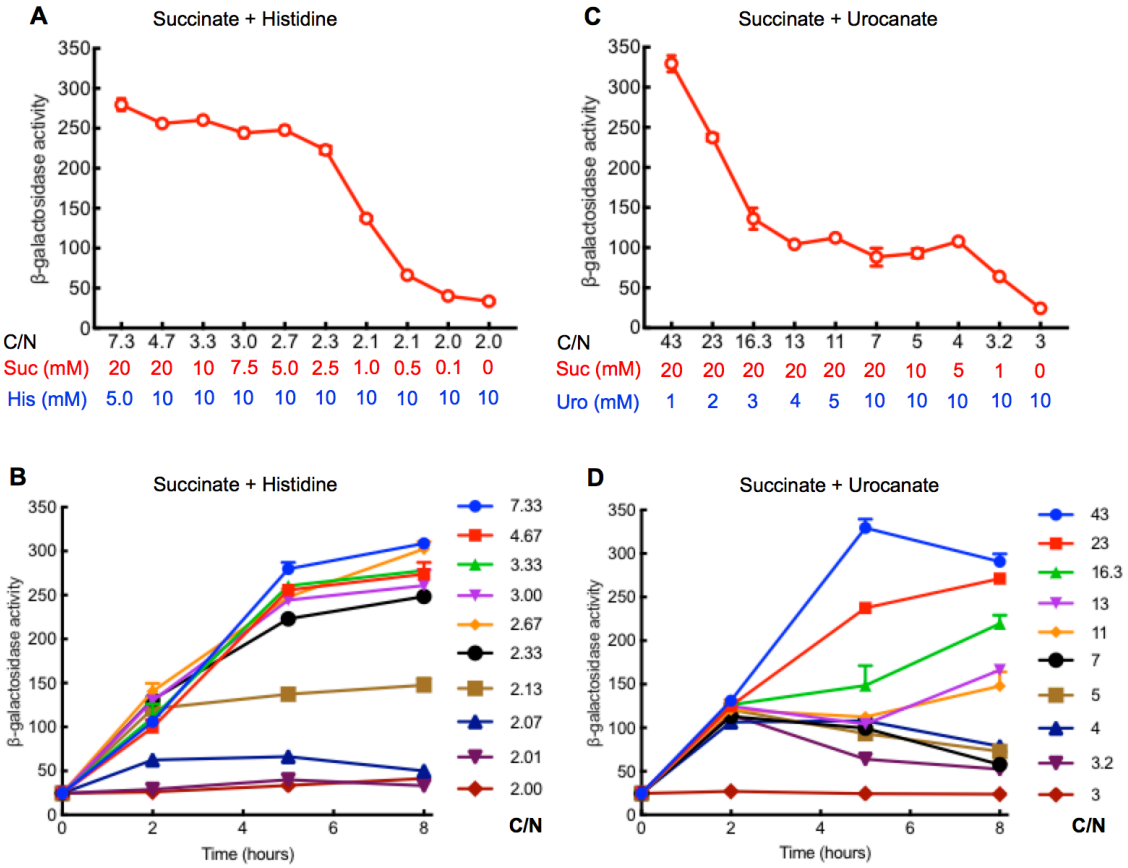

Figure 4.13. Variation in P_{ntrBC} promoter activities in response to changing ratios of C/N nutritional substrates in the medium. Bacteria were grown in minimal salts medium containing succinate (Suc) and histidine (His) or urocanate (Uro) at varying relative concentrations. β-galactosidase activities were measured at 0, 2, 5 and 8 hours after inoculation. Data are means and standard errors of three independent cultures.

(A) The 5-hour expression data were plotted against C/N ratios for cells grown on succinate + histidine. One-way ANOVA revealed significant difference ($F_{9,20}$ = 565.9, $P < 0.0001$). There was a significant correlation between P_{ntrBC} promoter activity and C/N ratio of the cultivation medium (r = 0.6387, P = 0.0468).

(B) P_{ntrBC} expression over time in the succinate + histidine media.

(C) The 5-hour expression data were plotted against C/N ratios for cells grown on succinate + urocanate. One-way ANOVA revealed significant difference ($F_{9,20}$ = 161.6, $P < 0.0001$). There was a significant correlation between P_{ntrBC} promoter activity and C/N ratio of the cultivation medium (r = 0.9587, $P < 0.0001$).

(D) P_{ntrBC} expression over time in the succinate + urocanate media.

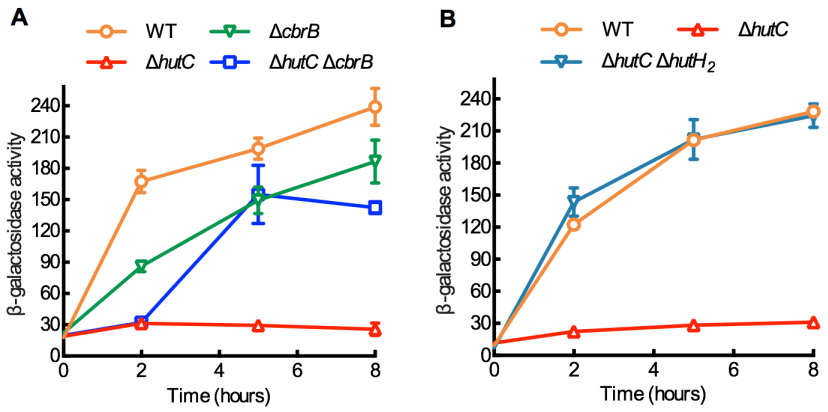

Figure 4.14. HutC is involved in fine-tuning P_{ntrBC} activity through maintaining a N-starved physiological condition during histidine utilization as a nitrogen source. Bacteria were grown in minimal salts medium with succinate (20 mM) and histidine (10 mM), and β-galactosidase activities were measured at 0, 2, 5 and 8 hours after inoculation. Data are means and standard errors of three independent cultures.
(A) Impacts of *cbrB* deletion on P_{ntrBC} expression in the wild type (WT) and Δ*hutC* genetic backgrounds. Two-way ANOVA revealed significant differences between genotypes ($F_{3,8}$ = 678.6, P < 0.0001). The differences among the four genotypes were highly significant at the three time points of 2, 5 and 8 hours (P < 0.001), except for Δ*hutC* versus Δ*hutC*Δ*cbrB* at 2 hours and Δ*cbrB* versus Δ*hutC*Δ*cbrB* at 5 hours.
(B) Impacts of $hutH_2$ deletion on P_{ntrBC} expression. Two-way ANOVA revealed no significant difference between wild type and Δ*hutC*Δ$hutH_2$ ($F_{1,16}$ = 4.795, P = 0.0437).

Finally, we compared the P_{ntrBC} and P_{hutU} promoter activities between wild-type SBW25 and Δ*hutC* mutant in minimal salts medium containing 20 mM succinate and varying concentrations of histidine. If HutC functions as a governor that controls *hut* catabolic rate in histidine-replete environments, P_{ntrBC} ought to be expressed at significantly lower or basal levels in the Δ*hutC* mutant when compared with wild type; and meanwhile P_{hutU} should also be expressed at lower levels (of note, the CbrAB system will provide weak P_{hutU} promoter activities as described above). The results shown in Figure 4.15 are fully consistent with these predictions. At low histidine concentrations (< 0.5 mM), P_{hutU} was expressed in a concentration-dependent manner in wild-type SBW25, but it was constitutively expressed at high levels in the Δ*hutC* mutant. This is consistent with the known function of HutC as a transcriptional repressor of *hut* operons.

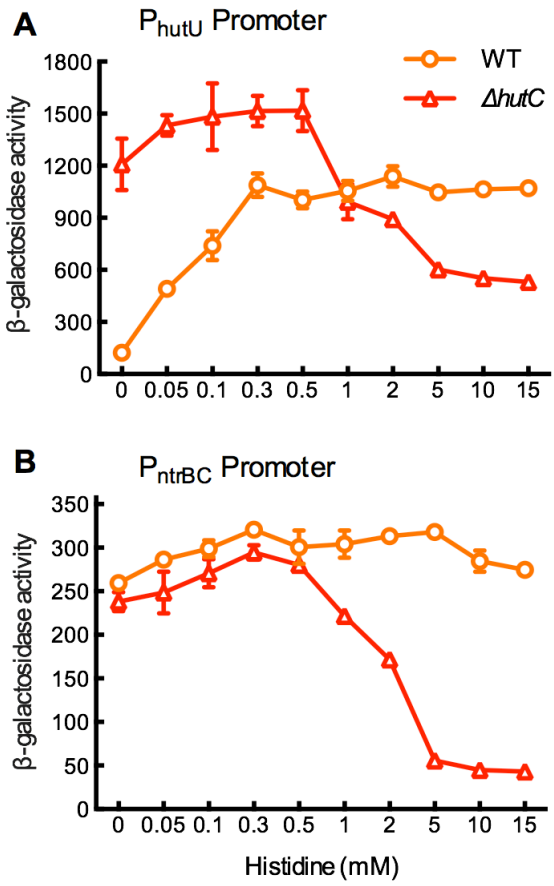

Figure 4.15. *hutC* is required for maintaining P_{hutU} and P_{ntrBC} promoter activities in histidine-replete environments. Data are means and standard errors of three independent cultures in minimal salts medium containing 20 mM succinate and varying concentrations of histidine as indicated in *x*-axis. β-galactosidase activities were measured using N- or C/N-starved cells at 0, 2 and 5 hours after inoculation, but only the 5 hour data are plotted here to show the most pronounced difference.
(A) Cells were C/N-starved in minimal salts medium for 2 hours before inoculation into the test media. Two-way ANOVA revealed a significant interaction between genotype and medium ($F_{9,40}$ = 99.92, $P < 0.0001$). Differences between wild type (WT) and Δ*hutC* mutant were highly significant ($P < 0.001$) in all media except succinate + histidine (1 mM).
(B) Cells were N-starved in minimal salts medium supplemented with 20 mM succinate, and then histidine was added at varying concentrations at time zero. Two-way ANOVA revealed a significant interaction between genotype and medium ($F_{9,40}$ = 141.3, $P < 0.0001$). Multiple *t*-tests show that differences between genotypes were highly significant ($P < 0.001$) when histidine was added at or higher than 1 mM.

4.3 Discussion

In the present study, we have defined a new biological function for the histidine-responsive regulator HutC, which acts in a manner analogous to the governor of a car engine, setting an upper bound to the level of pathway activity, thus preventing harm that can result from over activity (ammonium poisoning in the case of histidine utilization). HutC plays its

governor's role by specifically targeting the NtrC operator site in the *ntrBC* promoter. This finding has broader implications as it indicates that a local substrate-specific regulator can fine-tune the expression of a global regulator whose expression is subject to autoregulation. NtrBC is a master regulator for cellular nitrogen metabolism, and it is involved in the utilization of a wide range of nitrogen-containing organic compounds including histidine. Thus, the new mode of gene regulation discovered in this work with HutC likely exists in many other pathways whose activities are under the direct control of the NtrBC system.

Positive autoregulation is commonly found in bacteria, and it occurs when a transcriptional regulator activates its own expression. In *E. coli*, among the ~200 functionally characterized transcriptional regulators about half are autoregulated, and ~30 of them are positively autoregulated. Intriguingly, at least 10 of the 30 positively autoregulated regulators belong to the family of two-component signal transduction systems, including NtrBC (Gao & Stock, 2018). However, it has been well established that positive autoregulation of transcription results in a delayed response, while conferring benefits such as an increased sensitivity to signals, promoting bistability or a switch-like response or memory. A recent work by Gao and Stock (2018) show that in the two-component system PhoB-PhoR of *E. coli*, a coupled negative feedback mechanism has been adopted to accelerate the response, thus overcome the cost of positive autoregulation. A similar regulatory scheme has been previously reported with the NtrBC system in *E.coli*: a second weak NtrC-binding functions to repress NtrBC-activated transcription (Atkinson *et al.*, 2002). The HutC-mediated repression of the *ntrBC* promoter represents another fine example that a negative feedback control is involved to prevent over-expression of a positively regulated transcriptional factor.

In this work, we have also defined the molecular mechanisms of succinate-induced CCR on histidine utilization, which occurs at post-transcriptional level through the CbrAB-CrcYZ-Crc/Hfq cascade. Previous studies on *Pseudomonas* suggest that Crc protein may play no role in the succinate-induced CCR of histidine utilization, and other mechanisms might be involved. A study on *P. aeruginosa* PAO1 showed that the succinate-mediated repression on histidase and urocanase activities was not relieved in *crc* mutant strains (Collier *et al.*, 1996). However, *P. aeruginosa* PAO1 does have putative Crc/Hfq binding sites in the *hut* locus. CbrB activates the *hut* expression in *P. aeruginosa* PAO1 in response to carbon limitation (Itoh *et al.*, 2007; Li & Lu, 2007), and a putative CbrB binding site was identified in the *hutU* promoter (Fig. 4.6). Thus, in *P. aeruginosa* PAO1, CbrB may also

transcriptionally activate *hutU* and control the *hutU* translation via Crc/Hfq. That is a possible reason for the remained succinate-induced repression of Hut in *crc* mutants. In the presence of succinate, CbrB activity is low, which reduces the *hutU* expression in both transcription and translation. However, lack of Crc can only relieve the repression in the translational level, and the overall Hut expression is still repressed by succinate. In addition, a proteomic analysis of *P. putida* observed no difference between wild type and *crc* mutant on the expression of Hut enzymes when cells were grown in LB medium (Moreno *et al.*, 2009). LB is a nutrient-complex medium, which can generate strong catabolite repression, but also limit the induction of *hut* genes due to the lack of histidine (and urocanate) inducer. The *hutU* operon of *P. fluorescens* SBW25 is expressed at a very low level when growing in LB medium (unpublished data). Effect of *crc* deletion will not be observed if the *hut* genes are not induced transcriptionally in the testing medium. Thus, the assay conditions might be the reason for not detecting the Crc effect on Hut expression in previous studies.

Data presented in this work consistently indicate that CCR on histidine utilization is relatively weak when compared with other less preferred carbon sources, e.g., xylose. Transcription of xylose utilization (*xut*) genes including the xylose-responsive activator (XutR) is subject to strong CCR mediated by the Crc/Hfq complex (Liu *et al.*, 2017). Consequently, the Δ*cbrB* mutant (Xyl^-) was unable to grow on xylose because of strong repression as a result of CrcY and CrcZ non-expression. Therefore, *crc* deletion restored the growth defect of Δ*cbrB* on xylose (Δ*cbrB*Δ*crc*, Xyl^+). However, both the Δ*cbrB* and Δ*cbrB*Δ*crc* mutants were unable to grow on histidine as the sole carbon source (His^-). These phenotypes can be explained by the fact that CbrB is required as the direct transcriptional activator of *hut*, and the non-growth phenotype (His^-) for Δ*cbrB* is not caused by strong CCR as observed with xylose utilization genes. More importantly, the Δ*cbrB* mutant was able to grow on histidine as the nitrogen source (succinate + histidine). Under this nutrient condition, *hut* transcription is activated by NtrBC, and subject to strong CCR as a result of *cbrB* deletion. If the CCR is very strong like that of xylose utilization, the Δ*cbrB* mutant would not be able to grow on histidine. It makes sense that histidine utilization is subject to a weak CCR control as it will not eliminate the physiological demand for nitrogen.

Here, we have defined the molecular mechanism of positive regulation of *hut* operons,

showing that CbrAB and NtrBC function in a direct manner, and their interplay coordinates C/N balance for efficient histidine utilization. The mechanism is highly conserved in *Pseudomonas* (Fig. 4.6), except *P. putida*, *P. entomophila* and *P. mosselii*. The *hutU* promoter region of these three species does not contain any putative binding sites for CbrB, NtrC as well as σ^{54}. Of note, Hu and Phillips (1988) have used *P. putida* as a model for their studies of histidine utilization. Their work led to identification of catabolic genes, except *hutF*, and the *hutC* repressor in *Pseudomonas*. A recent study on *P. putida* show that deletion of CbrAB and NtrBC resulted in growth defects (Amador *et al.*, 2010): the Δ*cbrB* mutant was unable to grow on histidine as the sole carbon source. However, the double Δ*cbrB*Δ*ntrC* deletion mutant showed a significantly reduced growth on histidine as the sole nitrogen source (succinate as the carbon source), whereas the two single deletion mutants grew normally. The fact that the P_{hutU} promoter lacks clear binding sites for σ^{54}, CbrB and NtrC strongly indicate that CbrAB and NtrBC regulate the expression of *hut* in an indirect manner in *P. putida* strains. Furthermore, the dual control of CbrAB and NtrBC likely occurs beyond histidine catabolism. A search of putative NtrC-binding sites in *P. fluorescens* SBW25 genome revealed a total of 34 NtrC-regulated candidate genes, possessing a putative NtrC-binding site and σ^{54}-binding site in the promoter region (Table S4.1, Page 164). Among the 34 NtrC-regulated candidate genes, five are predicted to be regulated by CbrB at the same time. Taken together, our data implicate a central role of CbrAB and NtrBC in the coordination of cellular carbon and nitrogen metabolism in *Pseudomonas*.

4.4 Materials and Methods

4.4.1 Bacterial strains and growth conditions

One Shot® TOP10 (Invitrogen, Auckland) chemically competent *E. coli* was used for transferring pCR™8/GW/TOPO® vector (Invitrogen, Auckland) with cloning PCR products for subsequent sequencing. *E. coli* DH5αλ_{pir} was used for general gene cloning and tri-parental conjugation of *P. fluorescens* SBW25. *E. coli* BL21 (DE3) was used for protein purification. Bacterial strains and plasmids used in this work are listed in Table 4.2. Luria-Bertani (LB) medium was routinely used to grow *P. fluorescens* and *E. coli* strains at 28°C and 37°C, respectively. When bacteria were grown in the mininal M9 salt medium (Sambrook *et al.*, 1989), the components and concentrations of carbon and nitrogen

sources supplemented are as indicated in each assay. When required, antibiotics were used at the following concentrations: ampicillin (Ap), 100 μg/ml; tetracycline (Tc), 15 μg/ml; spectinomycin (Sp), 100 μg/ml; kanamycin (Km), 50 μg/ml; gentamicin (Gm), 25 μg/ml; nitrofurantoin (NF), 100 μg/ml.

To monitor growth kinetics *P. fluorescens* strains from -80°C stock were initially grown in LB broth overnight. One milliliter of cell culture was washed twice with MSM salt solution and starved at 28°C for 2 hours. Then the culture was mixed with the tested medium by 1:100 folds dilution and 200 μl aliquots of cell culture were placed onto a 96-well microtiter plate. Growth kinetics were monitored at 28°C by a Synergy 2 plate reader installed with Gen5 software (Bio-Tek). Absorbance at 450 nm was recorded every 5 minutes for a period of 24 or 48 hours.

Table 4.2. Bacterial strains and plasmids used in this work

Strain or plasmid	Genotypes and relevant characteristics	Reference
P. fluorescens		
SBW25	Wild-type strain isolated from phyllosphere of sugar beet	Bailey *et al.* (1995)
PBR810	Δ*cbrB*, SBW25 devoid of *pflu5237*	Zhang and Rainey (2007)
PBR829	Δ*ntrC,* SBW25 devoid of *pflu0343*	Zhang and Rainey (2008)
PBR830	Δ*ntrC* Δ*cbrB*::Km, SBW25 devoid of *pflu0343* and *pflu5237*	Zhang and Rainey (2008)
MU12-58	Δ*crc*, SBW25 devoid of *pflu5989*	Liu *et al.* (2017)
MU47-12	Δ*cbrB* Δ*crc,* SBW25 devoid of *pflu5237* and *pflu5989*	Liu *et al.* (2017)
MU34-61	SBW25Δ*crcZ* Δ*crcY*	Liu *et al.* (2017)
MU47-17	SBW25Δ*crc* Δ*crcZ* Δ*crcY*	Liu *et al.* (2017)
MU60-1	Δ*hutC*, SBW25 devoid of *pflu0359*	This work
MU11-90	Δ*hutC* Δ*cbrB*, SBW25 devoid of *pflu0359* and *pflu5237*	Zhang and Rainey (2007)
MU34-18	Δ*hutC* Δ*hutH2*, SBW25 devoid of *pflu0359* and *pflu0367*	Zhang and Rainey (2007)
Plasmid		
pCR8/GW/TOPO	Cloning vector, Sp^r	Invitrogen
pCR8-PntrB-Mut1	pCR8/GW/TOPO carrying P_{ntrB} promoter region with O_{NtrC1} site mutated	This work
pRK2013	Helper plasmid, Tra^+, Km^r	Ditta *et al.* (1980)
pUIC3	Suicide vector with promoterless '*lacZ*, Mob^+, Tc^r	Rainey (1999)

pUIC3-2	pUIC3 containing *hutF-lacZ* fusion, Tc^r	Zhang and Rainey (2007)
pUIC3-3	pUIC3 containing *hutC-lacZ* fusion, Tc^r	Zhang and Rainey (2007)
pUIC3-8	pUIC3 containing *hutU-lacZ* fusion, Tc^r	Zhang and Rainey (2007)
pUIC3-65	pUIC3 containing *crcZ-lacZ* fusion, Tc^r	Zhang *et al.* (2010)
pUIC3-155	pUIC3 containing *crcY-lacZ* fusion, Tc^r	Liu *et al.* (2017)
pUX-BF13	Helper plasmid for transposition of mini-Tn7 element, Ap^r	Bao *et al.* (1991)
pUC18-mini-Tn7T-Gm-*lacZ*	Mini-Tn7 vector for transcriptional fusion to promoterless *lacZ*, Ap^r, Gm^r	Choi *et al.* (2005)
pUC18-Tn7T-lacZ-P_{UA}	pUC18-mini-Tn7T-*lacZ* containing a transcriptional *lacZ* fusion to the P_{hutU}A promoter	This work
pUC18-Tn7T-lacZ-P_{UB}	pUC18-mini-Tn7T-*lacZ* containing a transcriptional *lacZ* fusion to the P_{hutU}B promoter	This work
pUC18-Tn7T-lacZ-P_{UC}	pUC18-mini-Tn7T-*lacZ* containing a transcriptional *lacZ* fusion to the P_{hutU}C promoter	This work
pUC18-Tn7T-lacZ-P_{UD}	pUC18-mini-Tn7T-*lacZ* containing a transcriptional *lacZ* fusion to the P_{hutU}D promoter	This work
pUC18-Tn7T-lacZ-P_{UE}	pUC18-mini-Tn7T-*lacZ* containing a transcriptional *lacZ* fusion to the P_{hutU}E promoter	This work
pUC18-Tn7T-lacZ-P_{UF}	pUC18-mini-Tn7T-*lacZ* containing a transcriptional *lacZ* fusion to the P_{hutU}F promoter	This work
pUC18-Tn7T-lacZ-P_{UG}	pUC18-mini-Tn7T-*lacZ* containing a transcriptional *lacZ* fusion to the P_{hutU}G promoter	This work
pUC18-Tn7T-lacZ-P_{UH}	pUC18-mini-Tn7T-*lacZ* containing a transcriptional *lacZ* fusion to the P_{hutU}H promoter	This work
pUC18-Tn7T-lacZ-P_{UI}	pUC18-mini-Tn7T-*lacZ* containing a transcriptional *lacZ* fusion to the P_{hutU}I promoter	This work
pUC18-Tn7T-lacZ-P_{UJ}	pUC18-mini-Tn7T-*lacZ* containing a transcriptional *lacZ* fusion to the P_{hutU}J promoter	This work
pUC18-Tn7T-lacZ-P_{UK}	pUC18-mini-Tn7T-*lacZ* containing a transcriptional *lacZ* fusion to the P_{hutU}K promoter	This work
pUC18-Tn7T-lacZ-P_{ntrBC}	pUC18-mini-Tn7T-Gm-lacZ containing *lacZ* fusion to P_{ntrBC} promoter	This work
pUC18-Tn7T-lacZ-P_{cbrB}	pUC18-mini-Tn7T-Gm-lacZ containing *lacZ* fusion to P_{cbrB} promoter	This work
pXY2-P_{crc}	pXY2 containing the P_{crc}-*lacZ* translational fusion, Ap^r, Gm^r	Liu *et al.* (2017)
pTrc99A	Protein expression vector, P_{tac} promoter, Ap^r	Amann *et al.* (1988)
pTrc99A-ntrC	pTrc99A carrying $NtrC_{His6}$, Ap^r	This work
pTrc99A-cbrB	pTrc99A carrying $CbrB_{His6}$, Ap^r	This work
pTrc99A-*hfq*	pTrc99A carrying Hfq_{His6}, Ap^r	Liu *et al.* (2017)
pTrc99A-hutC	pTrc99A carrying $HutC_{His6}$, Ap^r	This work
pCR2.1-TOPO	Cloning vector, Km^r, Ap^r	Invitrogen
pCR2.1-PhutU-MN1	pCR2.1-TOPO carrying P_{hutU} promoter region with NtrC-I mutated	This work

pCR2.1-PhutU-MC1	pCR2.1-TOPO carrying P_{hutU} promoter region with CbrB-I (NtrC-II) mutated	This work
pCR2.1-PhutU-MN3+4	pCR2.1-TOPO carrying P_{hutU} promoter region with NtrC-III and NtrC-IV mutated	This work
pCR2.1-PhutU-C3	pCR2.1-TOPO carrying P_{hutU} promoter region with CbrB-III introduced	This work

4.4.2 Strains construction

Standard protocols were used for isolation of plasmid DNA, restriction endonuclease digestion, ligation and PCR reaction. Restriction enzymes were obtained from New England Biolabs. Ligation reactions were conducted using T4 DNA ligase from Invitrogen (Auckland, New Zealand). PCR reactions were performed using *Taq* DNA polymerase from Invitrogen. All the oligonucleotide primers used in this work are summarized in Table 4.3. pCR8/GW/TOPO® Cloning Kit (Invitrogen) was used for TA cloning. For gene cloning from the genomic DNA of *P. fluorescens* SBW25, PCR product was first cloned into pCR8/GW/TOPO vector for DNA sequencing (Macrogen, South Korea). Then the desired insert DNA was subcloned into destination vectors and transferred into *P. fluorescens* strains by electroporation.

Site-directed mutagenesis of genes was achieved by a previously established procedure of SOE-PCR (splicing by overlapping extension PCR) (Horton *et al.*, 1989) in conjunction with a two-step allelic-exchange strategy using the suicide-integration vector pUIC3 (Rainey, 1999; Zhang & Rainey, 2007). Briefly, two pairs of primers were designed to PCR amplify flanking regions (~500 bp) of the target gene, wherein the two primers closer to the target gene are complementary for 20-23 bp at the join site. The two PCR products were used as DNA templates in the second-round PCR whereby the two DNA fragments were joined together. Then the resultant single DNA fragment was cloned into plasmid pUIC3. Next, the recombinant pUIC3 plasmid was transferred into *P. fluorescens* through conjugation with the helper plasmid pRK2013 (Ditta *et al.*, 1980). The desired allelic exchange mutants were selected by a previously described procedure of D-cycloserine enrichment (Zhang & Rainey, 2007).

Site-directed mutagenesis of the operator sites of NtrC and CbrB was performed using SOE-PCR mentioned above. The resultant mutated DNA fragment was cloned into

pCR8/GW/TOPO or pCR2.1-TOPO® (Invitrogen) and used as DNA template for PCR amplification of DNA probes for *in vitro* protein-DNA binding assays.

Table 4.3. Oligonucleotides used in this work

Primer	Sequence (5′ - 3′)[a]	Application
hutF1	gaagatCTGATCTGACGCGACAGTTC	*hutC* deletion
hutC-del2	aagctatgacGCACAGGGAATCCTTGCAG	
hutC-del3	attccctgtgCGTCATAGCTTGGAAGGAC	
hutD1	gaagatctTGGGTCAGTTCGATCAGGC	
PhutU_A	aaatttactagtGAAACTCGGCCATCACGATTG	Primers PhutU_A to PhutU_K were used to amplify the P_{hutU} variants for promoter mapping with the reverse primer PhutU_Rev
PhutU_B	aaatttactagtGCCTGATCGAACTGACCCAG	
PhutU_C	aaatttactagtGTCGGTACATCTATGACTGAAAC	
PhutU_D	aaatttactagtCACATTTGTTTTTGCGCTGTTTAC	
PhutU_E	aaatttactagtATTTGTTACCGAATGCCCCAGC	
PhutU_F	gactagtAATGCCCCAGCGTGGCGCAAAACC	
PhutU_G	aaatttactagtAATTTCATCATGCCTTGAAG	
PhutU_H	gactagtGCCTTGAAGCCTTAATTTCCAAG	
PhutU_I	gcactagtTCCAAGGCTTGCACGCACTTTCC	
PhutU_J	gactagtAAATCCAAACACCTCGCCCGGA	
PhutU_K	aaatttactagtCCCGGAAAGTTGGCCGCTCG	
PhutU_Rev	aaatttctgcagAGCTTGTTACCGTGGGCGGC	
ntrB-SpeI	gactaGTATTACCGGCAACACCCCGGTCGA	Transcriptional *lacZ* fusion to P_{ntrBC}
ntrB-HindIII	gaagcttGCTGATGGTCATTGGGACCTCTT	
cbrB-FB	gaagatCTGATCGTCGAAGATGAAGGT	Transcriptional *lacZ* fusion to P_{cbrB}
cbrB-RB	gaagatCTGAAGCATCTCGTCATGGTC	
NtrC-ProF	accatgggccatcatcatcatcatcatAGCCGTAGTGAAACCGTCTGGAT	NtrC protein expression
NtrC-ProR	gaagcttTCAGCCTTCATCGCCCTCGTCAT	
HisCbrBF	aaatttccatgggccatcatcatcatcatcatCCGCACATTTTGATCGTCGAAGAC	CbrB protein expression
CbrBR	aaatttctgcagTCAACTCTCGCTGGCCACACCG	
HutC-ProF	aaatttaccatgggccatcatcatcatcatcatCCGACTCCGCCCGCCAAGTCTC	HutC protein expression
HutC-ProR	aaatttgaagcttGCGCCAGACGCTTATTGCACTCAT	
hutU-MN1	aacaaatcttgaaGAGGACTGGAAACAGATTATG	Mutagenizing NtrC-I site in P_{hutU} promoter with primer PhutU_A
hutU-MN2	agtcctcttcaagATTTGTTACCGAATGCCCCAGC	
hutU-T7R1	AGCTTGTTACCGTGGGCGGCACGGAT	

hutU-MC1	gcattcgacggttAATTGGTGCGAGGACTGGAAAC	Mutagenizing CbrB-I site in P_{hutU} promoter with primer PhutU_A and hutU-T7R1
hutU-MC2	accaattaaccgtCGAATGCCCCAGCGTGGCGCAA	
hutU-MN3	tttacggttcgcgctttaATTCGGTAACAAATTGGTGC	Mutagenizing NtrC-III and NtrC-IV sites in P_{hutU} promoter with primer PhutU_A and hutU-T7R1
hutU-MN4	aattaaagcgcgaaccgtAAAACCTCGCTCTGGTGAC	
CbrB-T1	aggtttttgttacgGCTGGGGCATTCGGTAACA	Introducing CbrB-III site into P_{hutU} promoter with primer PhutU_A and hutU-T7R1
CbrB-T2	ccccagccgtaacaAAAACCTCGCTCTGGTGAC	
PntrB-mut3	atcatgatcatagcagaaGGTTTTATGAAGGTTGT	Mutagenizing O_{NtrC1} site in P_{ntrBC} promoter with primers ntrB-SpeI and ntrB-HindIII
PntrB-mut4	accttctgctatgatcatGATAGGCTGCACCCTTC	
PhutU_R4[b]	GGCATGATGAAATTTCTTAAGAGGC	Amplifying P_{hutU} promoter DNA probes
crcZ-Bio[b]	TGTGGCCAGCGAGAGTTGAG	Amplifying DNA probe PcrcZ171
crcZ-2	CCAGCAAAACCGGGAGGTTG	
Bio-ntrR[b]	GCTGATGGTCATTGGGACCTCTT	Amplifying DNA probe PntrBC-387 with primer ntrB-SpeI
Bio-ntrR1[b]	CTCCGAAAAGAAGCGTGCAAGC	Amplifying DNA probe PntrBC-300 with primer ntrB-SpeI
Bio-F-new2[b]	CAGCCCATCGGCGCTGACTT	Amplifying DNA probe PhutFC-256
hutF-F	aactagtACAAGGGCGCCGGACTTTCG	

[a] Artificial sequences integrated into the primers are shown in lowercase with restriction sites underlined.
[b] Primers are labeled by biotin at the 5′ end.

4.4.3 Assays for β-galactosidase and urocanate consumption

To construct transcriptional fusions to the promoterless *lacZ* the promoter region (~500 bp) of genes was cloned into pUIC3 or pUC18-mini-Tn7T-Gm-*lacZ*. The recombinant pUIC3 plasmid was introduced into *P. fluorescens* through conjugation with the help of pRK2013. The *lacZ* reporter was integrated into the chromosome via homologous recombination of the cloned DNA fragment. The *lacZ* fusion in pUC18-mini-Tn7T-Gm-*lacZ* was introduced into *P. fluorescens* together with plasmid pUX-BF13 by electroporation. The mini-Tn7 element carrying transcriptional fusion integrates into the chromosome at a single attTn7 site downstream of the *glmS* gene (Choi *et al.,* 2005).

β-galactosidase assays for measuring expression of *lacZ* fusions were performed using a standard protocol with 4-methylumbelliferyl-β-D-galactoside (4MUG) as the enzymatic substrate (Zhang *et al.,* 2006). Enzymatic reactions were performed using bacterial cells

grown in the tested media for 2-8 hours after inoculation. The fluorescent product, 7-hydroxy-4-methylcoumarin (4MU), was measured at 460 nm with an excitation wavelength of 365 nm using a Synergy 2 plate reader (Bio-Tek). β-galactosidase activity was expressed as the amount of 4MU (μM) produced per minute per cell (OD_{600}). To monitor urocanate utilization by bacteria in different nutrient conditions, the urocanate concentration was spectrophotometically determined at the wavelength of 277 nm in a 96-well microtiter plate by a Synergy 2 plate reader (Bio-Tek).

4.4.4 Electrophoretic mobility shift assays

The coding regions of NtrC, CbrB, HutC and Hfq were amplified by PCR from the genomic DNA of *P. fluorescens* SBW25 and subsequently cloned into the protein expression vector pTrc99A (Amann *et al.*, 1988) with the integration of six histidine residues at the N-terminal. The recombinant pTrc99A plasmids were transformed into *E. coli* BL21(DE3) for protein expression (Studier & Moffatt, 1986). IPTG was added at the final concentration of 1 mM to the *E. coli* culture (OD_{600}, 0.5~0.7) to induce protein expression for 4 hours at 37°C. Cells were lysed by sonication using the Sonicator S-4000 (Misonix, Inc). The His6-tagged proteins were purified using TALON® metal affinity resin (Clontech laboratories, Inc.) according to the manufacturer's instructions. The type and pH of buffer solution for protein preparation were adjusted based on the properties of proteins. 20 mM HEPES buffer (pH 7.4) was used for the purification of HutC and NtrC. 20 mM potassium phosphate buffer (pH 7.4) and 20 mM HEPES buffer (pH 7.0) were used for CbrB and Hfq, respectively. Concentrations of the purified proteins were determined by the Bradford method (Bradford, 1976).

DNA probes for EMSA were amplified by PCR and listed in Table 4.4. One of each pair of primers for PCR amplification is labeled by biotin at the 5'-end. DNA probes were purified using a standard protocol of phenol-chloroform extraction. EMSA reactions were set up by mixing 20 nM DNA probe, varying concentrations of protein, 1 μg salmon sperm DNA (Invitrogen) in EMSA binding buffer (10 mM HEPES, 50 mM KCl, 5 mM $MgCl_2$ and 1 mM DTT, pH 7.5) to a final volume of 20 μl. After incubation at room temperature for 30 minutes, reactions were electrophoresed on 6% native polyacrylamide gel in 0.5x TBE buffer at 120V at 4°C. The DNA in gel was transferred to positively charged Whatman® Nytran™ SuPerCharge nylon membrane (Sigma-Aldrich) by electroblotting and

immobilized by incubating the membrane at 80°C for 30 minutes. LightShift™ chemiluminescent EMSA kit (Thermo Fisher Scientific) was used to detect the biotin-labelled DNA probes, and the image was visualized by LAS-4000 Luminescent Imager equipped with ImageQuant™ LAS 4000 software (FujiFilm).

RNA probes for EMSA were supplied by Integrated DNA Technologies (Singapore) with 5′-end labelled by biotin. The protein-RNA interactions were assayed in a 20 µl reaction containing 0.1 µM RNA probe, varying concentrations of Hfq_{His6}, 1 µg yeast tRNA and RNA binding buffer (10 mM HEPES, 35 mM KCl and 2 mM $MgCl_2$, pH 7.9). After incubation at room temperature for 30 min, reactions were electrophoresed on 6% nondenaturing polyacrylamide gel in 0.5x TBE buffer at 100V at 4°C. Electroblotting and detection of the RNA probes followed the same procedure as described in EMSA with DNA.

Table 4.4. DNA probes used in this work

DNA probe	Primers for PCR amplification	Template for PCR amplification	Length (bp)	Characteristics
PC-WT	PhutU_C & PhutU_R4[b]	SBW25 genomic DNA	194	P_{hutU} promoter DNA
PC-NtrC1	PhutU_C & PhutU_R4[b]	pCR2.1-PhutU-MN1	194	P_{hutU} promoter DNA with NtrC-I mutated
PC-NtrC2	PhutU_C & PhutU_R4[b]	pCR2.1-PhutU-MC1	194	P_{hutU} promoter DNA with NtrC-II mutated
PC-NtrC3&4	PhutU_C & PhutU_R4[b]	pCR2.1-PhutU-MN3+4	194	P_{hutU} promoter DNA with NtrC-III and NtrC-IV mutated
PE-WT	PhutU_E & PhutU_R4[b]	SBW25 genomic DNA	95	P_{hutU} promoter DNA
PE-CbrB1	PhutU_E & PhutU_R4[b]	pCR2.1-PhutU-MC1	95	P_{hutU} promoter DNA with CbrB-I mutated
PE+CbrB3	PhutU_E & PhutU_R4[b]	pCR2.1-PhutU-C3	95	P_{hutU} promoter DNA with CbrB-III introduced
PcrcZ171	crcZ-Bio[b] & crcZ-2	SBW25 genomic DNA	171	P_{crcZ} promoter DNA
PntrBC-387	ntrB-SpeI & Bio-ntrR[b]	SBW25 genomic DNA	387	P_{ntrBC} promoter DNA
PntrBC-300	ntrB-SpeI & Bio-ntrR1[b]	SBW25 genomic DNA	300	P_{ntrBC} promoter DNA
PntrBC-Mut1	ntrB-SpeI & Bio-ntrR1[b]	pCR8-PntrB-Mut1	300	P_{ntrBC} promoter DNA with O_{NtrC1} site mutated
PhutFC-256	Bio-F-new2[b] & hutF-F	SBW25 genomic DNA	256	P_{hutFC} promoter DNA

[b] Primers are labelled by biotin at the 5′-end.

4.4.5 DNase I footprinting assays

Reactions were set up under the same condition described for EMSA but in a larger volume of 50 µl, wherein 2 µM DNA probe was used. After incubation at room temperature for 30 minutes, 50 µl of cofactor solution (5 mM $CaCl_2$ and 10 mM $MgCl_2$) was added. Then the samples were treated with 0.02 U of DNase I (Invitrogen) for 5 min at room temperature. After termination of the reactions with 100 µl of DNase I stop solution (200 mM NaCl, 20 mM EDTA and 1% SDS), DNA was extracted with an equal volume of 1:1 phenol/chloroform mixture and precipitated by adding 1 µl of glycogen (20 mg/ml, Fermentas), 1/10th volume of 3 M sodium acetate (pH 5.2) and three volumes of ethanol. Following incubation at -20^{o}C for at least 1 hour, DNA was pelleted by centrifugation and resuspended in 8 µl of loading buffer (95% formamide, 0.05% bromophenol blue and 20 mM EDTA). After denaturing at 95^{o}C for 10 min, the samples were electrophoresed on a 6% denaturing urea-polyacrylamide gel (21 x 40 cm) in 1x TBE buffer using the Sequi-Gen® GT electrophoresis system (Bio-Rad Laboratories Pty). Then DNA was transferred from the gel to positively charged nylon membrane by contact blotting (Petersen *et al.*, 1996). Detection of the DNA fragments was conducted as described above in EMSA. A G+A marker showing the sequence of DNA fragments was included in the gel. It was produced with the same biotin-labelled DNA probe by Maxam-Gilbert chemical sequencing reactions (Maxam & Gilbert, 1980).

4.5 References

Abdou, L., Chou, H. T., Haas, D., & Lu, C. D. (2011). Promoter recognition and activation by the global response regulator CbrB in *Pseudomonas aeruginosa*. *J Bacteriol, 193*(11), 2784-2792. doi: 10.1128/JB.00164-11

Alejandro-Marin, C. M., Bosch, R., & Nogales, B. (2014). Comparative genomics of the protocatechuate branch of the beta-ketoadipate pathway in the *Roseobacter* lineage. *Mar Genomics, 17*, 25-33. doi: 10.1016/j.margen.2014.05.008

Amador, C. I., Canosa, I., Govantes, F., & Santero, E. (2010). Lack of CbrB in *Pseudomonas putida* affects not only amino acids metabolism but also different stress responses and biofilm development. *Environ Microbiol, 12*(6), 1748-1761. doi: 10.1111/j.1462-2920.2010.02254.x

Amann, E., Ochs, B., & Abel, K. J. (1988). Tightly regulated tac promoter vectors useful for the expression of unfused and fused proteins in *Escherichia coli*. *Gene, 69*(2), 301-315.

Atkinson, M. R., Pattaramanon, N., & Ninfa, A. J. (2002). Governor of the *glnAp2* promoter of *Escherichia coli*. *Mol Microbiol, 46*(5), 1247-1257.

Bailey, M. J., Lilley, A. K., Thompson, I. P., Rainey, P. B., & Ellis, R. J. (1995). Site directed chromosomal marking of a fluorescent pseudomonad isolated from the phytosphere of sugar beet; stability and potential for marker gene transfer. *Mol Ecol, 4*(6), 755-763.

Bao, Y., Lies, D. P., Fu, H., & Roberts, G. P. (1991). An improved Tn7-based system for the single-copy insertion of cloned genes into chromosomes of gram-negative bacteria. *Gene, 109*(1), 167-168.

Bender, R. A. (2010). A NAC for regulating metabolism: the nitrogen assimilation control protein (NAC) from *Klebsiella pneumoniae*. *J Bacteriol, 192*(19), 4801-4811. doi: 10.1128/JB.00266-10

Bender, R. A. (2012). Regulation of the histidine utilization (*hut*) system in bacteria. *Microbiol Mol Biol Rev, 76*(3), 565-584. doi: 10.1128/MMBR.00014-12

Bradford, M. M. (1976). A rapid and sensitive method for the quantitation of microgram quantities of protein utilizing the principle of protein-dye binding. *Anal Biochem, 72*, 248-254.

Bruckner, R., & Titgemeyer, F. (2002). Carbon catabolite repression in bacteria: choice of the carbon source and autoregulatory limitation of sugar utilization. *FEMS Microbiol Lett, 209*(2), 141-148. doi: 10.1111/j.1574-6968.2002.tb11123.x

Choi, K. H., Gaynor, J. B., White, K. G., Lopez, C., Bosio, C. M., Karkhoff-Schweizer, R. R., & Schweizer, H. P. (2005). A Tn7-based broad-range bacterial cloning and expression system. *Nat Methods, 2*(6), 443-448. doi: 10.1038/nmeth765

Collier, D. N., Hager, P. W., & Phibbs, P. V., Jr. (1996). Catabolite repression control in the Pseudomonads. *Res Microbiol, 147*(6-7), 551-561.

Curnow, A. W., Hong, Kw, Yuan, R., Kim, Si, Martins, O., Winkler, W., . . . Soll, D. (1997). Glu-tRNAGln amidotransferase: a novel heterotrimeric enzyme required for correct decoding of glutamine codons during translation. *Proc Natl Acad Sci U S A, 94*(22), 11819-11826.

Deutscher, J. (2008). The mechanisms of carbon catabolite repression in bacteria. *Curr Opin Microbiol, 11*(2), 87-93. doi: 10.1016/j.mib.2008.02.007

Ditta, G., Stanfield, S., Corbin, D., & Helinski, D. R. (1980). Broad host range DNA cloning system for gram-negative bacteria: construction of a gene bank of *Rhizobium meliloti*. *Proc Natl Acad Sci U S A, 77*(12), 7347-7351.

Gao, R., & Stock, A. M. (2018). Overcoming the Cost of Positive Autoregulation by Accelerating the Response with a Coupled Negative Feedback. *Cell Rep, 24*(11), 3061-3071 e3066. doi: 10.1016/j.celrep.2018.08.023

Garcia-Maurino, S. M., Perez-Martinez, I., Amador, C. I., Canosa, I., & Santero, E. (2013). Transcriptional activation of the CrcZ and CrcY regulatory RNAs by the CbrB response regulator in *Pseudomonas putida*. *Mol Microbiol, 89*(1), 189-205. doi: 10.1111/mmi.12270

Gorke, B., & Stulke, J. (2008). Carbon catabolite repression in bacteria: many ways to make the most out of nutrients. *Nat Rev Microbiol, 6*(8), 613-624. doi: 10.1038/nrmicro1932

Goss, T. J., & Bender, R. A. (1995). The nitrogen assimilation control protein, NAC, is a DNA binding transcription activator in *Klebsiella aerogenes*. *J Bacteriol, 177*(12), 3546-3555.

Grant, C. E., Bailey, T. L., & Noble, W. S. (2011). FIMO: scanning for occurrences of a given motif. *Bioinformatics, 27*(7), 1017-1018. doi: 10.1093/bioinformatics/btr064

Guo, Z., & Houghton, J. E. (1999). PcaR-mediated activation and repression of *pca* genes from *Pseudomonas putida* are propagated by its binding to both the -35 and the -10 promoter elements. *Mol Microbiol, 32*(2), 253-263.

Hernandez-Arranz, S., Moreno, R., & Rojo, F. (2013). The translational repressor Crc controls the *Pseudomonas putida* benzoate and alkane catabolic pathways using a multi-tier regulation strategy. *Environ Microbiol, 15*(1), 227-241. doi: 10.1111/j.1462-2920.2012.02863.x

Hervas, A. B., Canosa, I., & Santero, E. (2008). Transcriptome analysis of *Pseudomonas putida* in response to nitrogen availability. *J Bacteriol, 190*(1), 416-420. doi: 10.1128/JB.01230-07

Horton, R. M., Hunt, H. D., Ho, S. N., Pullen, J. K., & Pease, L. R. (1989). Engineering hybrid genes without the use of restriction enzymes: gene splicing by overlap extension. *Gene, 77*(1), 61-68.

Hu, L., & Phillips, A. T. (1988). Organization and multiple regulation of histidine utilization genes in *Pseudomonas putida*. *J Bacteriol, 170*(9), 4272-4279.

Hug, D. H., Roth, D., & Hunter, J. (1968). Regulation of histidine catabolism by succinate in *Pseudomonas putida*. *J Bacteriol, 96*(2), 396-402.

Itoh, Y. , Nishijyo, T. , & Nakada, Y. (2007). Histidine catabolism and catabolite regulation. *Pseudomonas. Springer, Berlin, Germany, 5*, 371-395.

Lessie, T. G., & Neidhardt, F. C. (1967). Formation and operation of the histidine-degrading pathway in *Pseudomonas aeruginosa*. *J Bacteriol, 93*(6), 1800-1810.

Li, W., & Lu, C. D. (2007). Regulation of carbon and nitrogen utilization by CbrAB and NtrBC two-component systems in *Pseudomonas aeruginosa*. *J Bacteriol, 189*(15), 5413-5420. doi: 10.1128/JB.00432-07

Liu, Y., Gokhale, C. S., Rainey, P. B., & Zhang, X. X. (2017). Unravelling the complexity and redundancy of carbon catabolic repression in *Pseudomonas fluorescens* SBW25. *Mol Microbiol, 105*(4), 589-605. doi: 10.1111/mmi.13720

Magasanik, B. (1955). The metabolic control of histidine assimilation and dissimilation in *Aerobacter aerogenes*. *J Biol Chem, 213*(2), 557-569.

Magasanik, B. (1961). Catabolite repression. *Cold Spring Harb Symp Quant Biol, 26*, 249-256.

Maxam, A. M., & Gilbert, W. (1980). Sequencing end-labeled DNA with base-specific chemical cleavages. *Methods Enzymol, 65*(1), 499-560.

Moreno, R., Martinez-Gomariz, M., Yuste, L., Gil, C., & Rojo, F. (2009). The *Pseudomonas putida* Crc global regulator controls the hierarchical assimilation of amino acids in a complete medium: evidence from proteomic and genomic analyses. *Proteomics, 9*(11), 2910-2928. doi: 10.1002/pmic.200800918

Nishijyo, T., Haas, D., & Itoh, Y. (2001). The CbrA-CbrB two-component regulatory system controls the utilization of multiple carbon and nitrogen sources in *Pseudomonas aeruginosa*. *Mol Microbiol, 40*(4), 917-931.

Oshikane, H., Sheppard, K., Fukai, S., Nakamura, Y., Ishitani, R., Numata, T., . . . Nureki, O. (2006). Structural basis of RNA-dependent recruitment of glutamine to the genetic code. *Science, 312*(5782), 1950-1954. doi: 10.1126/science.1128470

Osuna, R., Boylan, S. A., & Bender, R. A. (1991). In vitro transcription of the histidine utilization (*hutUH*) operon from *Klebsiella aerogenes*. *J Bacteriol, 173*(1), 116-123.

Osuna, R., Janes, B. K., & Bender, R. A. (1994). Roles of catabolite activator protein sites centered at -81.5 and -41.5 in the activation of the *Klebsiella aerogenes* histidine utilization operon *hutUH*. *J Bacteriol, 176*(17), 5513-5524.

Petersen, I., Reichel, M. B., & Dietel, M. (1996). Use of non-radioactive detection in SSCP, direct DNA sequencing and LOH analysis. *Clin Mol Pathol, 49*(2), M118-121.

Phillips, A. T., & Mulfinger, L. M. (1981). Cyclic adenosine 3',5'-monophosphate levels in *Pseudomonas putida* and *Pseudomonas aeruginosa* during induction and carbon catabolite repression of histidase synthesis. *J Bacteriol, 145*(3), 1286-1292.

Prival, M. J., & Magasanik, B. (1971). Resistance to catabolite repression of histidase and proline oxidase during nitrogen-limited growth of *Klebsiella aerogenes*. *J Biol Chem, 246*(20), 6288-6296.

Rainey, P. B. (1999). Adaptation of *Pseudomonas fluorescens* to the plant rhizosphere. *Environ Microbiol, 1*(3), 243-257.

Reitzer, L. (2003). Nitrogen assimilation and global regulation in *Escherichia coli*. *Annu Rev Microbiol, 57*, 155-176. doi: 10.1146/annurev.micro.57.030502.090820

Rojo, F. (2010). Carbon catabolite repression in *Pseudomonas* : optimizing metabolic versatility and interactions with the environment. *FEMS Microbiol Rev, 34*(5), 658-684. doi: 10.1111/j.1574-6976.2010.00218.x

Romero-Rodriguez, A., Maldonado-Carmona, N., Ruiz-Villafan, B., Koirala, N., Rocha, D., & Sanchez, S. (2018). Interplay between carbon, nitrogen and phosphate utilization in the control of secondary metabolite production in *Streptomyces*. *Antonie Van Leeuwenhoek, 111*(5), 761-781. doi: 10.1007/s10482-018-1073-1

Romero-Steiner, S., Parales, R. E., Harwood, C. S., & Houghton, J. E. (1994). Characterization of the pcaR regulatory gene from *Pseudomonas putida*, which is required for the complete degradation of p-hydroxybenzoate. *J Bacteriol, 176*(18), 5771-5779.

Sambrook, J., Fritsch, E.F., & Maniatis, T. (1989). Molecular Cloning: A Laboratory Manual. *Cold Spring Harbor Laboratory Press, New York, USA*.

Schwacha, A., & Bender, R. A. (1993). The *nac* (nitrogen assimilation control) gene from *Klebsiella aerogenes*. *J Bacteriol, 175*(7), 2107-2115.

Sonnleitner, E., Abdou, L., & Haas, D. (2009). Small RNA as global regulator of carbon catabolite repression in *Pseudomonas aeruginosa*. *Proc Natl Acad Sci U S A, 106*(51), 21866-21871. doi: 10.1073/pnas.pnas.0910308106

Studier, F. W., & Moffatt, B. A. (1986). Use of bacteriophage T7 RNA polymerase to direct selective high-level expression of cloned genes. *J Mol Biol, 189*(1), 113-130.

Suh, S. J., Runyen-Janecky, L. J., Maleniak, T. C., Hager, P., MacGregor, C. H., Zielinski-Mozny, N. A., . . . West, S. E. (2002). Effect of vfr mutation on global gene expression and catabolite repression control of *Pseudomonas aeruginosa*. *Microbiology, 148*(Pt 5), 1561-1569. doi: 10.1099/00221287-148-5-1561

Zhang, X. X., George, A., Bailey, M. J., & Rainey, P. B. (2006). The histidine utilization (*hut*) genes of *Pseudomonas fluorescens* SBW25 are active on plant surfaces, but are not required for competitive colonization of sugar beet seedlings. *Microbiology, 152*(Pt 6), 1867-1875. doi: 10.1099/mic.0.28731-0

Zhang, X. X., Liu, Y. H., & Rainey, P. B. (2010). CbrAB-dependent regulation of *pcnB*, a poly(A) polymerase gene involved in polyadenylation of RNA in *Pseudomonas fluorescens*. *Environ Microbiol, 12*(6), 1674-1683. doi: 10.1111/j.1462-2920.2010.02228.x

Zhang, X. X., & Rainey, P. B. (2007). Genetic analysis of the histidine utilization (*hut*) genes in *Pseudomonas fluorescens* SBW25. *Genetics, 176*(4), 2165-2176. doi: 10.1534/genetics.107.075713

Zhang, X. X., & Rainey, P. B. (2008). Dual involvement of CbrAB and NtrBC in the regulation of histidine utilization in *Pseudomonas fluorescens* SBW25. *Genetics, 178*(1), 185-195. doi: 10.1534/genetics.107.081984

4.6 Supplementary data

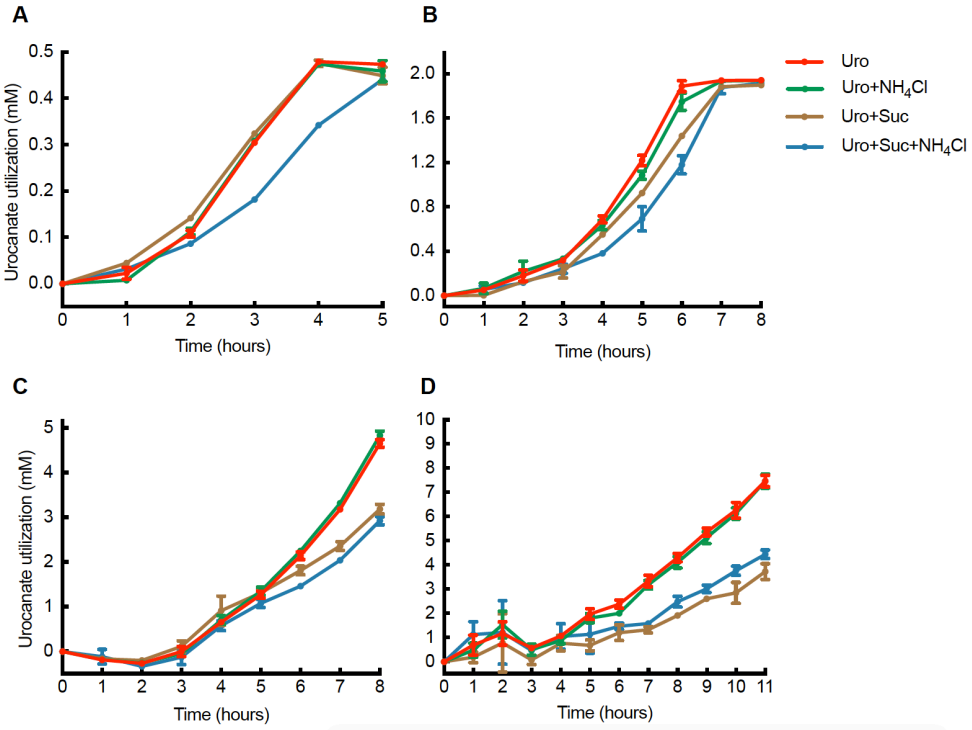

Figure S4.1. Variation of the effects of succinate and ammonium on urocanate consumption by wild-type *P. fluorescens* SBW25 when urocanate was added at different concentrations. Data are means and standard errors of six independent cultures. Succinate (Suc) and ammonium (NH_4Cl) were added at 20 mM and 18.7 mM, respectively.

(A) Urocanate added at 0.5 mM. Two-way ANOVA revealed significant difference among medium treatments ($F_{3,120}$ = 443.4, $P < 0.0001$). No significant difference between Uro and Uro + NH_4Cl. However, the differences were highly significant ($P < 0.001$) between Uro and Uro + Suc at 1, 2 and 3 hours; and Uro + Suc versus Uro + Suc + NH_4Cl at 2, 3 and 4 hours.

(B) Urocanate added at 2.0 mM. There were significant differences among medium treatments ($F_{3,180}$ = 271.3, $P < 0.0001$). Differences between each of the four media were highly significant ($P < 0.001$) at 5 and 6 hours after inoculation.

(C) Urocanate added at 5.0 mM. Two-way ANOVA revealed significant difference among medium treatments ($F_{3,180}$ = 299, $P < 0.0001$). The differences between Uro and Uro + Suc were highly significant at the three time points of 6, 7 and 8 hours ($P < 0.001$). Significant difference was also found between Uro + Suc and Uro + Suc + NH_4Cl ($P < 0.001$) at 6, 7 and 8 hours after inoculation.

(D) Urocanate added at 10 mM. There were significant differences among medium treatments ($F_{3,240}$ = 280.8, $P < 0.0001$). Differences were highly significant ($P < 0.001$) between Uro and Uro + Suc, and between Uro + NH_4Cl and Uro + Suc + NH_4Cl. However, addition of ammonium produced no significant difference (Uro versus Uro + NH_4Cl, Uro + Suc versus Uro + Suc + NH_4Cl).

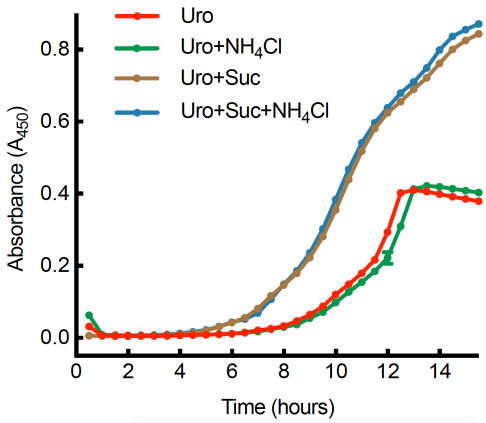

Figure S4.2. Growth dynamics of wild-type *P. fluorescens* SBW25 in minimal salts medium supplemented with urocanate with and without succinate and ammonium. Urocanate (Uro) was added at 5.0 mM. Succinate (Suc) and ammonium (NH_4Cl) were added at 20 mM and 18.7 mM, respectively.

Table S4.1. Predicted NtrC-binding sites in *P. fluorescens* SBW25

p-value	Matched Sequence	Motif Location		Putative or established function of candidate genes
		Start	End	
5.37E-10	GCACTATATTGGTGC	376928	376942	PFLU0344: NtrB
1.09E-07	GCACTAAATAGGTGC	380453	380467	PFLU0348: GlnA, glutamine synthetase.
2.13E-07	GCACTACATAGGTGC	2709388	2709402	PFLU2495: hypothetical protein.
3.25E-07	GCACCATATTGGCGG	6132971	6132985	PFLU5597: putative coenzyme PQQ (pyrroloquinoline quinone) biosynthesis-like protein.
4.68E-07	GCACCATATTGGTGA	5472022	5472036	PFLU4981*: InaA ortholog, pH-inducible protein involved in stress response.
4.88E-07	GCACCAGCATGGTGC	2303582	2303596	PFLU2123: putative methyl-accepting chemotaxis protein.
5.42E-07	GCGCCGTTTTGGTGC	613272	613286	PFLU0541: hypothetical protein. The homologue is IMP dehydrogenase (inosine-5'-monophosphate dehydrogenase).
5.73E-07	GCACCAGATAAGTGC	1837839	1837853	PFLU1674: putative amino acid transporter-like membrane protein. The homologue is ethanolamine permease. PFLU1676: KdpA, potassium-transporting ATPase subunit A.
5.75E-07	GCACTTGTTTAGTGC	1500581	1500595	PFLU1361*: PcaR, an activator of the pca genes for degradation of protocatechuate.
8.85E-07	GCGCCATCATGGTGC	4223167	4223181	PFLU3827: NADH dehydrogenase subunit K.
1.04E-06	GCACCTCATCGGTGC	2212207	2212221	PFLU2039: putative ABC transporter substrate-binding protein.
1.14E-06	GCACTCTAATGGTGC	2828874	2828888	PFLU2564: putrescine ABC transporter substrate-binding protein.
1.48E-06	GCTCCGGATTGGTGG	1752992	1753006	PFLU1599: Unknown function.
2.17E-06	GCGCTCTATTGGTGC	5516570	5516584	PFLU5024: GntR family transcriptional regulator that might be involved in aminosugars metabolism. It probably forms an operon with PFLU5025 encoding a putative N-acetylglucosamine-6-phosphate deacetylase.
2.51E-06	GCGCCAAATTGGTGC	639361	639375	PFLU0563: urease accessory protein UreE.
3.18E-06	GCTCTAGAACAGTGC	4202341	4202355	PFLU3808: isocitrate dehydrogenase, an enzyme that catalyzes the oxidative decarboxylation of isocitrate, producing α-ketoglutarate and CO2.
3.28E-06	GCACTGCAACGGTGC	2884590	2884604	PFLU2617*: putative glutamine ABC transporter periplasmic

				glutamine-binding protein.
3.61E-06	GCACCAGTTTGTTGC	5148129	5148143	PFLU4667: hypothetical protein.
3.73E-06	GCACCACGGTGGTGG	4111304	4111318	PFLU3714*: AraC family transcriptional regulator.
3.78E-06	GCACTTTTTTGGGGC	1185502	1185516	PFLU1072*: Amidase, exhibiting high similarity to the Glu-tRNA(Gln) amidotransferase subunit A (encoded by gatA2).
4.30E-06	GCACTGTTTTTGTGC	6509664	6509678	PFLU5953: GlnK, nitrogen regulatory protein P-II.
4.97E-06	GCGCTACCTTAGTGC	5292971	5292985	PFLU4811: putative gluconokinase, an enzyme participates in pentose phosphate pathway.
5.90E-06	GGTCTTTTTTGGTGC	936020	936034	PFLU0826: dppA3, dipeptide ABC transporter substrate-binding protein.
5.90E-06	GCACCAGGACGGTGC	5147341	5147355	PFLU4666: hypothetical protein.
6.03E-06	GCGCCACATGAGTGC	5789972	5789986	PFLU5273: OmlA, outer membrane lipoprotein.
6.49E-06	GTTCCTGATTGGTGC	921508	921522	PFLU0814: glycine/betaine ABC transporter substrate-binding protein.
6.49E-06	GCACCGCATTGGCGG	2455235	2455249	PFLU2265: AraC family transcriptional regulator
6.82E-06	GCACCGCTATGGCGC	4296596	4296610	PFLUs34: PrrF RNA involved in iron homeostasis.
7.00E-06	GCGCCTGTTCGGTGC	2468788	2468802	PFLU2271: putative exported isoquinoline 1-oxidoreductase subunit beta.
7.48E-06	GCACCAGGTTGGCGC	666981	666995	PFLU0588: putative amino acid ABC transporter substrate-binding protein.
7.61E-06	GCACCTTGTTGGCGC	4799000	4799014	PFLU4352: putative glutathione S-transferase protein.
8.54E-06	ACGCCGTATTGGTGC	1792657	1792671	PFLU1634: putative peptide ABC transporter ATP-binding protein.
9.13E-06	CCACCAGATGGGTGC	796372	796386	PFLU0697: putative metal transporter-like exported protein.
9.93E-06	GCACCTTCGTGGTGC	6425652	6425666	PFLU5870: hypothetical protein. The ortholog is ribonucleotide reductase.

The putative NtrC-binding sites in the *P. fluorescens* SBW25 genome were predicted using a matrix-based motif-scanning tool FIMO 4.11.2 (Grant *et al.*, 2011), resulting in 34 NtrC-regulated candidate genes (possess a putative NtrC-binding site and σ^{54}-binding site in the promoter region). Potential CbrB-binding sites were searched for in each NtrC-regulated candidate promoter by Motif Search module of Geneious 9.0.5. Five candidate genes are possibly subject to direct regulation by both CbrB and NtrC, including *pflu4981, pflu1361*, *pflu2617*, *pflu3714* and *pflu1072* (marked with *). *pflu1361* encodes the PcaR protein, an activator of *pca* genes for protocatechuate degradation. Protocatechuate degradation is one branch of the β-ketoadipate pathway, converting protocatechuate to β-ketoadipate. Subsequent degradation of β-ketoadipate produces intermediates of the TCA cycle (Alejandro-Marin *et al.*, 2014; Guo & Houghton, 1999; Romero-Steiner *et al.*, 1994). The product of *pflu2617* shows 98% identity to GlnH of *P. fluorescens* WH6, which is a glutamine ABC transporter periplasmic glutamine-binding protein. *pflu1072* encodes an amidase, which exhibits 71% identity to the Glu-tRNA(Gln) amidotransferase subunit A (encoded by *gatA2*) of *P. protegens* CHA0. Glu-tRNA(Gln) amidotransferase is an essential component in translation process as it catalyzes the production of Gln-tRNA(Gln) by transamidation of misacylated Glu-tRNA(Gln). Ammonia for the transamidation is produced via amidolysis of glutamine by the amidase GatA, a subunit of Glu-tRNA(Gln) amidotransferase (Curnow *et al.*, 1997; Oshikane *et al.*, 2006).

Chapter 5

Conclusions and future directions

5.1 The mode of HutC-mediated regulation of histidine utilization (*hut*) genes

HutC works as the regulatory protein of *hut* genes for bacterial histidine utilization. In the absence of histidine and urocanate, it represses the transcription of *hut* genes by binding to the operator site in the *hut* promoters. The repression is relieved via molecular interactions between HutC and urocanate (Allison & Phillips, 1990; Hu *et al.*, 1989; Newell & Lessie, 1970). Although the HutC-mediated repression of *hut* genes has been genetically characterized, the precise protein-DNA interaction has not been determined using purified HutC proteins.

In this study, we examined the detailed molecular interactions between $HutC_{His6}$ and the *hut* promoters of *P. fluorescens* SBW25, and the results of biochemical and mutational analysis allow us to propose updated models of HutC interacting with the P_{hutU} and P_{hutFC} promoters. First, we identified the operator site consisting of 10-bp short inverted repeat sequence (named Phut site), which is critical for HutC binding. Following recognition of the DNA targeting site, HutC forms complex oligomers in response to varying concentrations of urocanate. Moreover, simultaneously binding to the two half elements of Phut site is required for the proper oligomerization of HutC and HutC-mediated repression of *hut* genes. Second, the detailed modes of HutC action when interacting with the P_{hutU} and P_{hutFC} promoter DNAs are different with regard to oligomeric state and binding affinity of HutC. These differences imply the coordination of HutC in regulating the expression of the enzymatic and regulator genes.

More importantly, we have identified a novel HutC binding site (termed Pntr site) that is located adjacent to the abovementioned Phut site in the P_{hutFC} promoter of *P. fluorescens* SBW25. Consensus sequence of the Pntr site is distinct from that of the Phut site. Presence of the Pntr site extends the HutC-protected region into the *hutF* coding

region, which may contribute to a tighter control on the expression of *hutF* than *hutC*. Consequently, repression of the regulator gene *hutC* might be weaker than that of the enzymatic gene *hutF*. The biological significance of the Pntr site regarding the expression of *hutF* and *hutC* needs to be determined *in vivo* in future work.

5.2 The global regulatory role of HutC in *P. fluorescens* SBW25

HutC has long been known as a local regulator responsible for histidine concentration-dependent expression of *hut* genes. However, recent progress suggests that HutC plays an important role in global gene regulation for cellular metabolism, bacterial motility and production of virulence factors in different bacterial pathogens, including human pathogenic bacterium *P. aeruginosa*. Previous work in *P. fluorescens* SBW25 show that HutC contributes to enhanced ability to colonize the surfaces of sugar beet plants (Zhang & Rainey, 2007). In this work, we systematically examined the global regulatory role of HutC in *P. fluorescens* SBW25, and the results are presented in Chapter 3. First, we performed a genome-scale bioinformatic analysis of putative HutC-binding (Phut) sites. This led to the identification of 143 motif occurrences in the SBW25 genome. Eighty-eight of them are located within 500 bp upstream of a gene, which likely contains a promoter. A close examination of the HutC-regulated candidate genes revealed that a number of them are potentially involved in amino acid metabolism, energy production, cellular nitrogen metabolism and also type IV pili assembly. A panel of eight candidate Phut sites was selected and experimentally verified by EMSA with purified $HutC_{His6}$. In future work, it would be significant to further investigate whether and how HutC is involved in the regulation of the corresponding candidate genes.

Next, we focused on one of the HutC-regulated candidate genes, *ntrBC*. DNase I footprinting analyses identified a novel HutC-binding Pntr site in addition to the predicted upstream Phut site in the P_{ntrBC} promoter region. This is consistent with what has been found in Chapter 2 that HutC is able to bind to the Pntr site in the P_{hutFC} promoter. We show that HutC and NtrC are capable of binding to the same Pntr site in the P_{ntrBC} promoter on the basis of DNase I footprinting performed with the purified $NtrC_{His6}$ and $HutC_{His6}$ proteins and the same P_{ntrBC} promoter DNA. The presence of NtrC-binding sites and a putative σ^{54} binding site in the P_{ntrBC} promoter indicates that the

expression of *ntrBC* requires its own response regulator NtrC. The data suggest that HutC negatively regulates the expression of *ntrBC* via competing for the same operator site as the transcriptional activator NtrC. Unexpectedly, the Phut site in the promoter region of *ntrBC* plays no role in its expression. In addition, phenotypic analyses of the *hutC* deletion mutant showed that *hutC* is involved in the swimming and swarming motilities of *P. fluorescens* SBW25, but not biofilm formation.

Together, data presented in Chapter 2 and Chapter 3 confirmed that HutC is capable of binding to two distinct DNA sites, the Phut and Pntr sites, and the binding involves complex allosteric interactions between HutC and its target DNAs. Two distinct DNA operator sites for one regulatory protein has not been described in prokaryotes before. It would be interesting to examine the crystallographic structure of HutC interacting with the two targeting DNA sites, and determine the critical residues in both HutC and the DNA binding sites via site-directed mutagenesis to test the structure-function relationship.

5.3 Maintenance of carbon/nitrogen metabolic balance for histidine catabolism in *Pseudomonas*

Histidine is a source of both carbon and nitrogen for *Pseudomonas*, but it produces excess nitrogen over carbon. Thus, the rate of histidine utilization must be carefully regulated to maintain the cellular C/N balance. When growing in a nutrient-complex condition wherein histidine is provided as the sole nitrogen source along with succinate, one of the most preferred carbon sources for *Pseudomonas*, bacterial cells face a dilemma to increase *hut* expression as histidine is the sole nitrogen source, but meanwhile reduce the *hut* activities via carbon catabolite repression (CCR) provoked by succinate. These raise an important question how the carbon and nitrogen regulations are coordinated in the case of histidine utilization to maximize bacterial fitness in nutrient-complex environments.

In Chapter 4, we aimed to determine the underlying molecular mechanisms for the coordination of carbon and nitrogen regulations for histidine utilization in *P. fluorescens* SBW25. Two two-component regulatory systems CbrAB and NtrBC play a primary role in maintaining C/N metabolic balance via a complex interplay at the

operator sites in the P_{hutU} promoter. Besides directly activating *hut* transcription, CbrAB also controls Hut expression at the translational level via the CbrAB-CrcYZ-Crc/Hfq cascade. Notably, HutC works as a governor assisting NtrBC to directly activate the *hut* transcription in response to nitrogen limitation.

Specifically, when the bacteria are grown on histidine in the presence of low concentrations of succinate, CbrAB plays a major role in activating *hut* transcription. NtrBC is negligible under these nitrogen-replete nutrient conditions. The Crc/Hfq-mediated translational repression of *hut* is relieved due to a high-level expression of the antagonistic ncRNAs CrcY and CrcZ, whose expression is activated by CbrAB. In the contrast, when succinate is present at high concentrations, the CbrAB-mediated transcription of *hut* and *crcY*/*crcZ* genes is reduced, and consequently, *hut* expression is repressed by Crc/Hfq at the translational level. Under these nitrogen-limiting conditions, NtrBC starts to play the predominant role in activating *hut* transcription to meet the cellular demand for nitrogen. Of note, the translational repression of *hut* genes is relatively weak. A strong CCR of *hut* would lead to insufficient nitrogen supply, causing growth restriction.

Furthermore, a nitrogen-limited condition is required for expression of the *ntrBC* system. Hence, there is a risk that the *hut* genes are over-expressed, producing excess ammonia, which will quench the NtrBC system and cause no expression of NtrC-activated *hut* genes. To prevent this from happening, we show that HutC directly targets the P_{ntrBC} promoter to maintain the *ntrBC* expression at a proper level. This will avoid *hut* overexpression and buildup of excess ammonium during the growth on succinate and histidine. Together, we propose that HutC acts as a governor to maintain *ntrBC* expression in response to changing histidine availability.

The *hut* transcription is coordinately controlled by CbrB and NtrC. When *P. fluorescens* SBW25 is grown on succinate and histidine, NtrC plays a major role over CbrB in activation of the *hut* transcription. In future work, it would be interesting to monitor whether and how the predominance between CbrB and NtrC dynamically change responding to various concentrations of succinate and histidine. This will deepen the understanding of the regulatory roles of CbrB and NtrC in coordination of C/N metabolic balance for histidine utilization. Additionally, as mentioned in Chapter 4, the well-known model organism *P. putida* is quite different from most *Pseudomonas*

species in the regulation of *hut* genes. It does not contain any putative CbrB and NtrC binding sites nor σ^{54} binding site in the *hutU* promoter region. Interestingly, CbrB and NtrC are possibly involved in the regulation of *hut* genes of *P. putida* in an unknown indirect manner (Amador *et al.*, 2010). To date, little is known about the carbon and nitrogen regulation of *hut* genes in *P. putida*. Alternative mechanisms are likely to be involved to maintain carbon/nitrogen metabolic balance when growing on histidine, which is also worth further investigation.

5.4 References

Allison, S. L., & Phillips, A. T. (1990). Nucleotide sequence of the gene encoding the repressor for the histidine utilization genes of *Pseudomonas putida*. *J Bacteriol, 172*(9), 5470-5476.

Amador, C. I., Canosa, I., Govantes, F., & Santero, E. (2010). Lack of CbrB in *Pseudomonas putida* affects not only amino acids metabolism but also different stress responses and biofilm development. *Environ Microbiol, 12*(6), 1748-1761. doi: 10.1111/j.1462-2920.2010.02254.x

Hu, L., Allison, S. L., & Phillips, A. T. (1989). Identification of multiple repressor recognition sites in the *hut* system of *Pseudomonas putida*. *J Bacteriol, 171*(8), 4189-4195.

Newell, C. P., & Lessie, T. G. (1970). Induction of histidine-degrading enzymes in *Pseudomonas aeruginosa*. *J Bacteriol, 104*(1), 596-598.

Zhang, X. X., & Rainey, P. B. (2007). Genetic analysis of the histidine utilization (*hut*) genes in *Pseudomonas fluorescens* SBW25. *Genetics, 176*(4), 2165-2176. doi: 10.1534/genetics.107.075713

Appendix

I. Standard DNA techniques

1.1 Polymerase chain reaction (PCR)

PCR reactions were performed using a Palm-Cycler™ (Corbett Life Science). The reagents of a standard PCR reaction are shown in Table A1.1. Taq DNA polymerase for PCR amplification was purchased from Invitrogen. A dNTP stock (10 mM) was prepared from a 100 mM dNTP set (Bioline). The program for standard PCR reactions is shown in Table A1.2. When required, the annealing temperature was adjusted according to the sequence of primers.

Table A1.1. Reagents of PCR reactions

	Volume (µl)	Final Concentration
10x PCR Running Buffer	5	1x
$MgCl_2$ (50 mM)	1.5	1.5 mM
dNTP (10 mM)	1	0.2 mM
Forward Primer (10 µM)	1	0.2 µM
Reverse Primer (10 µM)	1	0.2 µM
Taq DNA Polymerase (5 U/µl)	0.2	1 U
Template DNA	5	1 ~ 5 ng
MilliQ H_2O	35.3	
Total Volume	50	

Table A1.2. Program of PCR reactions

	Temperature	Time	Cycles
Initial Denaturation	94°C	3 min	1
Denaturation	94°C	45 sec	30
Annealing	56°C	45 sec	
Elongation	72°C	1 min per kb	
Final Elongation	72°C	10 min	1
Hold	4°C		

1.2 Isolation of plasmid DNA

Plasmid DNA was extracted from overnight bacterial cultures using E.Z.N.A.® Plasmid DNA Mini Kit I (Omega Bio-Tek) according to manufacture's instructions and stored in DNase-free water at -20°C.

1.3 Restriction digestion

DNA was digested with restriction enzymes purchased from New England Biolabs. The appropriate NEB buffer and temperature for DNA digestion was used according to the manufacturer's instructions. Subsequently, the digested DNA was separated and purified from agarose gel.

1.4 DNA ligation

Ligation reactions were performed by mixing 1 U of T4 DNA ligase (Invitrogen), 2 µl of 5x ligation reaction buffer and insert DNA and vector at the molar ratio of 3:1. MilliQ water was added to a final volume of 10 µl. Reactions were incubated overnight at 16°C.

1.5 Agarose gel electrophoresis

DNA fragments were separated in 1% agarose gel containing 1x SYBR Safe™ DNA gel stain (Invitrogen). DNA loading dye (Fermentas) was added to DNA samples prior to loading onto the gel. Gels were run in SUB DNA cell (BIO-RAD) containing 1x TBE buffer (UltraPure™, Invitrogen) at 140 volts for 30-40 min. GeneRuler 1 kb DNA Ladder (Thermo Scientific) was used to estimate the size of DNA fragments. DNA bands were visualized using a High Performance Transilluminator (UVP, LLC).

1.6 DNA extraction from agarose gel

Desired DNA bands in agarose gel were excised from the gel and purified using a GeneJET Gel Extraction Kit (Thermo Scientific) following instructions from the manufacturer.

1.7 TA cloning

pCR8/GW/TOPO® Cloning Kit (Invitrogen) and TOPO® TA Cloning® Kit (with pCR2.1-TOPO® vector) (Invitrogen) were used for TA cloning. PCR products were firstly cloned into pCR8/GW/TOPO or pCR2.1-TOPO vectors for DNA sequencing. Then the desired insert DNA were restrictedly digested from pCR8/GW/TOPO vector and cloned into destination vectors, or the recombinant TA vectors were directly used as PCR templates.

II. Transformation techniques

2.1 Preparation of chemically competent *E. coli* cells

E. coli strains from -80°C stock were streaked out on LB plate and incubated at 37°C overnight. A single colony was inoculated into 30 ml of SOB broth in a 150ml flask and grown at 37°C overnight. Next morning, 8 ml of the overnight culture was added in a 1L flask containing 200 ml of SOB broth and grown at 37°C with shaking to an OD_{600} of 0.5-0.7. The culture was collected in four 50ml sterile centrifuge tubes and chilled on ice for 15 minutes. Then the cells were pelleted by centrifugation at 4000 g for 15 minutes at 4°C and resuspended in 16 ml of ice-cold transformation buffer I. The cells were incubated on ice for 15 minutes, and then pelleted by centrifugation as mentioned above. The cell pellet was resuspended in 2 ml of ice-cold transformation buffer II. 60 µl of aliquots were made in sterile 1.5ml tubes and stored at -80°C.

Transformation buffer I (250 ml)

RbCl	3.0 g
$MnCl_2 \cdot 4H_2O$	2.5 g
Potassium acetate (1M, pH 7.5)	7.5 ml
$CaCl_2 \cdot 2H_2O$	0.4 g
Glycerol	37.5 ml

Adjust pH to 5.8 with 0.2 M acetic acid and sterilized by filtration through a 0.22 µm filter.

Transformation buffer II (250 ml)

MOPS (0.5 M, pH 6.8)	5.0 ml
RbCl	0.3 g
$CaCl_2 \cdot 2H_2O$	2.75 g
Glycerol	37.5 ml

Sterilized by filtration through a 0.22 µm filter.

SOB medium (1 L)

Tryptone	20.0 g
Yeast extract	5.0 g
NaCl	0.6 g
KCl	0.5 g
2M Mg^{2+} stock	10 ml

Dissolve tryptone, yeast extract, NaCl and KCl in 990 ml of distilled H_2O and sterilize the medium by autoclaving. Add 10 ml of 2M Mg^{2+} stock into the medium prior to use.

2M Mg^{2+} stock (100 ml)

$MgCl_2$	20.3 g
$MgSO_4$	24.7 g

Sterilized by filtration through a 0.22 μm filter.

2.2 Heat-shock transformation of chemically competent *E. coli* cells

Two microliters of plasmid DNA or ligation products was added into chemically competent *E. coli* cells, which were thawed on ice. Cells were incubated on ice for 15 minutes and then heated at 42°C for 30 seconds. After heat shock cells were transferred to ice immediately. 400 μl of SOC medium was added and the cells were incubated at 37°C with shaking for 1 hour. The culture was spread onto prewarmed selective LB plates and incubated overnight at 37°C.

2.3 Electroporation of *P. fluorescens* cells

One milliliter overnight culture of recipient *P. fluorescens* strains was spun down at 12,000 rpm for 1 minute. Cells were washed with 1 ml of sterile glycerol/HEPES solution (10% glycerol and 1mM HEPES) three times. The cells were resuspended in 100 μl of glycerol/HEPES solution and mixed with interested plasmids (100-200 ng). The mixture was transferred into a pre-chilled gapped Gene Pulser® cuvette (Bio-Rad) and kept on ice for 15 minutes. Electroporation was performed using Electroporator 2510 (Eppendorf) at 1.8 kV. The cells were transferred to a sterile 1.5ml tube and immediately mixed with 400 μl of LB broth. Next, the cells were incubated at 28°C with shaking for 2 hours and spread onto selective LB plates. The plates were incubated at 28°C for 2 days.

III. Protein techniques

3.1 Protein expression and purification

3.1.1 Induction of protein expression

Cloning vector pTrc99A was used for protein expression and purification in *E. coli* BL21 (DE3). It contains a strong hybrid trc promoter repressed by LacI repressor. Expression of the cloned genes is induced by IPTG (Amann *et al.*, 1988). A N-terminal hexa-histidine tag was introduced for purification of expressed proteins in this study.

A small-scale protein expression was performed to test protein induction prior to large-scale protein purification. *E. coli* BL21 (DE3) strains harboring pTrc99A-based plasmid were grown in 5 ml of LB broth at 37°C overnight. 1 ml of overnight culture was inoculated into 20 ml of LB in

a 100ml flask. The culture was shaken at 37°C for ~2 hours to an OD_{600} of 0.5-0.7. IPTG was added to a final concentration of 1 mM, and one sample without IPTG was used as control. The culture was grown for further 4 hours for protein induction. 1 ml of samples were collected from the culture and centrifuged at 13,000 rpm for 1 minute. The cell pellets were resuspended in 100 µl of 2x sample buffer and subject to SDS-PAGE analysis (described below).

3.1.2 Protein solubility test

Protein induction was performed as described in section 2.7.1. Cell culture of *E. coli* BL21 (DE3) strains was spun down in a 50ml centrifuge tube at 4,000 g for 20 minutes. Cell pellet was resuspended in 15 ml of lysis buffer. Lysozyme (1.0 mg/ml), DNase I (20 µg/ml) and PMSF (0.1 mM) were added, following incubation on ice for 30 minutes. Cells were lysed by sonication at 60 mV for 10 cycles of 30s burst with 30s pause using Microtip™ of Sonicator S-4000 Ultrasonic Liquid Processor (Misonix, Inc). The cell lysate was centrifuged at 4,000 g for 20 minutes in 4°C. The supernatant was transferred into a new 50ml tube as the soluble fraction. The pellet was resuspended in 15 ml of lysis buffer as the insoluble fraction. 10 µl of soluble and insoluble fractions were mixed with 2x sample buffer and subject to SDS-PAGE analysis (described below).

Lysis buffer

HEPES, pH 7.4	20 mM
NaCl	500 mM
Imidazole	5 mM

pH value was adjusted according to isoelectric point (pI) of proteins.

3.1.3 Protein purification

A large-scale protein induction was performed prior to purification of proteins. 8 ml of overnight culture of *E. coli* BL21 (DE3) strains was inoculated into 400 ml of LB broth. Protein expression was induced by IPTG for 4 hours as described above. Cells were pelleted by centrifugation at 4,000 g for 20 minutes and resuspended in 30 ml pre-chilled lysis buffer. Lysozyme (1.0 mg/ml), DNase I (20 µg/ml) and PMSF (0.1 mM) were added, following incubation on ice for 30 minutes. Cells were lysed by sonication as shown above. The cell lysate was centrifuged at 4,000 g for 20 minutes at 4°C. The supernatant was collected and filtered through a 0.45 µm filter and placed on ice.

Hexa-histidine-tagged proteins were purified using TALON® metal affinity resin (Clontech laboratories, Inc.). 2 ml of TALON resin suspension was transferred to a 30 ml tube and pelleted at 700 g for 2 minutes. After removing the supernatant, the resin was washed twice with 10 ml of ice-cold lysis buffer and spun down at 700 g for 2 minutes. The filtered protein sample was

mixed with the resin in a 50ml tube and incubated at 4°C for 1 hour with slow shaking. The resin was centrifuged at 700 g for 5 minutes and washed with 10 ml of ice-cold lysis buffer. Following resuspension with 1 ml of lysis buffer, the resin was transferred to a 2 ml gravity-flow column. The column was washed with 10 ml of ice-cold lysis buffer and then 10 ml of ice-cold wash buffer. 5 ml of ice-cold elution buffer was added to the column to elute His-tagged proteins. 500 µl fractions of the eluate were collected in 1.5ml tubes. 10 µl of each fraction was subject to SDS-PAGE analysis (described below) to examine the purity of the proteins.

Wash buffer

HEPES, pH 7.4	20 mM
NaCl	500 mM
Imidazole	70 mM

Elution buffer

HEPES, pH 7.4	20 mM
NaCl	500 mM
Imidazole	200 mM

pH value was adjusted according to isoelectric point (pI) of proteins.

3.1.4 Sodium dodecyl sulfate-Polyacrylamide gel electrophoresis

Protein samples were mixed with 2x sample buffer and heated at 95°C for 10 minutes. The samples were spun down at 13,000 rpm for 1 minute and loaded onto a 5% stacking gel. SDS-PAGE was run at 200V for 30-50 minutes using an XCell SureLockTM mini-cell system (Invitrogen). Gels were stained with Coomassie brilliant blue for 1 hour with gentle shaking and then destained with destain solution overnight at room temperature. Preparation of buffers, stacking gel and resolving gel are listed below.

2x Sample buffer

Tris-HCl, pH6.8	125 mM
Glycerol	20%
SDS	4% (w/v)
β-mercaptoethanol	10% (v/v)
Bromophenol blue	0.02% (w/v)

10x SDS-PAGE running buffer, pH8.3 (1 L)

Tris base	30.3 g
Glycine	144.0 g
Sodium dodecyl sulfate (SDS)	10.0 g

Stacking gel (5% acrylamide) (10 ml)

MilliQ H_2O	6.1 ml
40% acrylamide/bis solution (29:1)	1.25 ml

0.5 M Tris-HCl, pH6.8	2.5 ml
10% (w/v) SDS	0.1 ml
10% (w/v) APS	50 µl
TEMED	10 µl

Resolving gel (12% acrylamide) (10ml)

MilliQ H_2O	4.4 ml
40% acrylamide/bis solution (29:1)	3.0 ml
1.5 M Tris-HCl, pH8.8	2.5 ml
10% (w/v) SDS	0.1 ml
10% (w/v) APS	50 µl
TEMED	5 µl

Coomassie blue stain

Coomassie brilliant blue R250	0.125%
Methanol	50%
Acetic acid	10%

Destain solution

Methanol	30%
Acetic acid	10%

3.1.5 Buffer exchange and protein storage

Proteins were loaded into Vivaspin 6 concentrators (GE healthcare) with 5 or 10 kDa molecular weight cut-off and centrifuged at 4,000 g at 4°C until the volume reached to ~1 ml. Proteins were repeatedly diluted with storage buffer in the concentrator until the components of elution buffer became negligible. During the final centrifugation, concentrate the proteins to a desired concentration. After adding 10% glycerol, proteins were stored at -20°C.

Storage buffer

HEPES, pH 7.4	20 mM
NaCl	100 mM

pH value was adjusted according to isoelectric point (pI) of proteins.

3.1.6 Determination of protein concentration

Concentration of proteins was determined by Bradford assay (Bradford, 1976). Protein standards (0, 125, 250, 500, 750, 1000, 1500, 2000 µg/ml) were first prepared with bovine serum albumin (BSA) and protein storage buffer. 5 µl of BSA standards and protein samples were added into 250 µl of Quick Start™ Bradford Dye Reagent (Bio-Rad) and loaded onto a 96-well plate. After incubation at room temperature for 15 minutes, absorbance of the protein samples and standards was measured at 595 nm using a Synergy 2 plate reader (Bio-Tek). The concentration

of proteins was determined according to the standard curve, which was made by plotting absorbance against BSA standards.

3.2 Electrophoresis mobility shift assay (EMSA) with DNA

3.2.1 Preparation of DNA probes

Biotin-labeled DNA probes were amplified by PCR. One of each pair of primers is labeled by biotin at the 5′ end. DNA probes were purified by extraction with an equal volume of 1:1 phenol/chloroform mixture. Following centrifugation at 10,000 rpm for 5 minutes, the upper layer was transferred to a microcentrifuge tube and mixed with an equal volume of chloroform to remove residual phenol. After centrifugation at 10,000 rpm for 5 minutes, the upper phase was transferred to a microcentrifuge tube. 1/10th volume of 3 M sodium acetate (pH 5.2) and 3 volumes of ethanol were added to precipitate DNA. The mixture was incubated at -20°C for at least 1 hour. DNA was pelleted by centrifugation at 15,000 g for 20 minutes and washed with 500 µl of ice-cold 70% ethanol. After air drying, DNA was resuspended in 30-100 µl of DNase-free water and stored at -20°C.

3.2.2 EMSA reactions

EMSA reactions were set up by mixing 20 nM DNA probe, 1 µg salmon sperm DNA (Invitrogen) (non-specific competitor), EMSA binding buffer and increasing concentrations of protein to a final volume of 20 µl. Reactions were incubated at room temperature for 30 minutes. After adding 3 µl of loading buffer, reactions were electrophoresed on 6% native polyacrylamide gel in 0.5x TBE buffer at 120V for 1.5-2 hours at 4°C using XCell SureLock™ mini-cell system (Invitrogen). The gel was pre-run in 0.5x TBE buffer at 120V for 20 minutes before loading samples.

6% Native polyacrylamide gel (12 ml)

10x TBE	0.6 ml
40% acrylamide/bis solution (60:1)	1.8 ml
50% Glycerol	1.2 ml
10% (w/v) APS	100 µl
TEMED	10 µl
MilliQ H_2O	8.3 ml

10x EMSA Binding buffer (pH 7.5)

HEPES	100 mM
KCl	500 mM
$MgCl_2$	50 mM
DTT	10 mM

0.5x TBE buffer	
Tris-HCl, pH 8.3	50 mM
Boric acid	45 mM
EDTA	0.5 mM

Loading buffer	
Glycerol	60%
Bromophenol blue	0.025%

3.2.3 Electroblotting and detection

DNA in native polyacrylamide gel was transferred to nylon membrane (Whatman® Nytran™ SuPerCharge) using XCell SureLock™ mini-cell system (Invitrogen). Electroblotting was performed in 0.5x TBE buffer at 30 V for 1 hour. The membrane was incubated at 80°C for 30 minutes to immobilize the DNA molecules. LightShift™ chemiluminescent EMSA kit (Thermo Fisher Scientific) was used to detect the biotin-labelled DNA probes following the manufacturer's instruction. The image was visualized by LAS-4000 Luminescent Imager equipped with ImageQuant™ LAS 4000 software (FujiFilm).

3.3 Electrophoresis mobility shift assay with RNA

25-nt biotin-labelled RNA probes for EMSA were supplied by Integrated DNA Technologies (Singapore) with 5′ end labelled by biotin. The RNA pellets were resuspended in RNase-free water and stored at -20°C.

EMSA reactions were set up by mixing 0.1 µM RNA probe, 1 µg yeast tRNA (non-specific competitor), RNA binding buffer and increasing concentrations of protein to a final volume of 20 µl. Reactions were incubated at room temperature for 30 minutes. After adding 4 µl of loading buffer, reactions were electrophoresed on 6% nondenaturing polyacrylamide gel in 0.5x TBE buffer at 100V for 1.5-2 hours at 4°C using XCell SureLock™ mini-cell system (Invitrogen). The gel was pre-run in 0.5x TBE buffer at 100V for 20 minutes before loading samples. RNA in nondenaturing polyacrylamide gel was transferred to nylon membrane (Whatman® Nytran™ SuPerCharge) using XCell SureLock™ mini-cell system (Invitrogen). Electroblotting was performed in 0.5x TBE buffer at 30 V for 1 hour. The nylon membrane was incubated at 80°C for 30 minutes to immobilize the RNA molecules. LightShift™ chemiluminescent EMSA kit (Thermo Fisher Scientific) was used to detect the biotin-labelled RNA probes following the manufacturer's instruction. The image was visualized by LAS-4000 Luminescent Imager equipped with ImageQuant™ LAS 4000 software (FujiFilm).

6% nondenaturing polyacrylamide gel (10 ml)

10x TBE	0.5 ml
40% acrylamide/bis solution (29:1)	1.5 ml
50% Glycerol	1 ml
10% APS	50 µl
TEMED	10 µl
MilliQ H2O	6.94 ml

RNA binding buffer

HEPES, pH7.9	10 mM
KCl	35 mM
$MgCl_2$	2 mM

Loading buffer

Glycerol	60%
Bromophenol blue	0.025%

3.4 DNase I footprinting assay

Biotin-labelled DNA probes used in DNase I footprinting assays were prepared as described in section 2.8.1. Reactions were set up by mixing 2 µM DNA probe, EMSA binding buffer and increasing concentrations of protein to a final volume of 50 µl. Reactions were incubated at room temperature for 30 minutes. 50 µl of cofactor solution was added and mixed gently. 0.02 U DNase I (Invitrogen) was added to digest DNA for 5 minutes at room temperature. Reactions were stopped by addition of 100 µl of DNase I stop solution. To extract DNA fragments from the reaction an equal volume of 1:1 phenol/chloroform mixture was added and centrifuged at 10,000 g for 5 minute at 4°C. The upper layer was transferred to a microcentrifuge tube and mixed with 1 µl of glycogen (20 mg/ml, Fermentas), $1/10^{th}$ volume of 3 M sodium acetate (pH 5.2) and three volumes of ethanol to precipitate DNA. The mixture was incubated at -20°C for at least 1 hour. DNA was pelleted by centrifugation at 15,000 g for 20 minutes and washed with 500 µl of ice-cold 70% ethanol twice. After air drying, DNA was resuspended in 8 µl of loading buffer. DNA samples and G+A marker were incubated at 95°C for 10 minutes and loaded onto a 6% sequencing gel. Electrophoresis was performed in 1x TBE buffer at 50W for 1.5-2 hours using Sequi-Gen® GT cell system (Bio-rad). Before loading samples, the gel was pre-run in the same condition for at least 30 minutes. DNA was transferred from the sequencing gel to positively charged nylon membrane (Whatman® Nytran™ SuPerCharge) by contact blotting overnight. A dry nylon membrane was carefully placed onto the gel and covered by three layers of Whatman 3MM paper. A glass plate and a weight of ~2 kg were placed on the Whatman 3MM paper. The nylon membrane was incubated at 80°C for 30 minutes to immobilize the

DNA molecules. Detection of DNA fragments and image visualization were performed as described above.

Cofactor solution

$CaCl_2$	5 mM
$MgCl_2$	10 mM

DNase I stop solution

NaCl	200 mM
EDTA, pH 8.0	20 mM
SDS	1%

6% sequencing gel (40 ml)

10x TBE	4.0 ml
40% acrylamide/bis solution (29:1)	6.0 ml
Urea	16.8 g
25% APS	50 µl
TEMED	50 µl

Loading buffer

Formamide	95%
Bromophenol blue	0.05%
EDTA	20 mM

3.4.1 Production of G+A marker

G+A marker showing the sequence of DNA fragments in DNase I footprinting assays was produced by Maxam-Gilbert chemical sequencing reactions. 10 µl of 20 µM biotin-labelled probe DNA was mixed with 25 µl of formic acid and incubated at 25°C for 5 minutes. 200 µl of hydrazine stop buffer and 750 µl of ice-cold ethanol were added and incubated at -80°C for 1 hour. DNA was pelleted by centrifugation at 15,000 g for 20 minutes and washed with 700 µl of ice-cold 70% ethanol twice. The DNA pellet was dried and resuspended in 100 µl of freshly prepared 10% piperidine. After reaction at 90°C for 30 minutes, 10 µl of 3 M sodium acetate (pH 7.0) and 300 µl of ice-cold ethanol were added and incubated at -80°C for 1 hour. DNA was pelleted by centrifugation at 15,000 g for 20 minutes and washed with 700 µl of ice-cold 70% ethanol twice. After air drying, the DNA pellet was resuspended in 20 µl of loading buffer and stored at -20°C. 7 µl of G+A marker was used for each assay.

Hydrazine stop buffer

Sodium acetate, pH 7.0	300 mM
EDTA	0.1 mM
yeast tRNA	20 µg/ml

Loading buffer	
Formamide	95%
Bromophenol blue	0.05%
EDTA	20 mM

IV. Mutant construction

4.1 Splicing by overlap extension PCR

Splicing by overlap extension PCR (SOE-PCR) (Horton *et al.*, 1989) was performed to generate DNA fragments for gene deletion by homologous recombination. Two pairs of primers were first designed to PCR amplify flanking regions (~500 bp) on each side of the target gene. The two primers closer to the target gene are complementary for 20-23 bp at the join site. Equal amount of the two DNA fragments amplified by PCR was used as templates to produce a single joint PCR product with the two distant primers. The PCR product was first cloned into pCR8/GW/TOPO vector for sequencing and subsequently ligated into plasmid pUIC3 (Rainey, 1999).

4.2 Tri-parental conjugation

Recipient *P. fluorescens* strains, *E. coli* DH5α (λ□) donor strain containing pUIC3-based plasmid and *E. coli* DH5α helper strain containing plasmid pRK2013 from -80ºC stock were inoculated into 5 ml LB medium and grown overnight at 28ºC and 37ºC, respectively. 500 µl of the *P. fluorescens* culture was heat shocked at 45ºC for 20 minutes. Meantime, 500 µl of the donor and helper cultures were spun down separately. After removing supernatants, the donor and helper cells were mixed using 500 µl of LB broth. After the heat shock, all cultures were spun down and mixed together with 50 µl of LB broth. The mixed culture was spread to ~4 cm^2 on a LB plate and incubated at 28ºC overnight. Next day, the inoculum was transferred from LB plate to 3 ml sterile water. 100 µl of the resuspension was plated onto LB plates containing Tc and NF for selecting transconjugants. After incubation at 28ºC for two days, single colonies were picked and inoculated into LB broth. The culture was ready for cycloserine enrichment described below.

4.3 Cycloserine enrichment

20 µl of transconjugant *P. fluorescens* culture was inoculated in 400 ml LB medium without antibiotics and grown overnight at 28ºC with shaking. Next morning, 400 µl of the culture was transferred into 20 ml of LB broth and shaken for 30 minutes at 28ºC. Tetracycline was added at the concentration of 15 µg/ml, and the culture was shaken for 2 hours at 28ºC. D-cycloserine was added at the concentration of 800 µg/ml and the culture was incubated for 4~5 hours with shaking. 1ml of culture was collected and centrifuged at 13,000 rpm for 1 minute. The cell pellet was resuspended with 500 µl sterile water and diluted to 10^{-1}, 10^{-2} and 10^{-3}. The dilutions were plated onto LB plates containing X-gal (60 µg/ml) and incubated at 28ºC for two days. White colonies were picked and gene deletion was screened by PCR.

V. β-galactosidase assay

β-galactosidase assays for measuring expression of *lacZ* fusions were performed with 4-methylumbelliferyl-β-D-galactosidase (4MUG) as an enzymatic substrate (Zhang *et al.*, 2006). 1 ml of cell culture containing *lacZ* fusion construct was harvested and mixed with 0.1% SDS and 40 µl of chloroform by vortex for 5 seconds. After incubation at room temperature for 5 minutes, the samples were diluted 50-100 folds with water. 40 µl of the diluted samples was transferred to a new 1.5ml tube and mixed with 160 µl of reaction cocktail. The reactions were incubated at 37ºC for 30 minutes. 50 µl of 25% (w/v) trichloroacetic acid was added to stop the reaction and the samples were cooled down on ice for 2-3 minutes. Following centrifugation at 13,000 rpm for 1 minute, 10 µl of the supernatant was mixed with 990 µl of glycine-carbonate stop buffer. Fluorescent 4MU (7-hydroxy-4-methylcoumarin) of 200 µl aliquots of samples was measured at 460 nm with an excitation wavelength of 365 nm using a Synergy 2 plate reader (Bio-Tek).

Reaction cocktail solution

Tris-HCl, pH 7.5	25 mM
NaCl	125 mM
$MgCl_2$	2 mM
β-mercaptoethanol	12 mM
4MUG	0.3 mM

Dissolve 2 mg of 4MUG in 100 µl of absolute ethanol and add it to reaction cocktail solution.

Glycine-carbonate stop buffer (pH 10.7)

Glycine	133 mM
Na_2CO_3	83 mM

4MU standards

1 μM 4MU (4-methylumbelliferone) stock solution was prepared and diluted to 100, 200, 300, 400, 500, 600, 700, 800 and 900 nM with glycine-carbonate stop buffer.